2002

Copper toxicity in the physiology and early development of Fucus serratus

Nielsen, Hanne Dalsgaard

Copper toxicity in the physiology and early development of *Fucus serratus*

by

Hanne Dalsgaard Nielsen

A thesis submitted to the University of Plymouth
In particular fulfillment for the degree of

Doctor of Philosophy

Department of Biological Sciences
Faculty of Science

In collaboration with
The Marine Biological Association of the UK

March 2002

Copper toxicity in the physiology and early development of *Fucus serratus*

BY Hanne Dalsgaard Nielsen

Abstract

Fucus serratus was used in a series of laboratory experiments to study the effects of Cu^{2+} exposure on the early development of zygotes and physiological effects on adults collected from Cu^{2+} polluted and clean habitats.

Comparative studies showed that Cu^{2+} tolerance in *Fucus* is an inherited character. Zygote development and growth of embryos and adults during Cu^{2+} exposure indicated that *Fucus serratus* from a Cu^{2+} polluted habitat had a higher tolerance limit than material from two clean habitats. Furthermore, there was no difference in the tolerance level of zygotes, embryos and adults from the same habitat.

Chlorophyll fluorescence measurements showed that Cu^{2+} affected photosynthetic electron transport at PSII, and increased the sensitivity of the alga to saturating light. These effects were most pronounced in non-resistant alga. The algae responded to reduced photosynthetic efficiency by increased non-photochemical quenching, that was more apparent in resistant than in non-resistant algae.

Copper accumulation and release of organic substances by non-resistant fronds was much higher than that of resistant fronds, and the algae may therefore possess different response mechanisms to Cu^{2+} exposure. The respiratory demand of non-resistant fronds was higher and the relative growth rate much lower than that of resistant fronds in the presence of Cu^{2+}.

Cu^{2+} affected zygote development in a very selective manner. Initiation of the polar growth axis was unaffected whereas there was an inhibitory effect on axis fixation and rhizoid elongation. Inhibitory effects on axis fixation resulted in an abnormal cell division pattern in the zygotes. The effects of Cu^{2+} on axis fixation were downstream of F-actin localisation, which was unaffected, and upstream of localised secretion of fucoidin, which was severely inhibited by Cu^{2+}.

By microinjecting the rhizoid cell of germinated zygotes with fluorescent Ca^{2+} dye and using confocal microscopy, it was determined that 1μM Cu^{2+} abolished the apical Ca^{2+} gradient and disrupted normal Ca^{2+} signalling dynamics in the rhizoid apex. Furthermore it was shown that acute exposure of zygotes to extreme [Cu^{2+}] resulted in a dramatic elevation in $[Ca^{2+}]_{cyt}$.

The observed effects of Cu^{2+} on Ca^{2+} signalling suggests that Cu^{2+} toxicity in *Fucus serratus*, in part, acts through induction of reactive oxygen species and inhibition of Ca^{2+} conducting ion channels.

List of contents

List of figures and tables

Acknowledgement

First of all, I would like to thank my supervisors Murray Brown at University of Plymouth and Colin Brownlee at the Marine Biological Association for offering me the opportunity to carry out this project, and for their help during planning and performance of experimental work and during write up of the thesis.

The majority of the experimental work has been carried out at the Marine Biological Association, and I would, in particular, like to thank Colin for providing me the facilities, use of the cofocal microscope and for his competent help with the cell physiological aspects of this project.

Data, of copper concentrations present in the estuaries studied, have been provided by the Environment Agency in Exeter and Bodmin and by Bill Langston (Plymouth Marine Laboratory), and I would like to thank for the kind assistance.

This project would not have been realised without the help and support from my friends and family.

I would like to thank Susana Coelho for her brilliant assistance during the long hours of chlorophyll fluorescence measurements, and Tean Mitchell and John Bothwell for proofreading the script of the thesis. My other friends at the Department of Biological Sciences and in the Brownlee lab in the MBA, Lorraine Berry, Maria Ganderton, Amanda Humble, Helen Goddard, Alison Taylor and Florance Corellou have contributed by encouraging, advising and entertaining me during the past 3½ years.

My parents, Claus and my friends in Denmark have supported me with their many letters, e-mails and phone calls and their visits to Plymouth, for which I am grateful. In particular, I want to thank my parents for their unique support, encouragement and understanding during my work on this project.

Author's Declaration

At no time during the registration for the degree of Doctor of Philosophy has the author been registered for any other University award.

This study was financed with the aid of a studentship from University of Plymouth and carried out in collaboration with the Marine Biological Association of the UK.

Relevant scientific seminars and conferences were regularly attended at which work was often presented.

Presentations at conferences attended:

Hong Kong (2001). 3rd International Conference on marine Pollution and Ecotoxocology. *Oral presentation*: 'Cu^{2+} toxicity in polar axis establishment in the *Fucus* zygote'

Plymouth (2001). 11th International Symposium on Pollutant Responses in Marine Organisms. *Oral presentation*: 'Copper toxicity in early development of the *Fucus* zygote'

Oporto (2000). 7th FECS Conference. *Poster presentation:* 'Effects of copper contamination on development and growth in the *Fucus* zygote'.

Birmingham (2000). The Annual Winter Meeting of the British Phycological Society. *Poster presentation*: Effects of copper on early development and growth in the *Fucus* zygote.

Dundee (1999). The Annual Winter Meeting of the British Phycological Society. Precentation of preliminary results.

Signed: Hanne D. Nielsen
Date: 07.06.02.

Author's Declaration

At no time during the registration for the degree of Doctor of Philosophy has the author been registered for any other University award.

This study was financed with the aid of a studentship from University of Plymouth and carried out in collaboration with the Marine Biological Association of the UK.

Relevant scientific seminars and conferences were regularly attended at which work was often presented.

Presentations at conferences attended:

Hong Kong (2001). 3rd International Conference on marine Pollution and Ecotoxocology. *Oral presentation*: 'Cu^{2+} toxicity in polar axis establishment in the *Fucus* zygote'

Plymouth (2001). 11th International Symposium on Pollutant Responses in Marine Organisms. *Oral presentation*: 'Copper toxicity in early development of the *Fucus* zygote'

Oporto (2000). 7th FECS Conference. *Poster presentation:* 'Effects of copper contamination on development and growth in the *Fucus* zygote'.

Birmingham (2000). The Annual Winter Meeting of the British Phycological Society. *Poster presentation*: Effects of copper on early development and growth in the *Fucus* zygote.

Dundee (1999). The Annual Winter Meeting of the British Phycological Society. Precentation of preliminary results.

Signed:

Date:

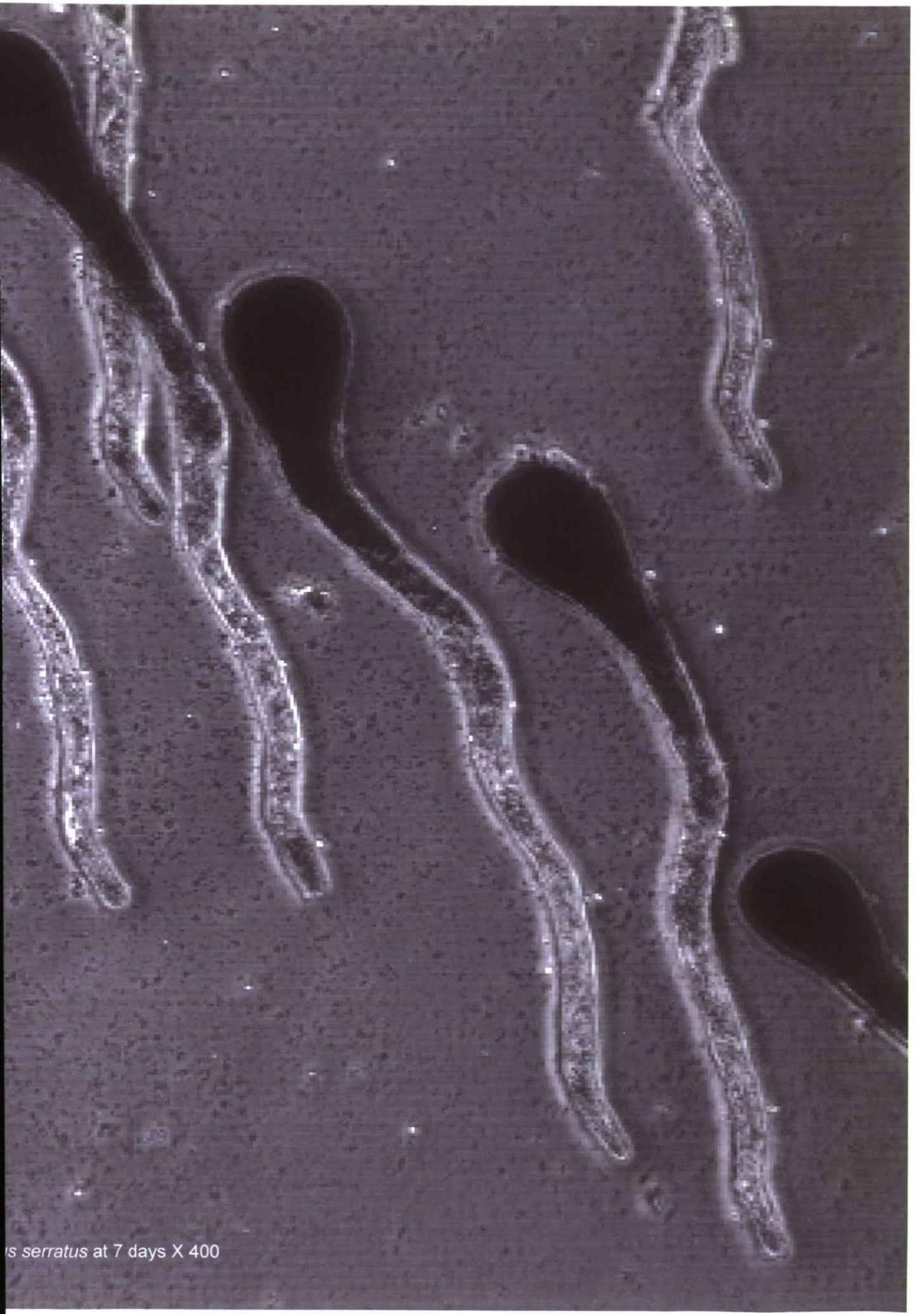

s serratus at 7 days X 400

CHAPTER 1

General Introduction

Mineral copper has been exploited commercially since prehistoric times and the refined form used as a valuable material in many industries. The activity of extracting copper, naturally bound in rocks as minerals such as chalcocite (Cu_2S), cuprite (Cu_2O), bornite (Cu_5FeS_4) and chalcopyrite ($CuFeS_2$), has resulted in the release of copper into the environment mainly as covellite (CuS) and the highly reactive and toxic form, the free copper ion, Cu^{2+} (Atkins, 1989). Concerns about the environmental impact of anthropogenic copper pollution have arisen over the last few decades as awareness of the potentially toxic effects of copper has increased. Copper contamination of air, soil and aquatic environments near metal mines and smelters still occurs, sometimes with devastating consequences for the biota (Fernández *et al.*, 2000; Dahmani-Muller *et al.*, 2000; Larsen *et al.*, 2001). Much of this contamination can end up in the marine environment (Larsen *et al.*, 2001), and effects of copper on marine organisms and ecosystems has become of particular interest for environmental researchers.

Copper is classified as a transition metal alongside nickel, lead, tin, gold, silver, zinc, cadmium and mercury which are often toxic (Bryan, 1971). The effect of Cu^{2+} and other toxic metals on biota, however, is dependent on the actual concentration present. Cu^{2+} is a naturally occurring trace metal, found in most waters and soils at very low levels, which are essential for plant growth (Marschner, 1995). At limiting concentrations, an increase in $[Cu^{2+}]$ can have a positive effect on animal and plant growth (Garansson, 1998; Tokarnia, 1999), whereas a further increases above the deficiency level saturate a plant's copper requirement, resulting in no further increase in growth. Concentrations of Cu^{2+} above levels required for growth may cause symptoms of toxicity and ultimately death.

1.1. Copper speciation in the marine environment

1.1.1. Copper complexation

Free Cu^{2+} is the dominating form of ionic copper in the marine environment, although ionic copper may also exist in the more reduced form, Cu^{+} (Sharma and Millero, 1988). However, auto-oxidation of Cu^{+} with O_2 to form Cu^{2+} and O_2^{-} in seawater occurs very quickly, as the rate constant of the reaction at 25°C and pH 7 is k=2.5 (Sharma and Millero, 1988). Consequently, Cu^{+} is usually only of significance under anoxic conditions. Cu^{2+} in seawater forms complexes with inorganic and organic ligands. The sum of free and complexed Cu^{2+} is termed the total dissolved copper (Cu_T), and is biologically available (Van den Berg, 1984; Allen and Hansen, 1996; Gledhill *et al.*, 1997). Free and complexed Cu^{2+} exists in equilibrium:

$[Cu^{2+}] + [L] \leftrightarrows [CuL]$

where $[Cu^{2+}]$ is the concentration of free copper, [L] is the concentration of the ligand and [CuL] is the concentration of Cu^{2+}-ligand complexes (van den Berg, 1984). The strength of a Cu^{2+}-ligand complex can be estimated from the stability constant, pK_{CuL}, of the Cu^{2+}-ligand equilibrium where high values are equivalent to a strong complex (Van den Berg, 1984):

$pK_{CuL} = \log([CuL]/[Cu^{2+}] \times [L])$

The Cu^{2+}-ligand equilibrium and therefore $[Cu^{2+}]$ are strongly influenced by pH, temperature, and salinity (Byrne *et al.*, 1988; Soli and Byrne, 1989; Meador, 1991; Lores and Pennock, 1998). pH in seawater is mainly governed by bicarbonate (HCO_3^{-}) and its equilibrium with carbon dioxide (CO_2) and hydroxide (OH^{-}) ($CO_2 + OH^{-} \leftrightarrows HCO_3^{-}$) (Madsen and Sand-Jensen, 1991). At 25°C an reduction in pH from 7.6 to 8.3, which represents a natural fluctuation in seawater, increased $[Cu^{2+}]$ three fold from 15% to 5% of total dissolved copper (Meador, 1991; Byrne *et al.*, 1988). pH of seawater in dense

photosynthetic active macrophyte stands may reach values as high as 10 (Madsen and sand-Jensen, 1991) at which Cu^{2+} by large is complexed with ligands. Lowering the temperature from 25°C to 5°C resulted in an increase in $[Cu^{2+}]$ to 12% and 32% of dissolved copper at pH 8.3 and 7.6, respectively (Byrne *et al.*, 1988).

1.1.2. Inorganic ligands

Traditionally, the principal inorganic copper ligands in seawater are considered to be hydroxyl (OH^-), carbonate (CO_3^-), chloride (Cl^-) and sulphate SO_4^{2-} (Turner *et al.*, 1981; Byrne and Miller, 1985; Byrne *et al.*, 1988; Soli and Byrne, 1989). The total concentration of dissolved inorganic copper (Cu'), in seawater can therefore be calculated as:

$[Cu'] = [Cu^{2+}] + [CuCO_3] + [Cu(CO_3)_2^{2-}] + [CuOH^+] + [Cu(OH^-)_2] + [CuCl^+]$ *etc.*

The natural inorganic ligands usually occur in mM concentrations in seawater and so are often present in excess of Cu^{2+}. Thus changes in $[Cu^{2+}]$ can result from small changes in the concentration of free inorganic ligands (Allen and Hansen, 1996). pK_{CuL} values estimated for the copper-carbonate complexes $Cu(CO_3)_2^{2-}$ and $CuCO_3$ are 8.60-8.92 and 5.75-6.75 respectively, which are relatively high compared with pK_{CuL} of about 3-4 for hydroxide and chloride copper complexes (Turner *et al.*, 1981). The prevailing interpretation of these results is, therefore, that the speciation of inorganic copper complexes is dominated by carbonate complexation which accounts for ~75% of dissolved inorganic copper when only carbonates, hydroxides and chloride are taken into account as inorganic ligands (Turner *et al.*, 1981; Byrne and Miller, 1985; Byrne *et al.*, 1988; Soli and Byrne, 1989). However, it has been suggested that ionic sulphide, HS^-, is potentially the most important inorganic ligand in seawater (Al-Farawati and Van den Berg, 1999). Hydrosulphite (H_2S) is normally associated with anoxic environments and is assumed to be oxidised by O_2 in seawater (Millero, 1991). However, a H_2S concentration of 0.1 to 2 nM has been demonstrated in normal seawater (Elliott *et al.*, 1987), where it is likely to be

stabilised by trace metal complexation (Dyrssen, 1988; Al-Farawati and Van den Berg, 1999). With a pK_{Cu} of 12.9 – 14.1, HS^- is a very competent copper complexing ligand, with the potential to influence the speciation of inorganic copper in marine environments in both the absence and presence of organic ligands (Dyrssen, 1988; Al-Farawati and Van den Berg, 1999), which have pK_{CuL} values comparable with that of HS^- (Moffett and Zika, 1983; Coale and Bruland, 1988, 1990; Moffett *et al.*, 1990).

1.1.3. Organic ligands

A wide range of organic ligands form stable complexes with copper and other trace metals (Van den Berg, 1979; Gledhill *et al.*, 1999; Croot *et al.*, 2000; Pandey *et al.*, 2000). Organic ligands can be released from micro-organisms and macroalgae (McKnight and Morel, 1979; Gledhill *et al.*, 1999; Croot *et al.*, 2000) or they can originate from the degeneration of organic material (Ashley, 1996; Alberts and Filip, 1998; Voelker and Kogut, 2001). Two groups of organic ligands, with high pK_{CuL} of about 11-13 (strong organic ligands) and low pK_{CuL} of about 5-8 (weak organic ligands) have been identified in the marine environment (Moffett and Zika, 1983; Coale and Bruland, 1988, 1990; Moffett *et al.*, 1990; Kogut and Voelker, 2001).

Degeneration of marine and terrestrial organic material is a source of humic acid, a heterogeneous group of organic ligands found in the marine environment particularly near the coast and in estuarine waters (Ashley, 1996; Alberts and Filip, 1998; Voelker and Kogut, 2001; Kogut and Voelker, 2001). Terrestrial humic acid with a pK_{CuL} normally in the range of 5.18-5.32 is a well-known contributor of weak organic ligands in aquatic systems (Pandey *et al.*, 2000; Kogut and Voelker, 2001). However, humic acid may also contribute to the class of strong organic ligands since pK_{CuL} values for humic acid in the

region of 10.4-13.2 have been demonstrated (Voelker and Kogut, 2001; Kogut and Voelker, 2001).

Phytoplankton and macroalgae are known to release copper complexing substances, which lower the availability of toxic copper species in their surroundings (Anderson and Morel, 1978; McKnight and Morel, 1979; Moffett *et al.*, 1990; Gledhill *et al.*, 1997, 1999; Croot *et al.*, 2000). Secretion of ligands from living algae contribute to the pool of both strong and weak organic ligands (Coale and Bruland, 1988; Moffett *et al.*, 1990; Croot *et al.*, 2000). One group of organism which contributes more than others is the cyanobacterium *Synechococcus*. This can be very sensitive to copper, which may cause a reduction in reproductive rates at concentrations as low as 10-100 pM (Sunda and Guillard, 1976; Jackson and Morgan, 1978; Brand *et al.*, 1986; Sunda and Huntsman, 1995). This is consistent with the evolution of *Synechococcus* in an anoxic ocean where Cu^{2+} was held at a very low level by CuS formation (Brand *et al.*, 1986). In oceanic waters there is a high correlation between the vertical profiles of strong organic ligands and chlorophyll. It is therefore believed that *Synechococcus* is a major source of strong organic ligands in the world's oceans, potentially controlling oceanic copper speciation in some areas (Moffett and Zika, 1983; Coale and Bruland, 1988; Moffett *et al.*, 1990; Moffett and Brand, 1996).

1.2. Copper distribution in the marine environment

Naturally occurring background levels of Cu^{2+} in marine environments are dependent on inputs from rivers, the continents, the atmosphere, hydrothermal venting and sediments *via* particulate and biological material (Klinkhammer, 1980; Boyle *et al.*, 1985; Saager *et al.*,

1992; Widerlund *et al.*, 1996). Anthropogenic sources also contribute to the input of Cu^{2+} to aquatic systems (Nriagu and Pacyna, 1988).

1.2.1. Oceanic copper

Open oceanic water is largely isolated from terrestrial influence and the distribution of many nutrients is governed by biological activity (Hunter *et al.*, 1997). The concentration profiles of the major phytoplankton nutrients carbon, nitrogen, phosphate and silica appear to be highly correlated with one another and exist at a molecular ratio very similar to the phytoplankton nutrient uptake ratio, which is known as the 'Redfield Ratio' (Redfield, 1958; Brzezinkski, 1995; Tyrell and Law, 1997). The major nutrients become simultaneously depleted from the euphotic zone, the upper 100 m or so of surface water, by phytoplankton growth (Bruland, 1980; Hecky and Kilham, 1988; Hunter *et al.*, 1997). A very steep nutrient concentration gradient occurs through the thermocline and reaches background levels of μM concentrations at about 1,000 m depth where remineralisation of nutrients takes place (Bruland, 1980). Essential trace metals in oceanic waters exist at nano- to pico-molar concentrations and are orders of magnitudes lower than macronutrients (Hunter *et al.*, 1997). However, many trace metals display surface depletion and deep-water regeneration, resulting in a high degree of correlation between the vertical profiles of some macro- and micro nutrients. There is, for example, a high degree of correlation between the profiles of cadmium and phosphate (Bruland, 1980; Boyle, 1988; Frew and Hunter, 1992; Saager *et al.*, 1992), and zinc and silica (Saager *et al.*, 1992).

In contrast, the concentration profile of total dissolved copper, Cu_T, deviates from the characteristic nutrient profiles in oceanic waters. Cu_T does not become entirely depleted from surface waters and the concentration of copper in the Northeast Pacific increases

linearly with depth (Bruland, 1980; Boyle *et al.*, 1985; Coale and Bruland, 1988, 1990; Moffett, 1990; Saager *et al.*, 1992). Bruland (1980) showed that the concentration of total dissolved copper increased almost linearly from ~0.5 nM at the surface to ~5 nM at about 4,000 m. Significant increases in the copper concentration can be found in near bottom waters with levels up to 10 nM (Klinkhammer, 1980; Shaw *et al.*, 1990; Saager *et al.*, 1992). Sediment pore water can hold concentrations about 10 fold higher than bottom water, and diffusion and up-welling are considered important factors in the oceanic copper budget (Moore, 1978; Klinkhammer, 1980; Saager, 1992).

Deviation of the vertical Cu_T profile from that of other nutrients may be the result of copper distribution being controlled by a combination of the uptake regeneration cycle and the high concentration of copper complexing ligands in oceanic surface water (Hunter *et al.*, 1997). Phytoplankton uptake of copper tends to lower the concentrations in surface waters and correlations between Cu_T and silica, and Cu_T and phosphate have been demonstrated in some areas (Saager *et al.*, 1992; Sunda and Huntsman, 1995), although such correlations tend to break down altogether (Orren and Monteiro, 1985). As much as 99.7% of Cu_T in oceanic surface water is bound in strong organic complexes which prevent depletion, as complexed copper is largely inaccessible to phytoplankton (Coale and Bruland, 1988; Moffett *et al.*, 1990). Due to the complexing properties of the ligands, the speciation of copper varies hugely with depth. Coale and Bruland (1988) showed that $[Cu_T]$ in the Northeast Pacific increased three fold from 0.6 to 1.8 nM as the depth increased to 400 m, whereas $[Cu^{2+}]$ increased three orders of magnitude from 10^{-14} to 10^{-11} M.

$[Cu_T]$ in oceanic waters increases in an inshore direction due to an increasing significance of wind-borne (eolian) deposits from the continents, river inflow and diffusion from

continental shelf sediment (Boyle *et al.*, 1985; Saager *et al.*, 1992). In the study by Saager and co-workers (1992) [Cu_T] of near shore surface water in the Indian Ocean was about 4 nM and decreased sharply to ~0.5 nM at 500 m depth. Combined with a 5-fold lower copper concentration of surface water at offshore stations, the data indicated a strong influence of eolian sources (Saager *et al.*, 1992). Similar results have been found for other near shore waters. For example, [Cu_T] of Mediterranean Sea surface water of up to 3.8 nM resulted mainly from inflow from local rivers containing concentrations of copper up to 10-fold higher (Boyle *et al.*, 1980). [Cu_T] in near shore waters, however, is very heterogenous, and huge variations can be found between locations. This is illustrated by the [Cu_T] of up to 39 nM in the surface water of the Irish Sea (Van den Berg, 1984) which is 10-fold higher than those reported for the Mediterranean Sea and near shore waters of the Indian Ocean (Boyle *et al.*, 1985; Saager *et al.*, 1992).

1.2.2. Estuarine copper

Inputs of copper from rivers and sediment often result in [Cu_T] in estuaries several orders of magnitude higher than in oceanic waters. Terrestrial input *via* rivers is the main source of trace metals in many estuaries and the metal concentration in both the water column and the sediment usually declines in an offshore direction (Apte *et al.*, 1990; Larsen *et al.*, 2001). Sediment, however, is also an important source of trace metal to the estuarine water column. Trace metals, including copper, are released from sediment by degradation of organic matter under aerobic conditions and from the particulate fraction into the pore water and overlying bottom water (Widerlund, 1996; O'Leary and Breen, 1998). [Cu_T] in pore water exceeds that of bottom water by a factor of 3-4 and transport usually occurs by diffusion and suspension of sediment (Widerlund, 1996).

Large spatial and temporal variation in [Cu_T], which is influenced by water currents, salinity, the particle and ligand concentrations and interactions between these parameters, can be found within an estuary (Ng *et al.*, 1996; Turner, 1996). Organic ligands within estuaries can play a crucial role in copper speciation. Brown algae, which are often important primary producers in estuaries, are found amongst the group of ligand releasing algae (Ragan *et al.*, 1980; Gledhill *et al.*, 1997). Brown algae are able to release copper-complexing polyphenols in response to elevated concentrations of copper, and can potentially influence the estuarine copper speciation in contaminated areas (Ragan *et al.*, 1980; Gledhill *et al.*, 1997).

Tidal fluxes in an estuary cause large variations in salinity, which can vary from 6‰ at low tide to 26‰ at high tide in the Humber Estuary, England (Ng *et al.*, 1996). The solubility of copper decreases with increasing salinity and the metal fraction adsorbed to suspended particles and in complexation with ligands consequently increases significantly (Ng *et al.*, 1996, Turner, 1996; Lores and Pennock, 1998). Lores and Pennock (1998) showed that approximately 28% of Cu_T was complexed with organic ligands at a 3‰ salinity and increased to 60% at 15‰ salinity. Furthermore, Ng and co-workers (1996) showed that the total trace metal concentration at the mouth of the main channel in the Humber Estuary was close to zero at high tide due to dilution factors whereas trace metals could be found in μM concentrations at low tide. The mechanism underlying the effect of salinity on trace metal complexation is poorly understood and complexation of other metals, such as zinc, cadmium and chromium, is unaffected by changing salinity above 3‰ (Lores and Pennock, 1998). As a consequence of salinity-dependent copper complexation mechanisms, sediment in suspension and organic ligands can act as both a source of copper at low salinity and as a sink for copper at high salinity in estuarine waters. In an estuary the input of river water is a source of both freshwater (*i.e.* low salinity) and organic ligands

which may have contrasting effects on [Cu^{2+}]. The salinity may be expected to increase towards the mouth of the estuary and result in an increase in the proportion of complexed Cu^{2+}. On the contrary, the concentration of organic ligands may be expected to decrease from river inlet towards the mouth of the estuary and could potentially result in a decrease in the proportion of complexed Cu^{2+}. Consequently estuaries naturally have a heterogeneous metal distribution but anthropogenic activity can, nevertheless, often be an overriding factor, which results in huge differences between estuaries. Average differences in the copper concentrations between estuaries can range from a few nM to μM concentrations in the water column, and the sediment copper content can vary from a few to several thousand $\mu g\ g^{-1}$ sediment (Bryan and Langston, 1992).

1.2.3. The Fal and Avon Estuaries

Figure 1.01 shows the location of the Fal Estuary and the Avon Estuary, which are good examples of the large differences in copper status to be found in British estuaries as a result of mineral exploitation. The Avon Estuary (Figure 1.02) has never been affected by mineral exploitation and is considered a 'clean' estuary (Bryan and Langston, 1992), whereas the Fal Estuary (Figure 1.03) is heavily contaminated with copper and zinc due to anthropogenic activities. Commercial exploitation of mineral sources in South West England was at its peak in the 19th century when more than 1,000 mines in the region accounted for up to 50% of the world's mineral supply (Dines, 1969). Around 1900 the number of mines started to decline rapidly (Dines, 1969) and, by 1983, there were only about five working mines left in the region (Bryan and Gibbs, 1983). Today all mining has ceased. The formerly most productive mining area in the South West is situated north of Falmouth and is drained by the Carnon River *via* Restronguet Creek into the Fal Estuary, which has, over the centuries, received vast quantities of copper, zinc and arsenic tailings from mining activities (Dines, 1969). Sources of metal contamination include erosion of

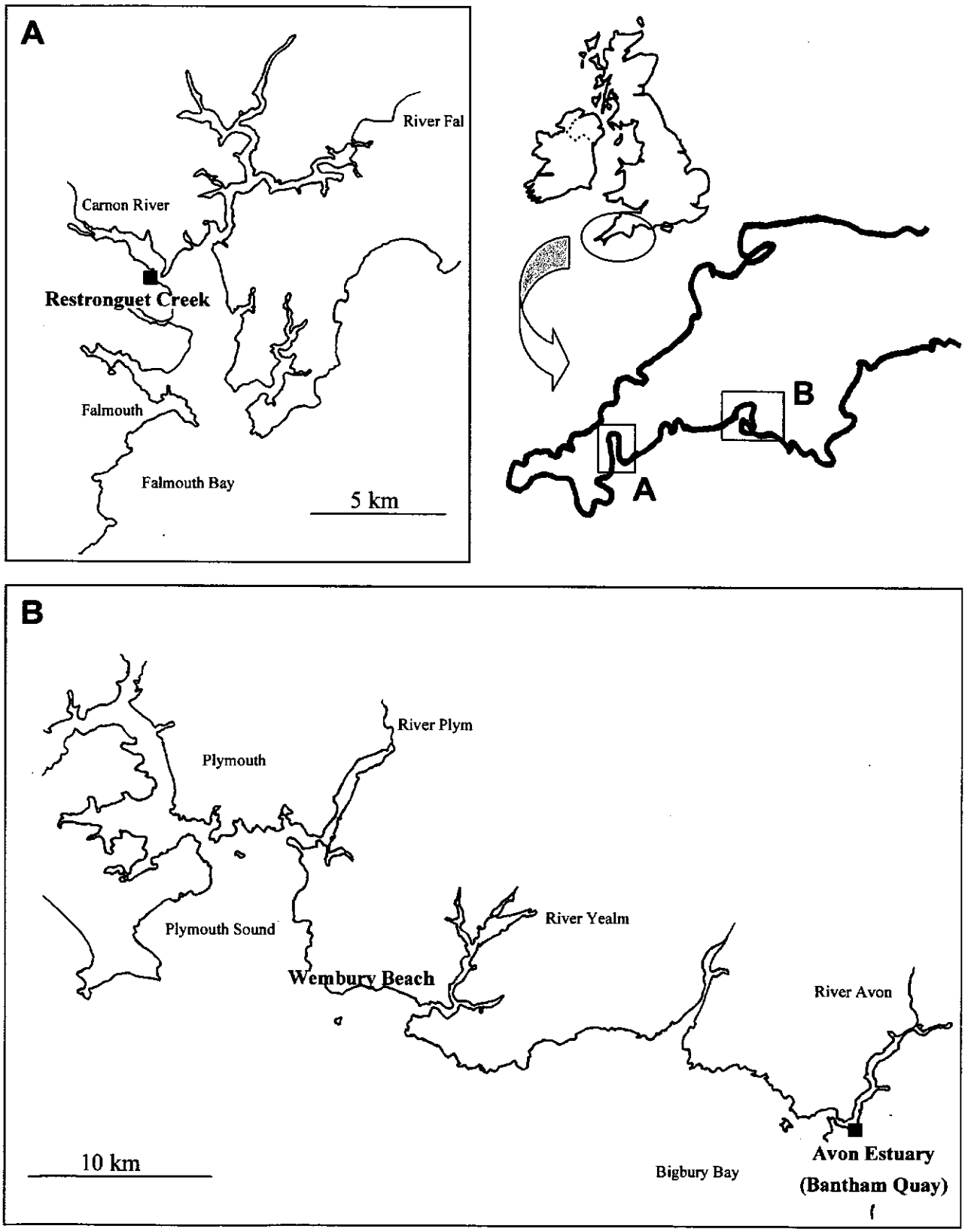

Figure 1.01. Map showing the location of Restronguet Creek (A), and Avon Estuary (B).

Figure 1.02. Avon Estuary by Bantham Quay

Figure1.03. Restronguet Creek in the Fal Estuary

spoil heaps (Larsen *et al.*, 2001) and flooding of abandoned mines by rainwater, resulting in the leaching of metals in acid solution into the drainage water (Marsden and DeWreede, 2000). Previous mining activity therefore constitutes a serious risk of metal contamination years after its termination (Gibb *et al.*, 1996), which is contributed to by diffusion of particulate waste from sedimentation in estuaries. Within the Fal Estuary system, Restronguet Creek represents the most heavily contaminated location, presently receiving copper from mine drainage water and the vast quantities of silt which have filled up the creek (Bryan and Gibbs, 1983; Bryan and Langston, 1992 Somerfield *et al.*, 1994). Acidic water, pH 4 (Perryman, 1996), carries about 9 μM Cu_T into Restronguet Creek (Bryan and Hummerstone, 1973). Concentrations of Cu_T measured at the mouth of the creek show large variations during a daily tidal cycle and annually, as illustrated in Figure 1.04. An average [Cu_T] of 200 nM has been measured in the water at Restronguet Creek over the last 7 years, which is 20-fold higher than values measured in the Avon and other 'clean' estuaries during the same period (Figure 1.05). The status of the Avon Estuary as one of the least polluted estuaries in the UK is also illustrated by the total copper content in the sediment of 18 $\mu g\ g^{-1}$, which is 2 to 3 orders of magnitude lower than in Restronguet Creek sediment (Bryan and Langston, 1992).

1.3. Determination of biologically significant copper

1.3.1. Chemical methods

The fraction of total dissolved copper (Cu_T) which exists as relatively inert forms, complexed with strong organic and inorganic ligands, are of less biological significance than free Cu^{2+} and copper bound to weak ligands. Knowledge of copper speciation is therefore relevant when monitoring copper in marine environments (Anderson and Morel,

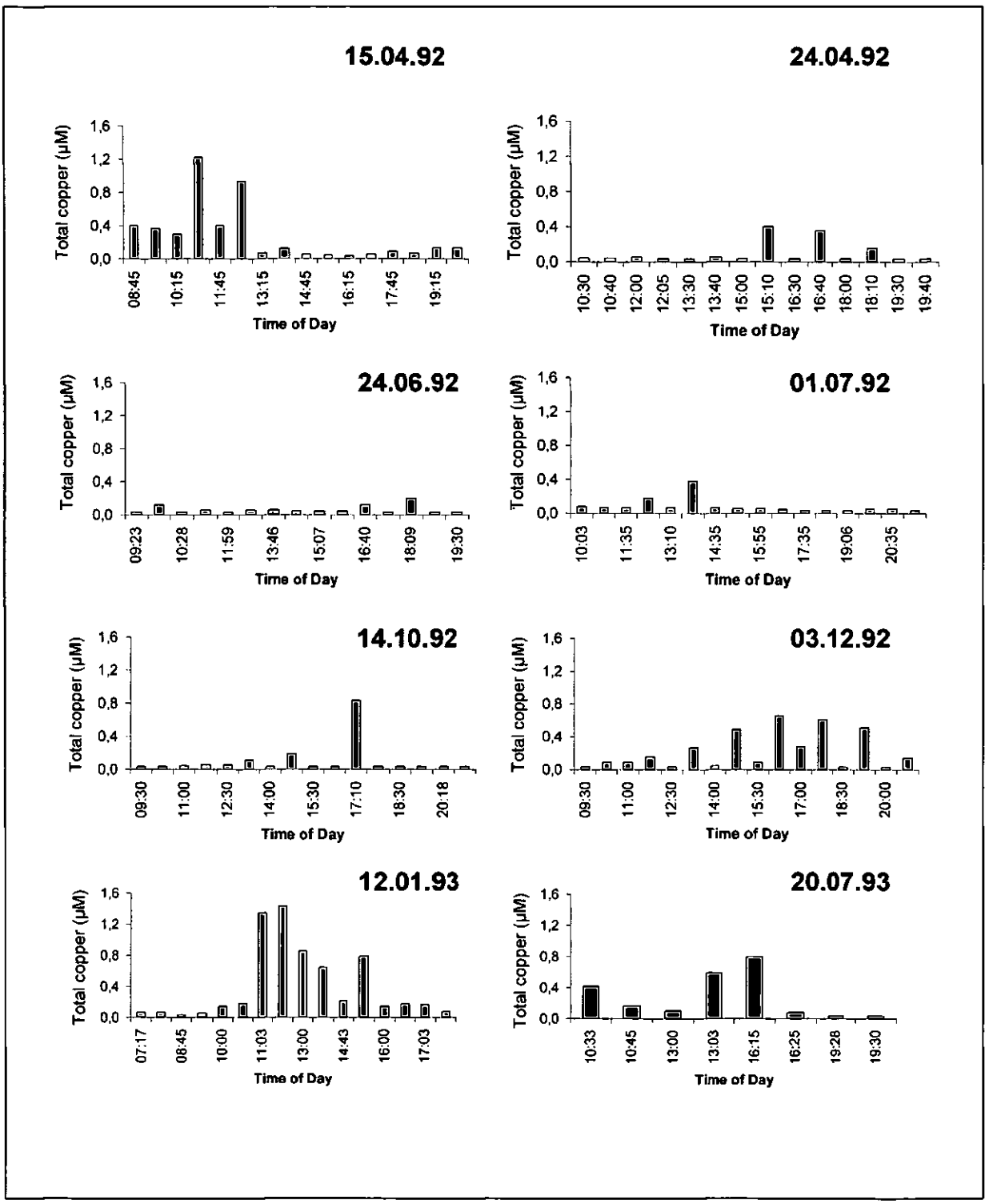

Figure 1.04. Variation in the total copper concentration in the water column at Restronguet Creek (Grid Ref. SW8161037010) at diferent times during the day from April 1992 to July 1993. Figures are drawn from data provided by the Environment Agency (2001).

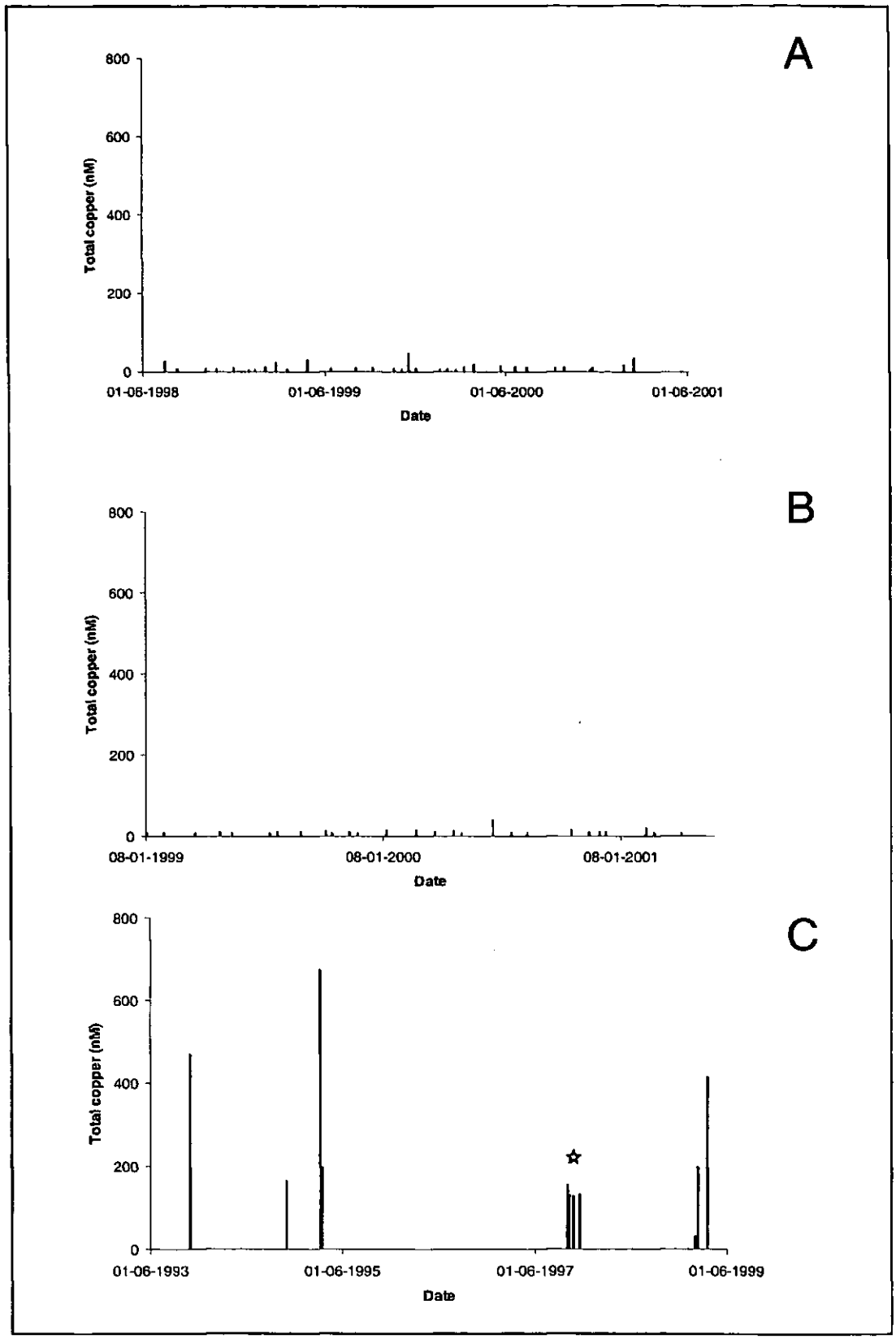

Figure 1.05. Concentrations of total copper in the water column in two clean estuaries, the Avon Estuary (Grid Ref. SX7142747251) (**A**), the Yealm Estuary (Grid Ref. SX5390047700) (**B**) and the copper contaminated Restronguet Creek (Grid Ref. SW8161037010) (**C**). Figures are drawn from data provided by the Environment Agency in Bodmin and Exeter (2001), and W. Langston, MBA (2001) (☆).

1978; Brand *et al.*, 1986; Moffett and Brand, 1996). Analytical techniques, such as the highly sensitive voltammetric stripping methods, are used to determine the chemical speciation of Cu_T and to measurement $[Cu^{2+}]$ (Van den Berg, 1984; Moffett and Zika, 1987; Sunda and Huntsman, 1991; Donat, 1994; Miller and Bruland, 1994; Compos and van den Berg, 1994; Gledhill *et al.*, 1999; Bruland *et al.*, 2000). Voltammetric stripping methods can be separated into two different approaches. 'Anodic stripping voltammetry' (ASV) is a direct technique for detecting kinetically the labile copper species, which usually comprises Cu^{2+} and inorganic copper complexes. 'Competitive ligand equilibration/adsorptive cathodic stripping voltammetry' (CLE-ACSV), an indirect method, measures the electrochemical equilibrium between a naturally occurring organic ligand and characterised ligand added to the sample.

ASV is performed on thin mercury film rotating glassy carbon disk electrodes. Labile copper species, Cu^{2+} and inorganic ligands, are reduced to atomic Cu forming a copper/mercury amalgam on the mercury electrode in response to the negative deposition potential (Bruland *et al.*, 2000). After a fixed deposition time, atomic Cu is oxidised (stripped) off the mercury electrode by changing its electrical potential to positive. The current resulting from oxidation of the copper/mercury amalgam gives a measure for the amount of Cu which is dissociated to Cu^{2+} (Donat *et al.*, 1994). Organic ligands are usually stronger chelating agents than inorganic ligands and electrochemically inactive so long as the electrical potential during the deposition step is low enough (Bruland *et al.*, 2000). The copper speciation and $[Cu^{2+}]$ can be calculated from $[Cu_T]$, [L], and pK_{CuL} of the different ligands in the sample. [L] and pK_{CuL} can be calculated from the stripping current.

In CLE-ACSV, the sample is titrated with copper and a ligand (AL) with known pK_{CuL} is added. AL forms complexes with copper ($Cu(AL)_2$) during the establishment of equilibria

(competition) with ligands naturally occurring in the sample (Bruland *et al.*, 2000). Ligands commonly used in competitive equilibrations include salicylaldoxime (Compos and van den Berg, 1994), acetylacetonate (Moffett and Zika, 1987), and EDTA (Sunda and Huntsman, 1991). After equilibration, the $Cu(AL)_2$ complexes are adsorbed onto a hanging-mercury-drop electrode. During the cathodic stripping step, Cu^{2+} in the $Cu(AL)_2$ complex is reduced to atomic Cu, and the resulting 'reduction current' is a measure for $[Cu(AL)_2]$. Complexation of Cu^{2+} by natural ligands results in a small decrease in the analytical signal, and gives an estimate of the strength of the naturally occurring organic ligand. As with ASV, the concentration of the different ligands and $[Cu^{2+}]$ originally occurring in the sample can be calculated from the stripping current.

1.3.2. Biomonitoring

Chemical analysis provides a good indication of the concentration of trace metals in the environment at the time when a sample is taken. This is, however, not always satisfactory when monitoring locations with highly fluctuating metal concentrations. Furthermore, chemical analyses do not provide any information on the effects of trace metals upon the organisms living within the environment, which are often of more interest than knowledge of the exact concentration present. The need to monitor the time-integrated concentration of trace metals, and to acquire knowledge of interactions between trace metals and organisms living within a particular environment, has resulted in the use of biomonitors (Phillips, 1990; Wolfe, 1992; Depledge *et al.*, 1994; Doust *et al.*, 1994; Langston and Spence, 1995).

Biomonitoring is generally defined as measurement of the response of living organisms to changes in their environment, which includes additive, synergistic and antagonistic effects, and changes in morphology and reproduction (Burton, 1986). Biomonitors are organisms

which can be used in qualitative and quantitative analysis of anthropogenicly induced environmental changes, and several criteria for such organisms have been described (Rainbow and Phillips, 1993; Langston and Spence, 1995): the organism should be stationary and representative for a particular environment, geographically widespread, allow-year round sampling, and provide sufficient material for analysis. Furthermore, correlation should exist between the concentration of metal in the environment and accumulation by the organism, which must be relatively tolerant to a range of concentrations.

Species which satisfy the requirements for biomonitoring in the marine environment include molluscs (Mostafa and Collins, 1995; O'Leary and Breen, 1997; 1998), some species of green algae (Seelinger and Cordazzo, 1982; Say *et al.,* 1990; Wong *et al.,* 1994; Muse *et al.,* 1999) and red seaweeds (McLean and Williamson, 1977; Phillips, 1990; Malea *et al.,* 1994). However, one of the brown seaweeds, fucoids, however, are considered a particularly suitable group of biomonitors. They are hyper-accumulators of heavy metals and are highly abundant in the intertidal zone of temperate rocky shores. Fucoids are considered to accumulate trace metals in a non-regulatory manner and the level of metals in the algae is considered to reflect that of the environment and they have been used in numerous monitoring studies (Bryan and Hummerstone, 1973; Fuge and James, 1974; Haug *et al.,* 1974; Foster, 1976; Melhuus *et al.,* 1978; Lignell *et al.,* 1982; Louma *et al.,* 1982; Bryan, 1983; Scanlan and Wilkinson, 1987; Fosberg *et al.,* 1988; Söderlund *et al.,* 1988; Ronnberg *et al.,* 1990; Riget *et al.,* 1995; Gibb *et al.,* 1996; Jayasekera and Rossbach, 1996; O'Leary and Breen, 1997; 1998; Stengel and Dring, 2000). Furthermore, brown seaweeds seem to be particularly resistant to elevated concentrations of trace metals and thrive in heavily contaminated locations such as

Restronguet Creek where Cu^{2+} levels reach toxic concentrations of 200-700 nM (Figure 1.06).

1.4. Copper - the essential nutrient

Copper is an absolute requirement for cellular metabolism and the highly reactive cupric ion (Cu^{2+}) is an irreplaceable co-factor in various enzymes. In plants, copper tissue levels of about 245-400 nmol g^{-1} DW are required for maintenance and growth, whereas during periods of deficiency the copper content of leaves may decrease to about 30 nmol g^{-1} DW (Droppa *et al.*, 1984; Herbik *et al.*, 1996; Garansson, 1998). In nature copper is usually available at suitable concentrations for growth and copper deficiency in plant leaves may be a side-effect of iron deficiency (Herbik *et al.*, 1996). For example, tomato plants displaying copper deficiency in leaves have been shown to accumulate copper in roots, where lack of the iron-binding enzyme, nicotianamine, caused by iron deficiency, results in an inability of the plant to mobilise copper from the roots for xylem transport (Herbik *et al.*, 1996). The immediate effect of copper deficiency in plants is reduced growth and die-back of young leaves (Garansson, 1998), whereas at a cellular level copper deficiency causes a reduction in copper requiring proteins (Droppa *et al.*, 1984; Herbik *et al.*, 1996; Molina-Heredia *et al.*, 2001).

1.4.1. Copper-requiring proteins

The cupric ion is employed as a co-factor in various enzymes in both prokaryotic and eukaryotic cells. The high redox potential of the Cu^{2+}/Cu^{+} ions ensures easy electron transfer between these forms, which makes them excellent electron carriers and allows them to react directly with molecular oxygen in terminal oxidases (Colman *et al.*, 1978).

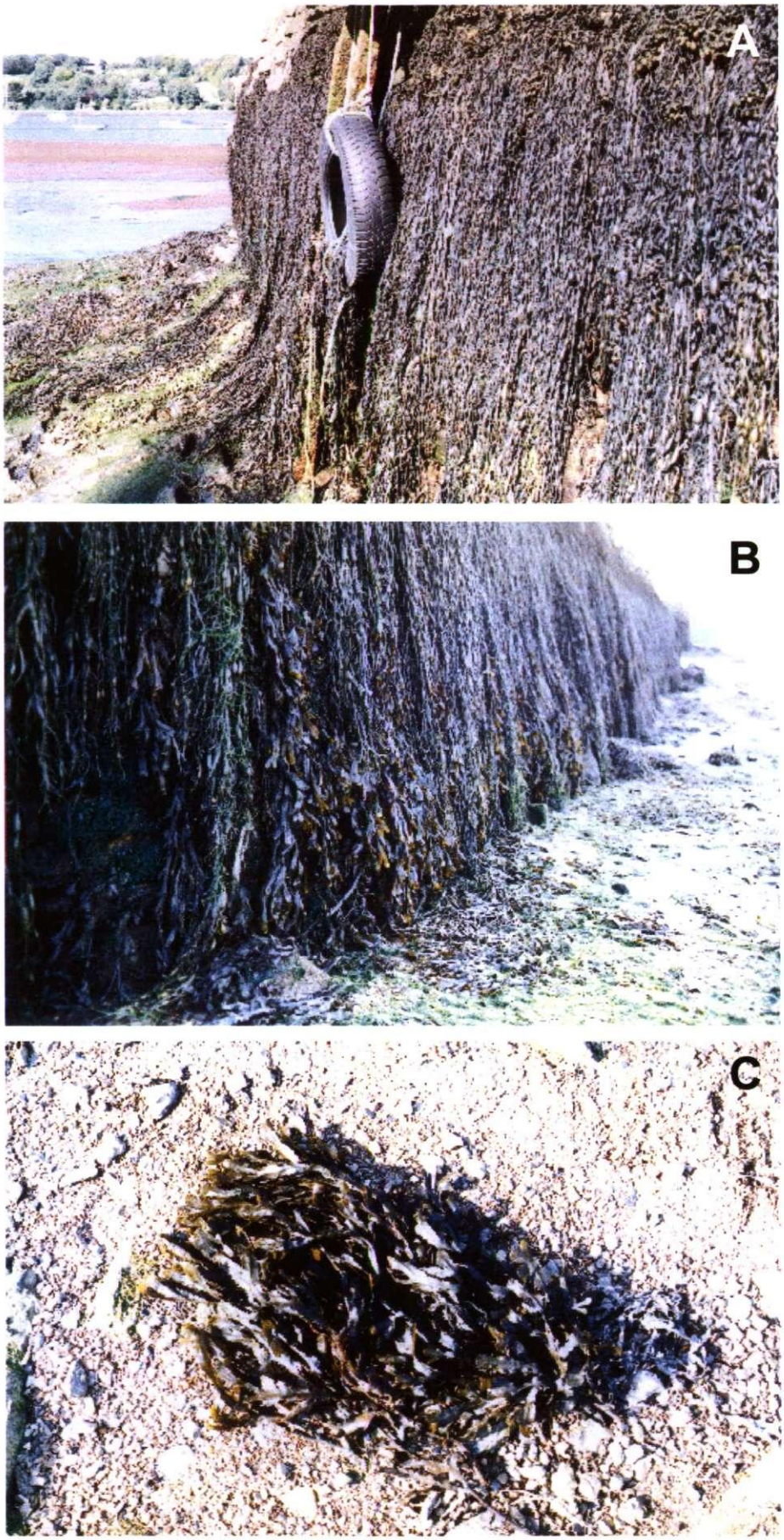

Figure 1.06. Brown seaweed in Restronguet Creek. *Ascophyllum nodosum* and *Fucus spiralis* (**A**). *F. serratus*, *F. vesiculosus* and *A. nodosum* (**B**), *F. serratus* (**C**)

Cytochrome *c* oxidase (COX) is the terminal oxidase in the respiratory electron transport chain in prokaryotes and in eukaryotic mitochondria where one Cu^{2+} reacts directly with molecular oxygen (Capaldi, 1990; Babcock and Wikström, 1992). Eukaryotic COX is a large membrane-spanning enzyme composed of 13 subunits of which two bind one Cu^{2+} each (Tsukihara *et al.*, 1996). Subunit I contains two heme complexes and one Cu^{2+}, Cu_B, which is coordinated by three histidine side chains, whereas one histidine and two cysteine side chains in subunit II coordinate a second Cu^{2+}, Cu_A (Capaldi, 1990; Babcock and Wikström, 1992; Tsukihara, 1996). The heme and copper reaction centres in COX are responsible for respiratory reduction of O_2 to H_2O and capture the energy from this reaction to promote proton transport across the inner mitochondrial membrane for ATP production ($4e^- + 8H^+_{matrix} + O_2 \rightarrow 2H_2O + 4H^+_{cytosol}$) (Babcock and Wikström, 1992). During this cyclic reaction, Cu_A is continuously reduced and oxidised by receiving electrons from cytochrome *c*, which becomes oxidised, and delivering the electrons to Cu_B in the iron-heme and Cu^{2+} reaction centre of subunit I, where the heme molecule mainly serves to stabilise O_2. Cu_B reacts directly with O_2 and catalyses its stepwise reduction to H_2O by a total of 4 electrons received from Cu_A and $4H^+$ from the mitochondrial lumen (Capaldi, 1990; Babcock and Wikström, 1992).

Plastocyanin (PC) is a 10.5 kDa mobile Cu^{2+}-requiring protein involved in photosynthetic electron transport between PSII and PSI in photosynthetic organisms. PC is located on the luminal side of the thylakoid membrane and represents up to 50% of chloroplast copper (Moore *et al.*, 1988; Marschner, 1995). One Cu^{2+} per PCmolecule is coordinated by the sulphur atoms in one cysteine and one methionine residue, and two nitrogen atoms from two histidine residues in the His87 Cu^{2+} complex (Colman *et al.*, 1978; Moore *et al.*, 1988; Molina-Heredia *et al.*, 2001). The copper ion changes between the Cu^{2+} and Cu^+-state during electron transport. Cu^{2+} in the reaction centre of PC is reduced to Cu^+ upon

receiving one electron from the cytochrome *bf* electron transport complex, and Cu^{+} is oxidised back to Cu^{2+} upon delivering the electron to PSI in a cyclic reaction (Colman, 1978).

Superoxide dismutase (SOD) is the name given to a group of methallo-proteins, which specifically scavenge the toxic superoxide ion ($O_2^{\cdot-}$) and form part of the general cellular protection against reactive oxygen species, which in addition to $O_2^{\cdot-}$ include $HO_2^{\cdot}$ and H_2O_2 (Fridovich, 1989). Increased levels of cellular $O_2^{\cdot-}$ occur as a by-product of the high oxygen turnover in photosynthesis and respiration (Elstner, 1982), and during exposure to high UV-B irradiances and elevated concentrations of trace metals (Willekens *et al.*, 1994; Buckley, 1994; Luna *et al.*, 1994; Navari-Izzo *et al.*, 1998). High levels of $O_2^{\cdot-}$ are accompained at a cellular level by increased production of SOD (Willekens, 1994). SOD comprises MnSOD and FeSOD in prokaryotes and in the eukaryotic mitochondrial and peroxisomal matrix (Fridovich, 1989; Bueno *et al.*, 1995), and Cu-Zn-SOD, which is unrelated to the other species of SOD occuring primarily in the cytoplasm, chloroplasts, and peroxisomes of eukaryotic cells (Kröniger *et al.*, 1992; Bueno *et al.*, 1995; Herbik *et al.*, 1996; Richards *et al.*, 1998). A histidine side chain at the active site in Cu-Zn-SOD binds one zinc ion, and coordinates one copper ion, which cycles between the Cu^{2+} and Cu^{+} oxidative states during dismutation of two superoxide ions into hydrogen peroxide and molecular oxygen ($2O_2^{\cdot-} + 2H^{+} \rightarrow H_2O_2 + O_2$) in a two step reaction (Fridovich, 1989). One electron is transferred from $O_2^{\cdot-}$ to Cu^{2+} forming O_2 and Cu^{+}. A second $O_2^{\cdot-}$ acquires one electron from Cu^{+} and two protons from other parts of the reaction centre of Cu-Zn-SOD to produce H_2O_2 and Cu^{2+} upon completion of the cycle. Catalase, a heme protein, then catalyses conversion of hydrogen peroxide into water and molecular oxygen (Fridovich, 1989).

1.5. Cu^{2+} toxicity

1.5.1. Cellular copper transport

Although copper is an essential nutrient, the toxic effects of Cu^{2+} even at relatively low concentrations have resulted in a requirement for specialised cellular uptake and transport of copper in order to maintain $[Cu^{2+}]_{cyt}$ close to zero (Valentine and Gralla, 1997; Pufahl *et al.*, 1997; Rae *et al.*, 1999; Peña *et al.*, 2000). The Cu^{2+} uptake mechanism has been most frequently studied in *Saccharomyces cerevisiae* (bakers yeast) and it is recognised as a model for Cu^{2+} uptake in other eukaryotic organisms (Culotta *et al.*, 1997; Peña *et al.*, 2000). Cu^{2+} uptake is initiated by reduction of Cu^{2+} to Cu^{+} by several different plasma membrane reductases (Hassett and Kosman, 1995; Georgatsou *et al.*, 1997) followed by transport of Cu^{+} across the plasma membrane by the high affinity Cu^{+} transporters, Ctr1 and Ctr3 (Dancis *et al.*, 1994; Peña *et al.*, 2000). Subsequently Cu^{+} is transported by different specialised Cu^{+} receptor and transport proteins, copper chaperones, which bind 2-3 Cu^{2+} ions at their reaction centre with two sulphur ions each, and insert Cu^{2+} directly into target enzymes (Pufahl *et al.*, 1997; Valentine and Gralla, 1997; Rae *et al.*, 1999). Amongst the copper chaperones are Cox17, which transports Cu^{2+} to the mitochondria for incorporation into cytochrome oxidase (Glerum *et al.*, 1996; Beers *et al.*, 1999), and Lys7, which targets and incorporates Cu^{2+} directly into cytosolic Cu-Zn-SOD (Rae *et al.*, 1999). Only a few of the copper chaperones have so far been identified, with most of the work carried out on yeast and human proteins, and little is therefore known about the existence of these specialised Cu^{2+} transport proteins in other organisms (Valentine and Gralla, 1997). However, a protein, Ran1, has been identified in *Arabidopsis*, where it functions to deliver Cu^{2+} to ethylene receptor proteins (Hirayama *et al.*, 1999). Ran1 encoding DNA has a sequence homologous to those of yeast and human Cu^{2+} transporting ATP-ase DNA

(Hirayama *et al.*, 1999). Furthermore, the high degree of conservation between the yeast and human DNA for Cu^{2+} transport proteins (Pufahl *et al.*, 1997) suggests that the copper transport mechanism described here is a general feature of eukaryotic Cu^{2+} uptake and transport.

1.5.2. Copper surplus

During exposure to Cu^{2+} contamination $[Cu^{2+}]_{cyt}$ may rise beyond cellular control and the highly toxic properties of Cu^{2+} may have undesirable effects on the biochemistry of a cell (Valentine and Gralla, 1997; Rae *et al.*, 1999; Peña *et al.*, 2000). Reduced growth is frequently observed in plants and algae exposed to elevated copper concentrations (Sunda and Guillard, 1976; Hophin and Kain, 1978; Chung and Brinkhuis, 1986; Strömgren, 1980; De Vos *et al.*, 1992; Sunda and Huntsman, 1995; Andersson and Kautsky, 1996; Bidwell *et al.*, 1998; Bond *et al.*, 1999) and may be a consequence of the inhibitory effects on photosynthesis (MacDowall, 1949; Plöz, 1991; Jegerschöld, 1995). Other physiological effects which contribute to the overall condition of plants and algae exposed to toxic concentrations of Cu^{2+} include reduced chlorophyll *a* content, reduced cell division rate (Rijstenbil *et al.*, 1994; Ciscato *et al.*, 1997), interference with membrane permeability (Sunda and Huntsman, 1983), and formation of free radicals (Luna *et al.*, 1994; Navari-Izzo *et al.*, 1998).

1.5.3. Cu^{2+} interactions with sulphydryl groups

High reactivity between Cu^{2+} and sulphydryl (SH) (Al-Farawati and van den Berg, 1999) may result in cytosolic Cu^{2+} reacting directly with enzymes and other proteins. This has been illustrated by the interactions between Cu^{2+} and glutathione (Stauber and Florance, 1986; Rijstenbil *et al.*, 1994). Glutathione, γ-Glu-Cys-Gly (GSH), is an antioxidant in eukaryotic cells, where it exists at mM concentrations. The –SH group of cysteine cycles

between the reduced and the oxidised form. Oxidation of the –SH groups of two GHS molecules result in their cross-linking by a disulphur bridge to form the oxidised form of glutathione (GSSG). Due to the interactions of the –SH group with Cu^{2+} and other metals, GSH serves as a major cytosolic ligand in cellular metal homeostasis, and elevated $[Cu^{2+}]_{cyt}$ can potentially deplete the cellular pool of GSH (Stauber and Florance, 1986; Rijstenbil *et al.,* 1994). Treating the diatom *Nizschia closterum* with 2.7 μM copper for 24h resulted in a reduction in cellular GSH pool from 3.68 nmol per 10^6 cells to 1.68 nmol per 10^6 cells (Stauber and Florance, 1986). Similar results have been presented by Rijstenbil and co-workers (1994), who showed that the cellular GSH pool of 0.9 μmol g^{-1} DW was oxidised completely in the diatom *Ditylum brightwellii* as the cellular total copper concentration increased to 15 nM. The reduction in the cellular pool of GSH in response to increasing $[Cu^{2+}]_{cyt}$, may be the result of the following interaction between Cu^{2+} and GSH:

$$4\,GSH + 2Cu^{2+} \rightarrow 2CuSG + GSSG + 4H^{+}$$

(Stauber and Florance, 1986; Rijstenbil *et al.,* 1994). Oxidation of enzymatic –SH groups by Cu^{2+} and formation of disulphide bridges and CuS complexes, may lead to cross-linking of different protein segments and conformational changes with consequent blockage of reaction centres and deactivation of enzymes. Inactivation of electron transport through photosystem II (PSII) (Yruela *et al.,* 1993; Scröder *et al.,* 1994; Jegerschöld *et al.,* 1995) and reduction in ion channel and ATP-ase activity (Viarengo *et al.,* 1996; Klusener *et al.,* 1997; Demidchik, 2001) are examples of the damaging effects of Cu^{2+} on proteins and enzyme activity.

1.5.4. Cu^{2+}-induced production of reactive oxygen species

Reactive oxygen species (ROS) occur as natural cellular metabolites but are potentially harmful to a cell as they cause lipid peroxidation and membrane damage. The superoxide

radical ($O_2^{\cdot-}$) is formed spontaneously due to the high oxygen turnover in respiratory and photosynthetic processes (Elstner, 1982) and scavenging of $O_2^{\cdot-}$ by superoxide dismutase (SOD) results in H_2O_2 production (Fridovich, 1989). Several experiments have shown that Cu^{2+} has the potential to elevate concentrations of ROS (Sandmann and Böger, 1980; Luna *et al.*, 1994; Yruela *et al.*, 1996; Navari-Izzo *et al.*, 1998; Teisseire and Guy, 2000). Treating wheat seedlings and oat leaves with 10-50 μM copper resulted in an 100-300% increase in stroma and thylakoid SOD activity, indicating Cu^{2+}-induced $O_2^{\cdot-}$ production (Luna *et al.*, 1994; Navari-Izzo *et al.*, 1998). $O_2^{\cdot-}$ accumulation during copper exposure may result from inhibition of photosynthetic electron transport chains (Sandmann and Böger, 1980; Jegerschöld *et al.*, 1995; Yrela *et al.*, 1996). In contrast to the results of Yrela and co-workers (1996), Navari-Izzo and colleagues (1998) found no effect of Cu^{2+} on electron transport, although Cu^{2+} clearly induced $O_2^{\cdot-}$ production, and the exact mechanism of Cu^{2+}-induced $O_2^{\cdot-}$ production is therefore unclear. Similarly, exposure of duckweed and oat leaves to 5-50 μM Cu^{2+} resulted in an increase in catalase and peroxidase activity of up to 240% (Navari-Izzo *et al.*, 1998; Teisseire and Guy, 2000). Catalase and peroxidase are both H_2O_2 scavengers (Fridovich, 1989; Yamasaki *et al.*, 1997) and their increased activity may be the result of Cu^{2+}-induced H_2O_2 production. Different species appear to react differently with respect to H_2O_2 in response to Cu^{2+}. In contrast to other researchers (Navari-Izzo *et al.*, 1998; Teisseire and Guy, 2000) Luna and co-workers (1994) found that Cu^{2+} exposure resulted in a slight decrease in peroxidase activity. Hence there was either no induction of H_2O_2 production in oat leaves during Cu^{2+} exposure, production or Cu^{2+} caused inhibition of peroxidase activity.

The evidence presented above suggests that Cu^{2+} has the potential to increase the cellular levels of $O_2^{\cdot-}$ and H_2O_2 (Luna *et al.*, 1994; Navari-Izzo *et al.*, 1998; Teisseire and Guy, 2000), which are substrates for the production of the more reactive oxidant, hydroxide

radical ($HO^{\cdot}$) (Elstner, 1982). Interactions between $O_2^{\cdot-}$ and H_2O_2 generate $HO^{\cdot}$ in the Haber-Weiss reaction ($O_2^{\cdot-} + H_2O_2 \rightarrow HO^{\cdot} + O_2 + HO^-$), which requires UV radiation or a catalyst such as iron and is unlikely to occur spontaneously in biological systems (Elstner, 1982). By using chloroplasts with a high rate of $O_2^{\cdot-}$ production, Sandmann and Böger (1980) showed that Cu^{2+} had the potential to act as a catalyst for the Haber-Weiss reaction during reduction of Cu^{2+} to Cu^+ especially in the presence of SOD (*i.e.* H_2O_2 production). Similarly Yruela and co-workers (1996) concluded that $O_2^{\cdot-}$ formed during Cu^{2+} exposure was converted to $HO^{\cdot}$ via a Cu^{2+}-catalysed Haber-Weiss reaction.

1.6. *Fucus serratus*

Algae comprise a group of organisms which are defined by having chlorophyll *a* as their primary photosynthetic pigment and by a zygote which never develops into a multicellular embryo while still inside the female reproductive tissue (Kristiansen *et al.*, 1981). The current classification presents six divisions of algae, the largest being the Chromophycota, which in turn contains nine classes including the Phaeophyceae, or brown algae (South and Wittick, 1988). The Phaeophyceae comprises about 1500 species, of which the vast majority are marine. One of the seven orders is the Fucales, which bears four families, the Cystoseiraceae, Sargassaceae, Himanthaliaceae and Fucaceae. Fucaceae include the three genera, *Pelvetia*, *Ascophyllum* and *Fucus*.

Fucus serratus, or serrated wrack, is indigenous to the temperate waters of the North Atlantic, where it dominates the lower intertidal zone of rocky shores. It thrives in both wave-exposed locations and in sheltered fjords and estuaries (Figure 1.07). The thallus is robust and can grow to about one metre in length. The branched, band-like fronds are

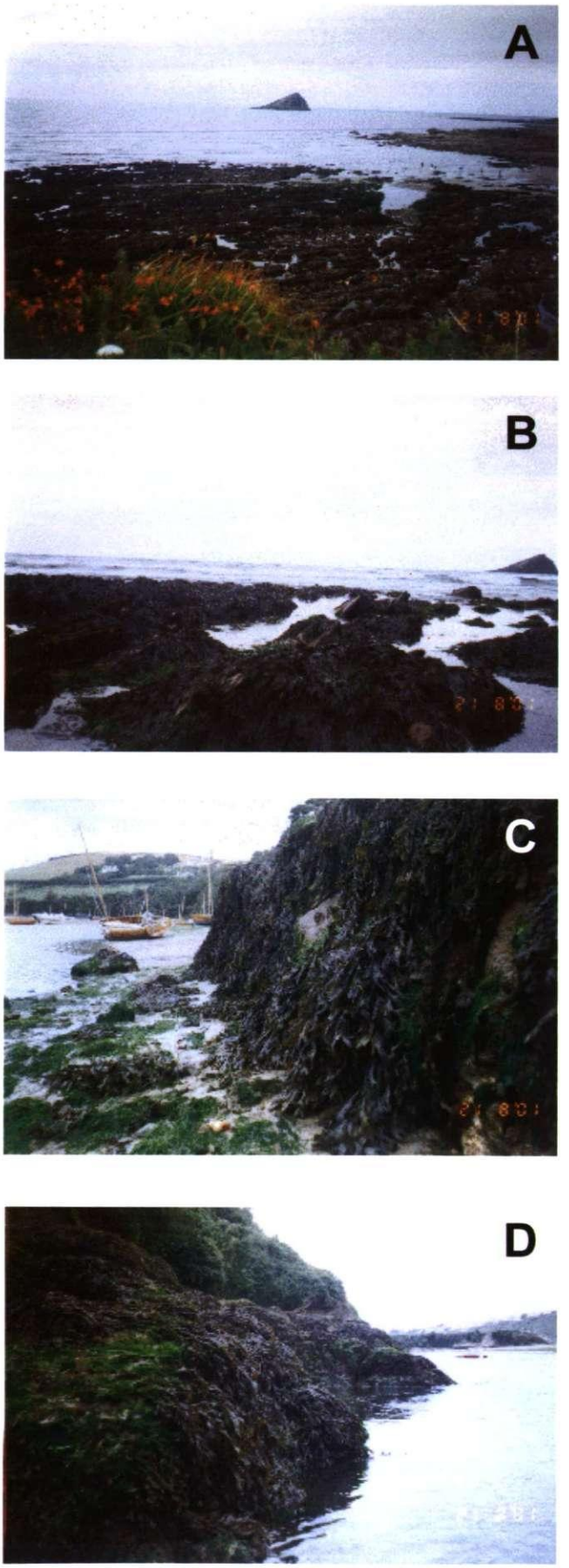

Figure1.07. *Fucus serratus* in a wave exposed location, Wembury Beach (**A, B**), and a sheltered location, Avon Estuary (**C, D**)

approximately 2 cm in width and possess an elevated midrib. The serrated edges of the fronds have given the species its name. The thallus is a parenchymatic structure growing from an apical cell which stimulates division of the surrounding cells. Occasional division of the apical cell results in dichotamous branching of the thallus (Kristiansen *et al.,* 1981).

Fucus serratus is reproductively active all year round although it is most active during the colder months (personal observation). It is dioecious and practices external oogamous fertilisation (Kristiansen *et al.,* 1981; South and Wittick, 1988). Thalli are always diploid, with the gametes being the haploid phase in the life cycle (Kristiansen *et al.,* 1981). Reproductive structures, called conceptacles, are located under the epidermis of the apical parts of the fronds, the receptacles, where they appear as small nodules. Conceptacles are approximately 0.5 cm in diameter and ripe gametes are secreted to the outside *via* the ostiore or pore (Levring, 1952; Müller and Gassmann, 1985). Mature algae can be sexed by the colour of the conseptacles as those of male gametes are bright orange, whereas female conceptacles are green. During spermatogenesis the antheridial mother cell produces 64 haploid spermatozoids of about 5 μm length through a succession of one meiotic and four mitotic divisions of the nucleus and subsequent cell division (Berkaloff and Rousseau, 1979). Each spermatozoid has one chloroplast (the eye spot), which is bright orange due to the accumulation of carotenoids within it (Callow *et al.,* 1985), and carries two flagella of unequal length (Levring, 1952). The anterior flagellum is much shorter than the posterior flagellum and carries membranous extensions believed to play a part in egg recognition (Jones *et al.,* 1988), whereas the posterior flagellum is used for propulsion (Levring, 1947). Oogenesis yields eight haploid eggs per oogonium through one meiotic and one mitotic division of the mother cell followed by cell division. Eggs are 60-80 μm in diameter. They are radially symmetrical and consequently possess no polar axis (Jaffe, 1958). The nucleus is located centrally in the egg and the organelles are evenly

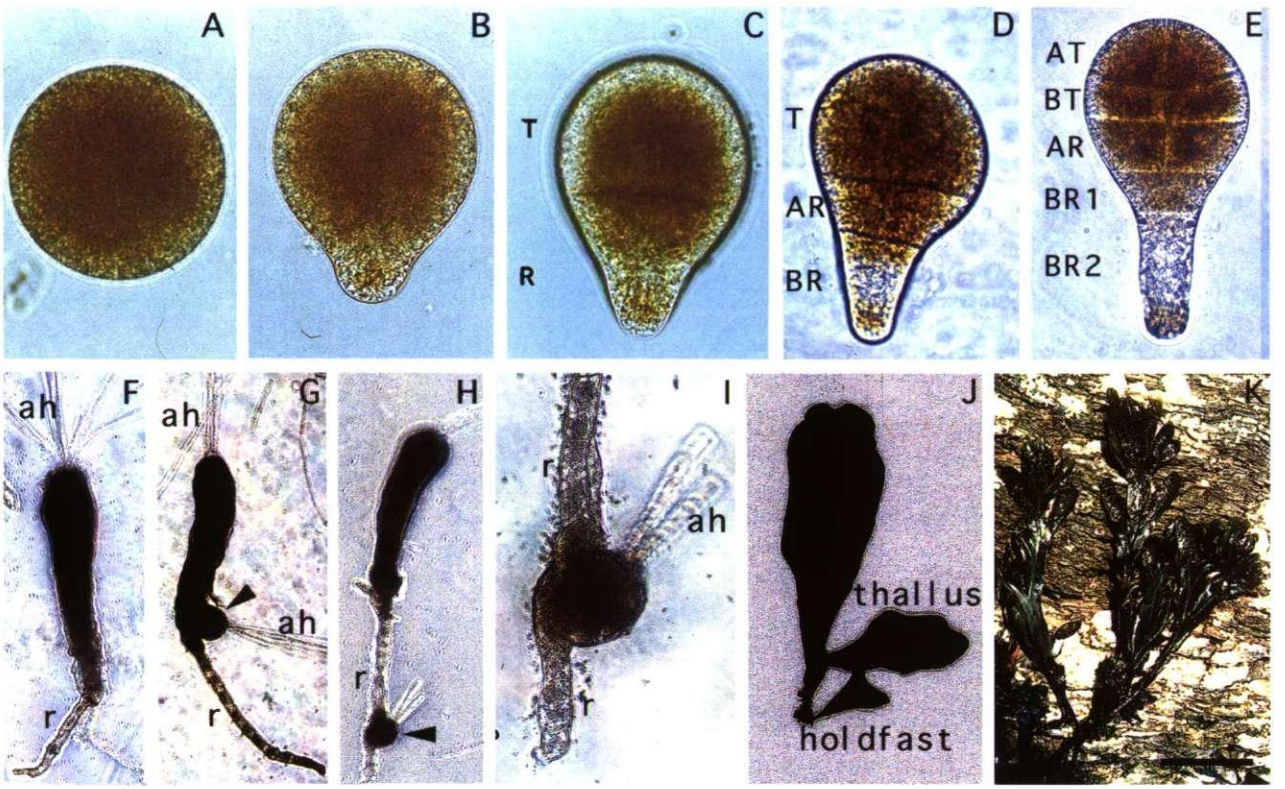

Figure 1.08. Embryo development in *Fucus serratus*. Fertilised egg (**A**), polarised egg 12 h after fertilisation (AF) (**B**), 20h AF, shoving the first cell division into thallus (T) and rhizoid cells (R) (**C**), 24h AF, the rhizoid cell into the apical rhizoid (AR) and basal rhizoid (BR) cells (**D**), 48h AF the thallus cell divides into apical (AT) and basal (BT) cells, whereas transverse division of the basal rhizoid cell yields the two basal rhizoid cells (BR1 and BR2) (**E**), apical hairs (ah) and a rhizoid (r) becomes apparent as cell division continues, and the embryo develops the thallus and stipe holdfast of the adult algae (**F-K**). Reproduced with permission from Bouget and co-workers (1998).

distributed. Fucoid eggs have no cell wall and are bound only by a plasma membrane (Levering, 1952).

Gametes are released directly into the sea, where fertilisation takes place. Fertilisation success declines as water velocity increases, due to quick dilution of gametes (Levitan *et al.*, 1992; Lasker *et al.*, 1996) and can be less than 1% (Denny and Shibata, 1989). *Fucus* usually restricts gamete release to periods of water motion below 0.2 ms^{-1}, under which condition the fertilisation success can be as high as 95% (Pearson and Brawley, 1996; Serrão *et al.*, 1996). Isolation of *Fucus* from the sea during low tide creates conditions of stagnant water depleted of dissolved inorganic carbon, which is favourable for fertilisation (Serrão *et al.*, 1996; Pearson and Brawley, 1996; Pearson *et al.*, 1995; 1998). Reproduction usually occurs in highly synchronised cycles and mass release of gametes is controlled by environmental factors and lunar rhythms which ensure that gamete release coincides with the spring tide (Brawley and Johnson, 1992). Immediately after fertilisation, eggs settle on the substratum and secrete a cell wall, which initiates attachment of the zygote (Quatrano and Stevens, 1976; Hable and Kropf, 1998). Germination of a rhizoid occurs a few hours after fertilisation (Hurd, 1920; Jaffe, 1958; Robinson, 1996) and is subsequently followed by the first cell division. This asymmetric cell division results in an elongate rhizoid cell, which forms the holdfast of the developing alga, and a rounded thallus cell which develops into the fronds and stipe of the adult alga (Figure 1.08).

1.7. Objectives of study

Although *Fucus serratus* forms vigorous populations in copper polluted locations such as Restronguet Creek, little is known about the effects of copper on the physiology and

reproduction of algae and the mechanism of adaptation of tolerant strains. This work sets out to investigate the effects of copper on the physiology and early development of *F. serratus* and to establish inter-population differences by including algae from Restronguet Creek, Avon Estuary and Wembury Beach in the experiments.

Chapter 2 of this thesis addresses the effects of copper on the physiology of adult *F. serratus*. The work aims to identify effects of copper on the metabolism of three different populations of *F. serratus*, their mechanism of handling the toxin, and to establish whether the physiological responses of the algae to copper are related to the copper status in the habitat from which they were acquired.

Chapter 3 addresses effects of copper on the early development of the *F. serratus* zygote. The work is focused on identifying developmental phases which are affected by copper, assessing effects of copper on the growth of germlings, and pinning down the underlying physiological processes.

The context of the results is discussed in the concluding chapter.

CHAPTER 2

Physiological Responses of *Fucus serratus* to Cu^{2+} Exposure

2.1. Introduction

The highly reactive properties of Cu^{2+} make it an essential nutrient. Cu^{2+} acts as a co-factor in enzymes, which are involved in the major physiological processes respiration and photosynthesis as well as dismutation of antioxidants (Babock and Wikström, 1992; Richards *et al.*, 1998; Molina-Heredia *et al.*, 2001). However, the high reactivity of Cu^{2+} may be toxic at elevated cytosolic concentrations. Cu^{2+} has a high affinity for sulfhydryl groups (Stauber and Florance, 1986) and may cause cross-linking of protein segments, which in turn could result in conformational changes and deactivation of enzymes (Demidchik *et al.*, 1997). When in excess, Cu^{2+} may also catalyse the production of reactive oxygen species, which has the ability to cause lipid peroxidation and consequently membrane damage (Murphy *et al.*, 1999). Therefore, Cu^{2+} at elevated concentrations has the ability to interfere with different metabolic processes and affect the overall condition of an organism.

2.1.1. Effects of Cu^{2+} on algal growth

Reduced growth rate is probably the most obvious response of algae to Cu^{2+} exposure and is manifested as a reduced cell division rate in phytoplankton (Brand *et al.*, 1986; Sunda and Huntsman, 1995) and reduced biomass gain of individual macroalgae (Stömgren, 1980; Bryan and Gibbs, 1983; Newman, 1998). Phytoplankton are generally very sensitive to Cu^{2+}, resulting in reduced cell division rates at pM concentrations (Brand *et al.*, 1986; Sunda and Huntsman, 1995). The cyanobacterium *Synechococcus* sp. is more sensitive to Cu^{2+} than any other known phytoplankton and $[Cu^{2+}]_{ext}$ above 10 pM resulted in cessation of cell division and cell death at exposure to 100 pM $[Cu^{2+}]_{ext}$ (Brand *et al.*, 1986). In

comparison, cell division rates in diatoms and coccolithophores, which are more Cu^{2+} tolerant than *Synechococcus* were reduced at $[Cu^{2+}]_{ext}$ above 0.1-1 nM (Brand *et al.*, 1986; Stauber and Florence, 1987; Sunda and Huntsman, 1995).

Marine macroalgae, including *Fucus* sp. appear to be more resistant to Cu^{2+} than phytoplankton and generally tolerate nM concentrations. In a comparative growth experiment, based on increases in length, Strömgren (1980) showed that the relative growth rates (RGR) of *Fucus serratus* and *Fucus vesiculosus* were unaffected after 10 days of exposure to 0.2 μM total copper whereas, at the same concentration, RGR of *Fucus spiralis* was reduced by 15% compared with controls. As the concentration of total copper was increased to 0.4 μM the RGR of *F. serratus* was reduced by 20% after 10 days of incubation, whereas the RGR of *F. vesiculosus* was unaffected until the total copper concentration reached 0.8 μM, which resulted in a 30% reduction in RGR (Strömgren, 1980). Similar results were presented by Bryan and Gibbs (1983), who found that the RGR of *F. vesiculosus* was reduced by 20% after 13 days of exposure to 0.8 μM total copper. Exposure to 2-5 μM total copper resulted in weight loss in the different species of *Fucus* studied, which was reflected by a negative RGR (Strömgren, 1980; Bryan and Gibbs, 1983). The effect of copper on growth of germinated *Fucus* embryos may be similar to that on the adult algae. Rhizoid germination of *F. vesiculosus* embryos was unaffected by total copper up to 0.6 μM when added just prior to germination (Andersson and Kautsky, 1996) and rhizoid elongation of germinated *F. spiralis* embryos was unaffected by total copper concentrations up to 0.2 μM (Bond *et al.*,; Gledhill *et al.*, 1999). These results are comparable to the tolerance limit for adult *Fucus* (Strömgren, 1980). The response to copper exposure of other species appears similar to that of fucoids. Exposure to 0.8 μM total copper for 8 days resulted in a 25% reduction in RGR in both the filamentous

cyanobacteria *Lyngbya nigra* (Gupta and Arora, 1978) and the red alga *Gracilariopsis longissima* (Newman, 1998).

2.1.2. Effects of Cu^{2+} on algal respiration

Information on the effects of Cu^{2+} on respiration in algae is both conflicting and very limited (Hopkin and Kain, 1978; Gupta and Arora, 1978; Newman, 1998). Concentrations of 0.8 to 20 μM total copper resulted in an increase in the respiration rate of *L. nigra* within a few days of exposure (Gupta and Arora, 1978). 8 μM total copper had a greater effect on respiration than higher and lower concentrations causing a 100% increase compared to controls after 4 days of exposure, which subsequently decreased to the respiration rate of controls after 8 days (Gupta and Arora, 1978). Other workers failed to demonstrate any effect of Cu^{2+} on respiration at concentrations within an environmentally relevant range (Hopkin and Kain, 1978; Newman, 1998). Exposure to 1.5 μM total copper for 8 days had no effect on oxygen consumption in *G. longissima* (Newman, 1998) and respiration of *Laminaria hyperborea* was unaffected by up to 160 μM total copper, but decreased rapidly at higher concentrations (Hopkin and Kain, 1978). However, respiration in *G. longissima* was only measured after 8 days of exposure to Cu^{2+} (Newman, 1998) and, considering that the work on *L. nigra* showed an increase in respiration of up to 100% followed by decrease to the level of controls within 8 days of exposure to Cu^{2+} (Gupta and Arora, 1978), it is possible that there was an effect of Cu^{2+} on *G. longissima*, which was not detected in the experiment by Newman (1998). Hence, the work on the effects of Cu^{2+} on respiration in algae is far from conclusive. On the basis on the available information it seems unlikely that Cu^{2+} decreases respiration within ecologically relevant concentrations, but whether Cu^{2+} has the ability to increase the respiratory rate of algae is unclear.

2.1.3. Effects of Cu^{2+} on photosynthesis

Cu^{2+} is widely recognised as a potent inhibitor of photosynthesis in plants and algae (MacDowall, 1949; Sandmann and Böger, 1980; Plötz, 1991; Yruela *et al.*, 1991, 1993; Schröder *et al.*, 1994; Jegerschöld *et al.*, 1995: Küpper *et al.*, 1996). Early work presented by MacDowall (1949) showed that treating isolated Swiss chard chloroplasts with 10 μM $CuSO_4$ resulted in a 50% decrease in the photolysis of H_2O in the Hill reaction: $2H_2O \rightarrow 4H^+ + O_2 + 4e^-$. Similarly, treating fronds of *F. vesiculosus* with 40 μM $CuSO_4$ at 18‰ salinity resulted in a 46% decrease in oxygen evolution within 20 minutes of exposure (Plötz, 1991).

2.1.3.1. Targets for Cu^{2+} in photosynthesis

Due to the highly reactive properties of Cu^{2+} there are several possible targets for Cu^{2+} in photosynthesis. An increase in the cellular total copper content to 15 nM in *D. brightwellii* resulted in a 33% decrease in both photosynthetic oxygen evolution and chlorophyll *a* content (Rijstenbil *et al.*, 1994). The high degree of oxidative damage in Cu^{2+}-treated *D. brightwellii* suggests that reduced photosynthesis may be the result of chlorophyll *a* damage caused by oxidative stress (Rijstenbil *et al.*, 1994). An additional damaging effect of Cu^{2+} on chlorophyll may be the ability of Cu^{2+} to substitute for the magnesium ion, which is bound in the centre of the chlorophyll molecule (Küpper *et al.*, 1996). Treating different species of macrophytes with concentrations of total copper ranging from 0.5 to 20 μM resulted in a cellular Cu-Chl content varying from 8 to 14% of the total chlorophyll content and it has been suggested that magnesium substitution may contribute to Cu^{2+}-induced photoinhibition (Küpper *et al.*, 1996). However, other workers offer an alternative

explanation of the inhibitory effects of Cu^{2+} on photosynthesis (Yruela *et al.*, 1991, 1993; Schröder *et al.*, 1994; Jegerschöld *et al.*, 1995).

Although Cu^{2+} is an essential co-factor in the photosynthetic electron carrier, plastocyanin, (Molina-Heredia *et al.*, 2000) inhibition of electron transport in photosystem II (PSII) is widely recognised as the major cause of Cu^{2+} toxicity in photosynthesis. Two major targets for Cu^{2+} in electron transport in PSII have been identified (Figure 2.01). Cu^{2+} may target electron transport in PSII by inhibiting electron transfer from the amino acid tyrosine to the primary electron acceptor, the reaction centre chlorophyll, P680 (Schröder *et al.*, 1994; Jegerschöld *et al.*, 1995) or it may inhibit electron transfer from P680 to the electron carrier plastoquinone A (Q_A) (Yruela *et al.*, 1991, 1993; Jegerschöld *et al.*, 1995). Concentrations of $CuSO_4$ up to 100 μM have been shown to inhibit the oxidation of tyrosine and in this way inhibit electron transport to P680 in intact PSII membranes and isolated PSII fragments of spinach (Schröder *et al.*, 1994; Jegerschöld *et al.*, 1995). Exposure of PSII to Cu^{2+} resulted in absorbance changes in P680, which were not observed in P680 and Q_A in the presence of an artificial electron donor. It was thus concluded that Cu^{2+} inhibition occurred on the donor side of PSII (Schröder *et al.*, 1994). However, Jegerschöld and co-workers (1995) showed that Cu^{2+} resulted in the absence of resonance signals, which can normally be recorded, from both tyrosine and Q_A when these molecules are changing between different molecular structures. This result indicated that Cu^{2+} targeted both tyrosine on the donor side and Q_A on the acceptor side of P680. Inhibition of electron transport through P680 resulted in radical formation, which may have been responsible for the observed degradation of PSII subunits (Jegerschöld *et al.*, 1995). Exposing sugar beet PSII membranes to 80 μM $CuCl_2$ strongly inhibited oxygen evolution (Yruela *et al.*, 1991). By using artificial substitutes for Q_A as electron acceptors for P680 and by measuring resonance signals and absorbance changes, it was indicated that the

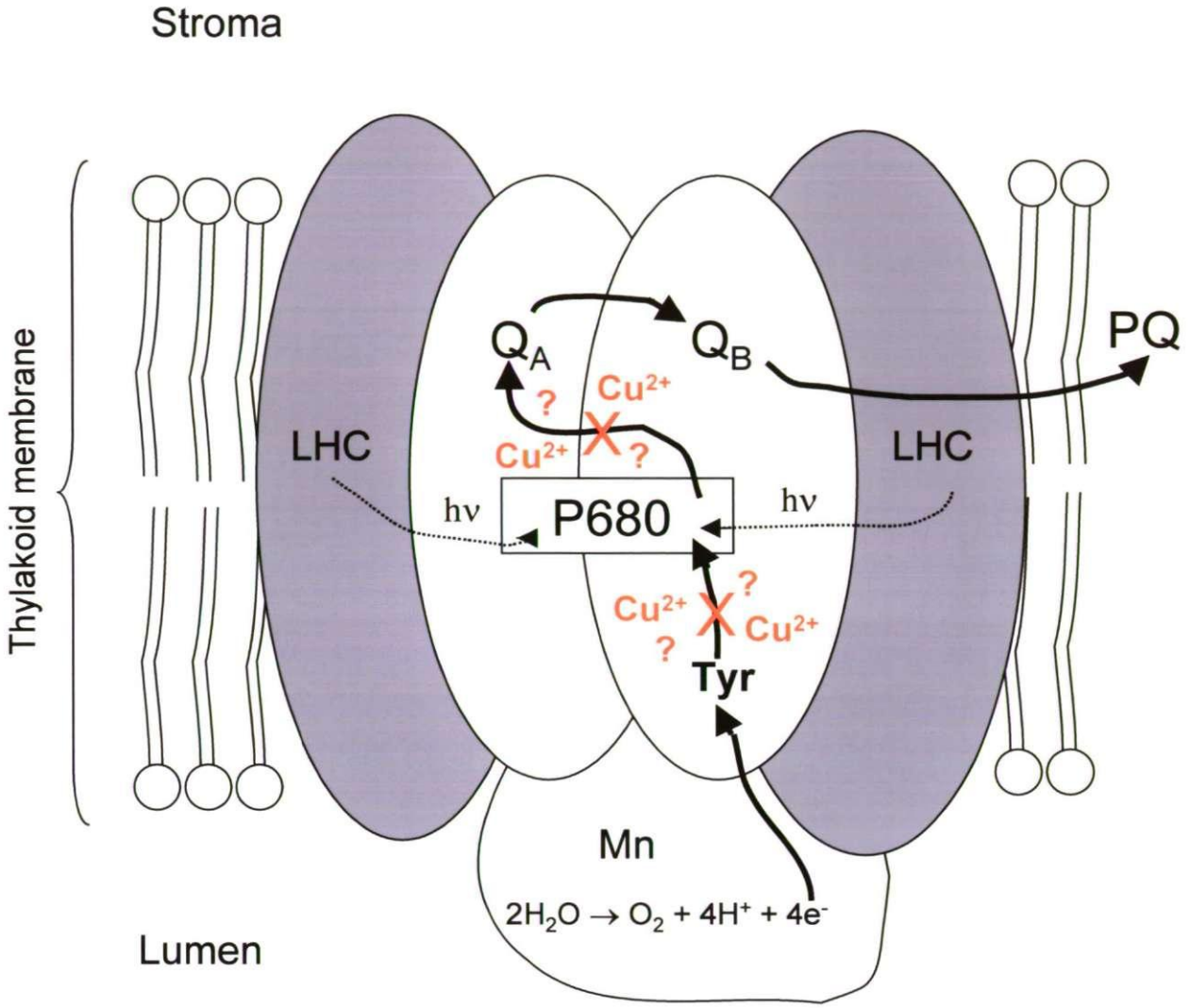

Figure 2.01. Two possible targets for Cu^{2+} in inhibition of electron transport through photosystem II. LHC: light harvesting complex, hν: light energy, Mn: manganese cluster at the site of H_2O reduction, Tyr: tyrosine, P680: chlorophyll reaction centre, Q_A: plastoquinone A, Q_B: plastoquinone B, PQ: mobile plastoquinone, which mediates electron transport to photosystem I. Cu^{2+} may either inhibit electron transport from tyrosine to the reaction centre or from the reaction centre to Q_A. Solid arrows show the electron path.

reduction in oxygen evolution by Cu^{2+} was caused by inhibition of electron transport through Q_A (Yruela *et al.*, 1991, 1993). The work discussed above suggests that Cu^{2+} has the potential to inhibit electron transport through PSII at more than one possible target site (Yruela *et al.*, 1991, 1993; Schröder *et al.*, 1994; Jegerschöld *et al.*, 1995).

2.1.3.2. Chlorophyll fluorescence

Effects of Cu^{2+} on the performance of the photosynthetic apparatus can be monitored by non-invasive measurements of chlorophyll fluorescence (Ouzounidou *et al.*, 1997; Ciscato *et al.*, 1997). Not all light energy harvested by chlorophyll is used to drive photosynthesis and the excess energy is either dissipated as heat or re-emitted as chlorophyll fluorescence at ~685 nm, accounting for 1-2% of the total absorbed light (Krause and Weis, 1991; White and Critchley, 1999; Maxwell and Johnson, 2000). The interrelationship between the three different fates of harvested light energy provides information about the efficiency with which photosynthesis is performed. During photosynthetic electron transport through PSII and acceptance by Q_A of one electron, the PSII reaction centre is 'closed' until the electron is passed on from Q_A to plastoquinone B (Q_B). As the proportion of closed reaction centres increases relative to the total number of reaction centres, the efficiency of light conversion into photosynthesis decreases, resulting in an increase in chlorophyll fluorescence. Upon transfer of PSII from dark to light a disproportionate number of reaction centres become closed, resulting in increased chlorophyll fluorescence. After a few seconds, PSII begins to adapt to the light and the chlorophyll fluorescence decreases over several minutes to a steady state level in a process termed 'chlorophyll quenching'. During this light adaptation, photosynthetic enzymes are gradually activated and the rate of electron transport away from PSII is increased in 'photochemical quenching' (*qp*) and an increasing number of reaction centres become open. Simultaneously, conversion of excess

energy into heat becomes more efficient, which results in 'non-photochemical quenching' (NPQ).

Information about non-photochemical quenching, photosynthetic efficiency and other related parameters can be acquired by exploiting the interrelationship between the different fate of harvested light in a series of fluorescence measurements, as illustrated in the typical fluorescence trace shown in Figure 2.02. The light source used to measure fluorescence is a modulating beam (MB) and, as the detector only measures wavelengths emitted by chlorophyll fluorescence, it allows for measurements in the presence of photosynthetically active radiation (PAR). Upon switching on MB, the minimal fluorescence in the absence of PAR, F_o, is measured. Subsequent application of a saturating light pulse (SP) of ms duration closes all PSII reaction centres transiently without increasing NPQ and allows measurement of the maximum fluorescence in the dark adapted state (F_m) in the absence of *qp*. Application of PAR, provided by an actinic light source (AL), allows for measurement of maximum fluorescence in the light (F'_m), by application of a saturating ms light flash (SP), once steady-state photosynthesis is reached. Minimum fluorescence during steady-state photosynthesis is termed F_t. Upon switching off AL, the fluorescence level decreases immediately to the minimum fluorescence level in the light, F'_o.

Calculation of the proportion of light absorbed by PSII, the quantum yield during steady state photosynthesis (Φ_{PSII}) is based on the difference between F'_m and F_t: $\Phi_{PSII} = (F'_m - F_t)/ F'_m$ (Genty *et al.*, 1989). The maximum quantum yield of PSII, the quantum yield of the dark adapted state, is expressed by: $F_v/F_m = (F_m - F_o)/F_m$ (Genty *et al.*, 1989). Photochemical quenching can be calculated as: $qp = (F'_m - F_t)/(F'_m - F'_o)$ or alternatively as: $\Phi_{PSII}/(F_v/F_m)$ (Maxwell and Johnson, 2000). Whereas Φ_{PSII} expresses the efficiency of energy conversion at a given light intensity, *qp* gives an indication of the proportion of

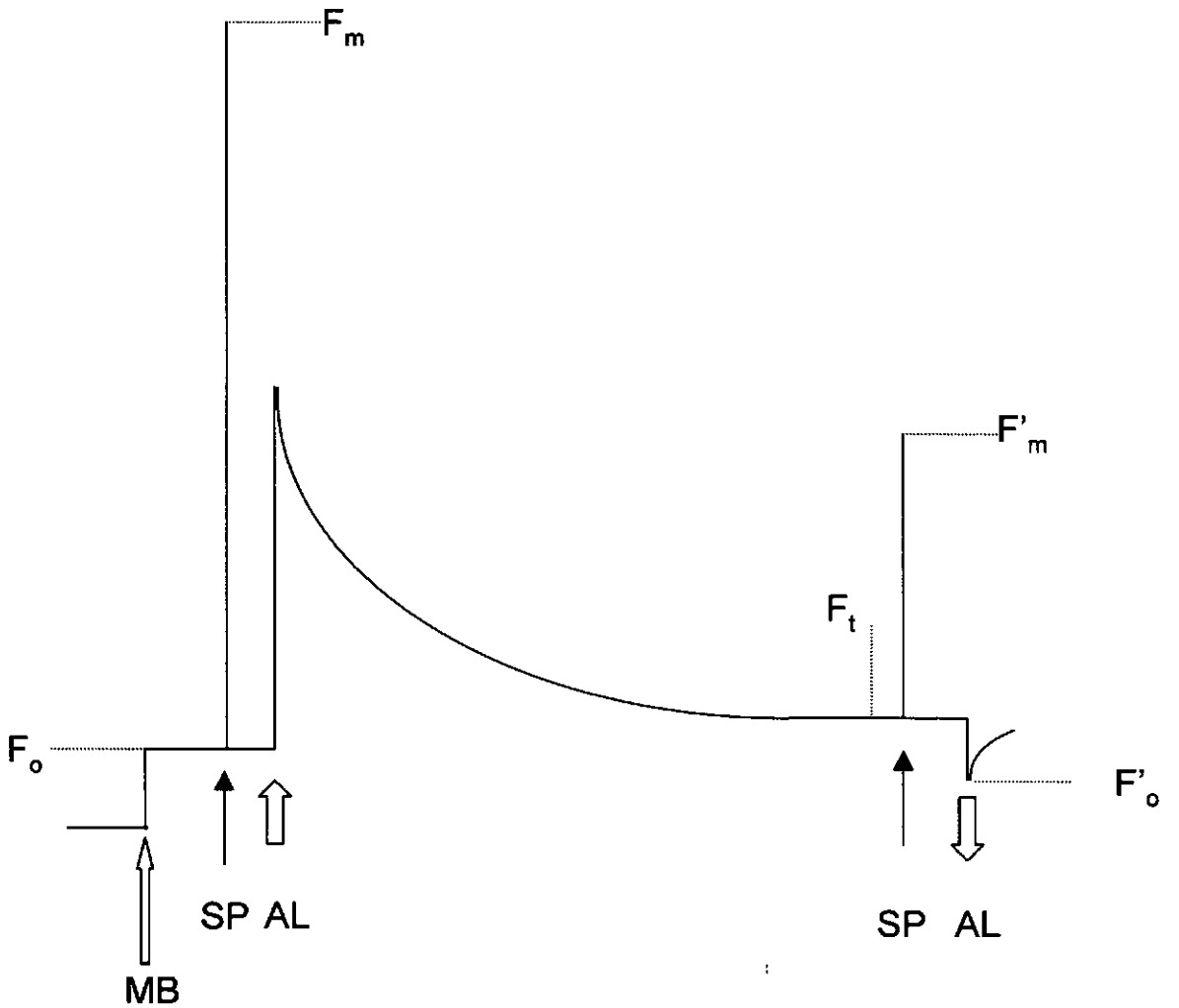

Figure 2.02. Sequence of a typical fluorescence trace. A measuring light is switched on (↑MB) and the zero fluorescence level is measured (F_o). Application of a saturating light flash (↑SP) allows measurement of the maximum fluorescence level F_m. A light to drive photosynthesis (↑AL) is then applied . After a period of time, another saturating light flash (↑SP) allows the maximum fluorescence in the light, F'_m, to be measured. The level of fluorescence immediately before the saturating flash is termed F_t. Turning off the actinic light (AL↓) allows measurement of zero fluorescence in the light, F'_o. Reproduced after Maxwell and Johnson (2000).

PSII reaction centres that are open, and F_v/F_m provides information about the general condition of PSII. F_v/F_m is generally expected to be around 0.83 and lower values are an indication that PSII is being exposed to stress, such as photoinhibition (Maxwell and Johnson, 2000). Non-photochemical quenching can be calculated as: $NPQ = (F_m - F'_m)/F'_m$ (Maxwell and Johnson, 2000).

2.1.3.3. Non photochemical quenching (NPQ)

Both reversible non-photochemical quenching (q_E) and irreversible non-photochemical quenching (q_I) may contribute to NPQ. q_E, however, is usually considered more important than q_I (Maxwell and Johnson, 2000). q_E is initiated by acidification on the luminar side of the thylakoid membrane during high rates of photosynthetic H^+ transport and large ΔpH across the thylakoid membrane which may occur at photosynthetically saturating irradiances (Horton *et al.*, 1996; Ruban and Horton, 1999). Very low lumen pH results in activation of de-epoxidase and de-epoxidation of the carotenoids violaxanthin to zeaxanthin in the xanthophyll cycle which coincide with thermal dissipation of excess light energy, *i.e.* q_E, in several species of flowering plants (Ruban *et al.*, 1993; Niyogi *et al.*, 1998; Demmig-Adams, 1998; Harker *et al.*, 1999; Ruban and Horton, 1999; Li *et al.*, 2000; Ort, 2001). Epoxidation of zeaxanthin restores the violaxanthin pool and completes the xanthophyll cycle upon relaxation of q_E. Xanthophyll is one of a group of carotenoids in the light-harvesting complex of plants and algae (Falkowski and Raven, 1997) which are bound to membrane spanning antenna proteins (Horton *et al.*, 1996; Li *et al.*, 2000).

Conformational changes of xanthophyll binding proteins may also be a requirement for q_E (Li *et al.*, 2000). Accumulation of zeaxanthin during q_E coincides with increased absorbance of thylakoid membranes at 505 nm and absorbance changes at 535 nm in *Arabidopsis* and the bromeliad *Gusmania monostachia* (Ruban *et al.*, 1993; Li *et al.*,

2000). Li and co-workers (2000) showed that *Arabidopsis* mutants, which lack the antenna protein PsbS were unable to perform the absorbance changes at 535 nm as well as q_E. This finding suggests that the absorbance changes observed for thylakoid membranes at 535 nm were caused by conformational changes of the antenna protein PsbS, and that these conformational changes are a requirement for q_E in addition to low lumen pH and de-epoxidation of violaxanthin to zeaxanthin (Li *et al.*, 2000).

The level of q_E and de-epoxidation of violaxantin in a plant or algae may reflect adaptation to specific environmental conditions (Demmig-Adams, 1998; Harker *et al.*, 1999). Demmig-Adams (1998) showed that sun adapted leaves of different plants generally contained higher levels of xanthophyll and had higher level of q_E than shade adapted leaves of the same species. Similarly, violaxanthin is a general constituent of brown algae carotenoid (Vershinin and Kamnev, 1996) and xanthophyll cycling may govern non-photochemical quenching in some algae (Urmacher *et al.*, 1995; Harker *et al.*, 1999; Coelho *et al.*, 2001). Harker and co-workers (1999) showed that NPQ of both *Pelvetia canaliculata* and *Laminaria saccharina* was highly correlated with de-epoxidation of violaxanthin to zeaxanthin in both desiccated d and hydrated states of the fronds. However, both the xanthophyll pool and NPQ of *Pelvetia* was 2-fold higher than that of *Laminaria*, and may reflect different adaptation to high irradiances and desiccation in these species (Harker *et al.*, 1999).

2.1.3.4. Chlorophyll fluorescence during Cu^{2+} exposure

Chlorophyll fluorescence measurement is a useful tool for monitoring the performance of PSII during Cu^{2+} exposure (Ouzounidou *et al.*, 1997; Ciscato *et al.*, 1997). Φ_{PSII} measured at 350 μmol m^{-2} s^{-2} PAR on maize seedlings grown for 15 days in water culture containing 80 μM $CuSO_4$ was reduced by 33% compared with controls, whereas F_v/F_m was largely

unaffected (Ouzounidou *et al.*, 1997). This result suggests that Cu^{2+} may cause a significant decrease in electron transport through PSII (Ouzounidou *et al.*, 1997). In contrast there was only a slight effect of Cu^{2+} on both Φ_{PSII} and F_v/F_m of wheat seedlings after 10 days of growth in water culture containing 20 μM $CuSO_4$ and the efficiency of electron transport was therefore unaffected by Cu^{2+} (Ciscato *et al.*, 1997). Furthermore, Ciscato and co-workers showed a significant decrease in both F_v and F_m which coincided with a >35% decrease in the chlorophyll *a* content in response to the Cu^{2+} treatment. Consequently, reduced photosynthesis in response to Cu^{2+} exposure in wheat seedlings may be the result of chlorophyll *a* breakdown rather than direct inhibitory effect on electron transport (Ciscato *et al.*, 1997).

2.1.4. Mechanisms of Cu^{2+} resistance in plants and algae

Exposure of an organism to elevated [Cu^{2+}] may result in physiological damage and even death. However, some species have the ability to adapt to and resist high concentrations of metal in their natural environment. Resistance to Cu^{2+} can be achieved either by avoidance, *i.e.* protection from external Cu^{2+}, or by tolerance, *i.e.* coping with effects of internal Cu^{2+} in a way which allows the organism to function normally. Tolerance may be based on genetic evolution of tolerance genotypes or acquired through acclimation of plastic phenotypes (Baker, 1987).

2.1.4.1. Cu^{2+} resistance

Different species of seaweed, including the green alga *Enteromorpha compressa* and several species of brown algae, are known for their tendency to resist elevated concentrations of metals, including copper (Seelinger and Coradzzo, 1982; Reed and

Moffat, 1983; Bryan and Gibbs, 1983; Correa *et al.,* 1996; Marsden and DeWreede, 2000). An excellent example of the ability of brown algae to resist extreme $[Cu^{2+}]_{ext}$ is the healthy population of *Fucus* which grows in the heavily Cu^{2+} polluted Restronguet Creek (Chapter 1). This population has a higher tolerance limit to copper than populations of *Fucus* from unpolluted estuaries. Growth in *F. vesiculosus* collected from Restronguet Creek was reduced by 20% when exposed to 1.5 μM copper for 22 days, whereas growth of *F. vesiculosus* from an unpolluted estuary was reduced by 85% in response to the same treatment (Bryan and Gibbs, 1983). Adaptation to copper toxicity in tolerant strains is illustrated by the fertility of *Fucus gardneri* growing near a copper mine drainage outflow, which was not significantly different from that of reference populations (Marsden and DeWreede, 2000).

Similarly, diverse communities of Cu^{2+}-resistant flowering plants such as *Calluna vulgaris* (heather) and *Silene vulgaris* (bladder campion) are often found on metal polluted soils near metal mines and smelters and in mine spoil heaps (Marrs and Bannister, 1978; Baker, 1987; Monni *et al.,* 2000; van Hoof *et al.,* 2001). Cytosolic chelation of Cu^{2+} with metal-binding proteins either exclusively in the roots (Rauser and Cuvetto, 1980) or throughout the plant (Schat and Kalff, 1992; Monni *et al.,* 2000) is a common tolerance mechanisms in Cu^{2+} resistant flowering plants (Murphy and Taiz, 1995; van Hoof *et al.,* 2001). Detoxification of Cu^{2+} by accumulation in senescing leaves before shedding may also occur, and allows flowering plants to resist high $[Cu^{2+}]$ in the environment (Monni *et al.,* 2000).

2.1.4.2. The role of polyphenols

Polyphenols are a group of organic acids which are found in high concentrations in specialised cytoplasmic vesicles, called physodes, within the cells of brown algae (Ragan,

1979; Smith *et al.*, 1986; Ilvessalo and Tuomi, 1989). The metal complexing capacity of brown algal polyphenols is very high. Complexation of Cu^{2+} with organic acid occurs by the reaction: $L\text{-}H + Cu^{2+} \leftrightarrows L\text{-}Cu^{+} + H^{+}$, with the stability constants between polyphenols and Cu^{2+} in the region of $pK_{CuL} = 10.15 - 10.50$ (Sueur *et al.*, 1982; Gledhill *et al.*, 1999). Hence, pK_{CuL} for polyphenols is slightly lower than $pK_{CuL} = 12.8$ for the strong organic ligands secreted by the hyper sensitive cyanobacterium *Synechococcus* (Moffett *et al.*, 1990), but still higher than the pK_{CuL} for ligands secreted by other macroalgae so far tested (Sueur *et al.*, 1982; Gledhill *et al.*, 1997). The chelation of divalent metal ions by polyphenols probably plays an important role in maintaining the cytoplasmic metal concentration below toxic levels during metal exposure in brown algae, either by binding metals to polyphenols stored internally in physodes (Smith *et al.*, 1986) and/or to polyphenols secreted to the external medium (Sueur *et al.*, 1982; Gledhill *et al.*, 1999).

Organic ligands such as polyphenols are secreted by brown algae in a concentration dependent manner in response to increased levels of metal ions, and have the potential to detoxify seawater by complex formation, resulting in changed metal speciation and lower concentrations of free metal ions, including Cu^{2+} (Sueur *et al.*, 1982; Gledhill *et al.*, 1997, 1999). Secretion of ligands by *Ectocarpus siliculosus* during 30 days of incubation was linearly dependent on an external total copper concentration in the range 0.3 to 5.5 μM and resulted in $[Cu^{2+}]_{ext}$ ranging from 1 to 10 nM (Sueur *et al.*, 1982). In the experiment by Sueur and co-workers (1982) there was no renewal of the incubation medium during the 30 days of the experiment, which may have allowed the algae to saturate the medium with ligands without exhausting their reserves. However, other workers (Gledhill *et al.*, 1999) have studied the effect of depleting the reserves of algae by continuously renewing the culture medium during the course of an experiment. By applying atomic stripping voltammetry to artificial seawater medium containing ~10 *Fucus* embryos per ml and

external total copper concentrations varying from 20 to 500 nM, it was shown that the ligand concentration ([Lig]) increased from ~150 nM to ~800 nM after 19 days of incubation, during which period the medium was renewed 4 times. Embryos exposed to 1 μM total copper secreted ~500 nM ligands, which was equivalent to [Lig] in treatments containing 20-100 nM total copper. However, when exposed to up to 100 nM total copper the [Lig] released by the *Fucus* embryos was sufficient to chelate the [Cu^{2+}], whereas embryos were unable to chelate higher concentrations, which resulted in highly decreased growth rates of embryos exposed to 500 and 1000 nM total copper (Gledhill *et al.*, 1999).

Brown algae are thought to accumulate metals including Cu^{2+} and their tissue concentrations may reflect the metal concentration in their environment (Bryan and Hummerstone, 1973; Stengel and Dring, 2000). The concentration of Cu^{2+} in mature *F. vesiculosus* collected from different estuaries containing total copper concentrations of 3.5, 4.1, 24, and 660 $\mu g\ l^{-1}$ was 9, 17, 68, and 301 $\mu g\ g^{-1}$ DW respectively (Bryan and Hummerstone, 1973). Similarly, samples of the mature thallus of *F. vesiculosus* collected from the heavily polluted Restronguet Creek (Chapter 1) contained 1450 μg total copper g^{-1} DW, which is two orders of magnitude higher than the 8-10 $\mu g\ g^{-1}$ DW in the same species collected from the Looe and Torridge Estuaries, which are considered 'clean' locations in terms of Cu^{2+} (Bryan and Gibbs, 1983). Other less dramatic examples of Cu^{2+} accumulation in brown algae include an average 30 μg total copper g^{-1} DW in mature thalli of *F. serratus* from the Bristol Channel between 1972 and 1995 (Martin *et al.*, 1997) and 140 μg total copper g^{-1} DW in *Ascophyllum nodosum* collected from Whiterock in the Irish Sea (Stengel and Dring, 2000). The Cu^{2+} content in seaweed tissue is dependent not only on the concentration in the surrounding water, but also on the age of the tissue, with less accumulation in younger tissue due to shorter exposure time and dilution of the copper content of growing tissue (Bryan and Hummerstone, 1973; Stengel and Dring, 2000). The

total copper concentration in growing tips of *F. vesiculosus* from the Tamar Estuary was 52 $\mu g\ g^{-1}$, whereas the concentration in stipe and mature fronds of the same alga was three fold higher, 128-149 $\mu g\ g^{-1}$ (Bryan and Hummerstone, 1973).

The ability of brown algae to accumulate high concentrations of heavy metals may be due, in part, to their high polyphenol content. By applying scanning transmission electron microscopy and X-ray microprobes to fronds of *F. vesiculosus* and *F. serratus* collected from the Cu^{2+} polluted Restronguet Creek, Smith and co-workers (1986) showed that Cu^{2+} was located mainly in the physodes. No accumulation of Cu^{2+} was found in the outermost cell layer, chloroplasts, or the cell walls (Smith *et al.,* 1986). This result is in contrast to the findings of Lignell and co-workers (1982) who found that accumulation of cadmium in fronds of *F. vesiculosus* occurred in high concentrations in the physodes as well as the cell wall of the outer cell layers. Differences between the capacity of different metals to bind to polysaccharides and polyphenols (Ragan *et al.,* 1980) may account for the different degree of copper and cadmium accumulation in *Fucus* cell walls (Lignell *et al.,* 1982; Smith *et al.,* 1986). However, polyphenols may be an integral component of the fucoid cell wall (Schoenwaelder and Clayton, 1998) and it is therefore possible that Cu^{2+} bound to cell wall polyphenols was lost during fixation and embedding of the material in the experiment by Smith and co-workers (1986). Electron microscopy of newly fertilised zygotes of the fucoids *Hormosira banksii* and *Acrocarpia paniculata* revealed that the contents of the physodes, which accumulated at the cell periphery, were secreted by exocytosis during cell wall formation, and that extensive deposition of polyphenols occurred in older walls together with other cell wall materials (Schoenwaelder and Clayton, 1998). Given the strong tendency for Cu^{2+} and polyphenols to complex (Sueur *et al.,* 1982; Gledhill *et al.,* 1999) and the presence of polyphenols (Schoenwaelder and Clayton, 1998), it is likely that

Cu^{2+} accumulation does occur in the fucoid cell wall, the findings of Smith and co-workers (1986) notwithstanding.

2.1.4.3. The role of metallothionein

Removal of free metal ions by chelation with intracellular ligands is a major detoxification mechanism. In addition to polyphenols one of the principal classes of such metal binding ligands in plants and algae are the metallothioneins (Rauser and Cuvetto, 1980; Hamer, 1986; Schat and Kalff, 1992; Murphy and Taiz, 1995; Morris *et al.,* 1999; van Hoof *et al.,* 2001). Metallothioneins are a group of low molecular weight cysteine (*i.e.* –SH) -rich cytoplasmic polypeptides with high metal-binding capacities, which form stable complexes between –SH groups and metal ions (Grill *et al.,* 1985; Hamer, 1986). There are three distinct types of metallothionein: the direct products class-1 and class-2 metallothionein genes, and the enzymatically synthesised class-3 metallothionein, the phytochelatins, which occur exclusively in plants, algae and yeast (Grill *et al.,* 1985; Rauser, 1990).

Phytochelatin production is induced in filamentous algae during exposure to metals including Cu^{2+} (Pawlik-Skowronska, 2001) and in a range of marine phytoplankton (Gekeler *et al.,* 1988; Ahner *et al.,* 1995; Morelli and Scarano, 2001). However, data on phytochelatin induction in marine macroalgae in response to metal exposure is limited. Exposure of the brown algae *Sargassum muticium* to 20 μM $Cd(NO_3)_2$ for up to 10 days resulted in accumulation of phytochelatin at a total concentration of 11.9 μmol, whereas no phytochelatin was detected in unexposed algae (Gekeler *et al.,* 1988). In comparison, phytochelatin production in the red alga *Porphyridium cruentum* was 15.6 μmol after exposure to 20 μM $Cd(NO_3)_2$ whereas the phytochelatin concentration in several species of phytoplankton of the class Chlorophyceae ranged from 8.0 to 43.8 μmol SH μg^{-1} protein

(Gekeler *et al.*, 1988). Phytochelatin induction may be a response to Cu^{2+} exposure in *Fucus*, given the above data on other species of algae.

In flowering plants, both non-tolerant and tolerant strains of *Silene cucubalus* and *S. vulgaris* produce phytochelatin upon exposure to Cu^{2+} and the threshold for the onset of phytochelatin production increases with the level of Cu^{2+} tolerance (Schat and Kalff, 1992; De Vos *et al.*, 1992). Phytochelatin production in a non-tolerant strain of *S. cucubalus* was induced at an external total copper concentration of 0.5 μM, and reached 25 μmol SH g^{-1} protein at 20 μM total copper, whereas phytochelatin production in a tolerant strain was unaffected at concentrations lower than 40 μM, which induced a phytochelatin production of just 10 μmol SH g^{-1} protein (De Vos *et al.*, 1992). Similar results were presented by Schat and Kalff (1992), who showed that both Cu^{2+} non-tolerant and tolerant strains of *Silene* possess the ability to produce phytochelatin once their tolerance limit is reached. However, the difference in the onset of phytochelatin production suggests that some special property of tolerant strains, other than phytochelatin production, allows them to cope with Cu^{2+}.

Expression of type 2 metallothionein encoding genes (*MT2*) in tolerant strains may determine the tolerance difference (Murphy and Taiz, 1995; van Hoof *et al.*, 2001). In plants *MT2* were first recognised in the grass *Agrostis* (Rauser and Curvetto, 1980) and have now been demonstrated to exist in *Arabidopsis* and *S. vulgaris* (Murphy and Taiz, 1995; van Hoof *et al.*, 2001). van Hoof and co-workers (2001) showed that *MT2* were responsible for significantly increasing Cu^{2+} tolerance and that the metallothionein genes were transcribed at higher rates in tolerant strains than in non-tolerant strains of *S. vulgaris*, regardless of $[Cu^{2+}]$. A Cu^{2+}-sensitive strain of yeast would tolerate and grow in up to 5 mM $CuSO_4$ when transformed with *MT2* from Cu^{2+}-tolerant *S. vulgaris*, whereas when not

transformed with *MT2*, the same strain only tolerated up to 1 mM $CuSO_4$ (van Hoof *et al.*, 2001). Furthermore, quantitative sequencing showed higher levels of *MT2* mRNA were found in tolerant than in non-tolerant *S. vulgaris*, both with and without exposure to 50 μM $CuSO_4$ (van Hoof *et al.*, 2001). The work discussed above suggests that induction of phytochelatin production is a general response to Cu^{2+} toxicity in both tolerant and non-tolerant strains of flowering plants, whereas metallothionein gene transcription occurs exclusively in tolerant strains and may be responsible for the different tolerance limits in tolerant and non-tolerant strains (van Hoof *et al.*, 2001).

The induction of a metallothionein gene in response to Cu^{2+} exposure has recently been shown in *F. serratus* and *F. vesiculosus* (Morris *et al.*, 1999). The *Fucus* metallothionein shows high sequence homology with both vertebrate class-1 and plant class-2 metallothionein (Morris *et al.*, 1999). Metallothionein gene expression in *F. vesiculosus* exposed to 19 μM $CuCl_2$ for 72h was two-fold higher than in control algae (Morris *et al.*, 1999). Furthermore, the resulting *Fucus* metallothionein does have the ability to bind cadmium but is preferentially a copper-binding protein (Morris *et al.*, 1999). Metallothionein genes are highly conserved between animals, plants and fungi (Hamer, 1986), which suggests that metallothionein may be a determining factor in the development of metal tolerance in many biological systems. It is, therefore, not surprising that this metallothionein coding gene also occurs in brown algae. However, sequestering of Cu^{2+} in brown algae is generally believed to occur by chelation with polyphenols stored in vesicles (Smith *et al.*, 1986). Therefore, the role of *Fucus* metallothionein may be to act as a specialised Cu^{2+} transport protein and ensure that $[Cu^{2+}]_{cyt}$ is kept close to zero during transport of Cu^{2+} through the cytoplasm to storage vesicles, analogous with the Cu^{2+} chaperones, which have been identified in yeast (Beers *et al.*, 1997).

2.1.5. Objectives

Brown algae have the ability to resist high concentrations of Cu^{2+} and form vigorous populations in polluted estuaries such as Restronguet Creek. Tolerant strains of *Fucus* cope very well when exposed to elevated concentrations of Cu^{2+}, whereas growth of non-tolerant strains can be severely reduced during Cu^{2+} exposure (Bryan and Gibbs, 1983). The ability of *Fucus* to accumulate Cu^{2+} and to form Cu^{2+}-tolerant and non-tolerant populations, is widely recognised. However, effects of Cu^{2+} on the physiology of *Fucus* and direct comparative studies on these effects in tolerant and non-tolerant populations are very limited. This study aims to determine the effects of Cu^{2+} on relative growth rate, dark respiration and photosynthesis of *F. serratus*, and to establish the effect of Cu^{2+} on secretion of organic substances and accumulation of copper, and to characterise the different response patterns during Cu^{2+} exposure of copper-tolerant and non-tolerant populations.

2.2. Material and methods

2.2.1. Experimental algae

Individuals of *Fucus serratus* were collected in September 2000 from three different locations with known copper status and transported to the laboratory within 2h in plastic bags. Algae collected from Restronguet Creek, which is subject to anthropogenic copper pollution, are exposed to a significantly higher copper level in their natural environment than algae collected from Wembury Beach and Bantham Quay, which are exposed to very low levels of copper (Chapter 1). The algae were cleaned by rubbing and rinsing them three times in filtered seawater (FSW). Tips were cut from the fronds approximately 3 cm from the apex (apical tips=fronds). Fronds were left to recover from cutting and acclimate to laboratory conditions in filtered aerated water from their respective locations to maintain their natural copper status. For 3 to 5 days after cutting, the fronds leaked yellow substance. They were considered recovered after 8 days. The water was changed every day during the acclimation period during which the fronds were kept at 15°C and 250 μmol m^{-2} s^{-1} photosynthetically active radiation (PAR) provided by fluorescent lamps on a 16/8h light/dark cycle.

2.2.2. The culture medium, Aquil

Following recovery from cutting, the fronds were incubated in the artificial culture medium, Aquil, modified from the original recipe formulated by Morel (Morel *et al.*, 1979; Price *et al.*, 1988/89). Aquil was originally developed as a phytoplankton culture medium

and lately has been successfully used for culturing microscopic stages of brown macroalgae (Bond *et al.*, 1999; Gledhill *et al.*, 1999). In Aquil the concentrations of the major salts yielding synthetic ocean water (SOW) correspond closely to the principal constituents of natural seawater. The main reason for using Aquil, rather than natural seawater supplemented with nutrients and trace metals, was to obtain a medium in which the availability of trace metals was known as precisely as possible. Precautions were taken to avoid trace metal contamination or unknown decreases of constituent concentrations in the medium. All flasks, funnels and pipette tips used in preparing the medium and storage containers were made from polyethylene, which is largely free from trace metals and adsorbs only small amounts of metals. Nano-pure water was always used for stock solutions and media, and all chemicals were of analytical grade purity. In order to reduce the risk of contamination further, the plasticware was acid washed prior to use by submerging it in 3% HCl for 24h and subsequently rinsing it 3 times in nano-pure water. Preparation and exchange of medium took place in a class 100 –laminar flow hood. Extra precautions, such as microwaving to avoid infection of the culture medium with bacteria, were not taken as the main source of such contamination was considered to be the seaweed itself.

Information on the composition and preparation of SOW, the stock solutions of nutrients and trace metals, mixing of these to yield Aquil and final total concentrations is summarised Appendix 1. In preparing SOW, complete dilution of the anhydrated salts was ensured before adding the hydrated salts. Stock solutions of nutrients (N, P, K, F and Sr) and trace metals were prepared individually at 1×10^3 the final concentration. Each solution was added at 1 ml l^{-1} to SOW to yield Aquil. The pH of Aquil was 8.2, buffered by the presence of HCO_3^- (2.38 mM). No other buffers were added to control the pH, as chelating ligands are known to be toxic to some algae and have been found to slightly

reduce growth in *Fucus* zygotes when compared with unchelated medium (Bond *et al.*, 1999).

To avoid loss of trace metals due to precipitation, trace metal stocks were prepared in 0.01 M HCl. In order to reduce the background contamination of trace metals in the N, P and K stocks, 1 g of the resin Chelex 100, prepared according to Price *et al.* (1988/89), was added to each solution. The PO_4 was stored in an acid-washed glass bottle since PO_4 is strongly adsorbed to polyethylene. Stocks were dark stored for up to three months at 4°C. Precautions taken to avoid trace metal contamination or loss in making Aquil were considered adequate, as analyses of media by cathodic stripping voltammetry showed concentrations within 10% of expected values (Gledhill *et al.*, 1999).

During experiments, Aquil was enriched with $CuSO_4 \cdot 5H_2O$ to yield total copper concentrations ranging between 0 and 20 μM. A 2 mM $CuSO_4$ stock was prepared by adding $CuSO_4 \cdot 5H_2O$ at 0.499 g l^{-1} to 0.01M HCl. Subsequently the 2 mM stock was diluted ×10 to yield a 0.2 mM stock. Preparation of copper-enriched Aquil and concentrations of total copper and free Cu^{2+} are summarised in Appendix 2. Free Cu^{2+} concentrations initially present in Aquil were calculated by applying the total concentrations of the Aquil constituents to the chemical equilibrium modelling program MINEQL+ (version 3.01) (Westall *et al.*, 1976), which was downloaded from the internet (www.agate.net). Copper speciation was calculated based on a temperature of 15°C, the temperature at which all experiments took place (Gledhill *et al.*, 1999; Bond *et al.*, 1999)

2.2.3. Physiological responses of *Fucus* to elevated Cu^{2+}

In order to establish whether the degree of Cu^{2+} resistance in the algae reflected the copper status at the location from which they were collected, different physiological responses were monitored during 23 days exposure to different [Cu^{2+}]. Fronds were transferred to individual beakers containing 100 ml Aquil with [Cu^{2+}] of 0, 42.2, 211, 422, or 844 nM, and incubated at 15°C and 250 μmol m^{-2} s^{-1} PAR. The Cu^{2+} treatments chosen were representative of the copper levels found in Restronguet Creek (Chapter 1), and within the range which has toxic effects on non-tolerant *Fucus* (Bond *et al.*, 1999). The beakers were placed on an orbital shaker to ensure aeration of the medium and facilitate exchange of substance between medium and algae. *Fucus* is known to release metal-complexing ligands during exposure to elevated concentrations of metal ions (Gledhill *et al.*, 1997; 1999). During the course of the experiment differences in relative growth rates resulted in different sized fronds. Small fronds would consequently be exposed to relatively more Cu^{2+} than large fronds in beakers holding the same volume of medium and [Cu^{2+}]. Adding Cu^{2+} on a biomass basis would have overcome the differences although this approach was not possible in the present experiment. In order to compensate for this, the release of ligands, and to maintain supply of nutrients, the medium was changed daily. Measurements of physiological conditions of the fronds were carried out after 2, 6, 12, and 23 days of incubation unless otherwise stated. One batch of fronds was used for measurements of relative growth rate, dark respiration, photosynthesis and final total copper content of fronds, whereas another batch was used for quantifying secretion of organic substances and measurement of final chlorophyll *a* content.

2.2.3.1. Relative growth rate

Measurements of relative growth rate (RGR) of fronds were based on fresh weight (FW) measurements. Fronds were blotted dry, weighed and RGR was calculated according to the equation by Hunt (1982):

$RGR\ (\%\ d^{-1}) = (\ln (m_f) - \ln (m_i) / t) \times 100$

where 'm_f' is mass of the frond (g FW) on the day of measurement, 'm_i' is mass of the frond (g FW) on the previous day of measurement and 't' is time in days between measurement of m_f and m_i.

2.2.3.2. Dark respiration

Dark respiration was measured as continuous oxygen consumption in darkness in a closed incubation chamber fitted with a Clark-type oxygen electrode (Hansatech Instruments Ltd., Norfolk, UK) connected to a data logger (Servogor 220, John Minister Instruments Ltd., Austria). The temperature in the chamber was maintained at 15°C by a circulating water jacket connected to a thermostatically controlled water bath (Termostirrer 100, Gallenkamp, EU). The system was calibrated to oxygen-depleted and atmospherically saturated Aquil and the oxygen concentration calculated according to the temperature and salinity of the medium (Green and Carrit, 1969). Fronds were dark adapted for 30 minutes and subsequently placed in the incubation chamber, in darkness, containing 10 or 15 ml Aquil which was stirred by a magnetic bar and contained the respective concentrations of Cu^{2+}. Dark respiration (μmol O_2 g^{-1} FW min^{-1}) was calculated as:

$(O_{2i} - O_{2f} \times v) / (t \times m)$,

where '$O_{2i} - O_{2f}$' is oxygen consumption (μmol ml^{-1}), 'v' is volume of incubation medium (ml), 't' is time (min), and 'm' is the mass of the frond (g FW).

2.2.3.3. Photosynthesis

The photosynthetic performance (PS) of the fronds was measured using two different methods: chlorophyll fluorescence and oxygen evolution.

Upon absorbing an electron during photosynthesis, the reaction centre of photosystem II (PSII) is in the closed state and cannot absorb more light energy until the electron is passed on to the electron carrier, plastoqinone A (Q_A). Excess light energy is dispersed as heat or emitted as chlorophyll fluorescence. The relationship between the three different fates of light energy harvested by chlorophyll can be exploited to estimate photosynthesis on the basis of chlorophyll fluorescence measurements. Chlorophyll fluorescence measurements were carried out by application of the Rapid Light Curve technique (RLC) (White and Critchley, 1999) and use of a modulated Fluorescence Monitoring System (FMS) (Hansatech Instruments Ltd., Norfolk, UK). Fronds were placed in a holder at a fixed distance from the measuring light and the fluorescence trace of the RLC recording was initiated. A 5.5 s far red light (6 μmol m^{-2} s^{-1}) treatment drained electrons from PSII, and ensured its full relaxation. Zero fluorescence (F_o) was measured immediately afterwards and was followed by application of a 0.8 s saturating light pulse (3000 μmol m^{-2} s^{-1} white light) and measurement of maximum fluorescence (F_m). Subsequently the actinic light source was switched on and the light intensity gradually increased in 13 steps from 17 to 657 μmol m^{-2} s^{-1} PAR, each lasting 30 s. Each step was followed by a saturating light pulse of 0.8 s, and simultaneous measurement of maximum fluorescence in the light (F'_m), with subsequent measurement of steady state fluorescence in the light (F_t). Standard total recording time of an RLC trace was 7 minutes.

The maximum efficiency of PSII (Genty *et al.*, 1989) was calculated as:

$F_v/F_m = (F_m - F_o)/F_m$,

and the electron transport rate of PSII, which is equivalent to PS (μmol e^- m^{-2} s^{-1}) was calculated according to Genty *et al.* (1989):

$PS = \Phi_{PSII} \times PAR \times 0.42$,

where PAR is the intensity of actinic light, '0.42' is a factor which accounts for partitioning of light energy between PSII and PSI, and 'Φ_{PSII}' expresses the efficiency of PSII photochemistry in the light, and is given by:

$\Phi_{PSII} = (F'_m - F_t)/F'_m$

Light response curves were plotted from the resulting data and the photosynthetic affinity (α) was calculated by linear regression from photosynthesis at the initial 4 steps of light irradiances from 0 to 43 μmol m^{-2} s^{-1}. The photosynthetic capacity (P_{max}) was taken as photosynthesis at the saturating irradiance of 365 μmol m^{-2} s^{-1}.

Photochemical quenching (*qp*) at 365 μmol m^{-2} s^{-1} PAR was calculated:

$qp = \Phi_{PSII}/ (F_v/F_m)$

and non-photochemical quenching (NPQ) at 365 μmol m^{-2} s^{-1} PAR was calculated:

$NPQ = F_m\text{-}F'_m/F'_m$

PS of the fronds was also estimated from measurements of oxygen evolution, using a closed system fitted with a Clark oxygen electrode as described above (section 2.2.3.2.). After 23 days of incubation, the maximal photosynthetic capacity P_{max} of the fronds was measured at a photosynthetically saturating irradiance of 500 μmol m^{-2} s^{-1} PAR, provided by a actinic light source, Red LEDs (Hansatech Instruments Ltd.) which was fitted to the incubation chamber. Dark respiration was added to the oxygen evolution measurements to yield gross photosynthesis (gross PS) and enable comparison with the results of the chlorophyll fluorescence measurements.

2.2.3.4. Copper content of fronds

The copper content of fronds was measured initially before the acclimation period and on the final day of measurements by Atomic Absorption Spectrophotometry (AAS). The

fronds were rinsed thoroughly in nano-pure water, frozen at -5°C and freeze-dried in a Super Modulyo freeze-dryer (Edwards, West Sussex, UK). Following freeze drying, the fronds were weighed and approximately 0.1 g of freeze dried material was added to 2 ml 69% NH_3 in a 7 ml polyethylene digestion vessel. The material was digested in a CEW 2000 microwave (CEM Microwave Technology Ltd., Birmingham, UK), the power was gradually increased from 3% to 15% during a 35 minutes digestion period, which included 10 min cooling. Following digestion, the samples were made up to 5 ml volume with nano-pure water and analysed for copper using a Varian 600 series AAS (Varian Ltd., Surrey, UK) in graphite furnace mode. Calibrations were carried out regularly and subtracted from the samples. Copper standards were made using a certified copper standard solution (Merck Ltd., Lutterworth, UK) acidified to the same pH as the samples with NH_3.

2.2.3.5. Measurements of organic substances

Fucoids are known to release organic ligands in response to Cu^{2+} exposure which effectively lowers [Cu^{2+}] of the surrounding environment (Gledhill *et al.*, 1997; 1999). To compensate for this, the growth medium was renewed every day during the 23 day incubation period. This procedure also allowed for quantitative analysis of organic substances secreted by the fronds over 24h on the different days of measurements. Absorbance of three samples was measured by UV-visible spectrophotometry (Cary 13, Varian Ltd., Walton-on-Thamse, Surrey, UK) at wavelengths varying from 200 to 900 nm at 5 nm intervals, resetting the spectrophotometer with Aquil at each step. It was determined that maximum absorbance of the incubation medium was in the UV region of the spectrum at around 235 nm (Figure 2.03). The absorbance of all samples was therefore measured at this wavelength and calculated as absorbance g^{-1} FW ml^{-1}.

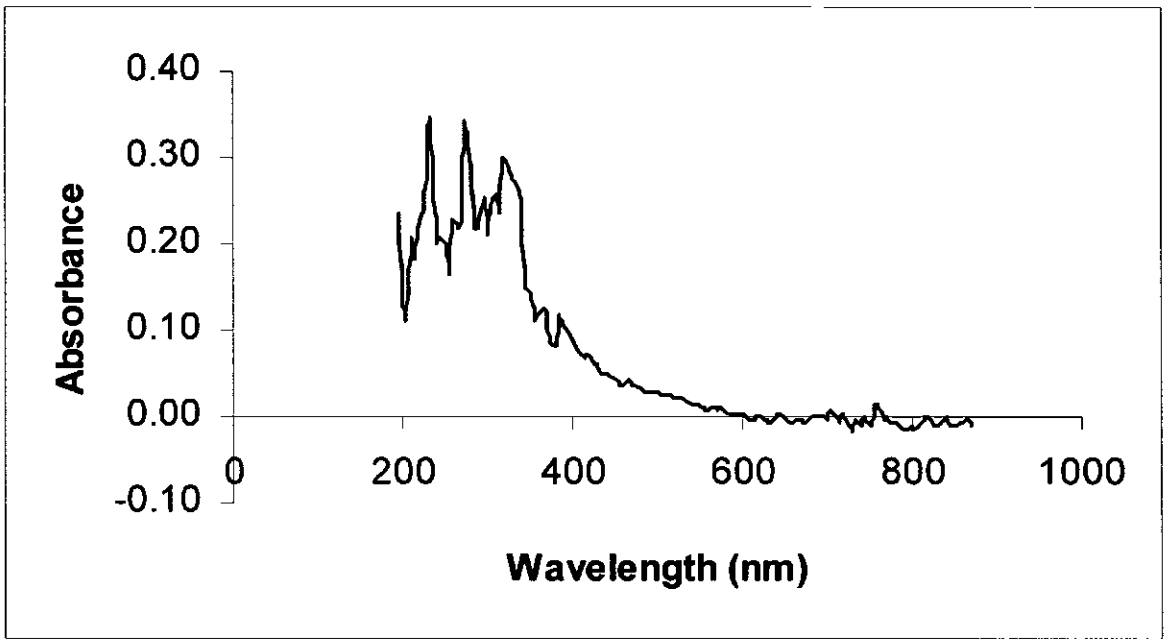

Figure 2.03. Representative curve of absorbance of the culture medium containing organic compounds secreted by *Fucus* during Cu^{2+} exposure. Absorbance was measured at wavelengths varying from 190 to 900 nm at 5 nm intervals. Clean medium was used to reset the spectrophotometer at each step.

2.2.3.6. Chlorophyll *a* content of fronds

The chlorophyll *a* content of the fronds was determined at the end of the experiment on day 23 by extraction from approximately 50 mg FW material. The material was homogenised and extracted in 5 ml ethanol for 3h at room temperature. Subsequently the samples were made up to 10 ml and absorbance measured at 665 and 750 nm on a spectrophotometer (Cary 13, Varian Ltd., Walton-on-Themse, Surrey, UK). Chlorophyll *a* was calculated as:

Chl *a* ($\mu g\ g^{-1}$ FW) = $((Abs_{665}-Abs_{750}) \times v)/83.4 \times m$

where 'Abs_{665}' and 'Abs_{750}' are the absorbances at 665 nm and 750 nm (cm^{-1}), 'v' is the volume of ethanol used for extraction (ml), '83.4' is the absorption coefficient of chlorophyll *a* in ethanol (ml μg^{-1} cm^{-1}), and 'm' is the mass of the extracted material (g) (Schierup *et al.*, 1995).

2.2.4. Statistical tests

Statistical tests of the data (Sokal and Rolf, 1981) were carried out using STATGRAPHICS plus 5.0. The small number of replicates (4-5) was considered inadequate to carry out analysis of normal distribution and it was therefore assumed that the data did apply to this rule for statistical testing (Ricketts, pers. comm.). No test of variance homogeneity was carried out although different variability in the data sets would increase the probability of accepting a false null hypothesis, *i.e.* highly variable data is more likely to conceal small differences between data sets. This was, however, considered acceptable.

Where repeated measurements were carried out on the same fronds, analyses of variance of data used a repeated measure design, to account for the fact that time was not an independent variable. A $p=0.01$ level of significance was accepted. When significant differences between means and interactions between the variables were found at different time intervals, further analyses of variance were carried out by one way ANOVA, and comparison of individual means by multiple range tests and accepted at a $p=0.01$ level of significance. The $p=0.01$ level of significance was chosen in order to compensate for multiple testing, which increases the probability of rejecting a true null hypothesis.

Where time was not included in the analysis, data was analysed by two way ANOVA and comparison of means and accepted at a $p=0.05$ level of significance. Data, which were distributed logarithmically were log transformed prior to analysis.

2.3. Results

The effect of Cu^{2+} on different physiological processes was studied in adult *Fucus* collected from locations with different Cu^{2+} statuses. Apical portions of individuals from a population growing in the Cu^{2+}-polluted Restronguet Creek and from unpolluted sites at Bantham Quay and Wembury Beach were incubated for 23 days in the artificial seawater medium, Aquil which contained varying [Cu^{2+}]. Physiological measurements were carried out at suitable intervals in order to establish physiological differences between the populations during Cu^{2+} exposure. Segments of adult *Fucus* grew well in Aquil throughout the 23 days of the experiment and the phytoplankton medium appears to be adequate for the culture of macroalgae.

2.3.1. Relative growth rate

Figure 2.04 shows the effect of Cu^{2+} on relative growth rate (RGR). RGR of Bantham and Wembury fronds was more sensitive to Cu^{2+} than RGR of Restronguet fronds. There was a pronounced inhibitory effect of Cu^{2+} on RGR of Bantham and Wembury fronds throughout the experiment, whereas RGR of Restronguet fronds was affected only by the highest [Cu^{2+}] tested and only towards the end of the experiment.

Bantham fronds appeared to be losing weight within the first two days of incubation and the weight loss was greater in the higher concentrations (Figure 2.04 A). RGR of control fronds was 0.7 ± 1.2 % d^{-1}, and RGR of fronds exposed to 211 nM Cu^{2+} was –0.7 ± 0.9 % d^{-1}. This difference was not significant due to the highly variable data ($p>0.01$). Further increase in [Cu^{2+}] to 844 nM resulted in a significant decrease in RGR to –5.6 ± 1.7 % d^{-1}

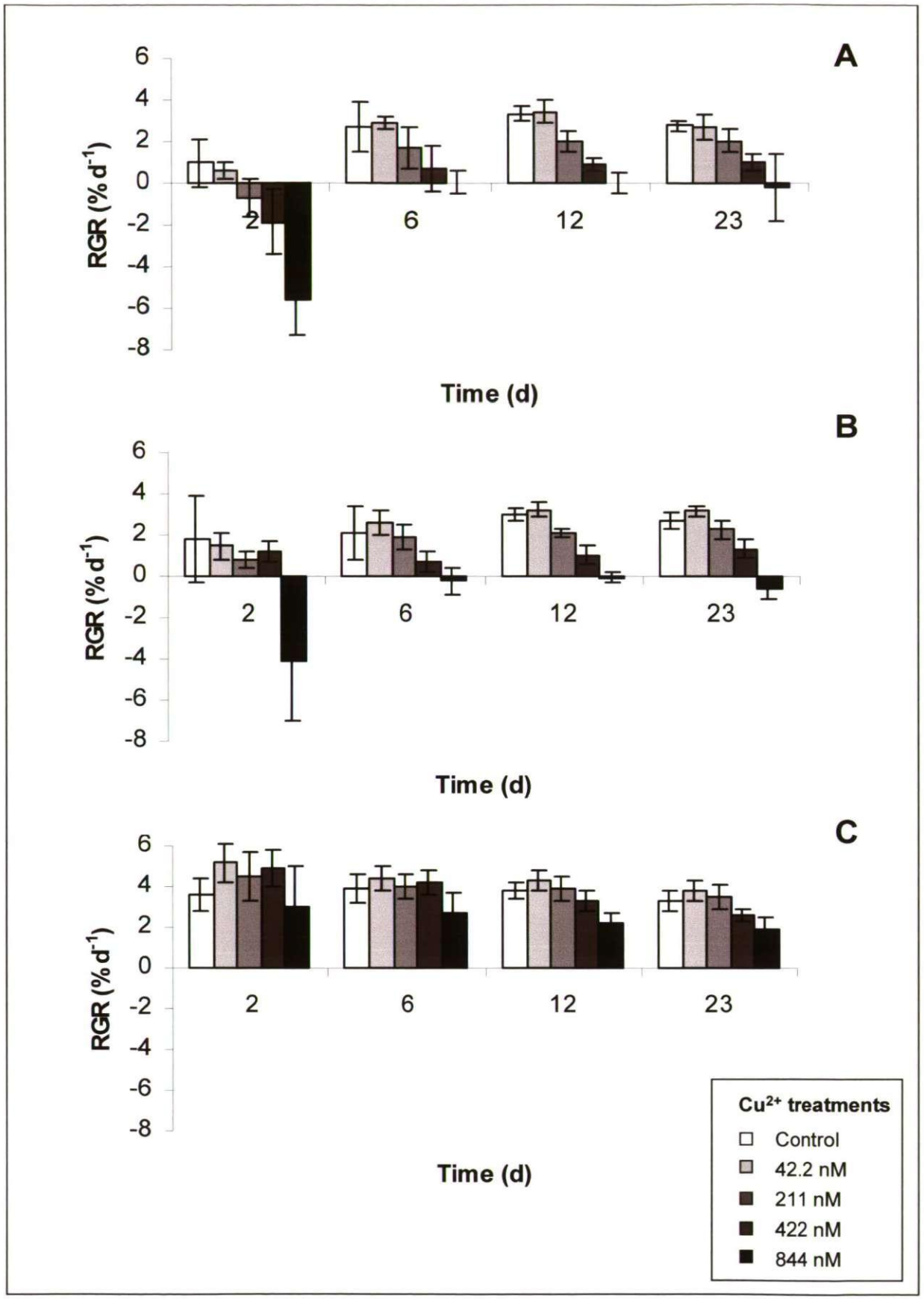

Figure 2.04. Effect of Cu^{2+} on relative growth rate (RGR) calculated from fresh weight measurements of Bantham (**A**), Wembury (**B**), and Restronguet (**C**) fronds during 23 days of exposure to Cu^{2+} concentrations varying from 0 to 844 nM. Values represents means ± 1 SD (n=5).

($p<0.05$). After 6 days there was a general increase in RGR. RGR of control fronds was 2.7 ± 1.2 % d^{-1}. RGR of fronds exposed to 211 nM had increased significantly compared with day 2 ($p<0.01$) to 1.7 ± 1.0 % d^{-1}, whereas RGR of fronds exposed to 422 nM Cu^{2+} was 0.7 ± 1.1 % d^{-1} and significantly lower than RGR of control fronds ($p<0.01$). The weight loss of fronds exposed to 844 nM Cu^{2+} had slowed down to 0.0 ± 0.6 % d^{-1} but RGR was still significantly lower than RGR of fronds exposed to 0 to 211 nM Cu^{2+} ($p<0.01$). After 12 days, RGR of control fronds had increased significantly to 3.3 ± 0.3 % d^{-1} ($p<0.01$). Exposure of fronds to [Cu^{2+}] above 42.2 nM had a significant inhibitory effect on RGR, which decreased gradually from 2.0 ± 0.5 % d^{-1} to 0.0 ± 0.5 % d^{-1} as [Cu^{2+}] increased from 211 to 844 nM ($p<0.01$). After 23 days, RGR of control fronds was 2.8 ± 0.2 % d^{-1} and significantly lower than after 12 days ($p<0.01$). There was an increasingly inhibitory effect of Cu^{2+} on RGR at concentrations above 211 nM ($p<0.01$). Similar to the previous days RGR of fronds exposed to 844 nM was arrested at –0.2 ± 1.6 % d^{-1} and significantly lower than RGR of fronds in all other treatments ($p<0.01$).

RGR of Wembury fronds exposed to varying [Cu^{2+}] was similar to that of Bantham fronds, although weight loss over the first two days was only seen at the highest concentration (Figure 2.04 B). RGR of control fronds was 2.4 ± 0.8 % d^{-1} during the course of the experiment. After 2 days, RGR of fronds exposed to 844 nM Cu^{2+} was reduced significantly compared with all other concentrations to -4.1 ± 2.9 % d^{-1} ($p<0.01$). After 6 days, there was an inhibitory effect of Cu^{2+} on RGR at concentrations above 211 nM. RGR was reduced significantly to 0.7 ± 0.5 % d^{-1} and –0.2 ± 0.6 % d^{-1} during exposure to 422 and 844 nM Cu^{2+} respectively. After 12 days at [Cu^{2+}] above 42.2 nM there was an increasingly inhibitory effect on RGR which was –1.0 ± 0.2 % d^{-1} for fronds exposed to 844 nM ($p<0.01$). After 23 days, RGR of fronds exposed to 211 nM Cu^{2+} was significantly reduced compared with RGR of fronds exposed to 42.2 nM ($p<0.01$), whereas RGR of

fronds exposed to 422 nM had decreased significantly to 2.3 ± 0.4 % d^{-1} ($p<0.01$) and RGR of fronds exposed to 844 nM was –0.6 ± 0.5 % d^{-1} and significantly different from RGR of fronds in any other treatment ($p<0.01$).

There was less effect of Cu^{2+} on RGR of Restronguet fronds than on Bantham and Wembury fronds (Figure 2.04 C). RGR of control fronds was 3.6 ± 0.3 % d^{-1} throughout the experiment. After 12 days, RGR of fronds exposed to 422 nM Cu^{2+} was significantly lower than RGR of fronds exposed to 42.2 nM Cu^{2+}. RGR of fronds exposed to 844 was 2.2 ± 0.5 % d^{-1} and lower than in any other treatment ($p<0.01$). After 23 days RGR of fronds exposed to 422 nM Cu^{2+} was significantly lower than RGR of fronds exposed to 42.2 and 211 nM Cu^{2+} ($p<0.01$), and RGR of fronds exposed to 844 nM was 1.9 ± 0.6 % d^{-1} and significantly lower than RGR of fronds exposed to between 0 and 211 nM Cu^{2+} ($p<0.01$).

2.3.2. Dark respiration

Figure 2.05 shows the effect of Cu^{2+} on dark respiration. Dark respiration of Bantham and Wembury fronds was more affected by Cu^{2+} than dark respiration of Restronguet fronds. Initially, dark respiration of Bantham and Wembury fronds increased strongly upon exposure to the highest [Cu^{2+}] tested. In contrast with Bantham and Wembury fronds, dark respiration in Restronguet fronds was unaffected by Cu^{2+} ($p>0.01$) (Figure 2.05 C). Rates of control fronds remained at about 0.13 ± 0.03 μmol O_2 g^{-1} FW min^{-1} throughout the experiment ($p>0.01$).

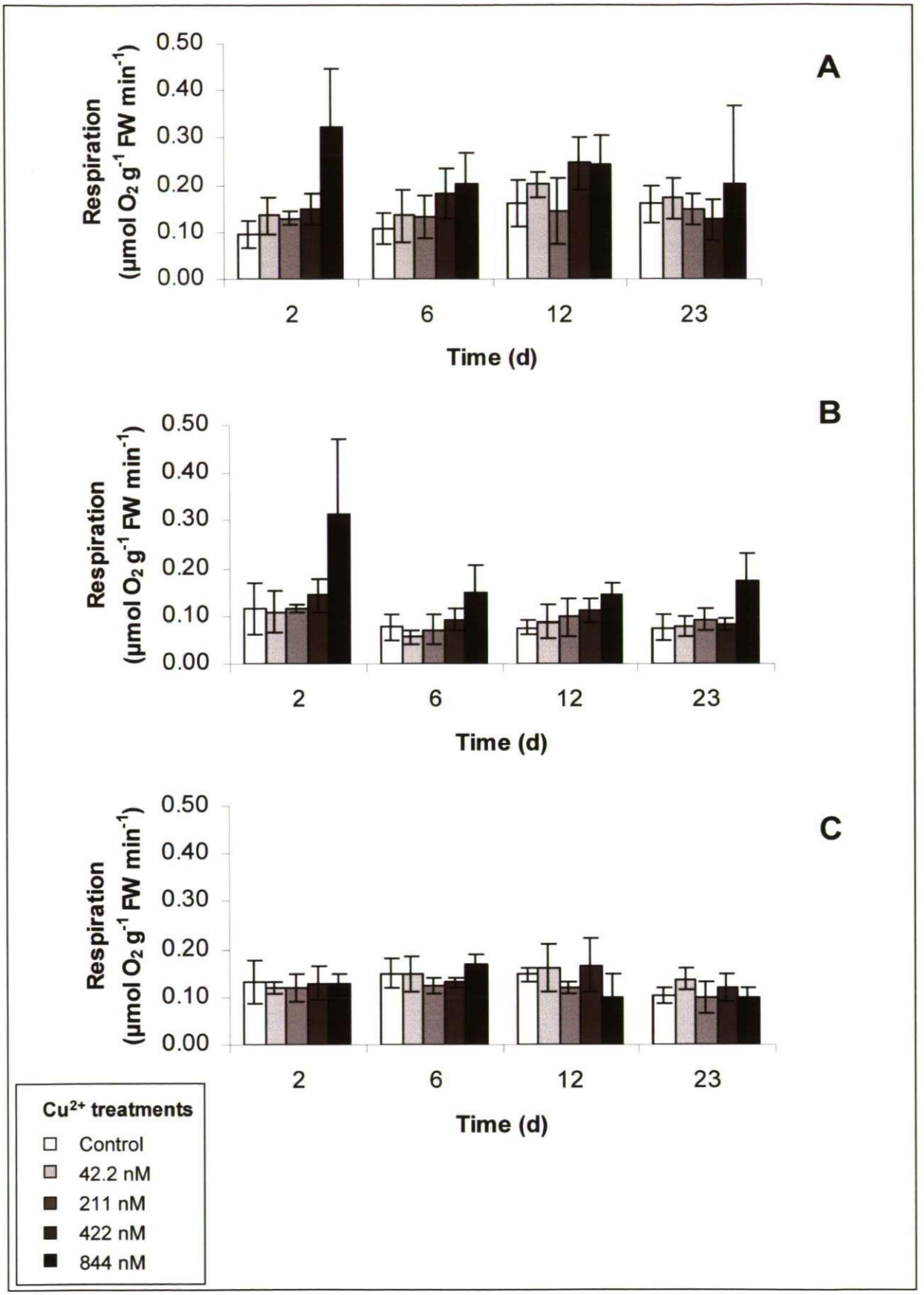

Figure 2.05. Effect of Cu^{2+} on dark respiration measured as oxygen consumption by Bantham (**A**), Wembury (**B**), and Restronguet (**C**) fronds during 23 days of exposure to Cu^{2+} concentrations varying from 0 to 844 nM. Values represents means ± 1 SD (n=5).

There was a slight but significant increase in dark respiration of Bantham control fronds from 0.10 ± 0.03 μmol O_2 g^{-1} FW min^{-1} after 2 days, to 0.16 ± 0.04 μmol O_2 g^{-1} FW min^{-1} after 23 days (Figure 2.05 A). After 2 days, 844 nM Cu^{2+} resulted in a 3-fold increase in dark respiration to 0.32 ± 0.12 μmol O_2 g^{-1} FW min^{-1}, which remained significantly higher than dark respiration of control fronds after 6 days ($p<0.01$). After 12 and 23 days, dark respiration of fronds exposed to 844 nM Cu^{2+} had decreased to the level of control fronds ($p>0.01$). After 23 days there was a high variability in the rates of dark respiration of fronds exposed to 844 nM Cu^{2+}.

Dark respiration in Wembury fronds followed a similar pattern to that of Bantham fronds (Figure 2.05 B). Throughout the experiment the rate of dark respiration of control fronds was 0.09 ± 0.03 μmol O_2 g^{-1} FW min^{-1}. After 2 days there was a 3-fold increase in dark respiration of fronds exposed to 844 nM Cu^{2+} to 0.31 ± 0.16 μmol O_2 g^{-1} FW min^{-1} ($p<0.01$). After 6 days, dark respiration rates of fronds exposed to 844 nM Cu^{2+} had decreased to 0.15 ± 0.06 μmol O_2 g^{-1} FW min^{-1} ($p<0.01$) and remained at this level until the end of the experiment ($p>0.01$); these rates were significantly higher than those of control fronds ($p<0.01$).

2.3.3. Chlorophyll fluorescence measurement

The electron transport rates of PSII (J) of fronds from the three populations were calculated on the basis of chlorophyll fluorescence measurements and expressed as the gross photosynthetic rate (gross PS) in μmol e^- m^{-2} s^{-1} (see Material and Methods). J was plotted as a function of the intensity of actinic light to produce photosynthetic light

response curves (Figures 2.06 – 2.08), from which the photosynthetic efficiency (α) and -capacity (P_{max}) were calculated.

2.3.3.1. α values

Values of α of fronds are presented in Figure 2.09. In all three populations there was significant effects of Cu^{2+} on α and significant interactions between Cu^{2+} and time ($p<0.01$). The differences in α did not correlate with $[Cu^{2+}]$ and, although significant, the differences in α were only slight during the whole of the experiment and there were only small differences in α between the days of sampling. Overall there are no notable effects of Cu^{2+} on α in any of the populations.

2.3.3.2. P_{max} values

Figure 2.10 A shows that P_{max} of Bantham fronds was unaffected by Cu^{2+} during the whole of the experiment ($p>0.01$). There was, however, a general effect of time on P_{max}. After 2 days, P_{max} of control fronds was 85.9±7.5 μmol e^- m^{-2} s^{-1} and decreased gradually to 45.8±4.4 μmol e^- m^{-2} s^{-1} after 23 days ($p<0.01$).

For Wembury fronds after, 23 days P_{max}, of control fronds was 56.6 ± 5.2 μmol e^- m^{-2} s^{-1} and significantly lower than the average 71.5 ± 7.5 μmol e^- m^{-2} s^{-1} on the previous days ($p<0.01$) (Figure 2.10 B). Furthermore, on day 23, P_{max} of fronds exposed to 211 to 844 nM Cu^{2+} was significantly lower than that of fronds exposed to 0 and 42.2 nM ($p<0.01$).

For Restronguet fronds, the average P_{max} of control fronds was 85.0 ± 7.1 μmol e^- m^{-2} s^{-1} throughout the experiment (Figure 2.10 C). After 23 days, P_{max} of fronds exposed to 844 nM Cu^{2+} was 43.3 ± 11.6 μmol e^- m^{-2} s^{-1} and significantly lower than P_{max} of fronds in any of the other treatments ($p<0.01$).

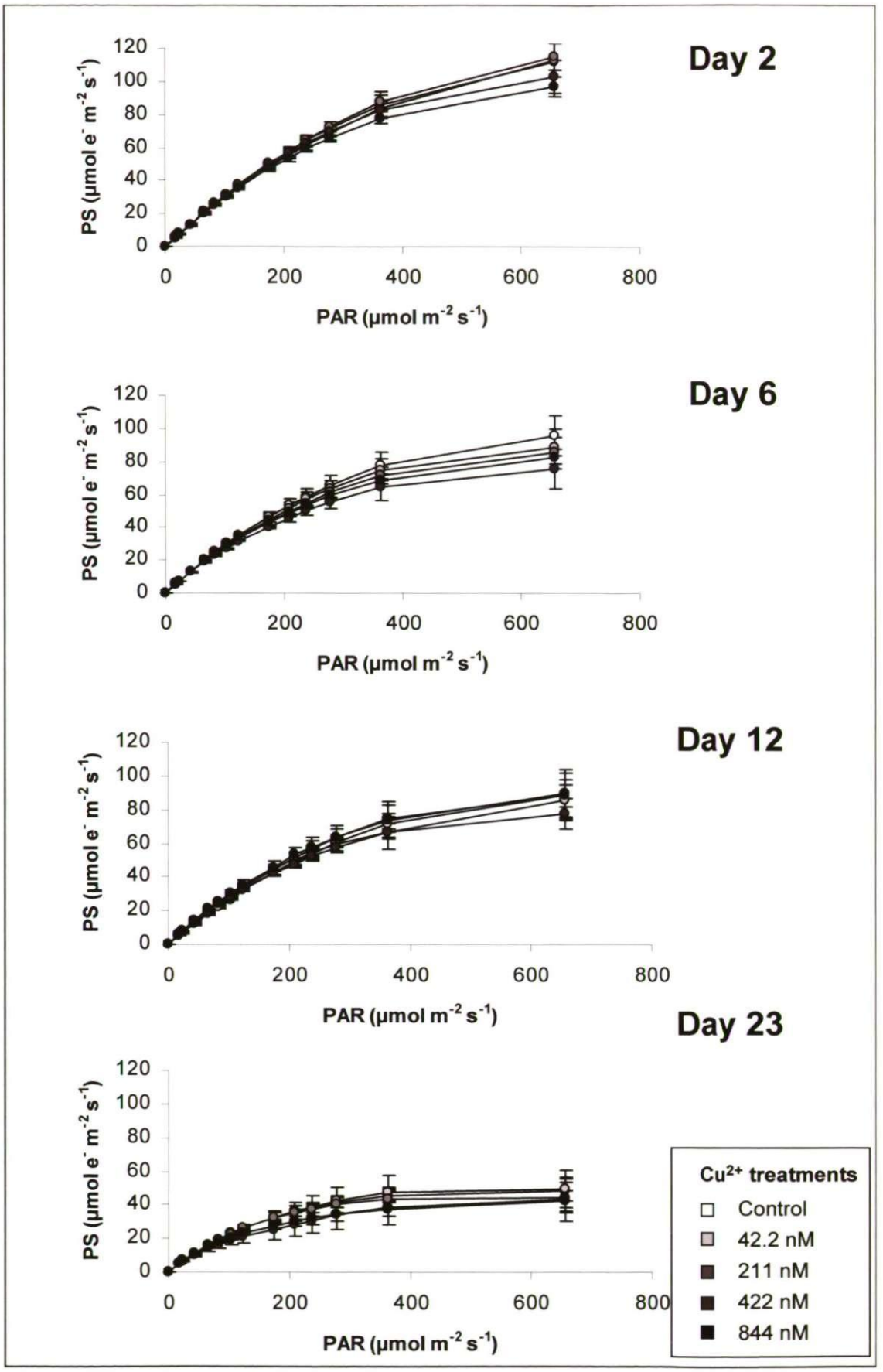

Figure 2.06. Effects of Cu^{2+} on gross photosynthesis estimated indirectly by measuring chlorophyll fluorescence of Bantham fronds after 2 to 23 days exposure to various concentrations of Cu^{2+}. Values for α and P_{max} were calculated and are presented in Figures 2.09 and 2.10. Values represents means ± 1 SD (n=5).

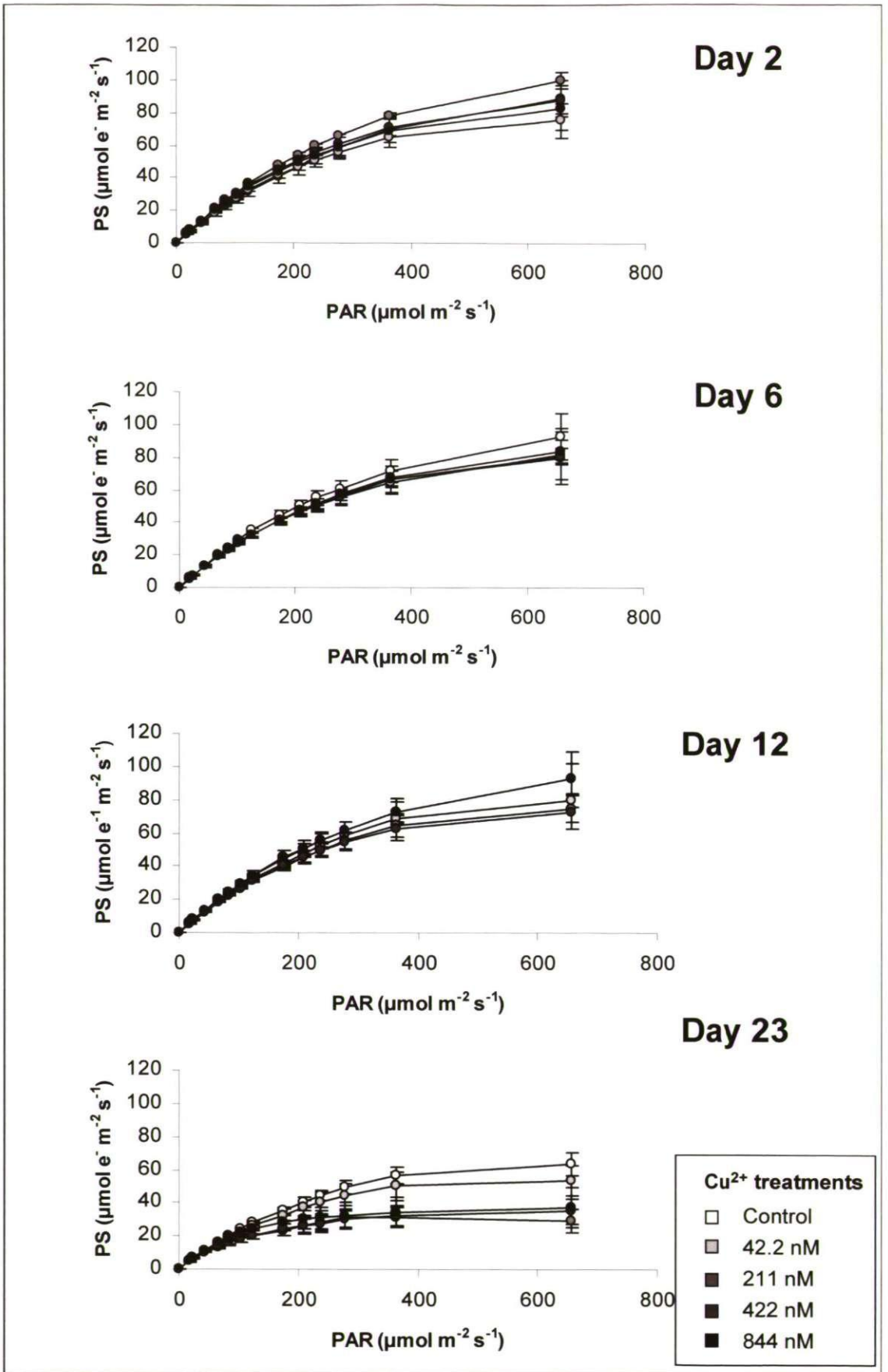

Figure 2.07. Effects of Cu^{2+} on gross photosynthesis estimated indirectly by measuring chlorophyll fluorescence of Wembury fronds after 2 to 23 days exposure to various concentrations of Cu^{2+}. Values for α and P_{max} were calculated and are presented in Figures 2.09 and 2.10. Values represents means ± 1 SD (n=5).

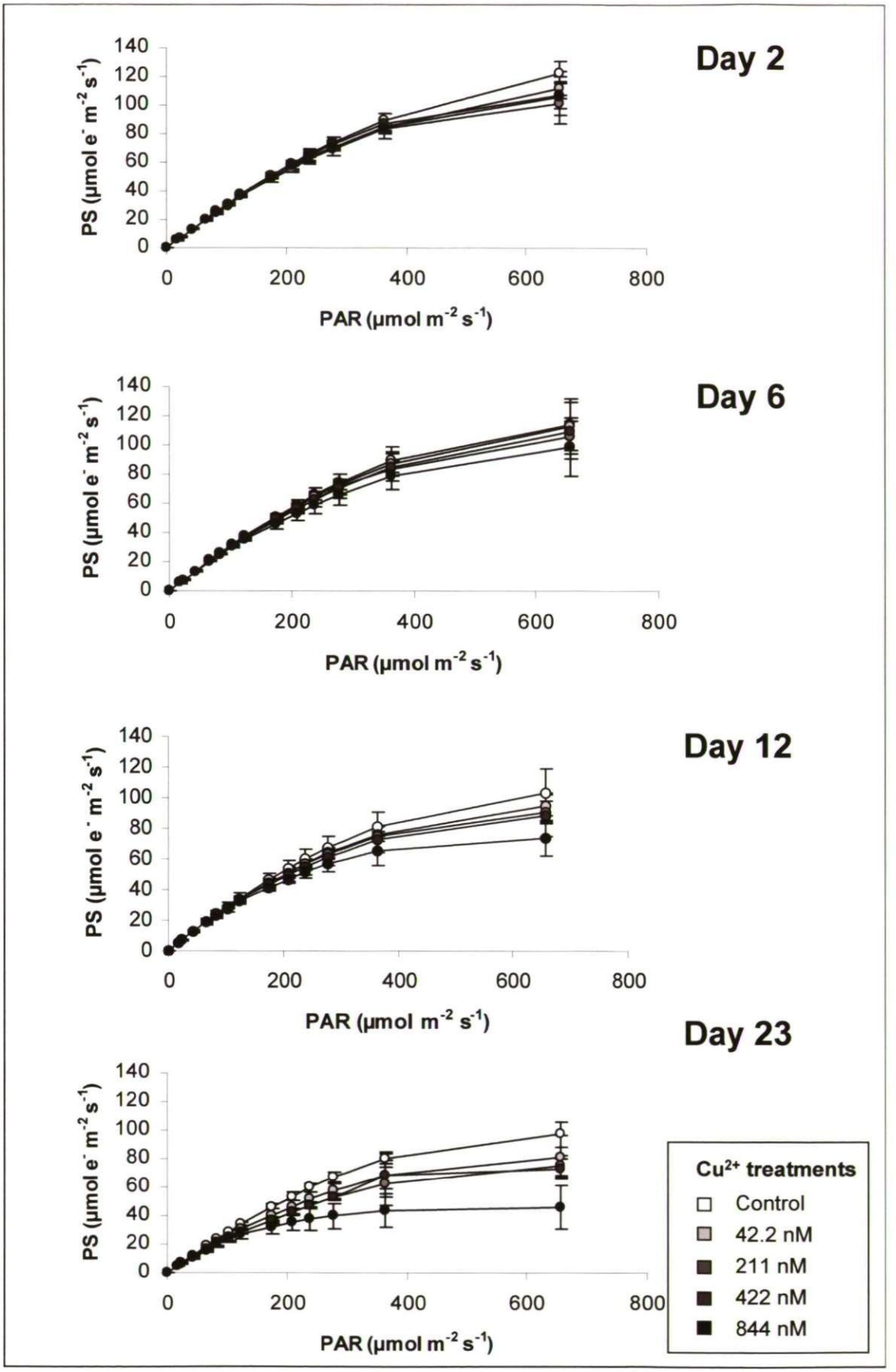

Figure 2.08. Effects of Cu^{2+} on gross photosynthesis estimated indirectly by measuring chlorophyll fluorescence of Restronguet fronds after 2 to 23 days exposure to various concentrations of Cu^{2+}. Values for α and P_{max} were calculated and are presented in Figures 2.09 and 2.10. Values represents means ± 1 SD (n=5).

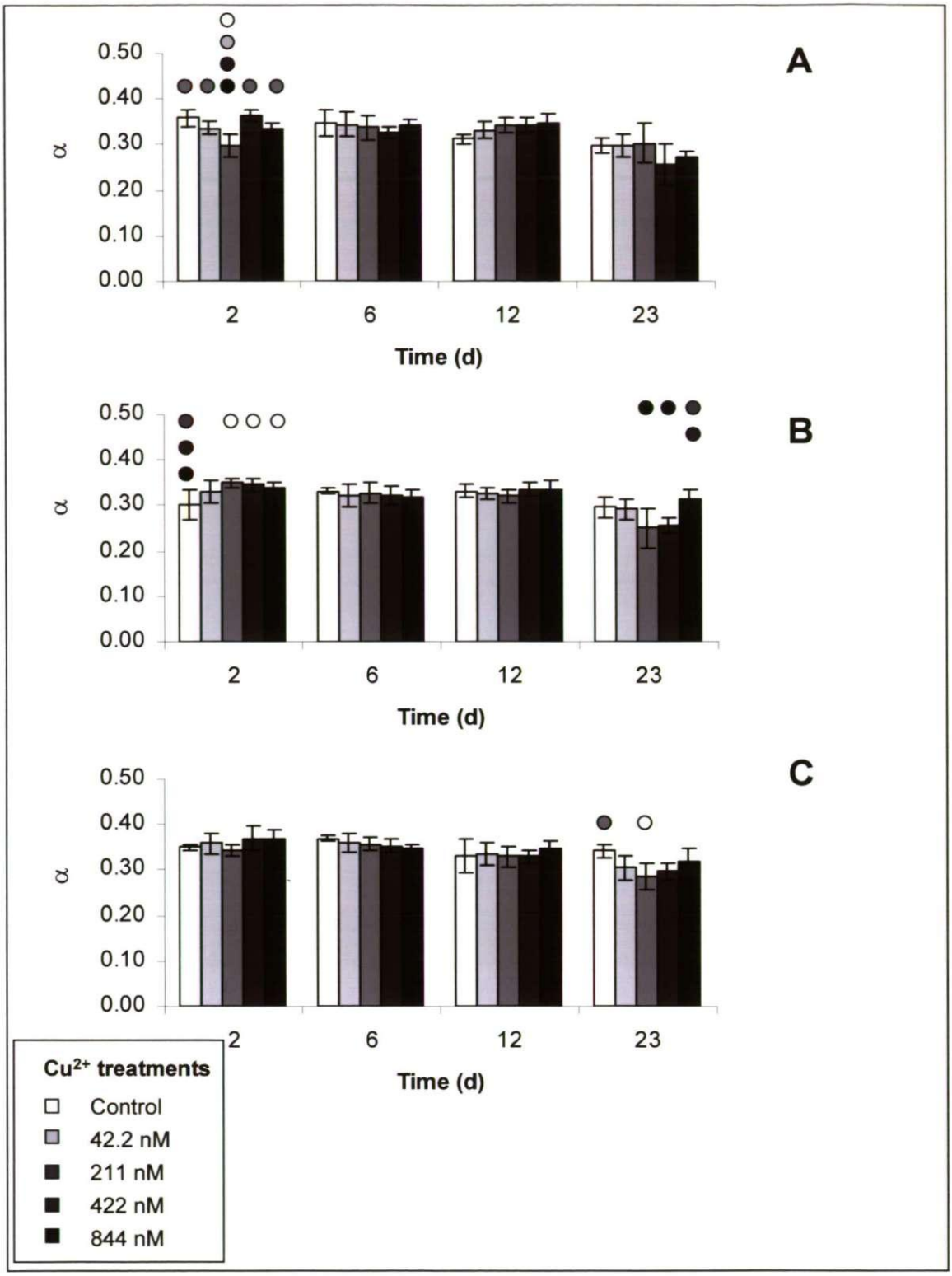

Figure 2.09. Effects of Cu^{2+} on photosynthetic efficiency (α) was calculated using chlorophyll fluorescence measurements of Bantham (**A**), Wembury (**B**), and Restronguet fronds (**C**). Fronds were incubated for 23 days in various Cu^{2+} concentrations. Significant differences ($p<0.01$) in the α values between fronds in two treatments within the populations on the different days are indicated by their appropriate colour code. Values represents means ± 1 SD (n=5).

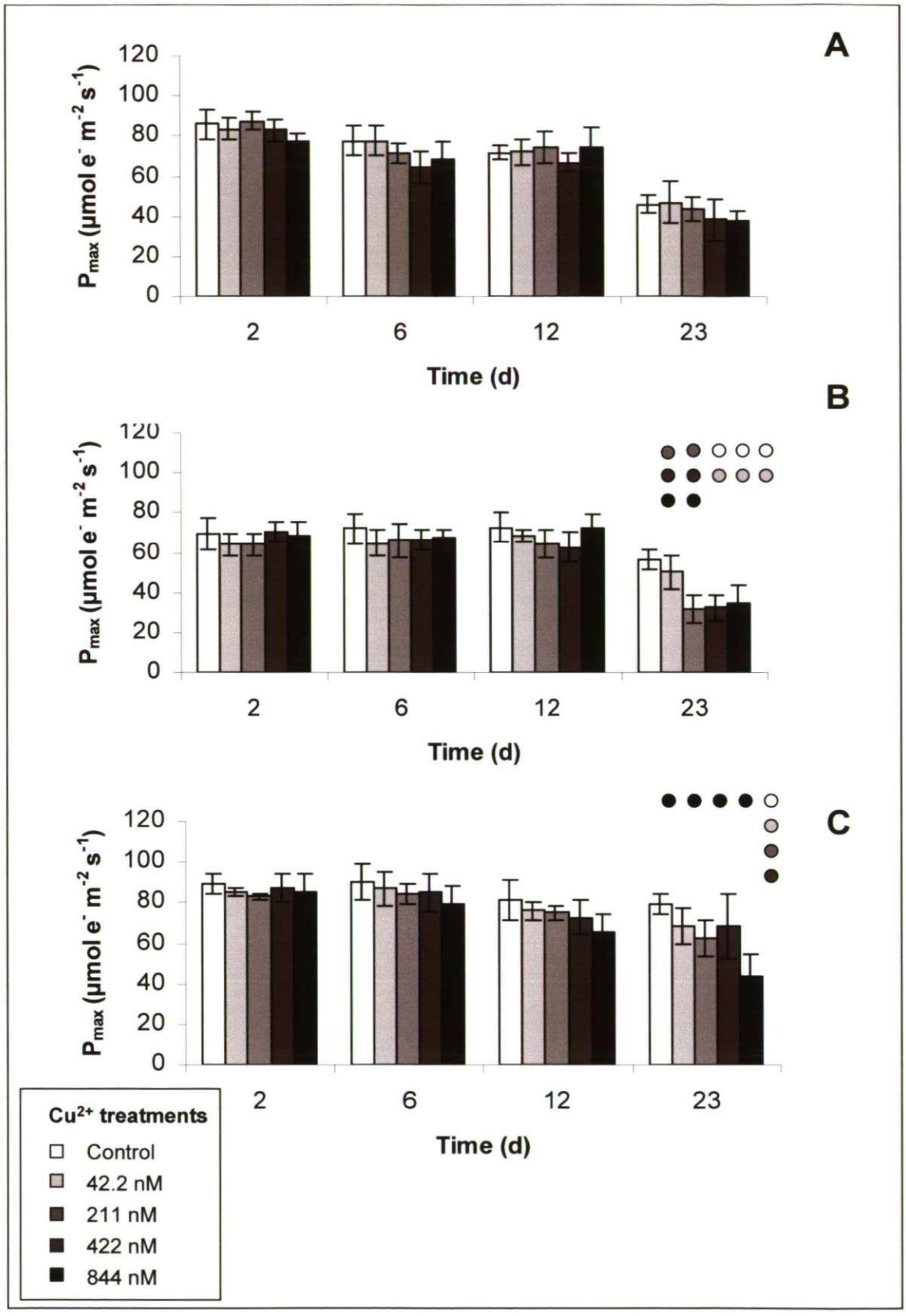

Figure 2.10. Effects of Cu^{2+} on photosynthetic capacity P_{max} calculated from chlorophyll fluorescence measurements of Bantham (**A**), Wembury (**B**), and Restronguet fronds (**C**). Fronds were incubated for 23 days various concentrations of Cu^{2+}. Significant differences ($p<0.01$) in the P_{max} values between fronds in two treatments within the populations on the different days are indicated by their appropriate colour code. Values represents means ± 1 SD (n=5).

2.3.3.3. F_v/F_m

There were significant differences in F_v/F_m between treatments and interactions between Cu^{2+} and time in all of the populations tested ($p<0.01$) (Figure 2.11). However, these effects were slight and did not correlate with [Cu^{2+}] and no obvious differences between the populations were observed.

2.3.3.4. Photochemical quenching (*qp*)

Some inhibitory effect of Cu^{2+} on *qp* was observed for the three populations towards the end of the experiment, though no pronounced differences between the populations were observed (Figure 2.12). *qp* values of Bantham control fronds were reduced significantly after 23 days compared with the previous days ($p<0.01$) (Figure 2.12 A). After 12 days, *qp* of fronds exposed to 422 nM Cu^{2+} was reduced significantly compared with *qp* of fronds exposed to 0 and 42.2 nM ($p<0.01$). After 23 days, there was no significant effect on *qp* of fronds exposed to up to 844 nM Cu^{2+} ($p>0.01$), although the data showed a decreasing trend in *qp* with increasing Cu^{2+}. *qp* of Wembury fronds exposed to 211 to 844 nM Cu^{2+} was reduced significantly compared to *qp* of fronds exposed to 0 and 42.2 nM Cu^{2+} after 23 days ($p<0.01$), although there were no significant differences in *qp* of fronds exposed to these concentrations ($p>0.01$) (Figure 2.12 B). For Restronguet fronds, no significant effect on *qp* was observed for all treatments apart from a reduction in *qp* at 844 nM Cu^{2+} after 23 days ($p<0.01$) (Figure 2.12 C).

2.3.3.5. Non-photochemical quenching (NPQ)

NPQ increased with time during the experiment for controls in all populations and significant effects of Cu^{2+} were found ($p<0.01$) (Figure 2.13). These were different for the different populations. For Bantham and Wembury fronds, the effect of Cu^{2+} on NPQ occurred

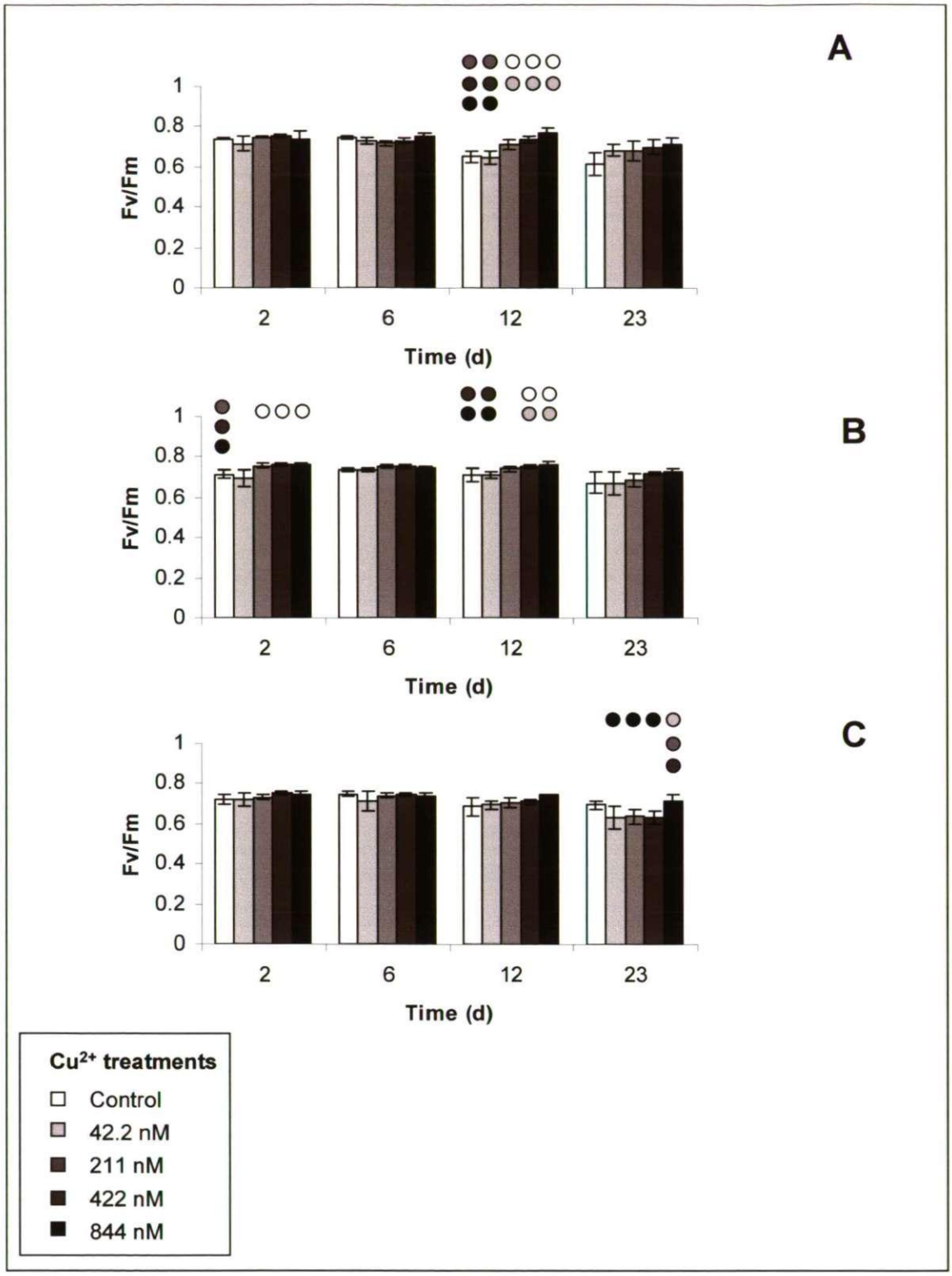

Figure 2.11. Effects of Cu^{2+} on F_v/F_m of Bantham (**A**), Wembury (**B**), and Restronguet fronds (**C**). Fronds were incubated for 23 days in various Cu^{2+} concentrations. Significant differences ($p<0.01$) in the F_v/F_m values between fronds in two treatments within the populations on the different days are indicated by their appropriate colour code. Values represents means ± 1 SD (n=5).

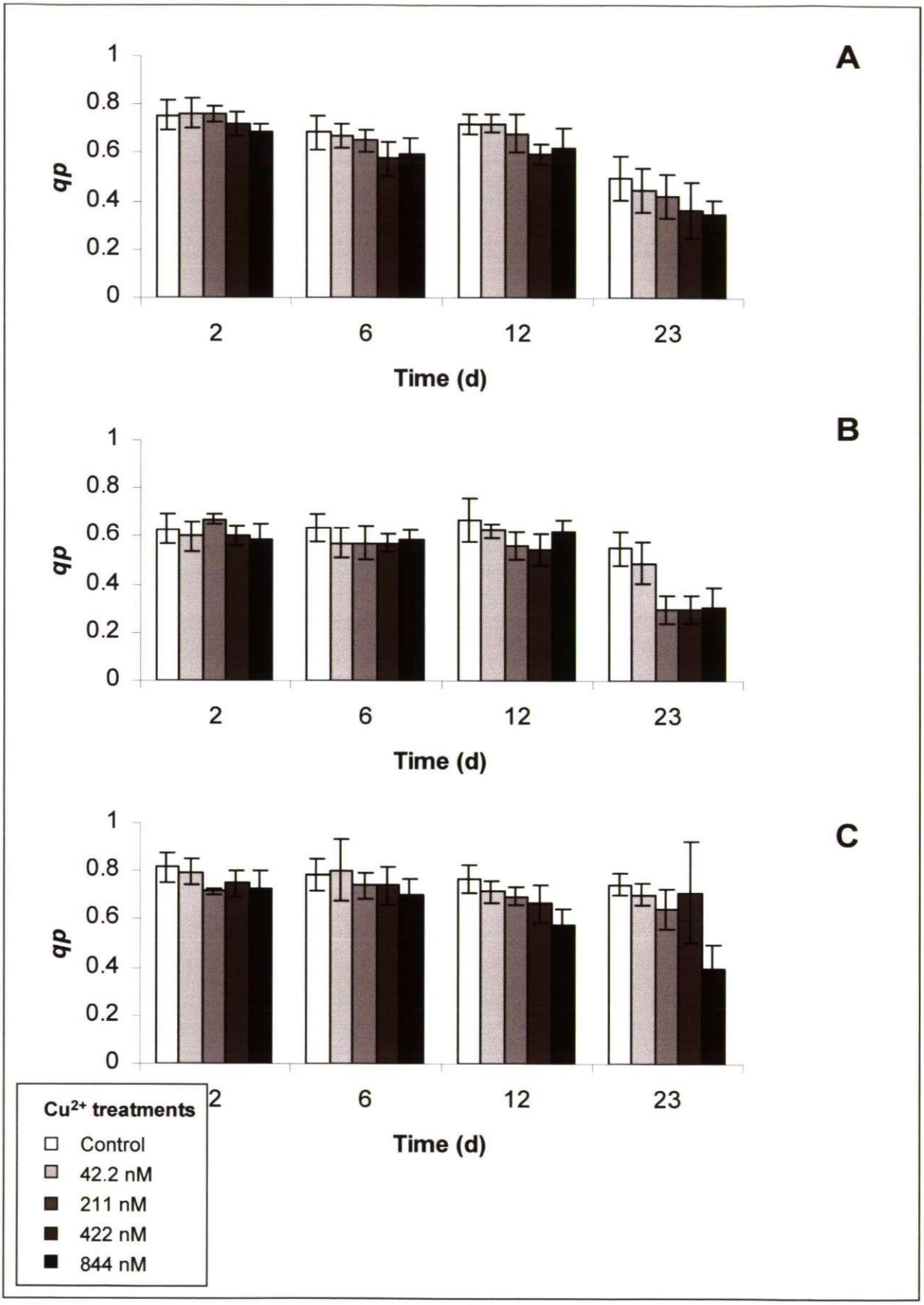

Figure 2.12. Effect of Cu^{2+} on the photochemical quenching ($qp = \Phi_{PSII}/(F_v/F_m)$) at 365 µmol m^{-2} s^{-1} PAR of Bantham (**A**), Wembury (**B**), and Restronguet (**C**) fronds during 23 days of exposure to Cu^{2+} concentrations varying from 0 to 844 nM. Values represents means ± 1 SD (n=5).

mainly at intermediate [Cu^{2+}], whereas the effect of Cu^{2+} on NPQ of Restronguet fronds was more pronounced at the highest [Cu^{2+}].

For Bantham fronds after 12 days, NPQ of fronds exposed to 422 nM was significantly increased compared with NPQ of fronds exposed to lower [Cu^{2+}] ($p<0.01$) (Figure 2.13 A). After 23 days there was no significant difference between NPQ of fronds exposed to up to 844 nM Cu^{2+} and control fronds ($p>0.01$). However, NPQ of fronds exposed to 422 and 844 nM Cu^{2+} was significantly lower than NPQ of fronds exposed to 42.2 nM ($p<0.01$).

A similar trend with different [Cu^{2+}] was also seen in Wembury fronds (Figure 2.13 B). After 6 days, NPQ of fronds exposed to 211 and 422 nM Cu^{2+} was increased significantly ($p<0.01$). However, there was no significant difference in NPQ of fronds exposed to 844 nM Cu^{2+} and any of the other treatments ($p>0.01$). After 23 days, NPQ of fronds exposed to 211 and 422 nM was increased significantly compared to NPQ of control fronds ($p<0.01$). When [Cu^{2+}] increased to 844 nM NPQ was significantly lower than that of fronds exposed to 211 and 422 nM ($p<0.01$), but not significantly different to NPQ of fronds exposed to 0 and 42.2 nM ($p>0.01$).

For Restronguet fronds, NPQ increased with experiment time and with increasing [Cu^{2+}] after 6, 12 and 23 days (Figure 2.13 C). After 6 days, NPQ of fronds exposed to 844 nM Cu^{2+} was significantly increased compared with NPQ of fronds in any other treatment ($p<0.01$). After 12 days, [Cu^{2+}] above 211 nM resulted in significantly increasing NPQ, which was 8-fold higher at 844 nM than NPQ of control fronds ($p>0.01$). After 23 days NPQ of fronds exposed to 422 nM was significantly higher than NPQ of control fronds

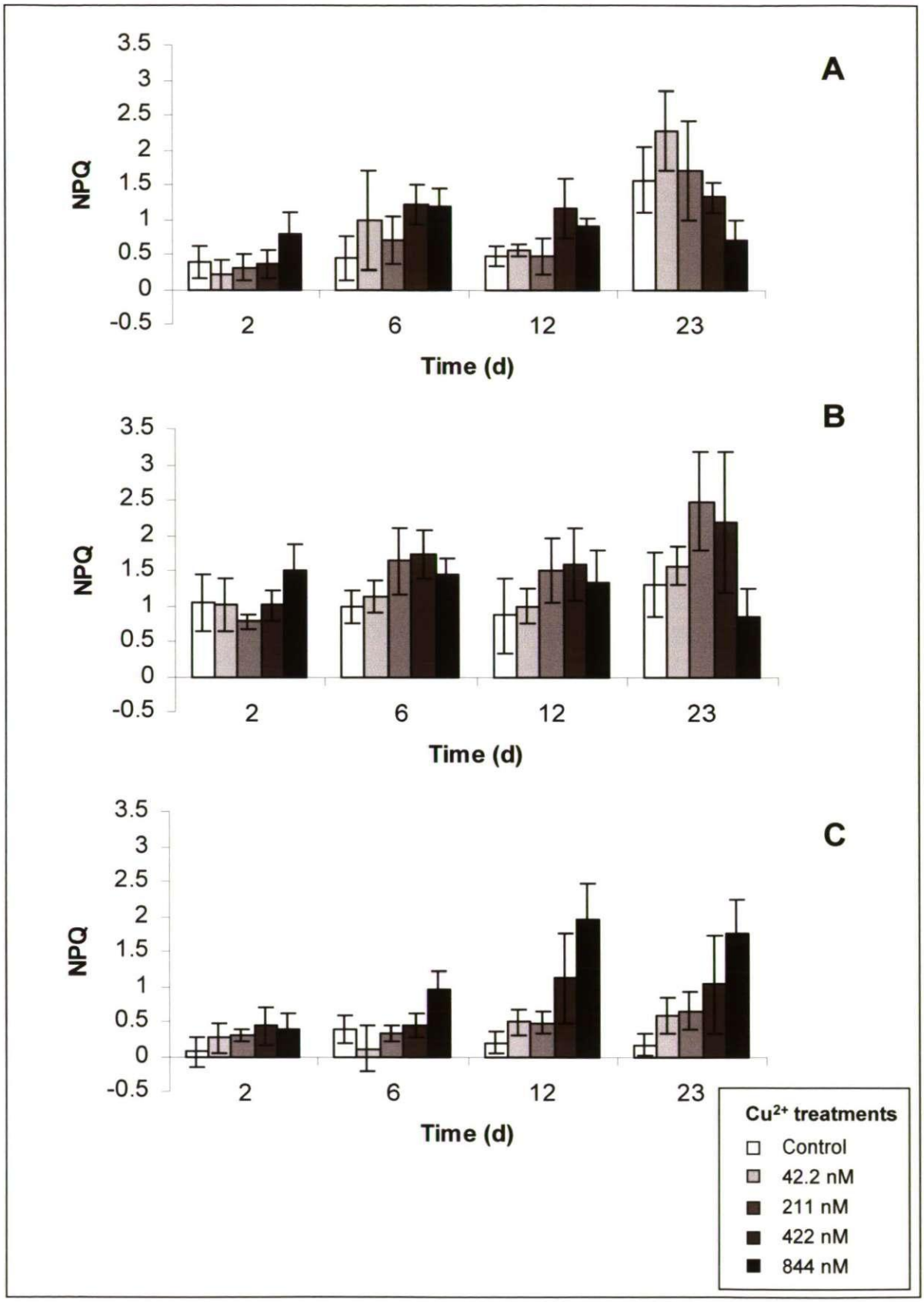

Figure 2.13. Effect of Cu^{2+} on non-photochemical quenching (NPQ = F_m-F'_m/F'_m) at 365 µmol m^{-2} s^{-1} PAR of Bantham (**A**), Wembury (**B**), and Restronguet (**C**) fronds during 23 days of exposure to Cu^{2+} concentrations varying from 0 to 844 nM. Values represents means ± 1 SD (n=5).

($p<0.01$). NPQ of fronds exposed to 844 nM was significantly higher than NPQ of fronds in any other treatment and 8-fold higher than NPQ of control fronds ($p<0.01$).

2.3.3.6. Values of F'_m and F_t

There were significant effects of Cu^{2+}on F'_m and significant interactions between Cu^{2+} and time ($p<0.01$) (Figure 2.14). The negative effect of Cu^{2+} on F'_m was most pronounced for Wembury fronds. The effect of Cu^{2+} on F'_m of Bantham fronds was inconsistent, whereas the effect on F'_m of Restronguet only occurred at the highest [Cu^{2+}] tested. Negative effects of Cu^{2+} on F_t were observed for all three populations tested, although this effect was more pronounced for Wembury than Bantham and Restronguet fronds (Figure 2.15).

2.3.4. Oxygen evolution

Gross PS of the fronds was calculated from measurements of oxygen evolution at photosynthetically saturating light and dark respiration after 23 days (Figure 2.16). Cu^{2+} had an inhibitory effect on gross PS of Bantham and Restronguet fronds whereas gross PS of Wembury fronds was unaffected. Oxygen evolution of control fronds from the three populations ranged from 0.34 ± 0.10 to 0.40 ± 0.08 O_2 g^{-1} FW min^{-1} and there were no significant differences between them ($p>0.01$).

For Bantham fronds [Cu^{2+}] above 211 nM had an inhibitory effect on gross PS, which declined significantly to 0.27 ± 0.04 O_2 g^{-1} min^{-1} in fronds exposed to 422 nM compared 0.46 ± 0.08 O_2 g^{-1} min^{-1} of fronds exposed to 42.2 nM Cu^{2+} ($p<0.01$). Gross PS of fronds exposed to 422 nM Cu^{2+} was not significantly different from gross PS of control fronds

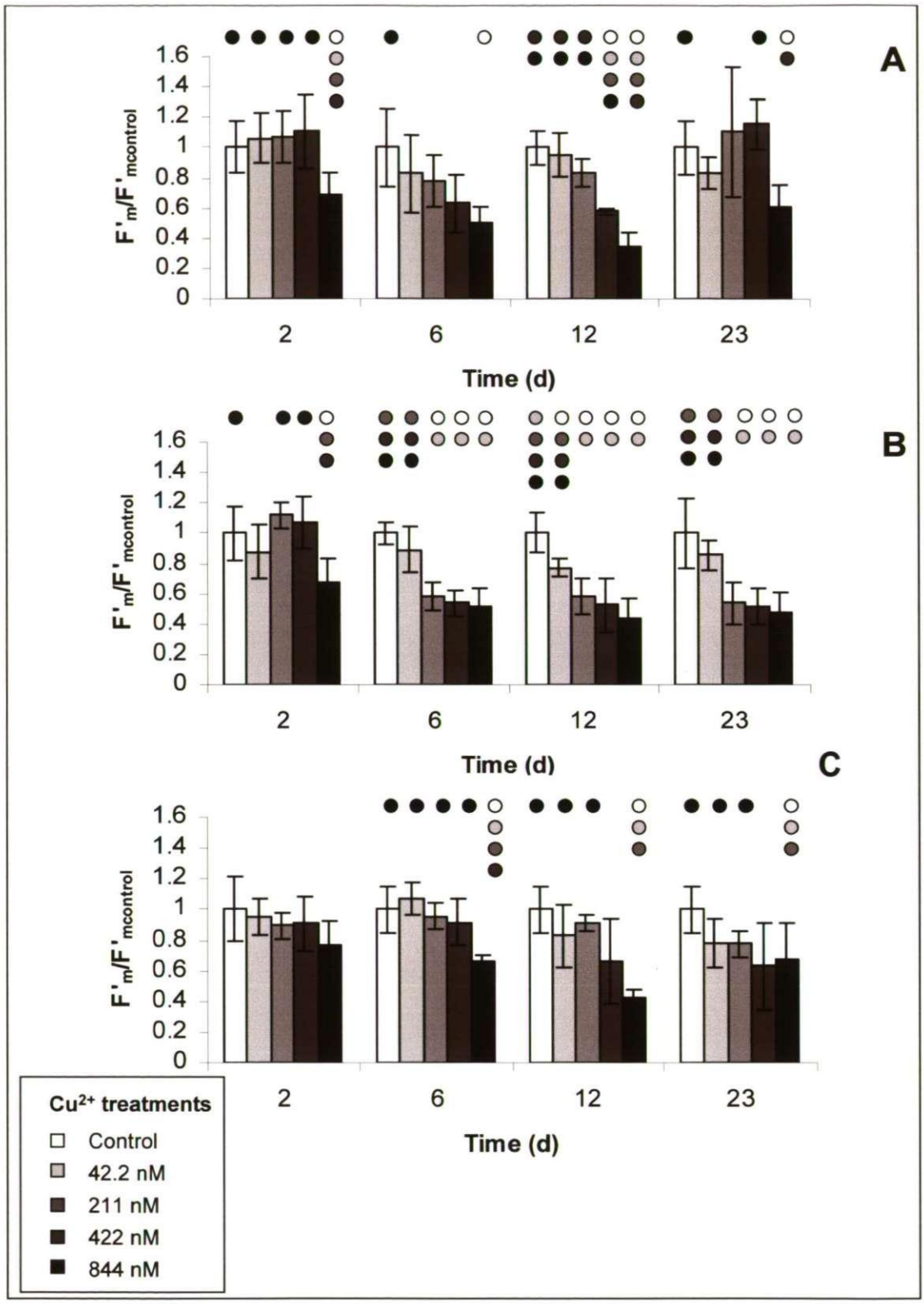

Figure 2.14. Effects of Cu^{2+} on F'_m measured as chlorophyll fluorescence at a photosynthetically saturating light intensity of 365 µmol m^{-2} s^{-1} PAR of Bantham (**A**), Wembury (**B**), and Restronguet (**C**) fronds. Fronds were incubated for 23 days in various Cu^{2+} concentrations. Significant differences ($p<0.01$) in the F'_m values between fronds in two treatments within the populations on the different days are indicated by their appropriate colour code. Values represents means ± 1 SD (n=5).

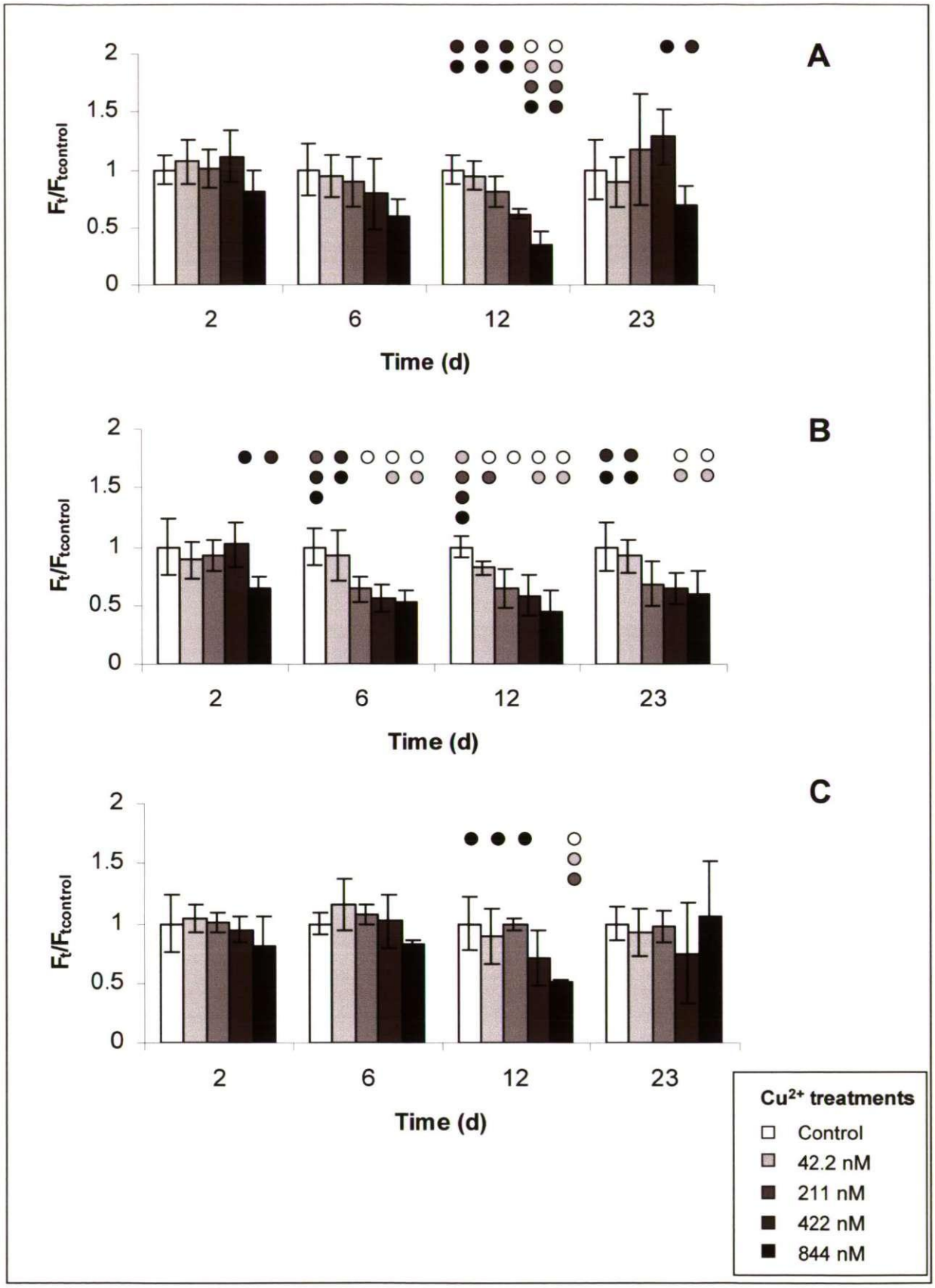

Figure 2.15. Effect of Cu^{2+} on F_t at 365 µmol m^{-2} s^{-1} PAR of Bantham (**A**), Wembury (**B**), and Restronguet (**C**) fronds during 23 days of exposure to Cu^{2+} concentrations varying from 0 to 844 nM. Significant differences ($p<0.01$) in the F_t values between fronds in two treatments within the populations on the different days are indicated by their appropriate colour code. Values represents means ± 1 SD (n=5).

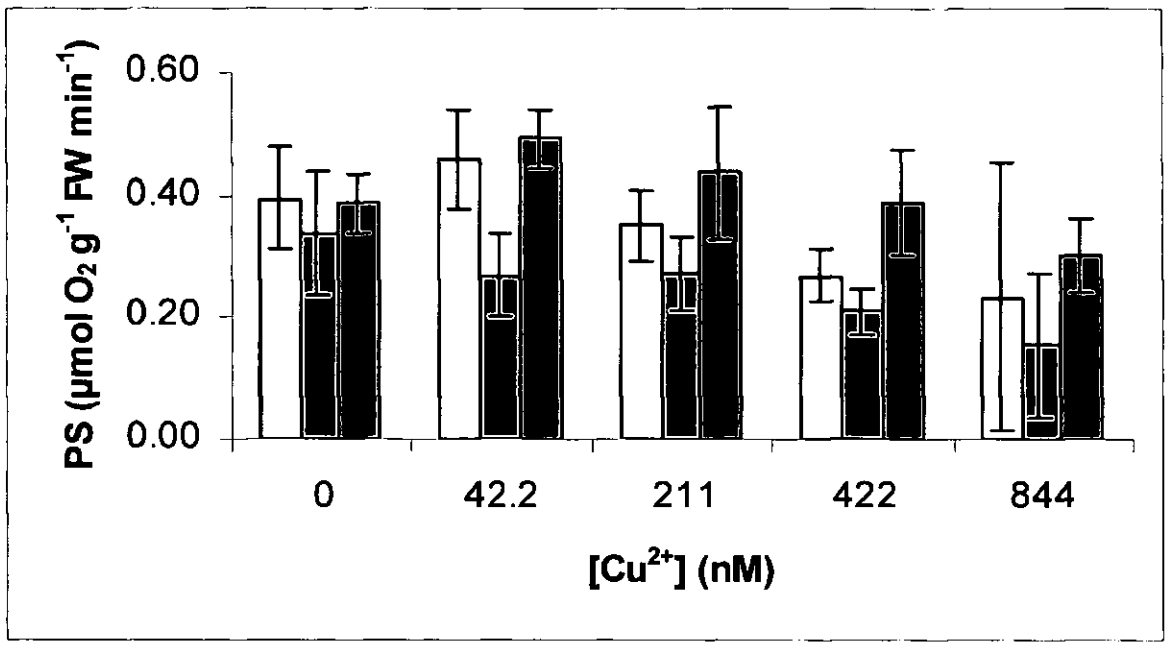

Figure 2.16. Effect of Cu^{2+} on gross photosynthesis based on oxygen evolution and consumption of Bantham (□), Wembury, (▣), and Restronguet (■) fronds measured at a saturating light intensity of 500 µmol m^{-2} s^{-1} PAR after 23 days of exposure to various Cu^{2+} concentrations. Values represents means ± 1 SD (n=5).

and fronds exposed to 211 and 844 nM Cu^{2+} ($p>0.01$) though a trend towards decreased gross PS with increasing Cu^{2+} was apparent. For Wembury fronds there was no significant effect on gross PS of $[Cu^{2+}]$ up to 844 nM ($p>0.01$). For Restronguet fronds there was no significant effect on gross PS of $[Cu^{2+}]$ up to 422 nM ($p>0.01$). Gross PS of fronds exposed to 844 nM was reduced significantly to 0.30 ± 0.06 O_2 g^{-1} min^{-1} compared to 0.49 ± 0.05 O_2 g^{-1} min^{-1} of fronds exposed to 42.2 nM ($p<0.01$) but was not significantly different to gross PS of control fronds and fronds exposed to 211 and 422 nM ($p>0.01$). The highly variable gross PS of both Bantham and Wembury fronds during exposure to 844 nM Cu^{2+} may be an expression of the generally very poor condition of the fronds exposed to this concentration.

During exposure to 42.2 nM Cu^{2+} gross PS of Bantham and Restronguet fronds was significantly higher than gross PS of Wembury fronds ($p<0.01$), whereas PS of Bantham and Restronguet fronds was not significantly different at this concentration ($p>0.01$). During exposure to 422 nM Cu^{2+} gross PS of Restronguet fronds was significantly higher than gross PS of Wembury fronds ($p<0.01$), whereas gross PS of Bantham fronds was not significantly different from gross PS of either Wembury or Restronguet fronds ($p>0.01$).

2.3.5. Chlorophyll *a* content of fronds

The chlorophyll *a* content of fronds from the three populations was measured after 23 days of exposure to various $[Cu^{2+}]$ (Figure 2.17). The chlorophyll *a* content of control fronds was 0.32 ± 0.05 to 0.39 ± 0.13 μg g^{-1} DW and there was no significant difference between the three populations ($p>0.01$). There was no significant effect of $[Cu^{2+}]$ up to 844 nM on the chlorophyll *a* content of Wembury and Restronguet fronds ($p>0.01$). In Bantham

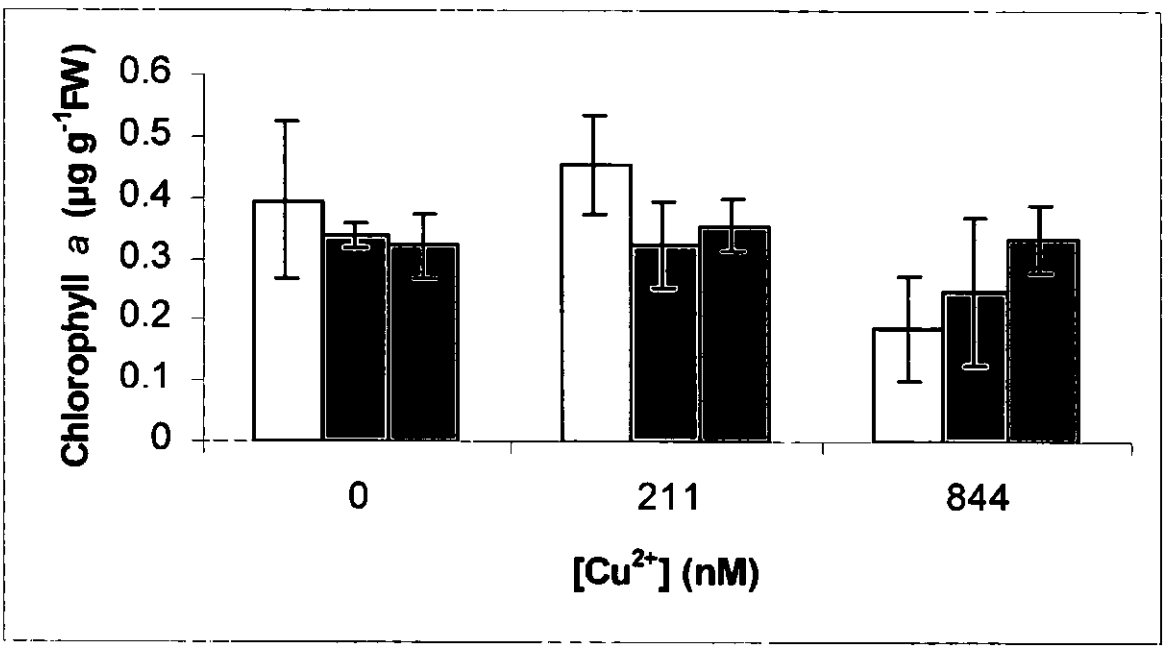

Figure 2.17. Chlorophyll *a* content of Bantham (□), Wembury (■), and Restronguet (■) fronds after 23 days of incubation in various Cu^{2+} concentrations. Values represents means ± 1 SD (n=5).

fronds the chlorophyll *a* content was unaffected by [Cu^{2+}] up to 211 nM ($p>0.01$), but it was reduced by about 50% to 18.7±0.08 when exposed to 844 nM Cu^{2+} ($p<0.01$).

2.3.6. Ligand and copper contents of fronds

2.3.6.1. Secretion of organic substances

For Bantham fronds, after 1 day, secretion of organic substances from fronds exposed to 844 nM was 6.2-fold higher than that of control fronds ($p<0.01$) (Figure 2.18 A). After 2 days secretion had decreased to 3-fold higher than of control fronds ($p<0.01$) and stayed at this level from day 6 until day 23 ($p>0.01$).

For Wembury fronds, after 1 day, secretion of fronds exposed to 844 nM Cu^{2+} was 3.4-fold higher than secretion of control fronds ($p<0.01$) (Figure 2.18 B). After 2 days up until 23 days, fronds exposed to 844 nM Cu^{2+} continued to secrete 2.1 to 3.6 fold more organic substances than control fronds ($p<0.01$).

For Restronguet fronds exposed to 844 nM Cu^{2+}, secretion was significantly 3-fold higher than that of control fronds after 1 day of exposure ($p<0.01$) (Figure 2.18 C). However, in contrast to Bantham and Wembury fronds, secretion of organic substances by Restronguet fronds had declined to the level of control fronds after 2 days of incubation ($p<0.01$). Secretion stayed at this level after 6 and 23 days of incubation ($p>0.01$), but after 12 days of exposure to 844 nM Cu^{2+} the fronds secreted 1.9 fold more organic substances than control fronds ($p<0.01$).

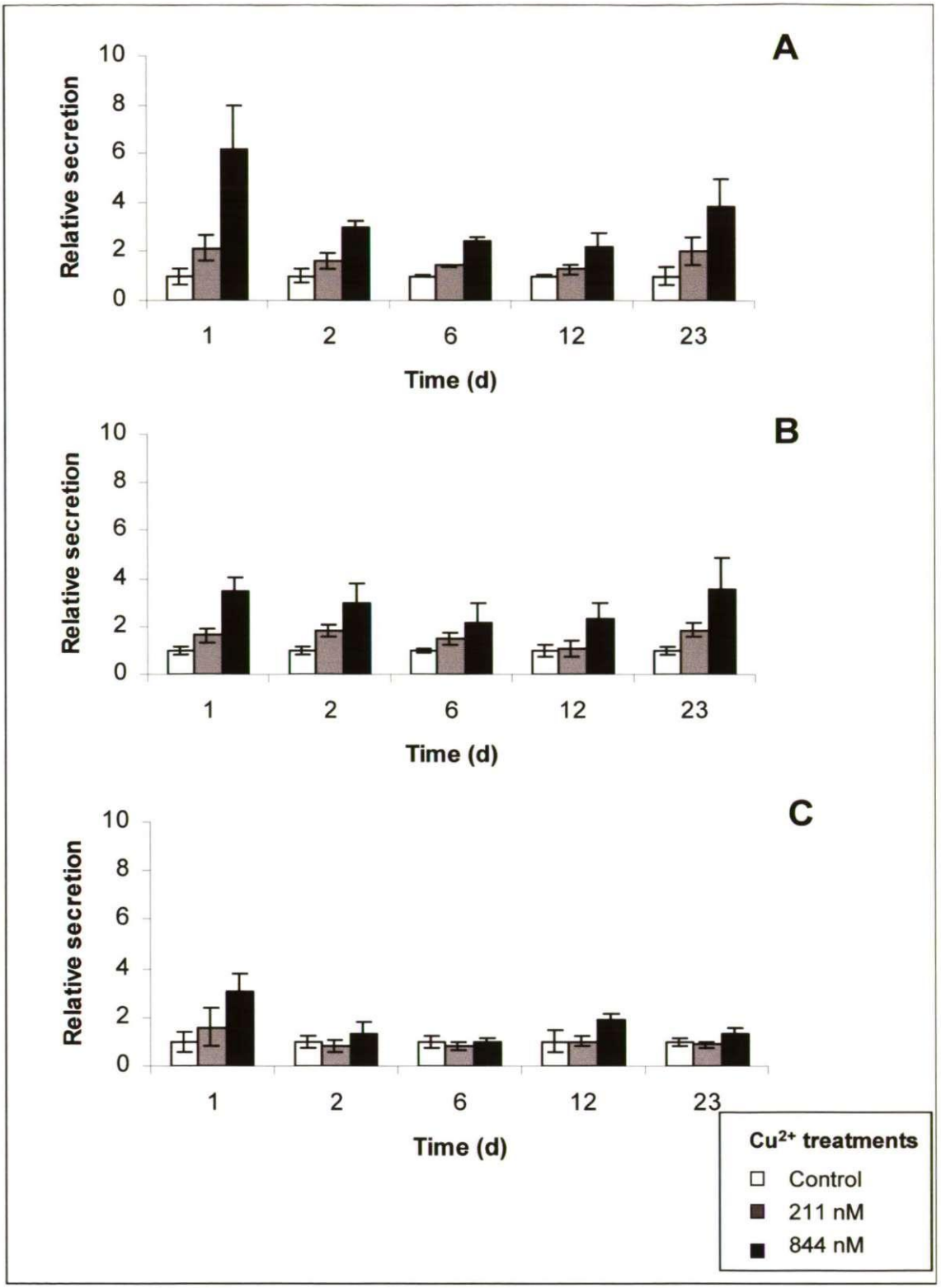

Figure 2.18. Secretion of organic substances by Bantham (**A**), Wembury (**B**), and Restronguet (**C**) fronds over 24 h following 1 to 23 days exposure to Cu^{2+} concentrations varying from 0 to 844 nM. Secretion (absorbance g^{-1} FW frond ml^{-1}) was estimated by measuring absorbance of the incubation medium. Relative secretion was calculated as 'secretion/secretion of control'. Values represents means ± 1 SD (n=5).

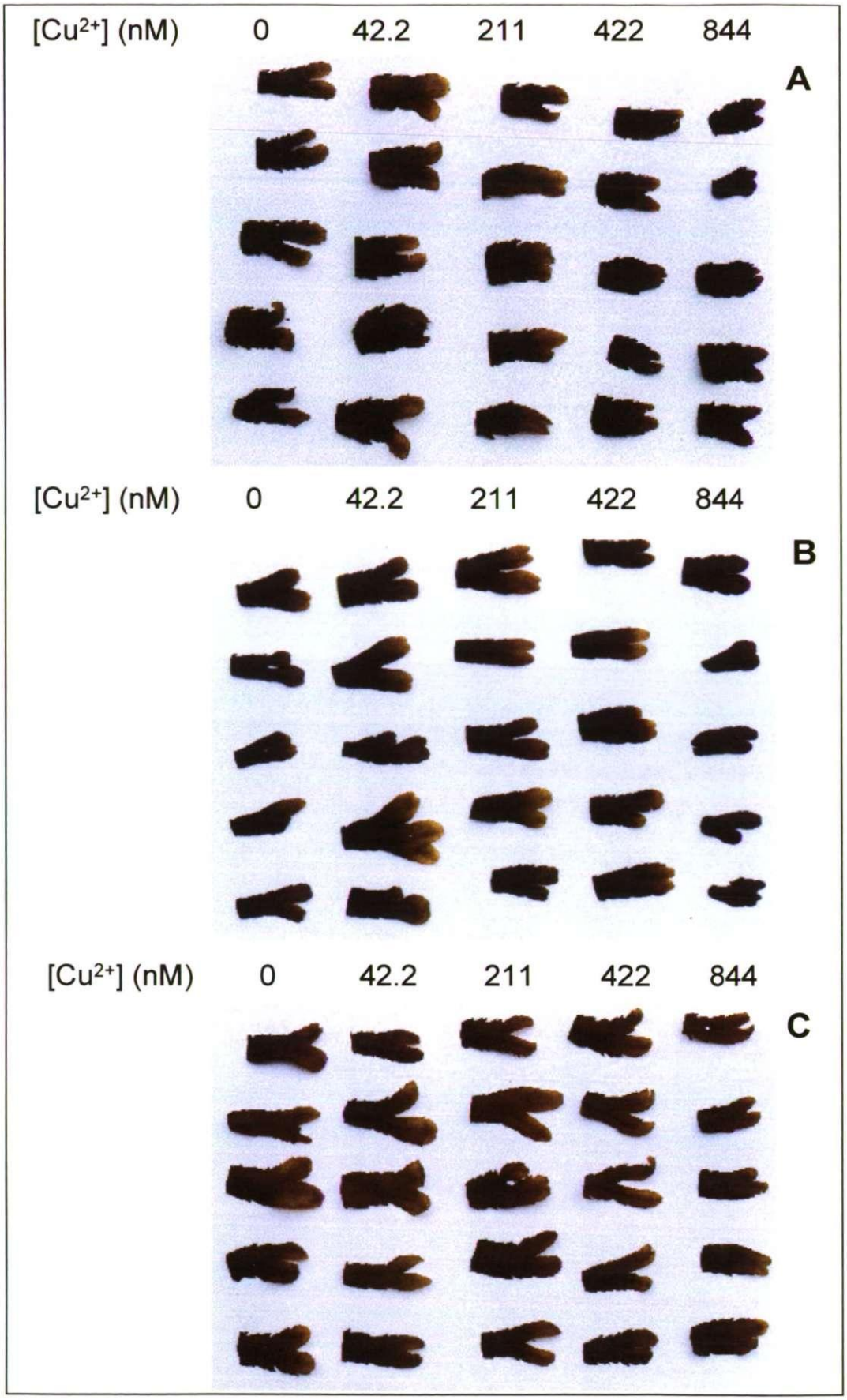

Figure 2.19. Pictures of fronds of *Fucus* after 23 days exposure to Cu^{2+} concentrations varying from 0 to 844 nM. There was a darkening, which was obvious to the naked eye, of Bantham (**A**) and Wembury (**B**) fronds with increasing concentrations of Cu^{2+}. There was no effect of Cu^{2+} on the colour of Restronguet fronds.

2.3.6.2. Darkening of fronds

Figure 2.19 shows pictures of the experimental fronds after 23 days of incubation in Aquil containing [Cu^{2+}] varying from 0 to 844 nM. Bantham and Wembury fronds exposed to 844 nM Cu^{2+} and Bantham fronds exposed to 422 nM Cu^{2+} were clearly darker brown in colour than fronds exposed to lower concentrations and control fronds. No apparent colour change of Restronguet fronds occurred during the course of the experiment.

2.3.6.3. Total copper content of fronds

The total copper contents of fronds were measured initially and after exposure to various [Cu^{2+}] for 23 days (Figure 2.20 A). The natural total copper content of Bantham and Wembury fronds prior to the experiment was 5.9 ± 1.7 $\mu g\ g^{-1}$ DW and 10.9 ± 2.4 $\mu g\ g^{-1}$ DW respectively, which was significantly lower than the natural total copper content of Restronguet fronds prior to the experiment (59.2 ± 20.8 $\mu g\ g^{-1}$ DW ($p<0.01$)). There was a significant effect of Cu^{2+} on the total copper content of fronds from all three populations and significant variation between populations ($p<0.01$). Bantham fronds were good copper accumulators over the whole of the concentration spectrum, whereas the increase in total copper content of Restronguet fronds was less pronounced than that of Bantham and Wembury fronds.

The total copper content of Bantham and Wembury control fronds was 6.7 ± 2.81 $\mu g\ g^{-1}$ DW and 2.5 ± 0.6 $\mu g\ g^{-1}$ DW respectively and significantly different ($p<0.01$), and significantly lower than the total copper content of Restronguet control fronds (24.2 ± 9.8 $\mu g\ g^{-1}$ DW ($p<0.01$)). At 42.2 and 211 nM the total copper content of Bantham and Restronguet fronds was not significantly different ($p>0.01$) but higher than that of Wembury fronds ($p<0.01$). At 211 nM Cu^{2+} the total copper content of Bantham fronds

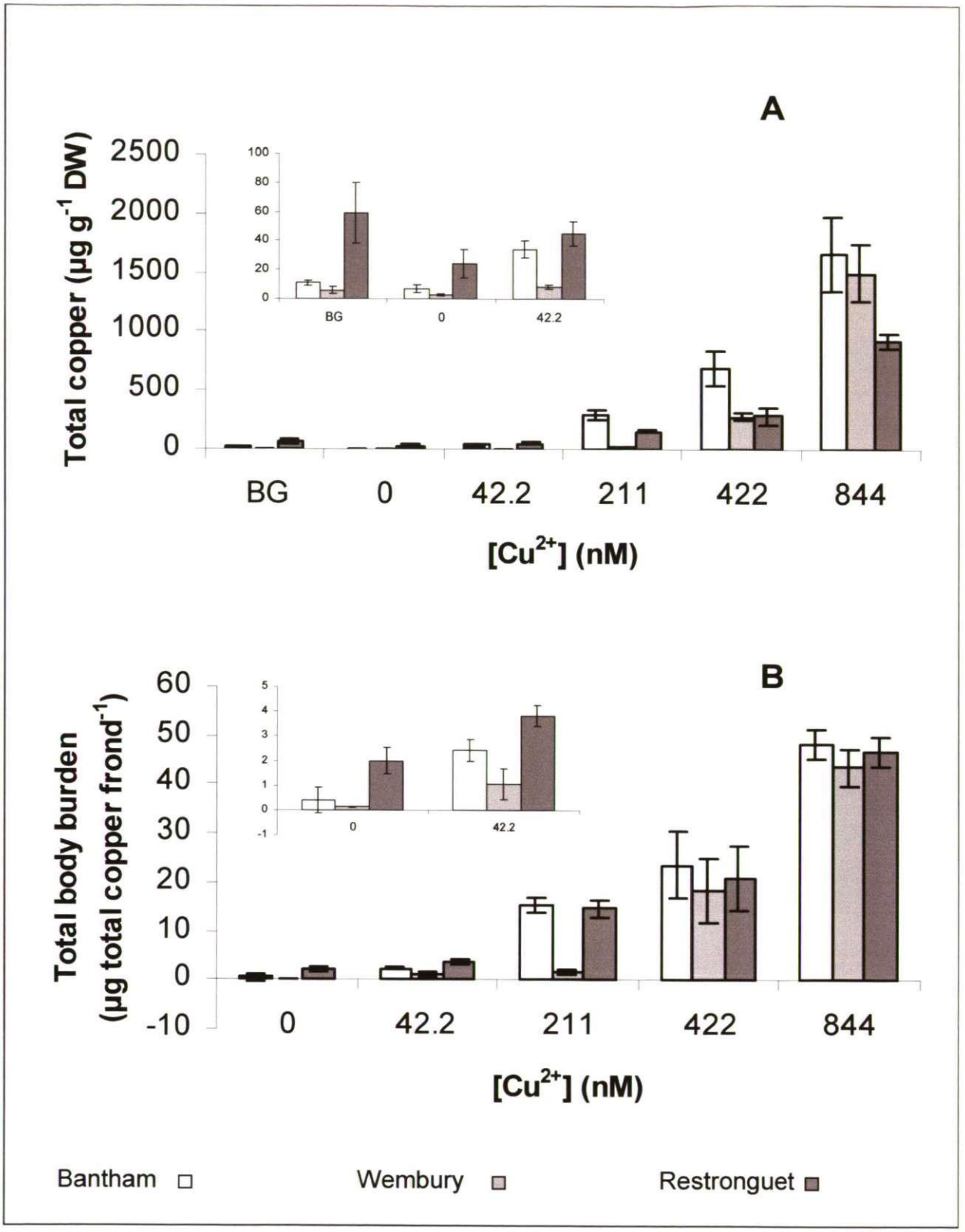

Figure 2.20. Total copper content after 23 days of incubation in Cu^{2+} concentrations ranging from 0 to 844 nM, and background (BG) total copper content of fronds prior to the pre-incubation period (**A**), and total body burden of fronds exposed to 0 to 844 nM Cu^{2+} for 23 days (**B**). Values represents means ± 1 SD (n=4).

was increased 43-fold compared with control fronds whereas the increase in the total copper content of Wembury and Restronguet fronds was 10- and 6-fold respectively. When exposed to 422 nM Cu^{2+} the total copper content of Bantham fronds was 696.1 ± 38.3 μg g^{-1} DW which was equivalent to a 103-fold increase and significantly higher than the total copper content of Wembury and Restronguet fronds ($p<0.01$) (282.9 ± 38.3 μg g^{-1} DW and 290.4 ± 13.8 μg g^{-1} DW respectively). The increase in the total copper content of Wembury fronds exposed to 422 nM Cu^{2+} was equivalent to a 113-fold increase compared with control fronds and that of Restronguet fronds to a 12-fold increase. At exposure to 844 nM, there was no significant difference in the total copper contents of Wembury and Bantham fronds which were 1496.7 ± 238.8 μg g^{-1} DW and 1662.1 ± 320.9 μg g^{-1} DW respectively ($p>0.01$), whereas that of Restronguet fronds (923 ± 54.4 μg g^{-1} DW) was significantly lower than that of Bantham and Wembury fronds ($P<0.01$). The total copper content of Bantham fronds exposed to 844 nM was equivalent to a 245-fold increase compared with control fronds, whereas that of Wembury fronds was equivalent to a 601-fold increase compared with control fronds and that of Restronguet fronds to a 38-fold increase.

2.3.6.4. Total copper burden of fronds

The total copper body burden of the fronds after 23 days exposure to various [Cu^{2+}] was also calculated as total copper content per frond (~3 cm apical thallus on day 0) (Figure 2.20 B). The copper burden of Bantham and Wembury control fronds was 0.41 ± 0.52 μg $frond^{-1}$ and 0.13 ± 0.03 μg $frond^{-1}$ respectively which was not significantly different ($p>0.01$), but 2-fold higher than the copper burden of Restronguet control fronds (2.0 ± 0.50 μg $frond^{-1}$ ($p>0.01$)). At 42.2 nM the copper body burden of Bantham fronds was significantly higher than that of Wembury fronds ($p<0.01$) and lower than that of Restronguet fronds ($p<0.01$). At 211 nM the copper body burden of Bantham and

Restronguet fronds was 15.3 ± 0.17 μg frond^{-1} and 14.6 ± 0.52 μg frond^{-1} respectively and not significantly different ($p>0.01$), but significantly 8.5-fold higher than the copper body burden of Wembury fronds which was 1.74 ± 0.042 μg frond^{-1} ($p<0.01$). At 422 and 844 nM Cu^{2+} the total copper body burden was 20.9 ± 6.7 and 46 ± 3.4 μg frond^{-1} respectively, and was not significantly different between the three populations.

2.4. Discussion

Fucus has the ability to develop Cu^{2+} tolerant and non-tolerant populations dependent on the Cu^{2+} status in their natural environment. In the present study it was shown that Restronguet fronds were more tolerant to Cu^{2+} exposure than Bantham and Wembury fronds, which had the same low tolerance limit. This finding reflected the Cu^{2+} status in the locations from which the algae were collected. The average copper concentration in Restronguet Creek was about 0.2 μM over the past 10 years, and 20-fold higher than the 10 nM which was average for the Avon Estuary during the same time period (Chapter 1). Similarly, Bryan and Gibbs (1983) showed that Restronguet Creek *Fucus* had a higher copper tolerance limit than *Fucus* from 'clean' estuaries.

2.4.1. Effects of Cu^{2+} on photosynthesis in *Fucus*

2.4.1.1. Effect of Cu^{2+} on the quantum yield of PSII

The photosynthetic apparatus of Restronguet fronds appeared to be better adapted to tolerate prolonged exposure to elevated [Cu^{2+}] than that of Bantham and Wembury fronds. The photosynthetic capacity (P_{max}) calculated from the quantum yield (Φ_{PSII}) at the photosynthetic saturating irradiance of 365 μmol m^{-2} s^{-1} PAR of Wembury fronds exposed to [Cu^{2+}] $\geq$ 211 nM decreased by about 40% compared with control fronds after 23 days (Figure 2.10 B). In comparison, P_{max} of Restronguet fronds was only inhibited at 844 nM Cu^{2+} which gave a reduction of nearly 50% compared to control fronds (Figure 2.10 C). Consequently, photosynthesis of Restronguet fronds had a higher tolerance threshold to Cu^{2+} than Wembury fronds. On the other hand, there was no significant difference in P_{max} of Bantham fronds exposed to 0 to 844 nM Cu^{2+} (Figure 2.10 A). This apparent Cu^{2+}

tolerance of Bantham fronds may have been caused by general effects of the long incubation period on P_{max} which was highly reduced in all treatments compare with the previous days, and may have offset any effects of Cu^{2+}.

The negative effect of Cu^{2+} on Φ_{PSII} and higher tolerance limit of the Restronguet fronds is confirmed by calculations of gross photosynthesis (gross PS) based on measurements of oxygen evolution (Figure 2.16). Gross PS of Bantham and Restronguet fronds in saturating light was reduced after 23 days of exposure to [Cu^{2+}] above 211 and 844 nM. Although there was no significant effect of exposure to 844 nM Cu^{2+} on gross PS of either Bantham or Wembury fronds, the highly variable data at this concentration suggests that there was indeed an effect of Cu^{2+} on gross PS, which was negative for some fronds. Consequently, the oxygen measurements point towards a higher tolerance limit for Restronguet fronds. The inhibitory effect of Cu^{2+} on Φ_{PSII} and oxygen evolution in the present study may be caused by inhibition of the electron transport through photosystem II (PSII). It has been shown in several experiments that Cu^{2+} has the potential to inhibit photosynthesis by targeting photosynthetic electron transport on either the donor or the receptor side of the reaction centre of PSII (Yruela *et al.*, 1991, 1993; Schröder *et al.*, 1994; Jegerschöld *et al.*, 1995). This inhibitory effect would result in a reduction in the efficiency of electron transport in PSII and may be the cause of the observed reduction in the quantum yield and oxygen evolution. However, there was no consistent effect of Cu^{2+} on the maximum quantum yield (F_v/F_m) of dark adapted *Fucus*, which was constant at about 0.74 for all three populations during the 23 days of exposure to up to 844 nM Cu^{2+} (Figure 2.11). Similar effects of Cu^{2+} on the quantum yield in light and darkness have been demonstrated for other species. Φ_{PSII} of maize seedlings was reduced by up to 70% at saturating irradiances after culture in 80μM $CuSO_4$ for 15 days whereas the quantum yield of dark-adapted leaves (F_v/F_m) was largely unaffected (Ouzounidou *et al.*, 1997). The results in the

present study and those by Ouzounidou and co-workers (1997) suggest that Cu^{2+} may inhibit tolerance to high irradiances at the reaction centre in PSII. The inhibitory effects of Cu^{2+} observed at photosynthetically saturating irradiances may also be the result of amplification of photoinhibition. This has been demonstrated previously for other systems, where Cu^{2+} may either cause direct damage to the membrane spanning subunit of PSII, the D1 protein *via* increased production of reactive oxygen species (ROS) (Yruela *et al.*, 1996), or inhibit the repair mechanism of photosynthetically damaged D1 protein (Pätsikkä *et al.*, 1998).

The Restronguet population seems to possess the ability to handle excess light energy better than the Bantham and Wembury population. The reduction in P_{max} of Restronguet fronds exposed to 844 nM Cu^{2+} coincided with an 8-fold increase in non-photochemical quenching after 23 days (NPQ) from <0.25 to about 2, and NPQ of fronds exposed to 422 nM increased 4-fold although there was no effect on P_{max} (Figure 2.13 C). A similar increase in NPQ occurred after 12 days although the corresponding decrease in P_{max} was not observed. Similarly, Ouzounidou and co-workers (1997) demonstrated a correlation between inhibited photosynthetic energy conversion in maize leaves during Cu^{2+} exposure and increased heat dissipation. The relationship between P_{max} and NPQ is usually expected during photoinhibition, as any decrease in photosynthetic energy conversion at a constant irradiance would normally result in an increase in the proportion of light dissipated as thermal energy (Demmig-Adams and Adams, 2000; Maxwell and Johnson, 2000). In contrast, Bantham and Wembury fronds were not well adapted to handle the negative effects on the photosynthetic apparatus caused by Cu^{2+}. There was some indication of increase in NPQ of both Bantham and Wembury fronds at 42.2-211 nM Cu^{2+}, which is lower than the concentrations, which affected NPQ of Restronguet fronds (Figure 2.13 A

and B). This finding indicated that Cu^{2+} induced photoinhibition in Bantham and Wembury fronds at lower concentrations than those which affected Restronguet fronds.

NPQ in brown algae is expected to occur mainly as heat dissipation in the xanthophyll cycle (Vershinin and Kamnev, 1996; Harker *et al.,* 1999; Coelho *et al.,* 2001), which is also considered the main path of NPQ in many flowering plants (Ruban *et al.,* 1993; Niyogi *et al.,* 1998; Demmig-Adams, 1998; Ruban and Horton, 1999). The results in the present experiment suggest that there is no inhibitory effect of Cu^{2+} on the xanthophyll cycle, which may even be increased in Restronguet fronds, whereas there are direct damaging effects of Cu^{2+} on the xanthophyll cycle in Bantham and Wembury fronds. The rate of NPQ is usually correlated with the size of the xanthophyll pool in the light harvesting complex and a high rate of de-epoxidation of violaxanthin to zeaxanthin, and a large pool of xanthophyll is one of the features, which distinguish sun-adapted plants and brown algae and allows them to have high levels of NPQ compared with shade adapted individuals (Demmig-Adams, 1998; Harker *et al.,* 1999). Consequently, the greater increase in NPQ of Restronguet fronds may be the result of more resistant xanthophyll pool than in Bantham and Wembury fronds. However, there are other features which are also determining for high NPQ. The xanthophyll cycle is dependent on conformational changes of the membrane-spanning pigment-binding protein, PsbS (Li *et al.,* 2000). Furthermore, the onset of the xanthophyll cycle occurs in response to acidification of the thylakoid lumen as excess light energy results in large ΔpH across the thylakoid membrane (Horton *et al.,* 1996; Ruban and Horton, 1999). In turn, acidification of lumen is dependent on Ca^{2+} release from stores at PSII (Krieger and Weis, 1999). Due to the high affinity of Cu^{2+} for polypeptide –SH groups (Stauber and Florance, 1986; Rijstenbill *et al.,* 1994), the PsbS protein, as well as the trans-membrane H^+-transport and release of Ca^{2+} from internal stores, are potential targets for Cu^{2+} in *Fucus* NPQ. Cu^{2+} has the potential to cause such

damage as it is known to inhibit channel-gated Ca^{2+} release (Kasai and Neher, 1992; Osipenko *et al.*, 1992; Klusener *et al.*, 1997), as well as ATPases and other ion transporters (Kiss *et al.*, 1991; Viarengo *et al.*, 1996; Amasheh and Weber, 1999; Demidchik *et al.*, 1997; 2001).

I propose that Cu^{2+} has the ability to reduce the tolerance of *Fucus* to saturating light. Furthermore, Restronguet fronds are better adapted to divert the excess light energy through thermal energy conversion in NPQ than Bantham and Wembury fronds. Restronguet fronds may be distinguished by a larger xanthophyll pool in the light-harvesting complex and/or other features, which prevents inhibition of proteins and ion transporters underlying the xanthophyll cycle.

2.4.1.2. Effects of Cu^{2+} on photosynthetic capacity

The inhibitory effect of Cu^{2+} on the efficiency with which electrons are transported through PSII in *Fucus* only appeared after prolonged (23 days) exposure. However, Cu^{2+} may cause oxidative damage to chlorophyll *a* which in turn may result in a negative effect on the total photosynthetic electron turnover in PSII. In the present experiment such an effect was indicated after short-term Cu^{2+} exposure, and was more distinct for Bantham and Wembury fronds than for Restronguet fronds (Figure 2.14 and 2.15). F'_m and F_t of Bantham and Wembury fronds decreased by more than 30% compared with controls in saturating light as early as 2 days after exposure to 844 nM Cu^{2+}, whereas such effects were only apparent for Restronguet fronds after 6 days of exposure. The negative effect of Cu^{2+} on F'_m and F_t coincided with a reduction in the chlorophyll *a* content, particularly of Bantham fronds, of 50% from 0.38 to 0.19 $\mu g\ g^{-1}$ FW after 23 days exposure to 844 nM Cu^{2+} (Figure 2.17). Negative effects of Cu^{2+} on the individual fluorescence values which were not reflected in

the quantum yield have also been shown for other systems. Exposure of wheat seedlings to 20 μM $CuSO_4$ for 10 days resulted in a reduction in F_m and F_v values without causing changes to F_v/F_m (Ciscato *et al.*, 1997). This reduction in F_m and F_v coincided with a 40% reduction in the chlorophyll *a* content (Ciscato *et al.*, 1997). Similarly, Rijstenbil and co-workers (1994) showed a 50% reduction in the chlorophyll *a* content of diatoms as $[Cu^{2+}]_{cyt}$ increased to 15 nM. The observed reduction in the chlorophyll *a* content may be an expression of a general reduction of the protein pool. However, Cu^{2+} may target chlorophyll *a* more specifically than other proteins, as the ratios chl *a*/chl *c* and chl *a*/chl *b* were shown to decrease by 33% and 40% respectively during Cu^{2+} exposure in diatoms and wheat (Rijstenbil *et al.*, 1994; Ciscato *et al.*, 1997).

Cu^{2+} induced oxidative damage (Luna *et al.*, 1994; Teisseire and Guy, 2000) may be the cause of chlorophyll *a* breakdown in the present and in other studies (Rijstenbil *et al.*, 1994; Ciscato *et al.*, 1997). Induction of reactive oxygen species (ROS) by Cu^{2+} may occur with (Sandmann and Böger, 1980; Yruela *et al.*, 1996) and without simultaneous inhibition of photosynthetic electron transport (Navari-Izzo *et al.*, 1998). Consequently, Cu^{2+}-induced oxidative damage may have caused chlorophyll *a* breakdown, which in turn may have resulted in a reduction in the overall electron turnover by shut down of entire photosynthetic units (reaction centres with light harvesting chlorophyll) without simultaneous inhibitory effects on the quantum yield in light and darkness (Φ_{PSII} and F_v/F_m).

Decreased oxygen evolution and electron turnover in PSII may be the result of indirect effects such as a decreased requirement for photosynthetic products, which could occur during direct inhibitory effects of Cu^{2+} on physiological processes other than electron transport in PSII. Effects of Cu^{2+} on processes downstream of PSII could result in a

decrease in the content of PSII chlorophyll resulting from feed back mechanisms that may ultimately lower the cost of maintenance. It has been shown that Cu^{2+} may have an inhibitory effect on the photoreduction of $NADP^+$ in photosystem I (PSI) (Sandmann and Böger, 1980). Sandmann and Böger (1980) showed that reduction of $NADP^+$ to NADPH with DCIP (dichlorophenolindophenol) as an electron donor was inhibited by 50% in spinach chloroplasts exposed to 2 μM $CuSO_4$. Furthermore, Cu^{2+} has the ability to inhibit H^+-ATPase activity (Uribe and Stark, 1982; Demidchik *et al.*, 1997) and may therefore inhibit photophosphorylation, which occurs downstream of PSII and PSI in chloroplasts. Exposure of spinach chloroplasts to 11 μM Cu^{2+} resulted in a 28% reduction of photophosphorylation within 3 min. (Uribe and Stark; 1982). The potential inhibitory effects of Cu^{2+} on PSI and H^+-ATPase activity would not be reflected in the efficiency of PSII. However, inhibition of H^+-ATPase and $NADP^+$ reduction may result in a lower requirement for electron delivery and mediation of H^+ transport across the thylakoid membrane by PSII, hence making part of this photosystem redundant.

Reduced demand for carbohydrates may be one result of Cu^{2+} inhibition of physiological processes downstream of photosynthesis which, however, is unlikely to be the cause of reduced photosynthesis in the present study. There was a dramatic 3-fold increase in dark respiration of Bantham and Wembury fronds after 2 days of exposure to 844 nM Cu^{2+} and respiration was not inhibited at any time during the course of the experiment (Figure 2.05).

The negative effect of Cu^{2+} on F'_m and F_t observed in the present study may be a true effect brought about by oxidative damage and chlorophyll *a* breakdown as indicated for Bantham fronds. The results could, however, also be an artefact caused by absorbance changes in the fronds. During exposure to 844 nM there was an obvious colour change of Bantham and Wembury fronds which became increasingly dark brown during the course of

the experiment and were almost black after 23 days of exposure (Figure 2.19). Darkening of the fronds may be the result of accumulation of accessory pigments such as fucoxanthin, which causes the brown colour of brown algae. Accumulation of organic acids and polyphenols, which is a well-known response of *Fucus* to exposure to high [Cu^{2+}] (Smith *et al.*, 1986) may also contribute to the darkening of the fronds. The colour change of the fronds was so intense that even very little absorbance by the accumulated substance at the main emission wave length of chlorophyll fluorescence at 685 nm (Falkowski and Raven, 1997) could potentially have caused the reduction in the measured fluorescence of fronds exposed to high [Cu^{2+}]. However, the correlation between reduced F'_m and F_t and darkening of the fronds was not consistent. For Restronguet fronds there was a pronounced negative effect of 844 nM Cu^{2+} on F'_m and F_t whereas no obvious colour change was observed. Hence the negative effects of Cu^{2+} on F'_m and F_t were not necessarily brought about by absorbance changes, at least not for Restronguet fronds, and the results may therefore reflect real quantitative effects of Cu^{2+} on PSII.

2.4.2. Mechanisms of Cu^{2+} tolerance in *Fucus*

The different levels of copper tolerance of fronds from the different populations may reflect their ability to avoid uptake and/or handle the metal internally, as the success of plants and algae in contaminated habitats is dependent on keeping $[Cu^{2+}]_{cyt}$ close to zero (Murphy and Taiz, 1995; van Hoof *et al.*, 2001). In the present study, organic substances, probably including polyphenols were released from *Fucus* during Cu^{2+} exposure (Figure 2.18). Secretion of polyphenols, which have high Cu^{2+} complexing capacity, in order to lower the external concentration of Cu^{2+} is believed to be one of the primary tolerance strategies of brown algae during exposure to high [Cu^{2+}] (Sueur *et al.*, 1982; Gledhill *et al.*,

1997). However, rather than chelating Cu^{2+} externally, secretion of polyphenols may be a mechanism of detoxifying the tissue of accumulated Cu^{2+}. Due to water movements, the water immediately surrounding the algae would be renewed quickly and therefore require continued secretion of organic compounds in order to chelate toxic metal ions in a polluted environment. It therefore seems possible that *Fucus* secrete the organic compounds with Cu^{2+} already attached in order to detoxify the tissue. The secretion from Bantham fronds exposed to 844 nM Cu^{2+} increased 6-fold compared to controls after 1 day, and that of Wembury and Restronguet fronds 3.5-fold. After 2 days of exposure to 844 nM, secretion from Restronguet fronds had returned to the level for control fronds, whereas secretion from Bantham and Wembury fronds continued for the rest of the experiment. Although the organic compounds secreted by the fronds may have been polyphenols, it is likely that at least part of the 6-fold increase in secretion by Bantham fronds was caused by the shock of sudden exposure to 844 nM [Cu^{2+}]. Such release may, in part, have been caused by lipid peroxidation and oxidative damage to the plasma membrane, which may have resulted in a general loss of cellular substances. This would, however, have contributed significantly, albeit indirectly, to lowering [Cu^{2+}] in the medium as organic substances in general are good chelators of heavy metals (Gledhill *et al.*, 1997).

The pattern of secretion suggests that Restronguet fronds coped better with a high degree of external un-chelated Cu^{2+} than Bantham and Wembury fronds. Yet, interestingly, Restronguet fronds were better adapted to avoid uptake of large concentrations of total copper. Brown algae usually accumulate high internal total copper concentrations during Cu^{2+} exposure (Bryan and Hummerstone, 1973; Bryan and Gibbs, 1983; Martin *et al.*, 1997; Stengel and Dring, 2000). However, the high content of polyphenols in fucoids (Ragan, 1979) may allow the algae to handle Cu^{2+} internally, by chelation away from the cytoplasm (Smith *et al.*, 1986).

At about 1500 μg g^{-1} DW, Bantham and Wembury fronds exposed to 844 nM for 23 days were accumulating 50% more total copper than Restronguet fronds (Figure 2.20). It is unlikely that the organic substances secreted by Restronguet fronds had a much higher capacity of chelating Cu^{2+} in the medium than those secreted by Bantham and Wembury fronds. Organic ligands secreted by fucoids in general have a pK_{CuL} = 10.15-10.50 (Sueur *et al.*, 1982; Gledhill *et al.*, 1999), which is amongst the highest Cu^{2+} complexing constants known for ligands secreted by algae (Gledhill *et al.*, 1997). The cellular mechanism of Cu^{2+} uptake offers an alternative explanation. Cellular Cu^{2+} uptake involves reduction of Cu^{2+} to Cu^{+} by membrane reductases (Hassett and Kosman, 1995; Georgatsau *et al.*, 1997) and subsequent transport by specialised Cu^{2+} transporters, Ctr1 and Ctr3 (Dancis *et al.*, 1994; Peña *et al.*, 2000). Populations of *Fucus* which are adapted to unpolluted habitats are exposed to very low [Cu^{2+}], which may even be limiting. To cope with this shortage of copper it is likely that they have developed a high number of Cu^{2+} uptake sites. Likewise *Fucus* in Cu^{2+} contaminated habitats, which are not suffering from Cu^{2+} deficiency, would be expected to have relatively few copper transporters in the cell membrane. Consequently when Cu^{2+} is in excess, it might be expected that Bantham and Wembury fronds would accumulate higher quantities than Restronguet fronds.

Remarkably, Wembury fronds were accumulating less copper than both Bantham and Restronguet fronds when exposed to [Cu^{2+}] below 422 nM. Wembury fronds were collected from a wave exposed location and consequently had tougher tissue with a lower surface area/weight ratio than Bantham and Restronguet fronds from wave protected locations, which may explain the lower uptake per gram biomass at low [Cu^{2+}] in Wembury fronds. This is however inconsistent with greater Cu^{2+} damage and induction of

secretion in Wembury fronds. Consequently, a very small $[Cu^{2+}]_{cyt}$ may be needed to induce damage in Wembury fronds.

The accumulation of copper in Bantham and Wembury fronds may have coincided with an increase in the internal polyphenol pool. The colour of Bantham and Wembury fronds became increasingly dark brown with increasing internal total copper concentration and $[Cu^{2+}]$ in the medium, which may have been the result of an increase in the internal polyphenol pool in order to cope with the increasing external $[Cu^{2+}]$. However, no colour change of Restronguet fronds was noticeable although they did accumulate levels of copper which were equivalent to the concentrations in the darkened Bantham fronds. Consequently, Restronguet fronds may have means of handling internal copper, in addition to chelating with polyphenols. A metallothionein-encoding gene has recently been identified in *Fucus* (Morris *et al.*, 1999) and increased metallothionein gene expression may, in part, explain the higher Cu^{2+} tolerance in Restronguet fronds than in Bantham and Wembury fronds. Metallothionin genes in *Fucus* are transcribed during exposure to high $[Cu^{2+}]$ and may contribute to Cu^{2+} tolerance in *Fucus* (Morris *et al.*, 1999). Morris and co-workers (1999) did not examine the expression of metallothionein genes of *Fucus* from populations naturally exposed to different levels of copper. However, it has been shown that metallothionin genes are transcribed at higher rates in tolerant than non-tolerant strains of *Arabidopsis* and *Silene* during copper exposure (Murphy and Taiz, 1995; van Hoof *et al.*, 2001). Consequently, it is possible that Restronguet fronds may express the metallothionin gene at higher levels than Bantham and Wembury fronds, which would provide them with higher concentrations of a cytosolic ligand with high copper complexing capacity.

The ability to chelate external Cu^{2+} by secretion of ligands, and to immobilise internal Cu^{2+} by binding it to polyphenols and storeing it in physodes and the cell wall, is a general feature of *Fucus*, which may allow un-adapted populations to cope with some degree of copper exposure. In spite of these abilities, non-tolerant Bantham and Wembury fronds were only capable of chelating 42.2 nM free Cu^{2+} in the external medium by secretion of organic substances and internal accumulation as any higher concentrations affected photosynthesis, dark respiration and growth. The tolerant Restronguet fronds are unlikely to have higher Cu^{2+}-chelating capacity than non-tolerant strains yet their metabolism was mainly unaffected by $[Cu^{2+}]_{ext}$ above 42.2 nM. The mechanism of tolerance in Restronguet fronds may therefore rely on reduced Cu^{2+} uptake, due to a limited number of Cu^{2+} transporters in the cell membrane and for high transcription of the metallothionein gene during copper exposure.

2.4.3. Metabolic responses to Cu^{2+} in tolerant and non-tolerant *Fucus*

Amongst the potentially toxic effects of Cu^{2+}, inhibition of photosynthesis and increased production and release of organic substances during exposure to high $[Cu^{2+}]$ in non-tolerant *Fucus* is reflected in the rate of dark respiration and the relative growth rate (RGR). In agreement with other experiments (Bryan and Gibbs, 1983), there was a pronounced negative effect of Cu^{2+} on RGR in non-adapted populations of *Fucus*, whereas RGR of Restronguet *Fucus* was only slightly affected at the high $[Cu^{2+}]$ of 844 nM. Similarly, dark respiration of Restronguet fronds was unaffected by $[Cu^{2+}]$ up to 844 nM, whereas the initial shock of exposure to this concentration resulted in a 2-fold increase in dark respiration of Bantham and Wembury fronds after 2 days, and remained slightly elevated for Wembury fronds throughout the experiment. The response pattern of dark

respiration of Bantham and Wembury fronds during exposure to high [Cu^{2+}] was similar to that of other algae. Four days of exposure to 8 μM copper resulted in a 2-fold increase in the dark respiration of *Nitella nigra* followed by a decrease to the level of controls after 8 days (Gupta and Arora, 1978).

The increased demand for production of Cu^{2+}-complexing ligands in the non-tolerant Bantham and Wembury populations could apply an extra cost to their metabolism during Cu^{2+} exposure due to the effects on Cu^{2+} homeostasis and general repair mechanisms. To similar effect, production of ROS during Cu^{2+} exposure may result in highly increased antioxidant production (Luna *et al.*, 1994; Yruela *et al.*, 1996; Navari-Izzo *et al.*, 1998; Teisseire and Guy, 2000). Consequently, exposure of non-adapted *Fucus* to elevated [Cu^{2+}] may induce cellular responses, which would increase the respiratory demands. Simultaneous inhibition of the photosynthetic performance presents the algae with a dilemma: They need to produce enough ligands to chelate Cu^{2+} to non-toxic levels as well as antioxidants, but not so much that their reserves are exhausted by increased respiratory demands. Consequently, whereas the Cu^{2+}-resistant Restronguet fronds seemed capable of avoiding this physiological dilemma during Cu^{2+} exposure and maintain an almost unaffected growth rate, failure of the non-tolerant Bantham and Wembury fronds to meet highly increased physiological demands resulted in a pronounced negative effects on their growth rates.

2.4.4. Summary of discussion

Effects of Cu^{2+} on the physiology of adult populations of *Fucus* with different tolerance limits were studied in the present chapter. *Fucus* from the heavily Cu^{2+} polluted

Restronguet Creek were better equipped to handle exposure to high concentrations of Cu^{2+} than *Fucus* from the unpolluted Bantham Quay and Wembury Beach.

Restronguet *Fucus* secreted less organic substances and accumulated lower concentrations copper during Cu^{2+} exposure than Bantham and Wembury *Fucus*. This finding led to the conclusion that the mechanism of Cu^{2+} resistance in tolerant *Fucus* may involve fewer sites for Cu^{2+} uptake in the plasma membrane as well as higher levels of metallothionien expression compared with non-tolerant specimens. Lack of such mechanisms of resistance in non-tolerant Bantham and Wembury *Fucus* may have resulted in the increased respiration and reduced growth rate through increased cost of polyphenol and antioxidant production as well as a greater demand for general repair mechanisms.

The ability of Cu^{2+} to reduce the quantum yield of PSII was expressed in both tolerant and non-tolerant *Fucus*. Increased non-photochemical quenching in the Restronguet population during Cu^{2+} exposure suggested that Cu^{2+} reduced the tolerance of *Fucus* to saturating light and that the Restronguet population was adapted to divert the resulting excess light energy through the xanthophyll cycle in contrast to the Bantham and Wembury populations.

Here I have addressed only the effects of Cu^{2+} on the adult life cycle stages of *Fucus*. It is, however, a general belief that young *Fucus* zygotes are very sensitive to Cu^{2+} exposure which may result in reduced growth and arrested development (Anderson and Kautsky, 1996; Bond *et al.*, 1999; Gledhill *et al.*, 1999). In Chapter 3 effects of Cu^{2+} on growth of *Fucus* germlings from Cu^{2+} tolerant and non-tolerant populations will be compared. The main emphasis will be on effects of Cu^{2+} on early development in the *Fucus* zygote from a non-tolerant population and on identifying the mechanism of arrested development and growth during Cu^{2+} exposure.

CHAPTER 3

Targets of Cu^{2+} Toxicity in the Early Development of *Fucus serratus*

3.1. Introduction

The presence of polar axes in an embryo is essential for correct development of the overall body plan. In animals there are two main axes, the antero-posterior axis defining head and tail, and the dorso-ventral axis laid down at a right angles to the former and defining front and back. In plants there is one main axis, the apical-basal axis, which defines shoot tip and root tip (Wolpert *et al.,* 1998). Distinct strategies to set up the primary embryonic axis have been developed in different groups of organisms (Kropf, 1992; Kimble, 1994; Kessler and Melton, 1994; Jürgens *et al.,* 1995). Axis establishment can occur either before or after fertilisation at either the single- or multicellular stage. In the fruit fly, *Drosophila*, maternal gene products establish the axes in the unfertilised egg and set up the framework for subsequent development when still inside the ovary (Kimble, 1994). Likewise, maternal factors define the antero-posterior axis in the toad, *Xenopus* egg, whereas the dorso-ventral axis is established by sperm entry (Kimble, 1994). In mammals, axis establishment does not occur until the multicellular level where the fate of the individual cell is dependent on its relative positioning in the cleaving embryo (Kessler and Melton, 1994). Still other strategies for establishment of a polar axis have developed in different types of plants and algae.

3.1.1. Polarisation in plants and algae

Polar axis organisation in flowering plant embryos is established during oogenesis (Goldberg *et al.,* 1994; Jürgens *et al.,* 1995). In many dicotyledon species such as *Arabidopsis*, polarity is determined by maternal factors and is apparent in the highly asymmetric unfertilised egg cell (Goldberg *et al.,* 1994; Jürgens, 1995). The nucleus and

most of the cytoplasm is located towards the antipodal side, while a large vacuole is located at the micropylar end of the egg cell (Goldberg *et al.*, 1994). Following fertilisation, reorganisation of the organelles occurs, which accentuates the polar organisation of the egg cell. In monocotyledons, such as maize, eggs are pear shaped and are also polarised, although the polarisation is less pronounced than in most dicotyledons (Schel *et al.*, 1984). In maize the position of the vacuole and nucleus are exchanged following fertilisation, so that the nucleus becomes orientated towards the micropylar end (Kranz *et al.*, 1995). The first zygote cell division in plants normally occurs transversely with respect to the polar axis of the zygote (Kropf *et al.*, 1990; Jürgens *et al.*, 1995; Kranz *et al.*, 1995). The first cell division in *Arabidopsis* embryos is highly asymmetric, and forms a small apical cell, which develops into the pro-embryo and the much larger basal cell which develops into part of the root meristem and mainly serves as extra-embryonic support tissue (the suspensor) (Jürgens *et al.*, 1995). In monocotyledons, the cell divisions following the first division appear to be very irregular and random and result in a multicellular, callus-like structure. The polarity in the embryo can only be observed again 10 to 12 days after fertilisation (Kranz and Lörz, 1993; Kranz *et al.*, 1995).

The angiosperm egg cell is surrounded by gametophyte cells and embedded in the female reproductive organ, where fertilisation takes place (Goldberg *et al.*, 1994). Consequently, studies of egg polarisation and embryo development in angiosperms are difficult. Methods have only recently been developed for *in vitro* fertilisation of isolated gametes and development of the resulting embryos (Kranz and Lörz, 1993; Breton *et al.*, 1995). *In vitro* fertilisation and culturing of zygotes facilitates the study of early development in flowering plants but obtaining embryos is difficult.

Research on seedling phenotypes in *Arabidopsis* mutants have revealed important information on pattern formation in plants (Mayer *et al.*, 1991; Mayer *et al.*, 1993; Vroemen *et al.*, 1996; Berleth *et al.*, 2000). It has been shown that the apical-basal axis in *Arabidopsis* is divided into apical, central and basal region, the differentiation of which is controlled by the expression of genes including *gurke*, *fackle* and *monopteros* (Mayer *et al.*, 1991; Vroemen *et al.*, 1996). In their work, Mayer and co-workers (1991) suggested that the *gnom* gene possibly played a special role in the organisation of the polar axis. Further work on the *gnom* mutant, which tends to have a symmetrical first cell division (Vroemen *et al.*, 1996), suggests that the *gnom* gene is directly involved in asymmetric cell division and is necessary for axis formation in *Arabidopsis* (Mayer *et al.*, 1993; Vroemen *et al.*, 1996). Work with mutants has also shown that auxin provides positional information and is important for expression of the polar axis in *Arabidopsis* embryos (Berleth *et al.*, 2000; Souter and Lindsey, 2000). Furthermore, it has been shown that the *gnom* mutants have defective auxin transport and effectively that the *gnom* gene is involved in regulation of the auxin transport mediator, *PIN1*, (Steinman *et al.*, 1999; Berleth *et al.*, 2000; Souter and Lindsey, 2000). Although methods such as *in vitro* fertilisation and embryonic mutants facilitates the research, studies of early development in flowering plants are still problematic. Studies on early development in other systems, which share similarities with plants, *i.e.* fucoid algae, are much easier since gametes and zygotes are very easily obtained and cultured.

Zygotes of fucoid algae (*Fucus* and *Pelvetia*) have long been used in experimental studies of development in plant embryos and provide an excellent model system. Unfertilised eggs and sperm are released from the conceptacles of adult algae into the surrounding environment where oogamous fertilisation and zygote development take place (Pearson and Brawley, 1996). Fucoid zygotes are easily obtained in large numbers and are simple to

culture and manipulate. The first experimental studies on fucoid zygotes were carried out by Thuret as early as 1854 (Thuret, 1854). Synchronous cultures of zygotes can be obtained and are therefore well-suited for studies of the factors controlling the developmental processes following fertilisation. In contrast to plant and most animal zygotes, the *Fucus* zygote is apolar before and several hours after fertilisation. The young zygote possesses no particular cytoplasmic order and is essentially radially symmetrical in all planes. The nucleus is located in the centre of the cell, and the cytoskeleton, various organelles and vesicles are uniformly distributed (Jaffe, 1966; Pu *et al.*, 2000). Unfertilised *Fucus* eggs are arrested in the G1 phase of the cell cycle (Corellou *et al.*, 2000) and their metabolism is restricted to a level essential for cellular maintenance. Once fertilised a whole range of cytological processes are initiated, all of which are dependent upon intracellular communication.

3.1.2. Early development in the *Fucus* zygote

3.1.2.1. Early fertilisation events

Fertilisation potential is the first detectable event following fertilisation of a *Fucus* egg and involves electrical depolarisation of the plasma membrane (Brawley, 1991; Taylor *et al.*, 1992; Taylor and Brownlee, 1993). The unfertilised *Fucus* egg maintains a resting membrane potential of about –60 mV mainly by efflux of K^+ ions from the cytosol into the surrounding environment (Brawley, 1991; Taylor and Brownlee, 1993; Roberts *et al.*, 1994). Contact of a sperm with a putative sperm receptor in the plasma membrane may induce the immediate opening of Na^+ channels, resulting in a large increase in inward Na^+ current and depolarisation of the membrane potential (Brawley, 1991; Taylor *et al.*, 1992). Depolarisation of the membrane potential may, in turn, induce the opening of voltage-

gated Ca^{2+} channels in the cell membrane, influx of Ca^{2+} into the cytoplasm and a further increase in the membrane potential (Taylor and Brownlee, 1993; Roberts *et al.*, 1994; Roberts and Brownlee, 1995). Depolarisation to about –5 mV induces the opening of voltage-regulated K^+-channels, and increased K^+ efflux, which restores the membrane potential to its normal resting level within a few minutes of fertilisation (Taylor *et al.*, 1992; Taylor and Brownlee, 1993; Roberts *et al.*, 1994). This fertilisation potential may play an important role in preventing polyspermy (Brawley, 1991).

Egg activation occurs upon fertilisation and involves resumption of arrested physiological processes such as protein synthesis and cell cycle. In animal cells, egg activation has been shown to depend on a large transient elevation of cytoplasmic Ca^{2+}, which propagates the egg as a wave of Ca^{2+} release from intracellular stores. Small, localised Ca^{2+} transients of about 200 nM can be detected in the cortical area of the *Fucus* zygote upon fertilisation. These Ca^{2+} elevations are dependent on the fertilisation potential and influx of external Ca^{2+}, whereas the role of internal Ca^{2+} release is uncertain (Roberts *et al.*, 1994). The fertilisation-induced Ca^{2+} transients may be a requirement for egg activation as the Ca^{2+} transient is involved in cell wall secretion in the *Fucus* zygote (Roberts *et al.*, 1994; Roberts and Brownlee, 1995). The unfertilised *Fucus* egg possesses no cell wall but cell wall synthesis can be observed in the zygote about 10 minutes after fertilisation (Quatrano and Stevens, 1976; Roberts *et al.*, 1994). It was shown that injecting the Ca^{2+} buffer BAPTA into eggs or removing Ca^{2+} from the external medium inhibits cell wall secretion in the *Fucus* zygote (Roberts *et al.*, 1994; Roberts and Brownlee, 1995).

3.1.2.2. Early polarisation

Establishment of the polar axis in the *Fucus* zygote takes place a few hours after fertilisation as spatial information provided by environmental vectors is translated into

developmental responses in a two-step process (Quatrano, 1973; Kropf, 1992). The direction of incident light is probably the principal external polarising vector but water current and chemical and electrical gradients can also bring about axis selection (Bentrup *et al.*, 1966; Gibbon and Kropf, 1993). Furthermore, zygotes in dense cultures orientate their axes towards one another (Hurd, 1920; Berger and Brownlee, 1994). If no external polarising stimulus is present, zygotes still form an axis and very early work suggests that the site of sperm entry could determine the orientation of this 'default' axis (Knapp, 1931). This theory has only recently been confirmed. Within a few minutes of fertilisation, an actin patch forms at the site of sperm entry and, supposedly, marks the 'default' axis, which becomes overwritten during subsequent developmental events (Hable and Kropf, 2000). The time course for the early developmental events in *Fucus* is summarised in Figure 3.01. During the phase termed 'axis formation' (3-8h after fertilisation, AF) a reversible polar axis is formed (Berger and Brownlee, 1994; Love *et al.*, 1997). This initial axis can be re-orientated by changing the direction of the polarising light vector until the period termed 'axis fixation' (8-14h AF), after which the orientation of the polar axis can no longer be changed (Berger and Brownlee, 1994). Essential irreversible structural modifications involving the cell wall and organisation of the filamentous actin cytoskeleton take place during axis fixation (Kropf *et al.*, 1988; Shaw and Quatrano, 1996b). Orientation of the polar axis is expressed by the germination of a rhizoid about 20h AF.

3.1.2.3. Detecting the light signal

Initial detection of the polarising light signal in the *Fucus* zygote may involve focusing light at photoreceptors but the exact mechanism of light detection is unclear, and the optical properties of the *Fucus* zygote appear to be complex (Berger and Brownlee, 1994). The ability of the zygote to polarise under a very wide range of irradiances (Jaffe, 1958;

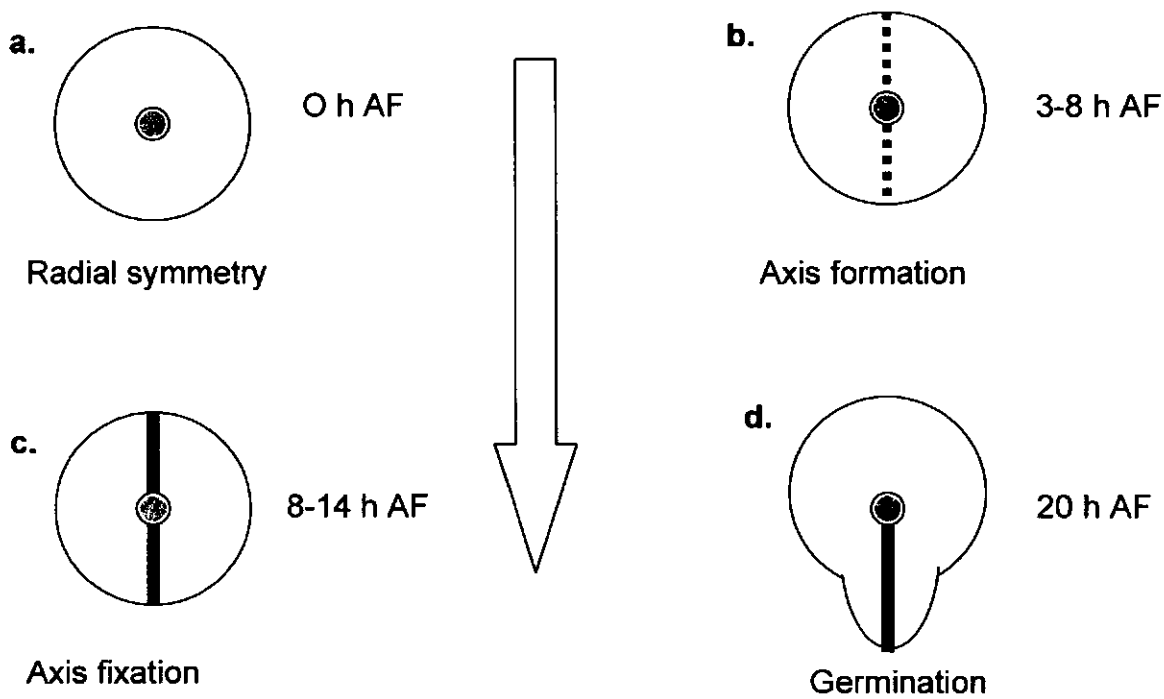

Figure 3.01. Axis formation, fixation and germination in *Fucus* zygotes in response to the direction of polarising light. The direction of light is indicated by the arrow. Before and just after fertilisation the zygote is apolar (**a**). From 3 to 8 h after fertilisation (AF) a polar axis is formed but can be re-orientated in response to light coming from another direction (**b**). At 8-14 h AF the polar axis is fixed in position (**c**), and at about 20 h AF the axis is expressed by the germination of a rhizoid (**d**).

Bentrup, 1963) indicates that the zygote responds to differences in light level in different regions of the cell and not to the absolute light intensity at any particular spot. Zygotes can be polarised by light pulses lasting less than one second given during the photosensitive period (Bentrup, 1963) and consequently possess the ability to memorise the light signal, which is subsequently translated by slower mechanisms, as axis formation takes at least one hour (Kropf 1992; Berger and Brownlee, 1994).

One established theory of light detection during polarisation suggests that early events in polar axis establishment involve unequal excitation of photoreceptors in the plasma membrane by the light vector (Jaffe, 1958; Berger and Brownlee, 1994). This may be associated with enhanced redox transport at the cell surface on the side of the zygote facing away from the light (Berger and Brownlee, 1994). Asymmetric activation of a plasma membrane electron transport chain may in turn induce localised increases in Ca^{2+} permeability of the plasma membrane through phosphorylation of Ca^{2+} channels (Berger and Brownlee, 1994). Increased Ca^{2+} influx and small cytosolic Ca^{2+} elevations on the shaded side of the zygote could provide a polar signal which is sufficient to initiate axis establishment.

An alternative model for translation of the light signal, which involves retinal and asymmetric actin polymerisation, has recently been proposed. The pigment, retinal, is known to form light sensitive complexes in association with opsins in animals, and the presence of retinal in *Pelvetia* zygotes (Robinson and Miller, 1997) led to the conclusion that similar complexes may exist in fucoid zygotes (Robinson *et al.*, 1998). In their analogy, Robinson and co-workers (1998) proposed a spatial variation in the level of their enzyme, cyclic GMP, in response to a light gradient within the zygote during early photopolarisation. The finding that blue light alone was sufficient to cause a two-fold

increase in the level of cyclic GMP on the side of the zygote facing the light supported this hypothesis (Robinson and Miller, 1997; Robinson *et al.*, 1998). Cyclic GMP is known to promote actin de-polymerisation (Furukawa and Fechheimer, 1997). It was therefore suggested that elevated levels of cyclic GMP on the side of the zygote which faced the light would result in actin de-polymerisation in this region and increased actin polymerisation at the rhizoid pole, and in this way mark the polar axis (Robinson and Miller, 1997; Robinson *et al.*, 1998).

3.1.2.4. The role of Ca^{2+} in polarisation

The free Ca^{2+} concentrations control many aspects of cell function (Bush, 1995; Gilroy *et al.*, 1993; Sanders *et al.*, 1999). Ca^{2+}_{cyt} is normally maintained at concentrations between 30 and 200 nM (Bush, 1995; Mahló *et al.*, 1998) which, in marine organisms is typically an order of 10^4 lower than $[Ca^{2+}]$ in the surrounding external environment. $[Ca^{2+}]_{cyt}$ must be kept low because highly abundant metabolic phosphate esters form insoluble calcium phosphates (Gilroy *et al.*, 1993). Binding of Ca^{2+} to regulatory proteins plays some role in lowering the $[Ca^{2+}]_{cyt}$ (Heizmann and Hunziker, 1991; Gilroy *et al.*, 1993) but low steady state $[Ca^{2+}]$ is mainly achieved by active Ca^{2+} export out of the cytosol into sub-cellular compartments such as ER and vacuoles and across the plasmamembrane (Koch, 1990; Poovaiah and Reddy, 1987; Bush, 1995; Malhó *et al.*, 1998), and is mediated by H^+/Ca^{2+} antiporters and ATP-ases, which drive transport of Ca^{2+} against the concentration gradient (Poovaiah and Reddy, 1987; Koch, 1990; Bush, 1995). Since most plant and algal cells maintain a negative potential across the plasma membrane, a large electrochemical potential difference for Ca^{2+} is present. Steep Ca^{2+} gradients present the cell with the opportunity of abruptly increasing $[Ca^{2+}]_{cyt}$ for signalling purposes (Trewavas and Gilroy, 1991; Schroeder and Thuleau, 1991; Malhó *et al.*, 1998). Ca^{2+} is an important second messenger in many different signalling pathways in plant, algal and animal cells and

interacts with target proteins directly or *via* calmodulin and Ca^{2+}-dependent kinases. There are many examples of Ca^{2+} transients in response to different environmental stimuli, such as touch, cold shock, oxidative stress, and hypo-osmotic shock in plants and algae (Knight *et al.,* 1996; Taylor *et al.,* 1997; Goddard *et al.,* 2000).

In flowering plants there is evidence for voltage independent, and both hyper polarisation and depolarisation, activated Ca^{2+} permeable channels (Alexandre *et al.,* 1990; Schroeder and Thuleau, 1991; Malhó *et al.,* 1998). Voltage sensitive channels can open in response to changes in plasma membrane potential, allowing Ca^{2+} entry and elevation of $[Ca^{2+}]_{cyt}$. Low cytosolic mobility of Ca^{2+} enables the cell to sustain a very localised rise in $[Ca^{2+}]_{cyt}$ (Malhó *et al.,* 1998), such as has been observed in the tip of elongating *Fucus* rhizoids (Berger and Brownlee, 1993).

Ca^{2+} binding proteins. Ca^{2+} is able to bind to a wide range of proteins, and is well suited for binding to irregular shaped crevices in proteins and can spurn other divalent cations such as Mg^{2+}. Generally the same reaction site, which co-ordinates eight oxygen atoms to each Ca^{2+}, occurs in many Ca^{2+} binding proteins. Ca^{2+} may also cross link different segments of proteins and induce large conformational changes (Williams, 1992).In parvalbumin, where the Ca^{2+} binding site was first mapped, it is formed by E and F helices, and resembles a hand, hence the name 'EF hand' (Babu *et al.,* 1988). Calmodulin is a major Ca^{2+} binding protein, comprising four modules based on the EF hand (Babu *et al.,* 1988), and serves as a Ca^{2+} sensor in nearly all eukaryotic cells. The sites in one lobe have high affinity for Ca^{2+} and those in the other lobe have lower affinity for the ion (Williams, 1992). Binding of Ca^{2+} to the two high affinity sites increases the affinity of the low affinity sites and activates calmodulin. Another important group of Ca^{2+} sensors in plants is the calcium-dependent protein kinases (CDPK's) which have a calmodulin-like reaction

site formed by four EF-hands (Harper *et al.*, 1991; Zhao *et al.*, 1993). A CDPK subfamily with modified EF-hands has been identified in plants (Hrabak *et al.*, 1996). The different CDPK isoforms may be involved in regulating separate signalling pathways as they are specific for different substrates (Lee *et al.*, 1998), and they may be activated by different $[Ca^{2+}]_{cyt}$. Different substrates for CDPK include Cl^- and K^+ channels in guard cells (Li *et al.*, 1996) and the plasma membrane proton pump (Camoni, 1998).

Ca^{2+}-activated ion channels form an important group of Ca^{2+} target proteins. Ca^{2+}-activated ion channels are targeted directly by Ca^{2+}, *via* other Ca^{2+} binding proteins, or *via* depolarisation of the membrane potential (Garrill *et al.*, 1992; Galione *et al.*, 1994; Ward and Schroeder, 1994). Examples of Ca^{2+}-activated ion channels are K^+-, Ca^{2+}-, and Cl^--channels, which are involved in cell turgor regulation in different systems including fungi, plants and algae (Garrill *et al.*, 1992; Taylor and Brownlee, 1993; Ward and Schroeder, 1994). One example of the involvement of Ca^{2+} in ion channel and cell turgor regulation is the model for guard cell closure proposed by Ward and Schroeder (1994). Loss of cell turgor during water stress induces an increase in the stress hormone abscisic acid (ABA) which, in turn, induces an increase in guard cell $[Ca^{2+}]_{cyt}$ to >1 μM. This level of cytosolic Ca^{2+} may be sufficient to activate vacuolar K^+-channels (VK-channels) in the membrane of the large central vacuole in the guard cell. Elevated $[Ca^{2+}]_{cyt}$ and K^+ flux from the vacuole into the cytoplasm could depolarise the vacuolar membrane potential further until a level is reached which activates voltage-dependent, slow vacuolar cation channels (SV-channels), and induces Ca^{2+} flux from the vacuole into the cytoplasm. This Ca^{2+}-induced Ca^{2+} release is likely to promote other regulatory roles during stomata closure (Ward and Schroeder, 1994).

The role of Ca^{2+} in polarisation. Increases in $[Ca^{2+}]_{cyt}$ on the side of the *Fucus* zygote facing away from the light (the rhizoid pole) is one of the first detectable responses in the *Fucus* zygote to a polarising light stimulus (Brownlee and Wood, 1986; Berger and Brownlee, 1993; Roberts *et al.*, 1993; Shaw and Quatrano, 1996a; Love *et al.*, 1997; Pu and Robinson, 1998). Confocal images of polarising *Fucus* zygotes have revealed that $[Ca^{2+}]$ at the rhizoid pole is 100 fold higher than $[Ca^{2+}]$ in the rest of the zygote, and appears as a gradient extending 5 μm beyond the cell membrane (Berger and Brownlee, 1993). The Ca^{2+} gradient is thought to be an absolute requirement for polar axis establishment in fucoid zygotes, as microinjecting polarising zygotes with the Ca^{2+} buffer BAPTA inhibits polarisation (Speksnijder *et al.*, 1989; Taylor *et al.*, 1992). Furthermore, calmodulin has been shown to be required for axis formation (Poovaiah and Reddy, 1987; Love *et al.*, 1997; Pu and Robinson, 1998). Exactly how the initial polar Ca^{2+} signal is established is unclear. In addition to Ca^{2+} influx from the external medium, apical Ca^{2+} may be supplemented from internal Ca^{2+} stores (Kropf and Quatrano, 1987; Love *et al.*, 1997). After the initial Ca^{2+} gradient has been established during axis formation, a positive ion current, entering at the rhizoid pole, can be detected by an extracellular vibrating electrode at about 5-6 hours AF (Jaffe, 1966; Nuccitelli and Jaffe, 1976). This current is carried in part by influx of Ca^{2+} and efflux of Cl^- through ion channels in the plasma membrane (Taylor *et al.*, 1992; Taylor and Brownlee, 1993) and may be involved in maintenance or amplification of Ca^{2+} asymmetries.

3.1.2.5. The role of F-actin in polarisation

Actin is a ubiquitous protein in eukaryotes and is critical for a wide range of physiological and developmental processes. In vertebrates, muscle contractions arise from interactions between myosin and actin (Cooke, 1987) but actin also serves multiple functions in non-muscle cells. Polymerised, filamentous actin (F-actin) is a component of the cytoskeleton

and serves many roles in intercellular transport and signal transduction, often in combination with tubulin (Small *et al.*, 1999; Goode *et al.*, 2000). Functioning of F-actin involves interactions with a range of proteins with signalling functions (Weeds, 1982; Frankel and Mooseker, 1996). F-actin is continuously dissolving and reforming, and is subject to a range of Ca^{2+}-dependent and independent interactions involving calmodulin, GTPases such as Cdc42, Rho and Rac, and ionic gradients (Welch *et al.*, 1997). Organelle and vesicle movement is often driven along F-actin and microtubule filaments by special motor proteins, such as myosin, dynein and kinesin (Shimmen and Yokota, 1994; Shimmen *et al.*, 1995; Rogers and Gelfand, 2000). The dynamic reorganisation of F-actin and vesicular transport along the filaments underlie multiple processes such as changes in cell shape, locomotion, and cell polarity (Small *et al.*, 1999). It has been suggested that F-actin and the actin-binding protein Tea-1-p which is involved in organising cortical actin patches, may be localised at the cell pole during polarised growth in yeast. F-actin would then be involved in directing secretory vesicles containing membrane- and cell wall-components towards the cell pole for secretion (Goode *et al.*, 2000). It is possible that F-actin has a similar role in polarising *Fucus* zygotes.

Re-organisation of F-actin in the zygotes of fucoid algae is a requirement for polar axis establishment. Staining zygotes with the fluorescent actin-specific probe, phalloidin, has revealed that F-actin becomes localised at the future rhizoid pole some time during axis establishment (Kropf *et al.*, 1989; Bouget *et al.*, 1998a; Alessa and Kropf, 1999; Pu *et al.*, 2000). Furthermore, application of cytochalasin, and other actin depolymerising agents such as latrunculin B, to polarising zygotes prevents polar axis fixation (Quatrano, 1973; Pu *et al.*, 2000). Although F-actin is an absolute requirement for polarisation in fucoid zygotes, the exact timing and patterning of F-actin localisation is controversial. Work presented by Pu and co-workers (2000) showed that a significant elevation in cellular actin

appeared in polarising *Pelvetia* zygotes within one hour after fertilisation. In this experiment there was a distinct actin elevation in cortical regions and a very slight increase in actin was detected at the rhizoid pole after 2h exposure to polarising light. However, definite accumulation of actin at the rhizoid pole was not detected until after germination (Pu *et al.*, 2000).

In contrast, results presented by Alessa and Kropf (1999) suggest that actin accumulation appears at the rhizoid pole much earlier in zygote development. A cortical actin patch was detected at the rhizoid pole in response to polarising light within 3h after fertilisation (AF) (Alessa and Kropf, 1999). By 4 h AF, changing the direction of polarising light resulted in relocation of the actin patch within 40-50 minutes (Alessa and Kropf, 1999).

The presented evidence does not allow firm conclusions of whether F-actin is a requirement for initiation of the Ca^{2+} gradient at the *Fucus* rhizoid pole, or whether F-actin accumulation is initiated in response to the Ca^{2+} gradient. Whatever the order of these events, they are both required for polar axis establishment in the *Fucus* zygote. Amongst the multiple functions of F-actin, one possible role in polarisation is to act as a cellular framework, which stabilises the polar axis by forming links with the extracellular matrix (see below). It is also possible that F-actin serves as a network for vesicular transport towards the rhizoid pole in a similar manner to that suggested for yeast (Goode *et al.*, 2000). Hence, the role of F-actin during axis establishment could be to provide a network for intracellular transport of cellular components such as vesicles towards the rhizoid pole (Goodner and Quatrano, 1993; Shaw and Quatrano, 1996b). The direction of the vesicular transport could then be controlled by the Ca^{2+} gradient.

3.1.2.6. The role of the cell wall in polarisation

Secretion of a cellulose/pectin cell wall in the *Fucus* zygote begins immediately after fertilisation and the polarising zygote possesses a rigid cell wall (Quatrano and Stevens, 1976; Hable and Kropf, 1998). Fixation of the axis previously stabilised by F-actin localisation is dependent on the presence of the cell wall. Experimental enzymatic removal of the wall inhibited axis fixation (Kropf *et al.*, 1988) and, in zygotes which had already fixed an axis, removal of the cell wall resulted in loss of the axis (Kropf *et al.*, 1993; Berger *et al.*, 1994). The role of the cell wall in axis fixation may be to provide anchoring points for molecular complexes which bridge the plasma membrane and form links with the F-actin network in the cytosol. Subsequent to F-actin accumulation, vesicles containing the cell wall component fucoidin, which is a Golgi-derived sulphated fucan F2 polysaccharide, are secreted preferentially at the rhizoid pole (Wagner *et al.*, 1992; Shaw and Quatrano, 1996b). Secretion of fucoidin is thought to play a key role in axis fixation and a model for axis fixation, which involves F-actin, the Ca^{2+} gradient, the cell wall and secretion of fucoidin has been proposed (Figure 3.02), (Goodner and Quatrano, 1993). Golgi-derived vesicles containing fucoidin are transported towards the rhizoid pole *via* the localised actin filaments in response to the polar Ca^{2+} signal and secreted into the cell wall. At the rhizoid pole, fucoidin may anchor the axis stabilising actin filaments into the cell wall. The membrane spanning protein, integrin, is expressed by all multicellular animals and mediates linkage between extracellular adhesion-molecules and the actin cytoskeleton (Humphries, 2000). The presence of integrin-like proteins has now been demonstrated in lily pollen tubes, where it appears to be involved in growth of the pollen tube tip (Sun *et al.*, 2000). This finding brings support to the hypothesis which suggests that integrin is involved in regulating tip growth in pollen tubes and the *Fucus* rhizoid (Quatrano *et al.*, 1991; Lord and Sanders, 1992). Integrin may bind to F-actin on the cytosol side of the plasma membrane and connect to the fucoidin anchor in the cell wall *via* a vitronectin-type

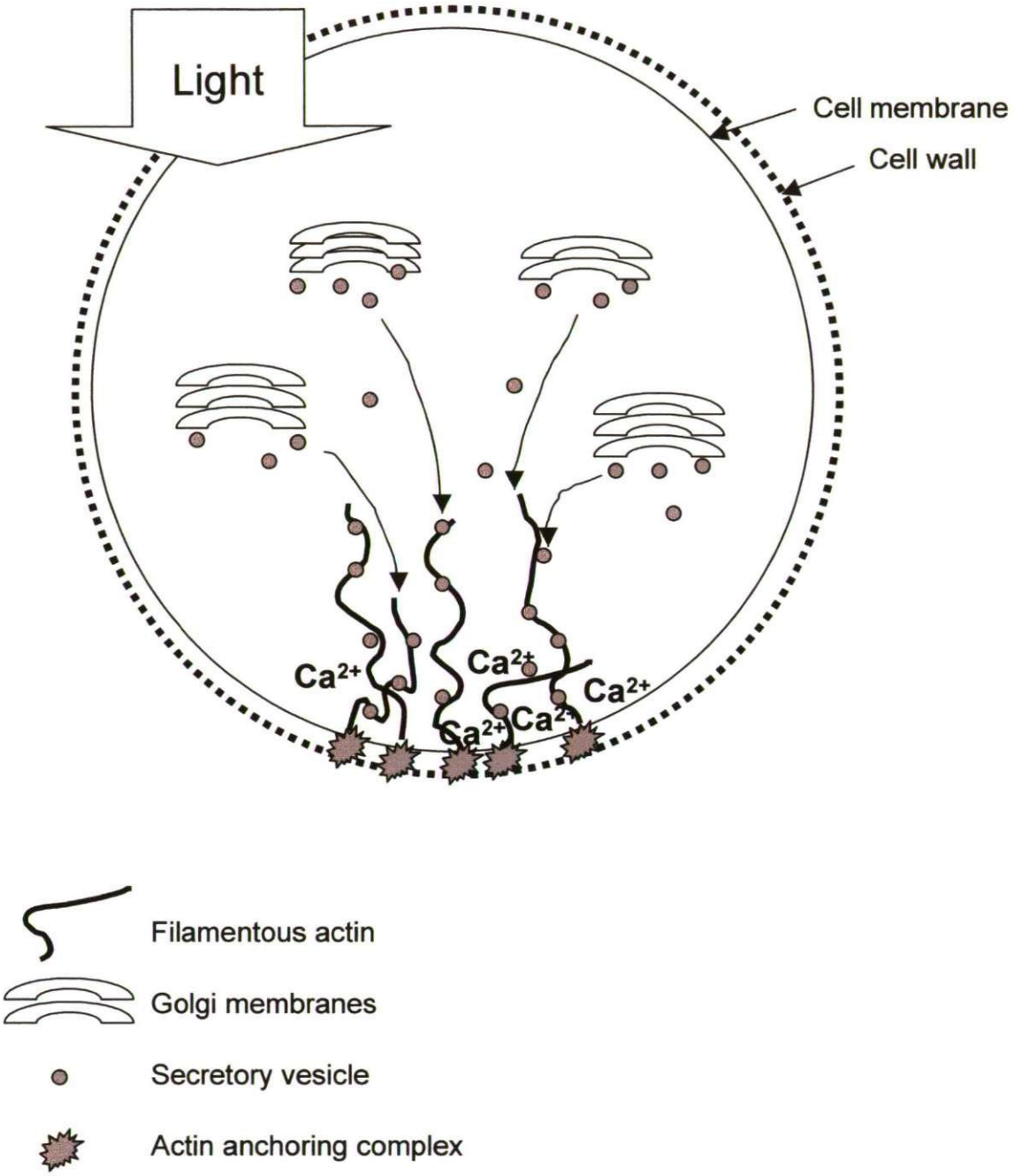

Figure 3.02. Summary of axis fixation in a *Fucus* zygote. F-actin is localised at the rhizoid pole, and guides secretory vesicles containing Golgi-derived fucoidin to the rhizoid pole. Fucoidin secreted into the cell wall stabilises the actin-anchoring complex and fixes the polar axis. Modified from Berger and Brownlee, 1995.

protein in the space between membrane and wall (Goodner and Quatrano, 1993). Anchoring of F-actin to the cell wall irreversibly fixes the polar axis in the *Fucus* zygote.

3.1.3. The developing embryo

3.1.3.1. Rhizoid germination and elongation

Establishment of the polar axis in *Fucus* is manifested by the germination of a rhizoid, which first appears as a small swelling (Hurd, 1920; Jaffe, 1958; Robinson, 1996). Rhizoid germination and elongation occur as tip growth, which takes place exclusively at the apex of an elongating cell, in contrast to diffuse growth where expansion occur over the entire cell surface (Kropf *et al.*, 1998). Tip growth is a common phenomenon in different systems including fungal hyphae (Garrill *et al.*, 1992), pollen tubes (Rathore *et al.*, 1991), root hairs (Miller *et al.*, 1999) and algal rhizoids (Kropf *et al.*, 1998). Organelles such as mitochondria, Golgi membranes and secretory vesicles become highly abundant at the apex of tip growing systems (Brawley *et al.*, 1977; Kropf *et al.*, 1998; Miller *et al.*, 1999), where cell membrane and newly synthesised cell wall are continuously secreted (Kropf, 1992; Battey and Blackbourn, 1993). In pollen tubes and root hairs, the organelles and secretory vesicles are guided to the rhizoid pole by axially arranged F-actin (Shimmen *et al.*, 1995), which is anchored into a cortical ring near the growing tip (Lord and Sanders, 1992; Miller *et al.*, 1999). It is generally believed that the apex of pollen tubes and root hairs is an F-actin-free zone (Lord and Sanders, 1992; Miller *et al.*, 1999) but an inability to stain for F-actin may reflect high polymerisation/depolymerisation rates in the tip of growing pollen tubes (Fu *et al.*, 2001). A sub-apical cortical actin ring has also been reported in fucoid rhizoids, although there are also F-actin hotspots in the rhizoid tip itself (Henry *et al.*, 1996; Alessa and Kropf, 1999; Pu *et al.*, 2000). Furthermore, a sub-apical ring of F-actin has also been demonstrated in the polarised apical cell of the brown algae

Sphacelaria rigidula which displays tip growth (Karyophyllis *et al.,* 2000). Elongation of tip growing cells occurs by continuous secretion of new wall at the rhizoid apex but may depend on the generation of turgor pressure. Turgor pressure develops in fucoid zygotes during axis fixation (Allen *et al.,* 1970) and its role during rhizoid elongation has been demonstrated by Wright and Reed (1990), who found that hyper-osmotic treatment inhibited rhizoid germination and elongation. As the cell wall matures, it becomes more rigid, hardens and the cell diameter reaches a maximum at about 15 μm in *Fucus* rhizoids.

3.1.3.2. Ca^{2+} and apical growth

The Ca^{2+} gradient, which is established during zygote polarisation, is a requirement for rhizoid germination and elongation, although apical [Ca^{2+}] is higher and the gradient more localised, providing a much stronger polar signal (Roberts *et al.,* 1993; Berger and Brownlee, 1993; Taylor *et al.,* 1996). Similarly a gradient of high [Ca^{2+}] is confined to the growing tip of pollen tubes (Malhó and Trewavas, 1996; Pierson *et al.,* 1996) and root hairs (Wymer *et al.,* 1997). The apical Ca^{2+} gradient is a requirement for apical growth, as microinjection of Ca^{2+} buffers such as BAPTA into rhizoids and root hairs, or adding the Ca^{2+} chelator, EGTA to the medium extinguishes the Ca^{2+} gradient and inhibits elongation (Kropf and Quatrano, 1987; Speksnijder *et al.,* 1989; Roberts *et al.,* 1993; Pierson *et al.,* 1996; Taylor *et al.,* 1996).

Exactly how the Ca^{2+} gradient is maintained is not clear. One theory suggests re-distribution of Ca^{2+} channels in an F-actin-dependent process (Kropf, 1994; Shaw and Quatrano, 1996a). By the use of fluorescent dihydropyridine, which may bind to Ca^{2+} channels, it was suggested that the putative Ca^{2+} channels become more abundant at the rhizoid pole than in the rest of fucoid zygotes during axis establishment (Shaw and Quatrano, 1996a). Ca^{2+} channels could be guided to the rhizoid pole by F-actin and the

increased concentration of Ca^{2+} channels may result in increased Ca^{2+} influx causing the Ca^{2+} gradient detected in the region (Shaw and Quatrano, 1996a). However, new evidence (Taylor *et al.*, 1996) challenges this view. Patch clamping of voltage-activated mechano-sensitive Ca^{2+} permeable channels in polarised *Fucus* zygotes revealed no asymmetrical distribution of Ca^{2+} permeable channels (Taylor *et al.*, 1997). The presence of turgor pressure and a soft cell wall at the cell apex in tip growing cells (Kropf *et al.*, 1998) may give rise to spatial regulation of evenly distributed mechano-sensitive Ca^{2+} permeable channels (Pierson *et al.*, 1996; Taylor *et al.*, 1997). The higher elasticity of the cell wall at the rhizoid apex, than in the rest of the zygote, would allow the cell membrane at the apex to stretch and consequently activate mechano-sensitive Ca^{2+} permeable ion channels in response to increased internal turgor (Taylor *et al.*, 1997). This system potentially allows a very simple way of maintaining an apical Ca^{2+} gradient during polar growth.

3.1.3.3. Cell fate and division patterns

Subsequent to rhizoid germination, the zygote divides perpendicular to the polar axis and two distinctively asymmetric cells, with very different fates, are formed (Figure 3.03 a-b). One is the spherical thallus cell, which is the precursor for the stipe and thallus, and the other is the elongate rhizoid cell, which develops into the disk holdfast of the adult. Cell fate and orientation of the cell division plane in the cleaving embryo is determined by the orientation of the polar axis, spatial information stored in the cell wall, and communication between cells (Berger *et al.*, 1994; Bouget *et al.*, 1998; Bisgrove and Kropf, 1998). The orientation of the first cell division is determined by alignment of the spindle with the polar growth axis and involves the microtubular cytoskeleton (Kropf *et al.*, 1990; Bisgrove and Kropf, 1998; Corellou *et al.*, 2000). Subsequent to germination the nucleus is rotated to a position parallel with the growth axis in a microtubule-dependent process, which results in division perpendicular to the polar axis (Kropf *et al.*, 1990). It has been shown that

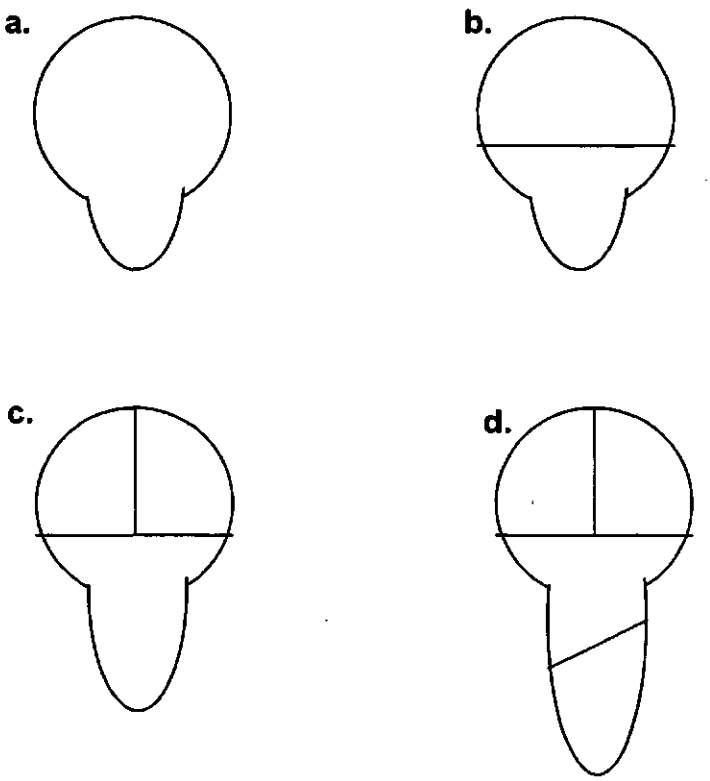

Figure 3.03. Early cell division in *Fucus* zygotes, showing an undivided, germinated cell (**a**), first cell division resulting in the thallus and rhizoid cells (**b**), second cell division, symmetrically dividing the thallus (**c**), and third cell division, asymmetrically dividing the rhizoid (**d**).

inhibition of axis fixation resulted in loss of the ability of the zygote to orientate the first division plane perpendicular to polarising light (Allen and Kropf, 1992; Shaw and Quatrano, 1996b). Subsequent embryo growth was reduced and malformations such as multiple rhizoids appeared (Allen and Kropf, 1992; Shaw and Quatrano, 1996b). The cell wall may play a key role in axis fixation by anchoring an F-actin stabilising complex and may play a position-dependent role in cell fate determination (Brownlee and Berger, 1995; Bouget *et al.,* 1998b). In the germinating and elongating rhizoid, secretory vesicles are continuously transported towards the rhizoid pole and it is possible that components involved in cell fate determination are being secreted into the cell wall. Embryonic *Fucus* cells are totipotent and possess the ability to de-differentiate completely when isolated as protoplasts or single cells. Their fate is therefore not determined exclusively by intracellular factors (Berger and Brownlee, 1995; Bouget *et al.,* 1998b). Laser microsurgery experiments showed that thallus and rhizoid cells isolated within their own wall continued to develop as normal, whereas their fate was switched when brought into contact with the wall of another cell type (Berger *et al.,* 1994). This finding clearly showed that some property of the cell wall plays a crucial role in cell differentiation in the developing embryo. Furthermore, Bouget and co-workers (1998b) showed that cell fate determination in *Fucus* embryos is dependent on cell-to-cell communication, and that this communication involved the transport of inhibitory messengers. Within the frame set by the polar axis, intracellular communication and the cell wall, the embryo continues to develop. The second cell division in the embryo is normally a symmetric division of the thallus cell perpendicular to the first cell division. Third cell division is an asymmetric division of the rhizoid cell transverse to the growth axis (Figure 3.03 c-d). The rhizoid continues to divide into large elongate cells perpendicular to the growth axis. This pattern of division would be conditioned by continued nuclear rotation prior to each cell division (Allan and Kropf, 1992). Divisions of the thallus cells are always perpendicular to the

previous cell division and these quickly continue to form many small cells, rich in chloroplasts (Kropf *et al.*, 1998).

3.1.4. Stress responses in the *Fucus* embryo

Living in the intertidal zone, *Fucus* embryos are naturally exposed to highly varying conditions of stress such as solar irradiance, salinity and temperature to which they must respond and adapt in order to develop into adult algae. At low tide the inhabitants of the intertidal zone can be exposed to high levels of solar irradiance and a varying osmotic environment. During high tide, intertidal organisms experience low solar irradiances and highly variable osmotic conditions.

3.1.4.1. Osmoregulation

A common response of plant and algal cells to environmental stress is a transient elevation in cytosolic Ca^{2+} (Sanders *et al.*, 1999). The amplitude and duration of the Ca^{2+} signal may be dependent on the strength of the stimulus (Malhó *et al.*, 1998; Goddard *et al.*, 2000). Examples of this stress response include an increase in cytosolic Ca^{2+} as in the response to cold shock in tobacco and *Arabidopsis* seedlings, involving flux of Ca^{2+} into the cytoplasm from both internal and external sources (Knight *et al.*, 1996). Oxidative stress inflicted upon tobacco seedlings by exposing them to H_2O_2 induced a cytoplasmic Ca^{2+} elevation which in turn resulted in changed superoxide dismutase activity (Price *et al.*, 1994). These examples demonstrate the importance of Ca^{2+} in stress control in plant cells. Ca^{2+} involvement in response to changing external osmotic pressure in *Fucus* embryos is well documented (Taylor *et al.*, 1996; Goddard *et al.*, 2000). Like most plant cells, the thallus cell of the *Fucus* zygote is surrounded by a rigid cell wall which forms a physical barrier to

the expansion of the protoplast within it. Consequently the volume of the thallus cell remains relatively constant when exposed to hypo-osmotic conditions (Taylor *et al.*, 1996). In contrast, the soft cell wall at the apex of the *Fucus* rhizoid provides less resistance against swelling during hypo-osmotic exposure. Consequently the surface area of a *Fucus* rhizoid cell increases by up to 20% in response to a 50% hypo-osmotic shock (Taylor *et al.*, 1996). To avoid uncontrolled swelling and bursting, the rhizoid cell possesses the ability to osmoregulate by controlling the amount of ions and water in the cell. Osmoregulation in algal cells of different species which do not possess a rigid cell wall is highly dependent on Ca^{2+} signalling (Okazaki *et al.*, 1987; Tazawa *et al.*, 1995). Hydration of the cytoplasm results in a transient elevation of $[Ca^{2+}]_{cyt}$, which can be prevented by microinjection of BAPTA into the cell or by removing Ca^{2+} from the medium (Okazaki *et al.*, 1987; Tazawa *et al.*, 1995; Taylor *et al.*, 1996, 1997). In the *Fucus* zygote the Ca^{2+} response during hypo-osmotic treatment occurs at the cell apex where Ca^{2+} is elevated during tip growth (Taylor *et al.*, 1996, 1997). Subsequent to hypo-osmotic swelling of the *Fucus* rhizoid, Ca^{2+} influx at the rhizoid apex is followed by a Ca^{2+} wave which spreads to the sub-apical region by release from internal stores as the rhizoid continues to swell (Goddard *et al.*, 2000). Ca^{2+} activation of Ca^{2+}-, Cl^-- and K^+-channels is involved in volume regulation in different systems (Garrill *et al.*, 1992; Taylor and Brownlee, 1993; Ward and Schroeder, 1994). The cytosolic Ca^{2+} wave in the *Fucus* rhizoid during exposure to hypo-osmotic conditions could stimulate Ca^{2+}-activated ion channels in the plasma membrane and in this way mediate efflux of K^+-and Cl^--ions (Taylor *et al.*, 1996, 1997). Hypo-osmotic shock has been shown to induce an increased efflux of Cl^- and K^+ from the cytoplasm of *Pelvetia* zygotes, which was sufficient to significantly decrease the cell volume by promoting osmotic efflux of water (Nuccitelli and Jaffe, 1976).

3.1.4.2. Other stress factors

In addition to a highly varying osmotic environment, *Fucus* embryos are naturally exposed to the stress inflicted upon them by high solar irradiances and disturbances caused by wave movements. Wave action may be a major mortality factor amongst seaweed embryos, with consequences for their distribution and abundance (Vadas *et al.*, 1992). The proportion of embryos settling on the substratum decreases with increasing water velocity, and large numbers may be swept away from the shore (Norton, 1978). Gentle wave movements bring sand in suspension and consequently move it around on the beach, whereas more violent waves can move stones and turn over boulders. Consequently the embryos are in danger of being covered or crushed under the sediment. Adult *Fucus*, however, has a very tough thallus and a strong stipe and holdfast and is therefore adapted to cope with these conditions (Norton *et al.*, 1982). Even with a great loss of embryos *Fucus* still dominates the North Atlantic beaches due to mass production of new recruits.

Fucus embryos are naturally shade adapted (Coelho *et al.*, 2001) and high irradiances of photosynthetically active radiation (PAR) and UV are lethal to the microscopic stages (Lüning and Neushul, 1978; Graham, 1996; Franklin and Foster, 1997). Recovery rates of *Laminaria* gametophytes exposed to sub-lethal irradiances are very slow (Hanelet *et al.*, 1997) and high level PAR+UV reduces the proportion of gametophyte and sporophyte germination and growth rate (Dring *et al.*, 1996; Yabe *et al.*, 1997). These microscopic stages, however, can adapt to increased UV irradiances (Han and Kain, 1996; Franklin and Foster, 1997), although shelter under the adult canopy is the major factor in avoiding high irradiances.

Both high irradiances and wave action are naturally-occurring hazards which can be amplified by human activities, where global warming may result in more violent storms,

and damage to the ozone layer is concomitant which increases the UV irradiance. Anthropogenic activities can also result in other and more direct environmental hazards. Macroalgae in coastal environments, in particular in industrialised areas, are exposed to nutrient enrichment, contamination from organic matter, and toxins such as pesticides and heavy metals, including copper, which may present a real threat to fucoids in some of their natural habitats.

3.1.5. Effects of copper on early stages of *Fucus*

Copper is a potential hazard to brown algae and may have severe effects on the physiology of the adult algae (Chapter 2). Microscopic life cycle stages of brown algae have also been subject to research in recent years but, the exact target of copper toxicity in the early development of the algae is largely unknown. Standardised protocols for the use of the microscopic life history stages of *Laminaria* and *Macrocystis* in toxicity testing have been developed and several studies address their response to copper exposure (Chung and Brinkhuis, 1986; Anderson *et al.*, 1990; Bidwell *et al.*, 1998). Gametophyte development and growth of the young sporophytes of *Laminaria* and *Macrocystis* are more sensitive to copper than meiospore release and germination. Meiospore release, spore settlement and gametophyte germination in *Laminaria* and *Macrocystis* were unaffected by copper at concentrations below 0.8-1.0 μM (Chung and Brinkhuis, 1986; Anderson *et al.*, 1990; Bidwell *et al.*, 1998). On the other hand, 0.08 μM copper had an inhibitory effect on gametophyte development and 0.16 μM copper resulted in abnormal growth patterns, with gametophytes failing to reach maturity (Chung and Brinkhuis, 1986). At 0.28 μM there was no sporophyte development at all (Chung and Brinkhuis, 1986; Anderson *et al.*, 1990). The microscopic stages of kelp may be more sensitive to elevated metal concentrations

Macrocystis, whereas there were no toxic effects on spore germination at concentrations below 47μM (Bidwell *et al.*, 1998).

Studies of copper toxicity have also focused on the different life history stages of fucoids. The toxic effects of copper on fertilised eggs of *F. vesiculosus* are highly dependent on the timing of exposure of the eggs. Exposing eggs of *F. vesiculosus* to 0.3 μM copper at the time of fertilisation had no effect on fertilisation, whereas pre-incubating eggs in the same concentration 30 minutes before sperm was added resulted in a 50 % decrease in fertilisation success (Andersson and Kautsky, 1996). Germination of *F. vesiculosus* zygotes is a critical stage in terms of copper toxicity. As little as 0.04 μM copper, added at the time of fertilisation, reduced germination by up to 50%, whereas germination of embryos was unaffected by up to 0.6 μM copper when added 24h AF (Andersson and Kautsky, 1996). Furthermore, rhizoid elongation of *F. vesiculosus* embryos exposed to copper after germination was unaffected by up to 0.5 μM copper after 7 days of exposure (Gledhill *et al.*, 1999). Consequently the *F. vesiculosus* embryos have developed some degree of copper tolerance at 24h AF, which is comparable to the tolerance limit between 0.4 and 0.8 μM for the adult algae (Strömgren, 1980). Evidently, the tolerance limit for Cu^{2+} in developing *Fucus* embryos changes rapidly, and increases several fold within a few hours (Andersson and Kautsky, 1996). Exposure of *F. spiralis* zygotes to copper after fertilisation, but prior to germination, resulted in a pronounced inhibitory effect on rhizoid elongation although all the zygotes germinated (Bond *et al.*, 1999). In that study, copper was added at an early stage in zygote development and it is impossible to distinguish exactly which developmental stage was targeted. Although there was a striking effect on rhizoid elongation, this could reflect damage to earlier developmental events as well as an effect directly on rhizoid elongation. Andersson and Kautsky (1996), however, exposed

the processes prior to rhizoid germination are particularly sensitive to Cu^{2+}. Although the sparse studies on effects of copper on *Fucus* embryos give some indications of the most vulnerable developmental stages, the more precise targets for Cu^{2+} toxicity in the early development of the *Fucus* zygote still need to be established.

3.1.6. Objectives

This work sets out to determine targets of copper toxicity in the development and growth of the *Fucus* zygote.

- The copper sensitivity of different developmental stages of zygotes, *i.e.* axis formation and fixation, is determined.
- Effects of copper on the rate and pattern of cell division and on osmoregulation are established.
- Effect of copper on rhizoid elongation of embryos from three different populations is measured and inter-population differences established.
- Effects of copper on the physiological processes underlying early development and rhizoid elongation are determined by studying effects of copper on:

  1. F-actin localisation
  2. Localised secretion of fucoidin
  3. The Ca^{2+} gradient

3.2. Material and methods

3.2.1. Experimental algae

Adult *F. serratus* bearing mature fronds were collected at low tide from a population with known Cu^{2+} tolerance status. It was previously established that adult *F. serratus* from the Cu^{2+} exposed Restronguet Creek have a significantly higher Cu^{2+} tolerance limit than adult *F. serratus* from unexposed locations (Wembury Beach and Bantham Quay) which have the same low Cu^{2+} tolerance limit (Chapter 2). Mature receptacles were cut from separate male and female fronds. Fronds were rinsed in seawater, blotted dry and stored in a single layer between paper towels and wrapped in plastic in the dark at 3-5°C for up to two weeks. Gametes could be obtained from conceptacles within 3-4 days of collection.

3.2.2. Obtaining and culturing zygotes

To obtain eggs, female receptacles were rinsed thoroughly in tap water to remove any previously released oogonia and to stimulate new release. To further stimulate release, receptacles were placed in natural light or under fluorescent white light for 15 min. Subsequently fronds were placed in UV-treated and filtered (0.45 μm cellulose nitrate membrane) natural seawater (FSW) in the light for about 1h. Receptacles were removed and the oogonia were collected with a pasteur pipette and transferred to fresh FSW, which induced release of eggs from the oogonia. Eggs were separated from the empty oogonia by filtering through a 100 μm nylon mesh and rinsing them in FSW.

Rinsing male receptacles in tap water and placing them in natural or fluorescent light induced sperm release, which appeared as orange secretions on the surface of the receptacles. Sperm was collected and activated by rinsing secretions of a receptacle into approximately 15 ml FSW. Sperm activity was monitored under the microscope at magnification ×20.

To induce fertilisation sperm and eggs were mixed under fluorescent white light at 16°C for 30 min. Fertilisation was stopped by filtering the zygotes several times through a 100 μm nylon mesh into fresh FSW. Zygotes were sown sparsely onto small petri dishes (d=2.5 cm) with coverslip bases and incubated at 16°C in unidirectional white light. Adhesion of the zygotes to the coverslips started immediately and after one hour the FSW was gently replaced with 5 ml of the artificial seawater medium, Aquil, modified from the original recipe by Morel *et al.* (1979) as described in Chapter 2, until the beginning of the experiment. One dish of zygotes was equivalent to one population and contained >200 zygotes.

3.2.3. Manipulating the orientation of the polar axis

Polar axis orientation in the *Fucus* zygote occurs in response to the direction of unidirectional light (L1) experienced by the zygote during the first few hours after fertilisation (Figure 3.04a) (Quatrano, 1973; Kropf, 1992; Berger and Brownlee, 1994). Therefore, the orientation of the polar axis is easily manipulated by different light treatments during axis establishment. Zygotes transferred to dark prior to axis formation germinate in random directions (Figure 3.04b). Exposure to L1 during axis formation and subsequent transfer to darkness during the axis fixation period results in the zygotes fixing

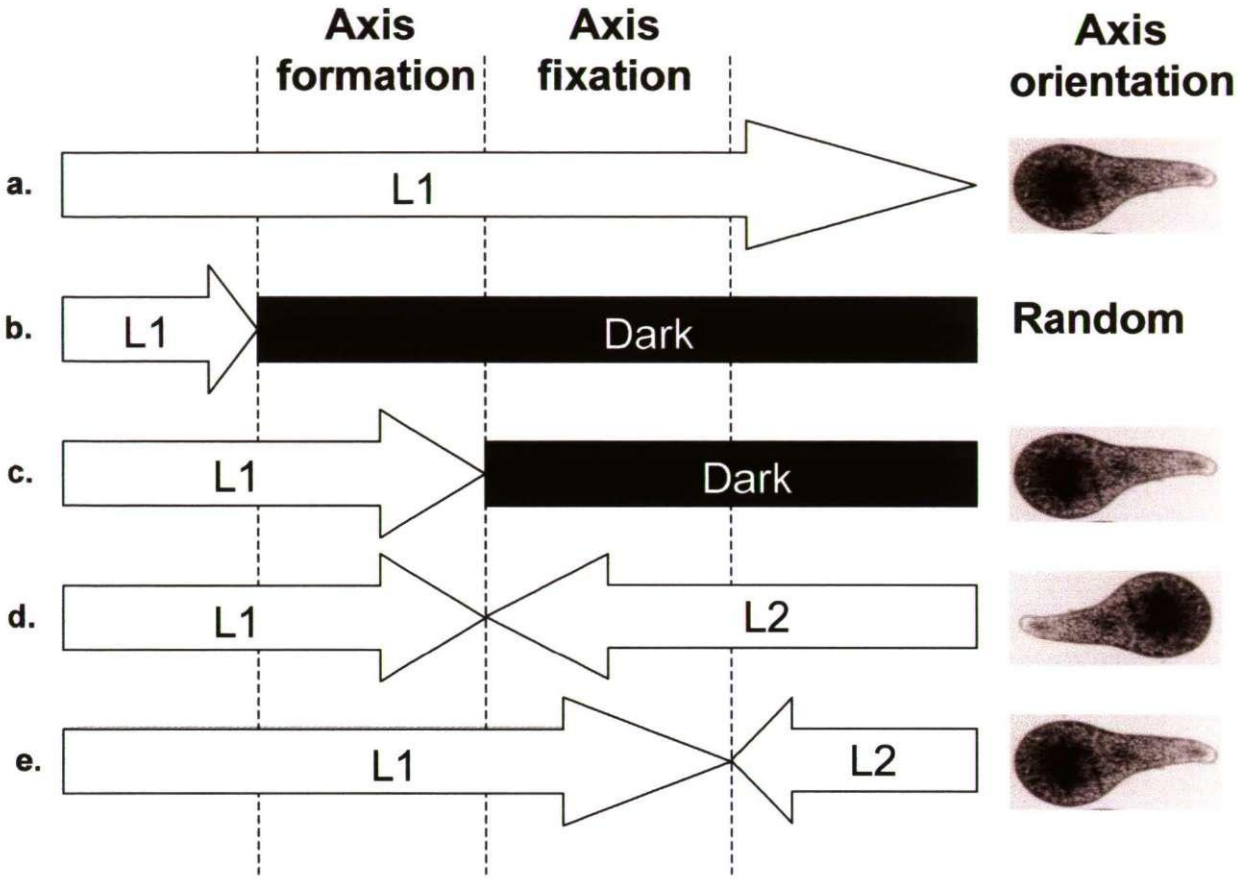

Figure 3.04. Manipulation of the light environment experienced by *Fucus* zygotes controls the orientation of the polar axis. The polar axis is expressed by rhizoid germination. The figure shows zygotes exposed to unidirectional light (L1) during axis establishment (**a**), zygotes transferred from L1 to darkness prior to axis formation (**b**), zygotes transferred from L1 to darkness prior to axis fixation (**c**), zygotes transferred from L1 to reversed unidirectional light (L2) prior to axis fixation (**d**), and, zygotes transferred from L1 to L2 after axis fixation (**e**).

their axes according to the polarising signal received during axis formation. Therefore, transfer of zygotes from L1 to darkness immediately after axis formation will result in germination away from L1 (Figure 3.04c). Light from the opposite direction of L1 (L2), immediately following exposure to L1 during axis formation will cause the polar axis to be re-orientated according to L2 (Figure 3.04d). However, zygotes which have irreversibly fixed their polar axes during exposure to L1 and subsequently transferred to L2 will be unaffected by L2 and germinate according to L1 (Figure 3.04e).

3.2.4. Establishing the period of axis formation and fixation

To determine the periods of axis formation and fixation, populations of synchronously developing zygotes from the same batch were grown in FSW at 16°C in L1. At one-hour intervals from 2 to 14h AF, populations of zygotes were either transferred to darkness to determine the proportion which had formed an axis or to L2 to determine the proportion of zygotes which had fixed an axis at the given time.

The proportion of zygotes, which formed their axes prior to transfer to dark and fixed their axes prior to transfer to L2 was scored during germination after 24h (Figure 3.04 c and e). Polarisation was calculated as:

(number of zygotes germinating in the hemisphere away from L1) / (total number of germinated zygotes).

Populations of zygotes transferred to dark before the onset of axis formation germinated in random directions and an even number of zygotes germinated towards and away from L1. Consequently total inhibition of axis formation occurred at 50% polarisation and complete axis formation at 100% polarisation. At total inhibition of axis fixation, all zygotes would germinate towards L1 and therefore occurred at 0% polarisation (Figure 3.04 d), whereas

all zygotes would germinate away from L1 in the event of complete axis fixation (*i.e.* 100% polarisation, Figure 3.04 e).

3.2.5. Effects of Cu^{2+} on axis formation and fixation

Effects of Cu^{2+} on axis formation were studied on zygotes from the Wembury population whereas effects of Cu^{2+} on axis fixation were carried out on zygotes obtained from both the Wembury Beach and the Restronguet Creek population. The time of axis formation and fixation was determined as described above. Axis formation occurred between 3 and 7h AF and axis fixation occurred between 7 and 13h AF (Figure 3.05). Populations of zygotes were first incubated in Cu^{2+}-free Aquil at 16°C in L1. Subsequently, in either the phase of axis formation or fixation, populations of zygotes were transferred to Aquil containing $[Cu^{2+}]$ ranging from 0 to 2110 nM while still kept in L1. Zygotes were then transferred to darkness in Cu^{2+}-free Aquil to determine the proportion which had formed their axes during the treatment, or to L2 in order to determine the proportion which had fixed their axes during the treatment. Upon germination the proportion of zygotes (>200 per dish) which had formed/fixed their axes during the experiment was scored as described above.

3.2.6. Effects of Cu^{2+} on F-actin localisation

Wembury zygotes were incubated in either Aquil with or without 2110 nM free Cu^{2+} in L1 at 16°C during axis fixation, which was previously determined to be 7-13h AF. At 13h AF the incubation was terminated and F-actin distribution was visualised using the F-actin specific fluorescent probe Texas Red phalloidin (Molecular Probes, Eugene, Oregon,

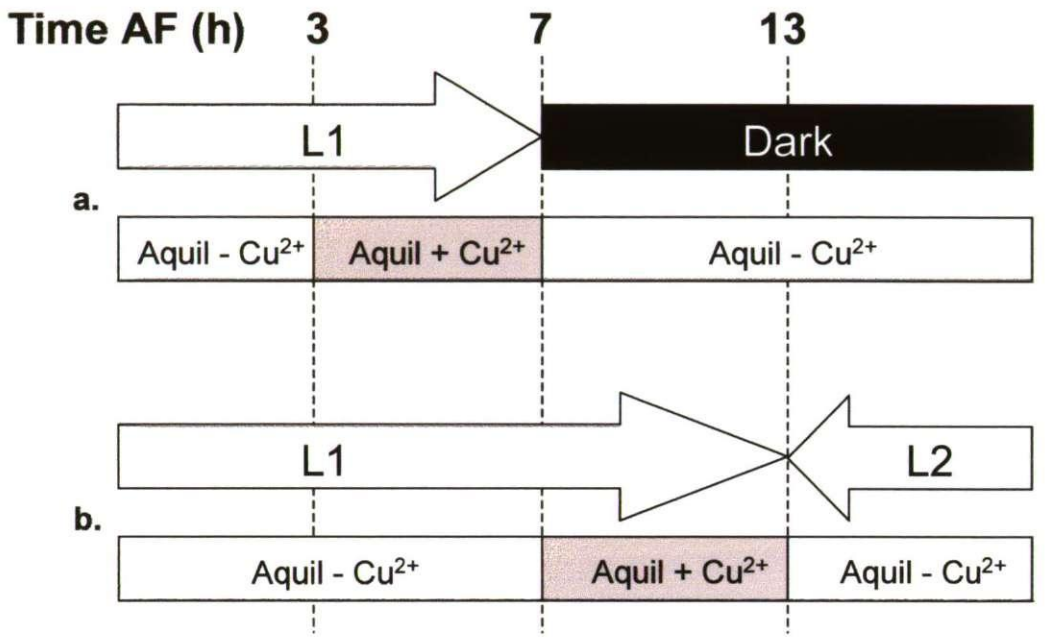

Figure 3.05. Experimental design for the study of the effect of Cu^{2+} on axis formation and fixation in *Fucus* zygotes. Zygotes were exposed to Cu^{2+} and unidirectional light (L1) during axis formation and subsequently transferred to Cu^{2+} free medium and darkness (**a**). Zygotes were exposed to Cu^{2+} and L1 during axis fixation, and subsequently transferred to Cu^{2+} free medium and reversed unidirectional light (L2) (**b**). The ability of the zygotes to form/fix their axis during Cu^{2+} exposure was calculated as the proportion of zygotes germinating away from L1.

USA) and confocal microscopy. Stock solutions contained 300 units of the product in 1.5 ml of methanol to yield an approximate concentration of 6.6 μM. Zygotes were fixed, permeabilised and stained using the following protocol modified from Henry *et al.* (1996). Aquil in the incubation dishes was replaced with 1 ml formaldehyde fixitive (0.1 mM maleimidobenzoyl-N-hydroxysuccinimide ester, 3.8% formaldehyde, 0.2% dimethylsulfoxide in artificial seawater (ASW)). After 30 minutes the fixitive was removed and the zygotes were washed 3 times for 5 minutes in ASW + 0.2 M sorbitol. Fixed zygotes were stained for 30 minutes in Texas Red phalloidin solution (1.3 μM Texas red phalloidin in ASW + 0.2 M sorbitol). Stained zygotes were washed three times for five minutes in ASW + 0.2 M sorbitol. Fluorescent images of stained zygotes were obtained using a confocal scanning laser microscope (Bio-Rad, UK). An argon/krypton laser excited the Texas Red-stained zygotes at 568 nm and emission was recorded at 605 nm. Each image was an average of five scans in the same optical section. By using a 10 nm bandwidth 605 nm emission filter, chlorophyll fluorescence was minimised. The proportion of zygotes which had localised F-actin was scored.

3.2.7. Effects of Cu^{2+} on secretion of fucoidin

Wembury zygotes were transferred to Aquil containing [Cu^{2+}] ranging from 0 to 2110 nM and incubated at 16°C in L1 during axis fixation. At 13h AF the incubation was stopped and secretion of fucoidin in the zygotes was visualised by staining with Toluidine Blue O (TB-O) (Sigma Chemicals, Dorset, UK) which binds to sulphated fucoidin. Zygotes were transferred directly to the TB-O solution (0.1% TB-O in ASW, pH 1.5 with HCl), and after 15 minutes they were washed three times for 5 minutes in 99% ethanol (Shaw and Quatrano, 1996b). Stained zygotes were immediately mounted in ASW and the proportion

of zygotes, which had secreted fucoidin into the cell wall was scored under a light microscope.

3.2.8. Effects of Cu^{2+} on osmoregulation

Wembury zygotes were grown in Cu^{2+}-free Aquil to allow the early developmental events and rhizoid germination to take place. At 18h AF embryos were transferred to Aquil containing [Cu^{2+}] varying from 0 to 2110 nM for 6 hours. Zygotes were then exposed to ASW diluted with distilled water to either 50% or 25%. To allow rapid solution exchange around the embryos during the hypo-osmotic treatment, as much medium as possible was removed from the chambers and the embryos were flushed with 5 ml of diluted ASW by the use of a 5 ml pipette. The proportion of embryos (>200 per dish) which were able to osmoregulate during hypo-osmotic treatment was determined as:

(1-bursting embryos/total number of embryos).

3.2.9. Rhizoid elongation and Cu^{2+} tolerance

To determine the effect of Cu^{2+} on rhizoid elongation, sparsely plated Wembury and Restronguet zygotes were allowed to develop in the incubation chambers in 5 ml Cu^{2+}-free Aquil under standard lab conditions (see above, section 3.2.2.) until 18h AF. At this time the early developmental events had occurred and the embryos had just started to germinate. Subsequently embryos were transferred to Aquil containing [Cu^{2+}] varying from 0 to 844 nM. *Fucus* embryos release metal-complexing ligands when exposed to metals, which bring about a decrease in [Cu^{2+}] (Gledhill *et al.*, 1999). To compensate for ligand release

from the growing embryos the medium was changed every day. Embryos were grown for a total of 10 days. At suitable intervals transmission images of >25 embryos per dish were recorded on a confocal microscope (Bio-Rad, UK) at x10 magnification. The length of the rhizoid defined as the distance from the rhizoid/thallus dividing wall to the rhizoid tip was measured using analytical software (KALCIUM ANALYSE, Kinetic Imaging, Liverpool, UK). Rhizoid length was calibrated with a graticule.

To allow for any population differences caused by factors other than Cu^{2+} a comparative experiment examining effects of Cu^{2+} on rhizoid elongation in embryos obtained from the two Cu^{2+} intolerant populations, Wembury Beach and Bantham Quay was carried out. The protocol described above was followed except embryos were grown in Aquil containing 0 and 211 nM Free Cu^{2+} and measurements were taken on day 2, 5, and 8 AF.

3.2.10. Cell division

Fertilised Wembury zygotes were allowed to settle in the incubation dishes. At 2 h AF zygotes were transferred to Aquil containing [Cu^{2+}] varying from 0 to 844 nM. To visualise the number of cell divisions by 24 h and 40 h AF, zygotes were immersed for 10 minutes in the membrane-specific dye N-(3-triethyl-ammonium propyl)-4-(4-(dibutylamino) styryl) pyridinium dibromide (FM 1-43, 1 μM) (Molecular Probes, Eugene, Oregon, USA). This effectively labelled the partition membranes (Goddard *et al.*, 2000). The number of cell divisions was monitored by imaging at least 25 embryos per dish on a confocal laser scanning microscope (Bio-Rad, UK) at 488 nm excitation and 530 nm emission.

3.2.11. Effect of Cu^{2+} on cytosolic Ca^{2+} in the *Fucus* rhizoid

To study the effects of Cu^{2+} on cytosolic free Ca^{2+} in the *Fucus* zygote, two experiments were carried out. **1).** Effects on Ca^{2+} signalling in the rhizoid apex of a moderate Cu^{2+} treatment given as a short term pulse or as chronic exposure were studied by monitoring Ca^{2+} during hypo-osmotic shock. **2).** The effect on global cell Ca^{2+} of acute exposure to high [Cu^{2+}] in the *Fucus* rhizoid was investigated.

Both experiments were carried out on germinated Wembury zygotes. Rhizoid cells were microinjected with the Ca^{2+} specific dye Calcium Green and the Ca^{2+} indifferent dye Texas Red in order to obtain simultaneous fluorescent images by confocal laser scanning microscopy (see below).

3.2.11.1. Microinjection of Calcium Green/Texas Red

Germinated *Fucus* zygotes at the two-cell stage were pressure microinjected with artificial intracellular solution (5 mM Hepes, 200mM KCl, 550 mM Manitol at pH 7.4; Berger and Brownlee, 1993) containing 1 mM Calcium Green, 10,000 dextran, and 1 mM Texas Red, 10,000 dextran (Molecular Probes, Oregon, USA). Incubation chambers containing embryos were placed and held in position on the stage of a Nikon inverted microscope fitted with a ×40 (N.A. 1.3) oil immersion objective. Micropipettes were pulled from 0.69 mm (inner diameter) GC120F filamented borosilicate glass capillaries (Clark Electromedical Instruments, UK) on a horizontal electrode puller (model p-87 Sutter Instruments, USA). Dry bevelling of electrodes produced sharp tips with a larger opening relative to the tip diameter. This improved the impalement success and reduced pipette blockage (Kaila and Voipoi, 1985; Taylor *et al.*, 1996). Microelectrodes were backfilled with the injection solution. The incubation medium was replaced with ASW containing

0.6 M sorbitol to reduce the cell turgor sufficiently to prevent bursting during the period immediately following microinjection. The natural adhesion of embryos to the coverslip bases of the incubation chambers was sufficient to hold the embryos in position. Before impalement of an embryo, a holding pressure of 20 kPa was established in the pipette by a Pico-injector PLI-100 (Medical Systems, USA) in order to avoid backflow of medium into the pipette or blockage of pipettes with cytoplasm on impalement. Impalement of an embryo 20-30 μm from the tip was carried out under white light illumination. After impalement the injection pressure was switched to 220 kPa and injection was monitored visually by dye fluorescence at 530 nm. Excitation light was provided by a xenon bulb (Burke Electronic) and dye emission passed through a 520-560 nm filter. Following microinjection, the micropipette was carefully removed and embryos were gradually transferred from hyperosmotic ASW to Aquil over 30 minutes. Embryos were allowed to recover under incubator conditions for at least 90 minutes before Ca^{2+} measurements were made.

3.2.11.2. Acquiring ratio confocal Ca^{2+} images

Embryos in incubation chambers were viewed on the stage of the Nikon inverted microscope with a ×40 (N.A. 1.3) oil immersion objective. Calcium Green and Texas Red images were acquired with a MRC 1024 confocal laser scanning imaging system (Bio-Rad, UK) (Figure 3.06). An argon-krypton laser exited Calcium Green at 488 nm and Texas Red at 568 nm. Embryos were normally scanned at 10% laser power, which was appropriate to yield a good signal/noise ratio without significant photobleaching of the dyes. The excitation wavelengths were reflected by a tricroic mirror and focused into a scanning beam by a lens before reaching the embryo. Emission light of 530 nm for Calcium Green and 605 nm for Texas Red was reflected from the focal point and passed back through the lens and straight through the tricroic mirror. A dicroic mirror reflected green light at

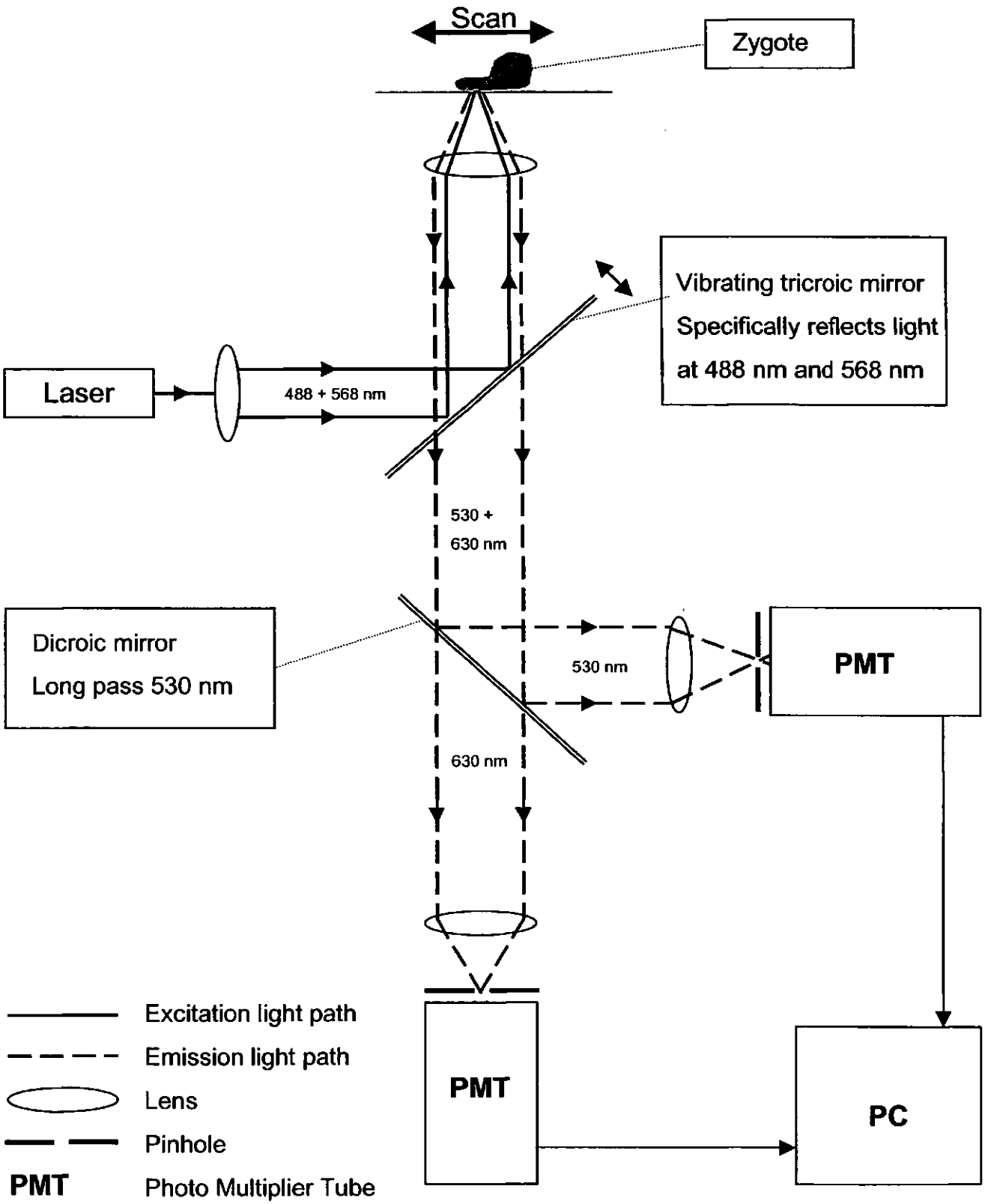

Figure 3.06. Schematic diagram of the laser scanning confocal microscope and light paths during acquisition of fluorescence ratio images.

wavelengths below 530 nm towards a second lens, which focused it through a pinhole in a photomultiplier. The red emission light at 605 nm passed straight trough the dicroic mirror and was focused through the pinhole in a second photomultiplier tube. The confocal pinhole apertures serve to block any light which does not originate from the focal plane, so that any unfocused information is not included in the final image. The light signal received by the photomultiplier tubes in response to the scanning laser beam was converted into digital images based on 255 grey levels in the analytical software package LASERSHARP 3.2 (Bio-Rad, UK). The Bio-Rad Time Course software package was used to ratio the Calcium Green image against the Texas Red image in order to calibrate for dye distribution and yield the true quantitative Ca^{2+} distribution in the cell (Goddard *et al.*, 2000).

3.2.11.3. *In vitro* calibrations

To estimate the amount of dye injected into the embryos, *in vitro* calibration of the dye concentration was obtained by measuring the fluorescence intensity in droplets of intracellular solution containing Texas Red concentrations varying from 0 to 250 μM. Droplets were placed on the stage of the confocal microscope and excited at 568 nm. Emission was recorded at 605 nm and the fluorescence intensity measured by using the analytical software KALCIUM ANALYSE (K.I., Liverpool, UK). The fluorescence values obtained were used to produce a calibration curve for the intracellular dye concentration (Figure 3.07a). Fluorescence measured in Texas Red images of the embryos was calibrated to the curve and a final intracellular dye concentration in the rhizoid of about 50 μM was ensured to avoid buffering of cytosolic Ca^{2+} by the injected calcium green.

In vitro calibrations of $[Ca^{2+}]$ were carried out in order to estimate $[Ca^{2+}_{cyt}]$ in the rhizoid cell. Ratio images of Calcium Green/Texas Red fluorescence were obtained from droplets

Table 3.01. Composition of solutions containing known free Ca^{2+} concentration. Each contained 550 mM mannitol. KOH was used to adjust pH (Tsien and Rink, 1980).

pCa^{2+}	$[CaCl_2]$ (mM)	Ca^{2+} ligand (10 mM)	[KCl] (mM)	pH buffer (10 mM)	pH
5	5	NTA	90	TAPS	8.42
6	5	HEDTA	90	HEPES	7.70
7	5	EGTA	90	MOPS	7.29
8	5	EGTA	100	HEPES	7.80

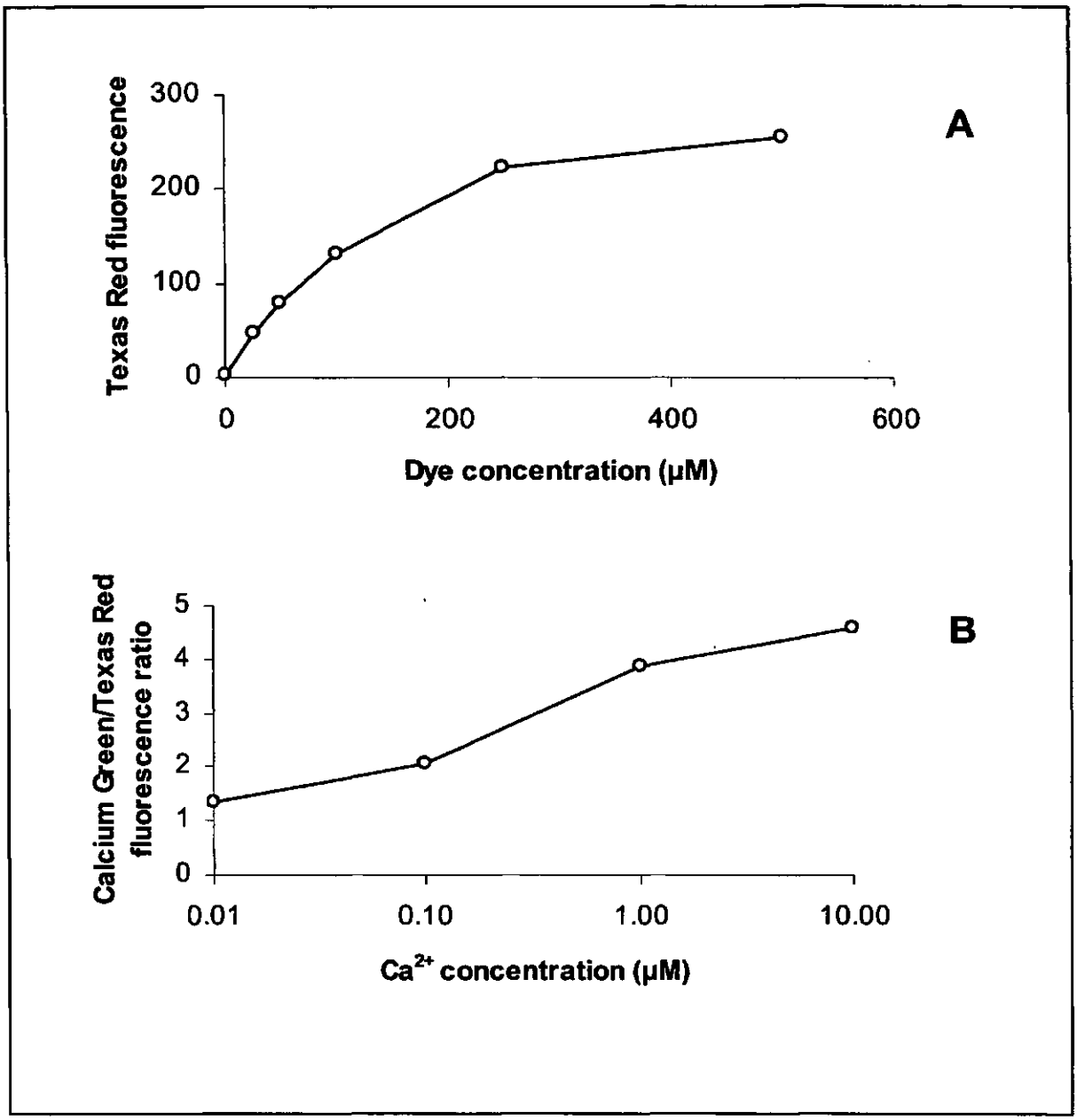

Figure 3.07. *In vitro* calibration curves for dye concentration and Ca^{2+} concentration. Calibration of the dye concentration was carried out by measuring fluorescence intensity at 605 nm of droplets of intracellular solution containing concentrations of Texas Red varying from 0 to 250 μM (**A**). Calibration of the Ca^{2+} concentration was carried out by calculating the ratio of the intensity of the Calcium Green signal to the intensity of the Texas Red signal of droplets containing 0 to 10 μM Ca^{2+} and 50 μM Calcium Green/Texas Red (**B**). Values represents means of 3 measurements.

of different Ca^{2+} buffer solutions (Table 3.01) containing 50 μM Calcium Green/Texas Red by use of a scanning laser confocal microscope and KALCIUM ANALYSE. The fluorescence values of the ratio images were used to produce a calibration curve for $[Ca^{2+}]$ (Figure 3.07b). *In vitro* and *in vivo* calibrations have previously been shown to differ by only 3-8% (Roberts *et al.*, 1994; Goddard *et al.*, 2000), and the *in vitro* calibrations were therefore considered sufficient to monitor dye- and Ca^{2+}-concentration in the rhizoid cells.

3.2.11.4. Effect of Cu^{2+} on cytosolic Ca^{2+}

To monitor the effect of short term and chronic exposure to moderate $[Cu^{2+}]$ on the apical Ca^{2+} gradient in the *Fucus* rhizoid, embryos were transferred to Aquil containing 422 nM free Cu^{2+} at 16°C for 3 hours, or were placed directly onto the stage of an inverted microscope in the incubation chambers and perfused with Aquil containing 422 nM Cu^{2+} for 5 minutes. During perfusion, embryos were placed directly in the perfusion flow provided by a gravity-driven perfusion system to ensure good exchange of medium around the embryo. The perfusion tube was fitted to a mixing chamber which was connected to reservoirs containing experimental media. This allowed rapid change of the medium. A pump removed excess medium from the incubation chamber. Subsequent to the Cu^{2+} pre-treatment, embryos were perfused with hypo-osmotic solution (80% Aquil containing 422 nM Cu^{2+}). Microinjected control zygotes were perfused with 80% Aquil without added Cu^{2+}. Calcium Green/Texas Red fluorescent images of the embryos before and during the hypo-osmotic treatment were recorded every 5 seconds for up to 2 minutes.

To monitor the effect of acute exposure to high $[Cu^{2+}]$ on $[Ca^{2+}]_{cyt}$, microinjected embryos were placed onto the microscope stage without any Cu^{2+} pre-treatment. Calcium Green/Texas Red fluorescent images of rhizoids before and during acute exposure to Aquil

containing [Cu^{2+}] varying from 0.844 to 8.44 μM were recorded at suitable intervals for up to 60 minutes.

To quantify the observed changes in [Ca^{2+}_{cyt}] in response to moderate [Cu^{2+}], fluorescence in the Calcium Green/ Texas Red ratio images of the embryos was measured in the apical and sub-apical region of the rhizoid using the image analytical software KALCIUM ANALYSE (K.I., Liverpool). The measured fluorescence was converted into [Ca^{2+}_{cyt}] on the basis of the Ca^{2+} calibration curve (Figure 3.07b). The effect on Ca^{2+}_{cyt} of acute exposure to high [Cu^{2+}] was expressed as relative changes in globular Ca^{2+} in the rhizoid. The fluorescence measured in the Calcium Green/Texas Red ratio images at any one time during the experiment was normalised to the fluorescence measured immediately before Cu^{2+} was applied.

3.2.12. Statistical tests

Statistical testing of the data (Sokal and Rolf, 1981) was carried out where required by using STATGRAPICS plus 5.0. Assuming variance homogeneity and normal distribution of data (Ricketts, per. Com.), and treating the time factor as an independent variable analysis of variance were calculated as one and two-way ANOVA's and a p=0.05 level of significance was accepted. When significant difference between means was indicated by the ANOVA further comparison of means was carried out by multiple range tests, and also accepted at a p=0.05 level of significance. Where data were presented in percentage, arcsine transformation of the data was carried out prior to any statistical testing.

3.3. Results

3.3.1. Cu^{2+} toxicity in early development

3.3.1.1. Establishing the period of axis formation and fixation

The period for axis formation and fixation in Wembury zygotes was found to occur from 3 to 7h AF (Figure 3.08). Prior to 3h AF, the zygotes were unresponsive to unidirectional light (L1), and orientated their polar axes at random upon transfer to dark. An increasing number of zygotes transferred from L1 to dark from 3 to 7h AF orientated their polar axes according to L1. There was no further increase in the proportion of zygotes polarising according to L1 when transferred to dark later than 7h AF.

Axis fixation was determined to occur from 7 to 13h AF. Although zygotes formed a polar axis according to L1 as early as 3h AF, the axis could still be re-orientated until 7h AF. Transfer of zygotes from L1 to reversed unidirectional light (L2) before 7h AF resulted in re-orientation of the polar axis in response to L2 in the vast majority of zygotes. However, an increasing proportion of zygotes became committed to the axis established during exposure to L1 when transferred to L2 later than 7h AF. By 13h AF all zygotes were fully committed to the polar axis established during exposure to L1, and consequently they were unresponsive to exposure to L2.

3.3.1.2. Effects of Cu^{2+} on axis formation and fixation

Axis formation of Wembury zygotes was not affected by Cu^{2+} at the concentrations used (Figure 3.09). When exposed to [Cu^{2+}] varying from 0 to 2110 nM at least 93% of zygotes polarised within the normal time of axis formation. Due to the high proportion of axis

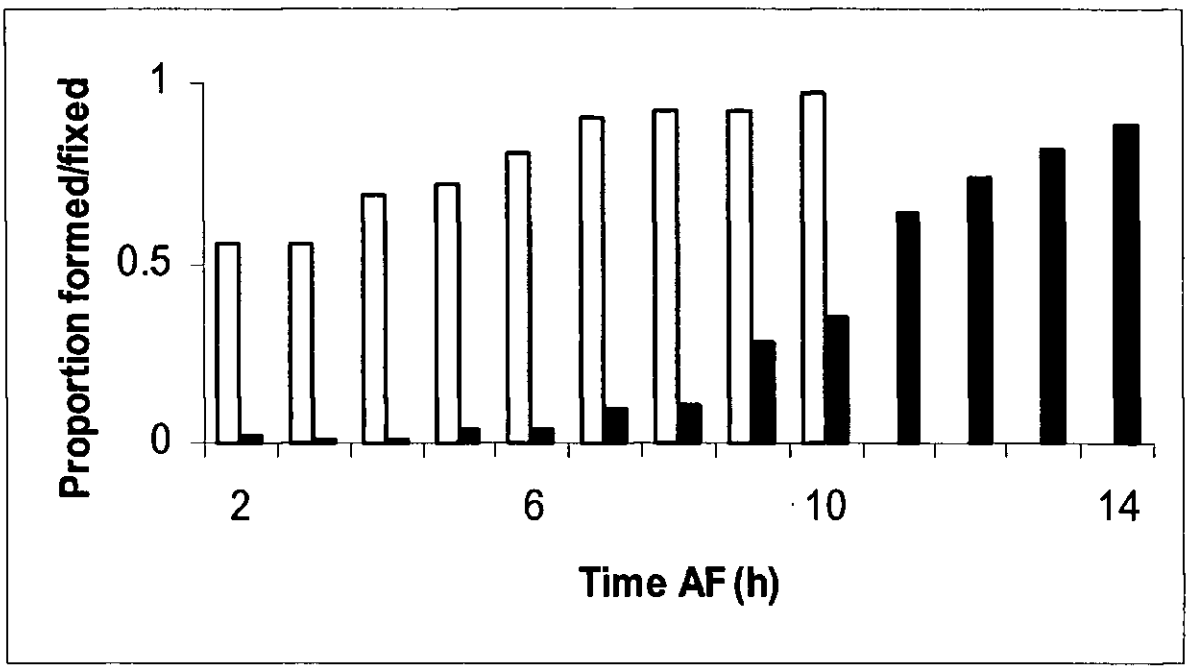

Figure 3.08. Determination of the time for axis formation (○) and fixation (●) in the *Fucus* zygote. Zygotes were incubated in unidirectional light (L1). At various times after fertilisation (AF) zygotes were transferred to dark or to reverse unidirectional light (L2). The proportion of zygotes (>200 in each measurement), which had formed/fixed an axis was scored upon germination. Each data point represents an average of two measurements.

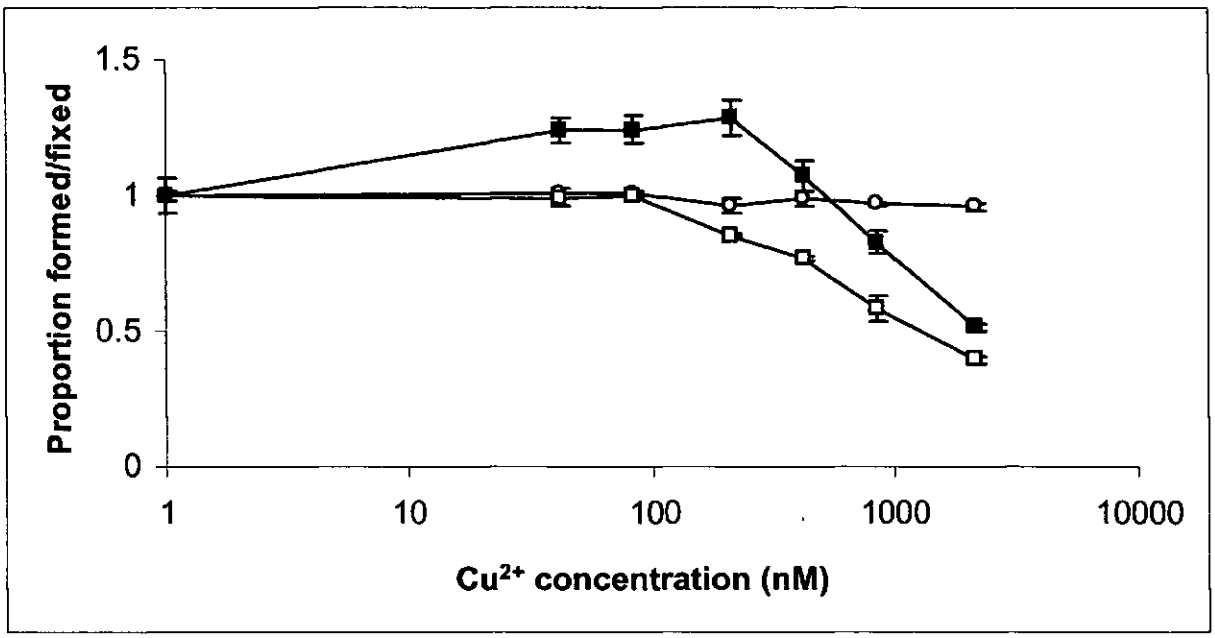

Figure 3.09. Effect of Cu^{2+} on axis formation and fixation in the *Fucus* zygote. Zygotes were incubated with a range of Cu^{2+} concentrations in unidirectional light (L1) during either axis formation or fixation. Subsequently they were transferred to Cu^{2+} free medium and kept in the dark or reversed unidirectional light (L2) until germination. The figure show axis formation in Wembury zygotes (O), and axis fixation in Wembury (□) and Restronguet zygotes (■). Data were normalised to control. Values represents means ± 1 SD (n=4).

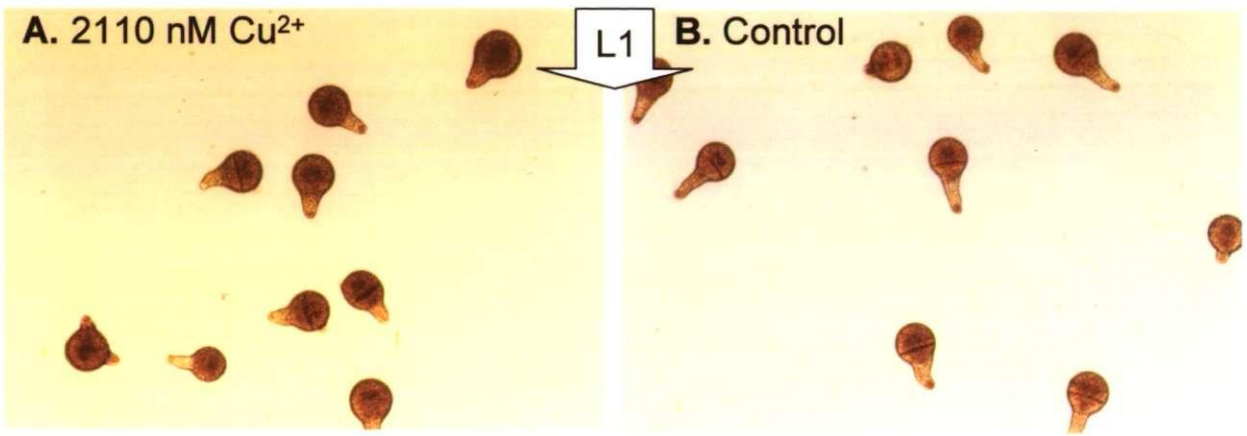

Figure 3.10. Examples of *Fucus* zygotes forming their axes in response to unidirectional light (L1) during axis formation, when exposed to 2110 nM Cu^{2+} (**A**) and in control zygotes not exposed to Cu^{2+} (**B**). Although some of the Cu^{2+} exposed zygotes in this example have orientated their polar axes at a right angle to L1, overall there is no significant difference between the treatments.

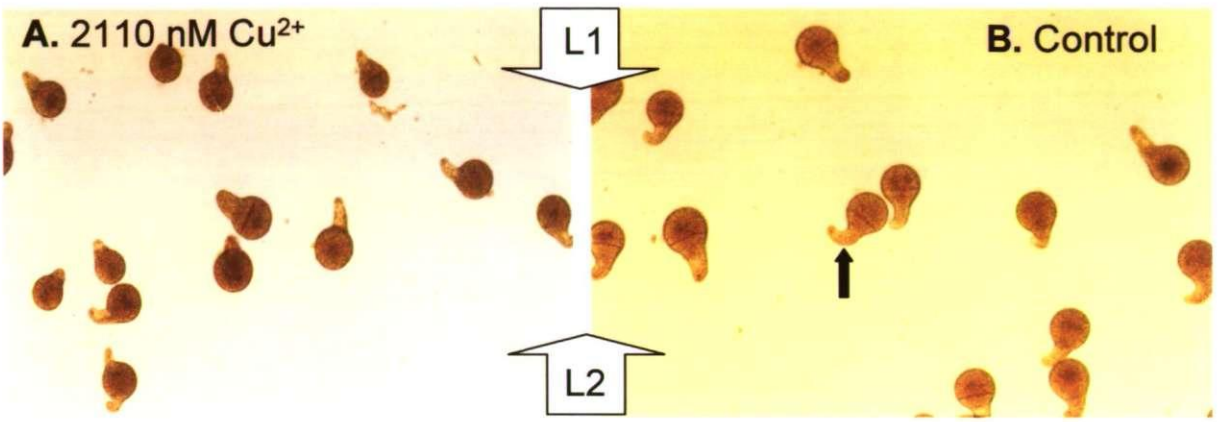

Figure 3.11. Zygotes exposed to 2110 nM Cu^{2+} did not fix their axes during exposure to unidirectional light (L1), but did fix their axes in response to reversed unidirectional light (L2) (**A**). Control zygotes not exposed to Cu^{2+} (**B**) fixed their axis during exposure to L1, and the orientation of the polar axes was unaffected by exposure to L2, although some of the rhizoids started to orientate their growth away from L2. This is indicated by an arrow.

formation in all treatments, the minor significant differences between them ($p<0.05$) were considered negligible. Examples of axis formation in zygotes exposed to 2110 nM Cu^{2+} and unexposed control zygotes are shown in Figure 3.10.

Axis fixation was inhibited by elevated concentrations of Cu^{2+} (Figure 3.09). Axis fixation in Wembury zygotes was unaffected by [Cu^{2+}] up to 84.4 nM ($p>0.05$). Further increase in [Cu^{2+}] had a significant inhibitory effect on axis fixation ($p<0.05$). Axis fixation was 50% lower in zygotes exposed to 2110 nM Cu^{2+} compared with zygotes exposed to 84.4 nM Cu^{2+} and Cu^{2+} free medium. Examples of axis fixation in zygotes exposed to 2110 nM free Cu^{2+} and in unexposed control zygotes are shown in Figure 3.11. Moderate [Cu^{2+}] had a positive effect on axis fixation in Restronguet zygotes, increasing polarisation by about 20%. Axis fixation was significantly higher in zygotes exposed to 42.2 to 211 nM Cu^{2+} than control zygotes unexposed to Cu^{2+} ($p<0.05$). Further increases in [Cu^{2+}] above 211 nM had a significant inhibitory effect on axis fixation in Restronguet zygotes ($p<0.05$). However, only in zygotes exposed to 844 and 2110 nM Cu^{2+} was axis fixation significantly inhibited when compared with control zygotes ($p<0.05$). Axis fixation in Restronguet zygotes exposed to 2110 nM Cu^{2+} was about 65% lower than in zygotes exposed to 42.2 to 211 nM Cu^{2+}.

3.3.1.3. F-actin localisation and secretion of fucoidin

Requirements for axis fixation include F-actin localisation and secretion of fucoidin (Bouget *et al.*, 1996; Shaw and Quatrano, 1996b). To determine the cause of Cu^{2+} toxicity during axis fixation, effects of Cu^{2+} on these physiological processes were studied. Zygotes were exposed to Cu^{2+} during axis fixation and subsequently stained with Texas Red phalloidin to image the F-actin distribution with the confocal microscope, or stained with

TB-O, which resulted in a blue colouring of the rhizoid pole in secreting zygotes when examined under a light microscope.

Examples of F-actin localisation in zygotes are shown in Figure 3.12. 80% of zygotes had localised F-actin at the rhizoid pole after exposure to 2110 nM Cu^{2+} during axis fixation (n=56). This is considerably higher than the proportion of zygotes which had irreversibly fixed their axes (35%) when exposed to 2110 nM Cu^{2+} within this time period. 97% of control zygotes (n=32) not exposed to Cu^{2+} during axis fixation had localised F-actin at the rhizoid pole by the end of the treatment. Even with the difference in the proportion of zygotes localising F-actin when exposed to 0 and 2110 nM Cu^{2+}, it is evident that disruption of F-actin localisation alone can not account for inhibition of axis fixation. Therefore the main target for Cu^{2+} in axis fixation was considered to be a process operating in parallel with or downstream of F-actin localisation.

Elevated [Cu^{2+}] had a considerable inhibitory effect on polar secretion of fucoidin in the *Fucus* zygote during axis fixation (Figure 3.13). At low [Cu^{2+}] (up to 84.4 nM) there was no effect of Cu^{2+} on secretion ($p>0.05$), whereas further increase in the [Cu^{2+}] had an abrupt inhibitory effect on secretion. An increase in the [Cu^{2+}] from 84.4 to 422 nM decreased the number of zygotes showing polar secretion by 75%. Increasing [Cu^{2+}] from 422 to 2110 nM resulted in no further decrease in the proportion of secreting zygotes ($p>0.05$). The effect of Cu^{2+} on secretion occurred within the same range of concentrations as that which had an inhibitory effect on axis fixation. The effect on secretion, however, was much more pronounced and it is evident that the main effect of Cu^{2+} is either directly on secretion or on physiological processes, which are upstream of secretion, and downstream of F-actin localisation.

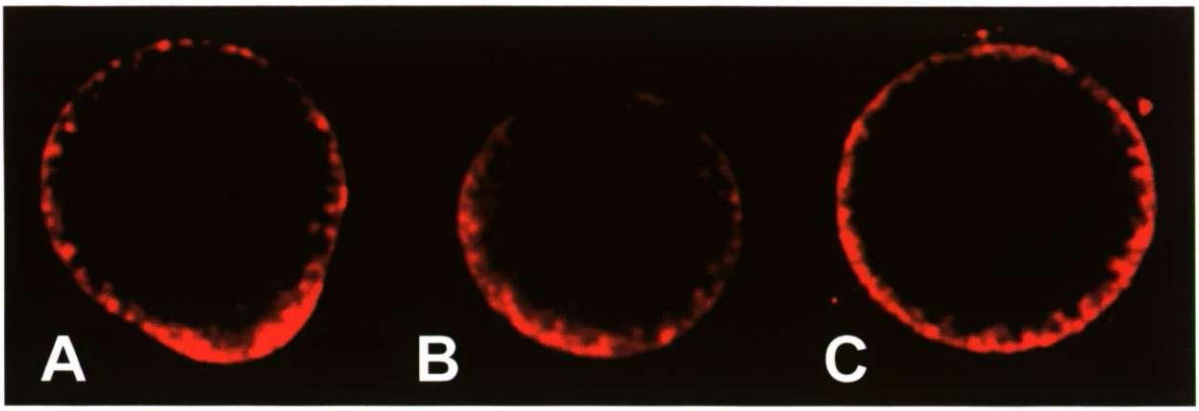

Figure 3.12. Confocal images of the distribution of F-actin in zygotes by 13h after fertilisation. F-actin localised at the rhizoid pole in an unexposed control zygote (**A**). F-actin localised at the rhizoid pole in a zygote incubated in 2110 nM free Cu^{2+} (**B**). Cu^{2+} treated zygote with uniform F-actin distribution (**C**).

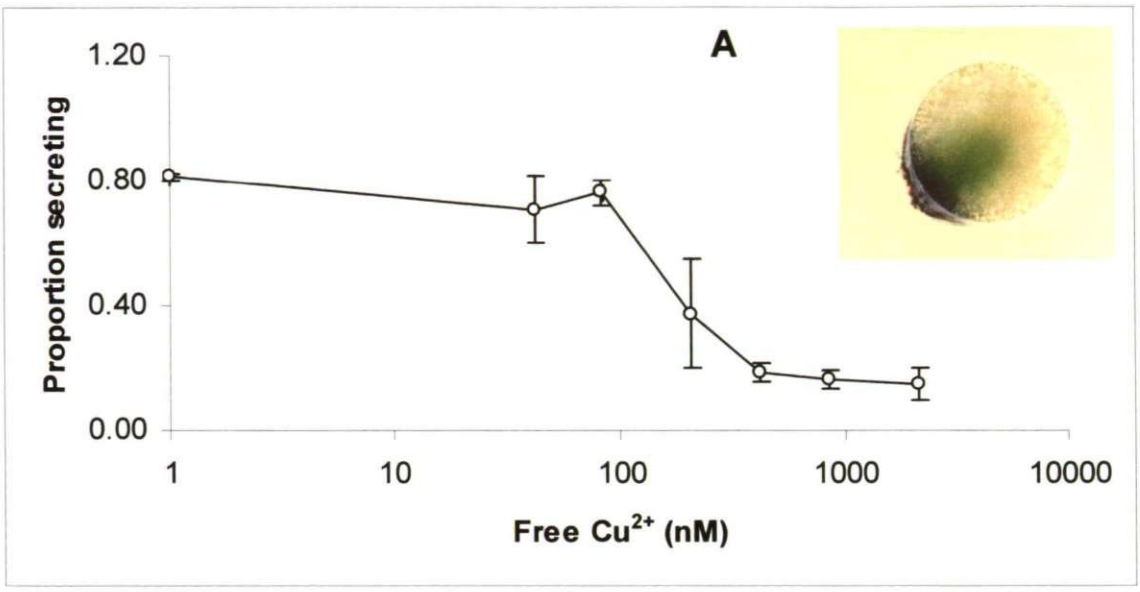

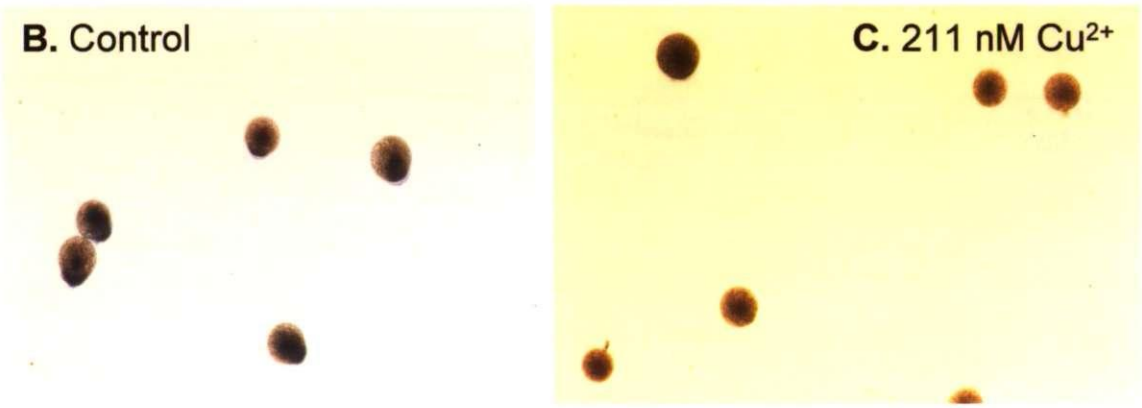

Figure 3.13. Effect of Cu^{2+} on the secretion of fucoidin in Wembury zygotes. Zygotes were incubated in a range of Cu^{2+} concentrations during axis fixation. At 13h AF they were stained with Toludine Blue O and the proportion of zygotes, which had secreted fucoidin was scored; values represents means ± 1 SD (n=3) (**A**). Secretion of fucoidin in TB-O stained zygotes appeared as a blue colouring at the rhizoid pole. Pictures show secretion in control zygotes (**B**), and inhibition of secretion in zygotes exposed to 211 nM Cu^{2+} during axis fixation (**C**).

3.3.2. Effects of Cu^{2+} on osmoregulation and embryo growth

3.3.2.1. Osmoregulation

Figure 3.14 shows the effect of free Cu^{2+} on osmoregulation during exposure to 25 and 50% hypo-osmotic shock. Osmoregulation was quantified as the number of two celled embryos able to withstand bursting in response to a hypo-osmotic treatment (transfer from seawater to 50 or 25% seawater). Pre-treatment of embryos with 0 to 844 nM free Cu^{2+} for 18h prior to exposure to a 50% and 25% hypoosmotic shock had no significant effect on the ability of the embryos to osmoregulate ($p>0.05$). However, some positive effect of high [Cu^{2+}] on osmoregulation was indicated. Incubating zygotes with 2110 nM Cu^{2+} significantly improved their ability to osmoregulate during exposure to a 50% hypo-osmotic shock compared with any other treatment ($p<0.05$). 96% of embryos pre-treated with 2110 nM free Cu^{2+} could osmoregulate during exposure to a 50% hypoosmotic shock. This is significantly higher than the average 68% of osmoregulating embryos in the other treatments ($p<0.05$). Similar results were found when exposing zygotes to a 25% hypo-osmotic shock after 18 h of pre-incubation. Zygotes incubated with 2110 nM Cu^{2+} had a significantly better ability to osmoregulate than zygotes incubated with 42.2, 84.4, and 211 nM Cu^{2+} ($p<0.05$). However, the ability of zygotes to osmoregulate during exposure to a 25% hypo-osmotic shock was not significantly different when incubated with 2110 nM Cu^{2+} and 422 and 844 nM Cu^{2+} and in control zygotes ($p<0.05$).

3.3.2.2. Rhizoid elongation and Cu^{2+} tolerance

The effect of Cu^{2+} on rhizoid elongation in *Fucus* embryos was investigated. Embryos obtained from the Cu^{2+}-contaminated Restronguet Creek population and the Cu^{2+}-intolerant Wembury Beach population (Chapter 2) were grown in varying [Cu^{2+}] (Figure 3.15). The *Fucus* zygotes grew well in the artificial seawater medium Aquil and each

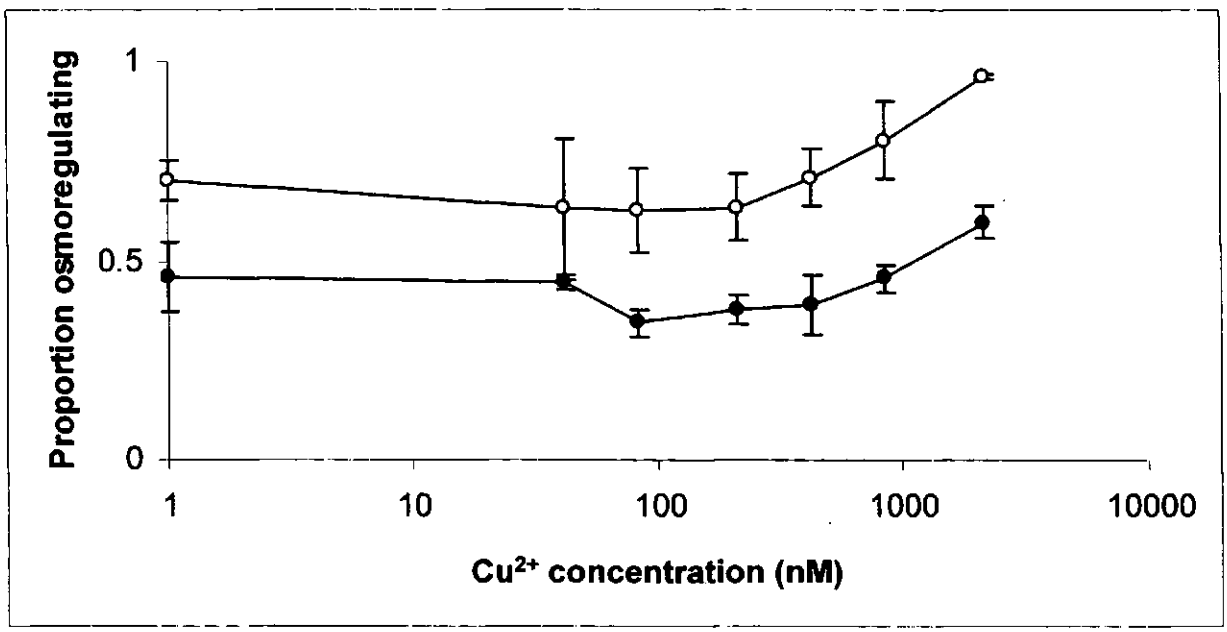

Figure 3.14. Effects of Cu^{2+} on osmoregulation in embryos pre-incubated with Cu^{2+} for 18 h and subsequently given a 50% hypo-osmotic shock (○) or a 25% hypo-osmotic shock (●). Values represents means ± 1 SD (n=3).

produced a 700-750 μm long rhizoid within 10 days of incubation in control medium. Elevated [Cu^{2+}] significantly reduced or inhibited rhizoid elongation in embryos from both populations, although Restronguet embryos had a higher Cu^{2+} tolerance limit than Wembury embryos. The Cu^{2+} tolerance limit for rhizoid elongation was 42.2 nM in Wembury embryos and 221 nM in Restronguet embryos. Examples are shown in Figure 3.16.

Rhizoid length in Wembury embryos incubated in 0-211 nM Cu^{2+} increased significantly throughout the experiment ($p<0.05$) and rhizoid elongation was unaffected in [Cu^{2+}] up to 42.2 nM Cu^{2+} (Figure 3.15A; $p>0.05$). Exposure of embryos to [Cu^{2+}] above 42.2 nM significantly reduced rhizoid elongation. Incubation in 211 nM Cu^{2+} resulted in significantly reduced, but not arrested, rhizoid elongation throughout the experiment when compared with control embryos ($p<0.05$). Exposure of embryos to 844 nM Cu^{2+} had a significant inhibitory effect on rhizoid elongation, resulting in complete growth arrest after seven days of incubation. Embryos exposed to 844 nM Cu^{2+} had significantly shorter rhizoids than embryos in all other treatments on all days of measurement ($p<0.05$). Although there was a significant increase in rhizoid length in embryos exposed to 844 nM Cu^{2+} until the 7^{th} day of incubation (Figure 3.15A; $p>0.05$), thereafter rhizoid length did not increase significantly ($p>0.05$).

Rhizoid length in Restronguet embryos increased significantly throughout the experiments in all concentrations tested ($p<0.05$) and after two days of incubation there was no significant difference in rhizoid length between the treatments (Figure 3.15B; $p>0.05$). Cu^{2+} had no negative effect on rhizoid elongation in zygotes incubated in concentrations up to 211 nM Cu^{2+} on any day of measurement ($p>0.05$). On day 4, zygotes incubated in 42.2 nM Cu^{2+} had produced significantly longer rhizoids than control embryos and embryos

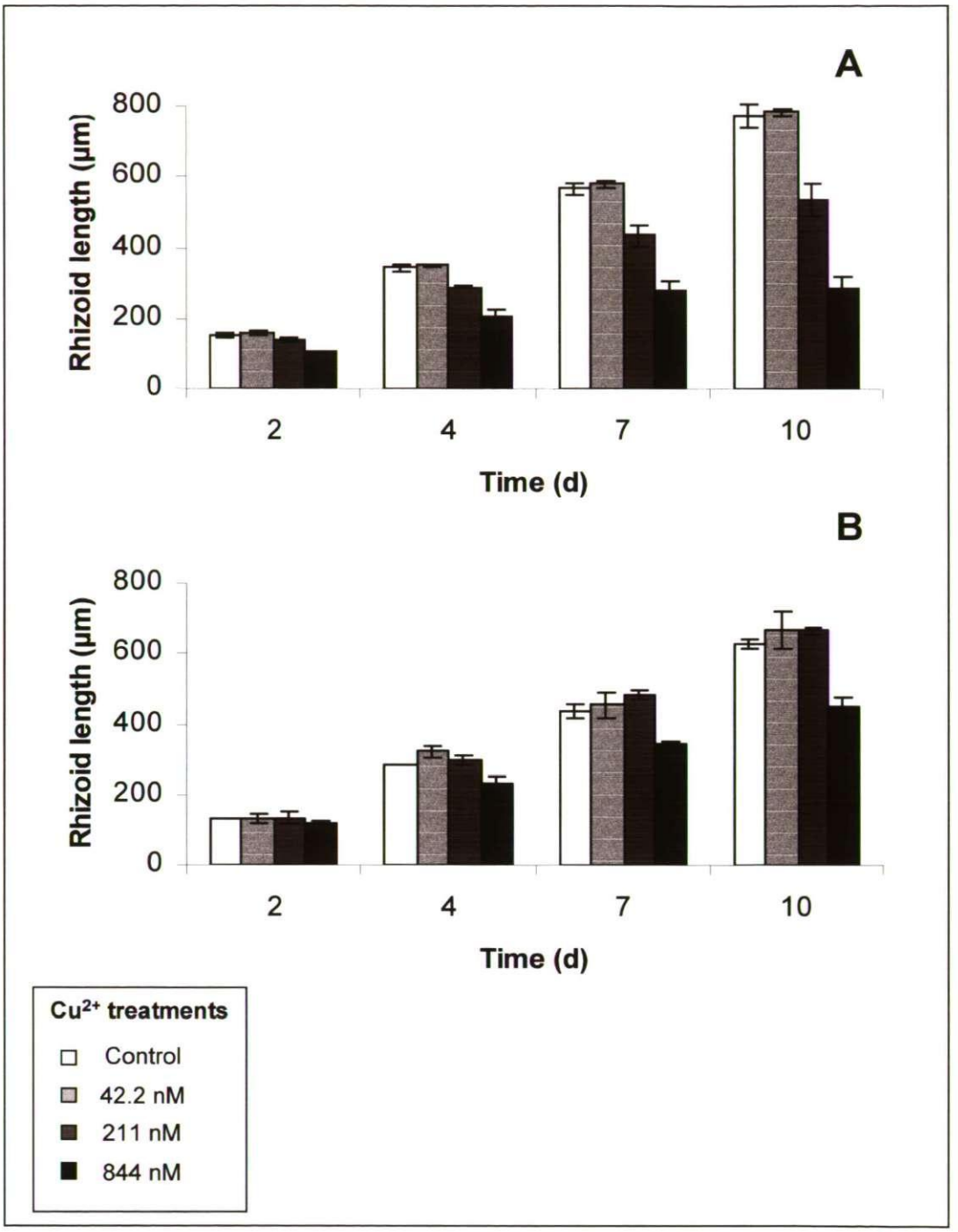

Figure 3.15. Effect of Cu^{2+} on rhizoid elongation in *Fucus* embryos obtained from Wembury Beach (**A**), and Restronguet Creek (**B**). Germinated embryos were incubated for 10 days in varying Cu^{2+} concentrations. Average rhizoid length for >25 embryos in each treatment was measured. Values represents means ± 1 SD (n= 3)

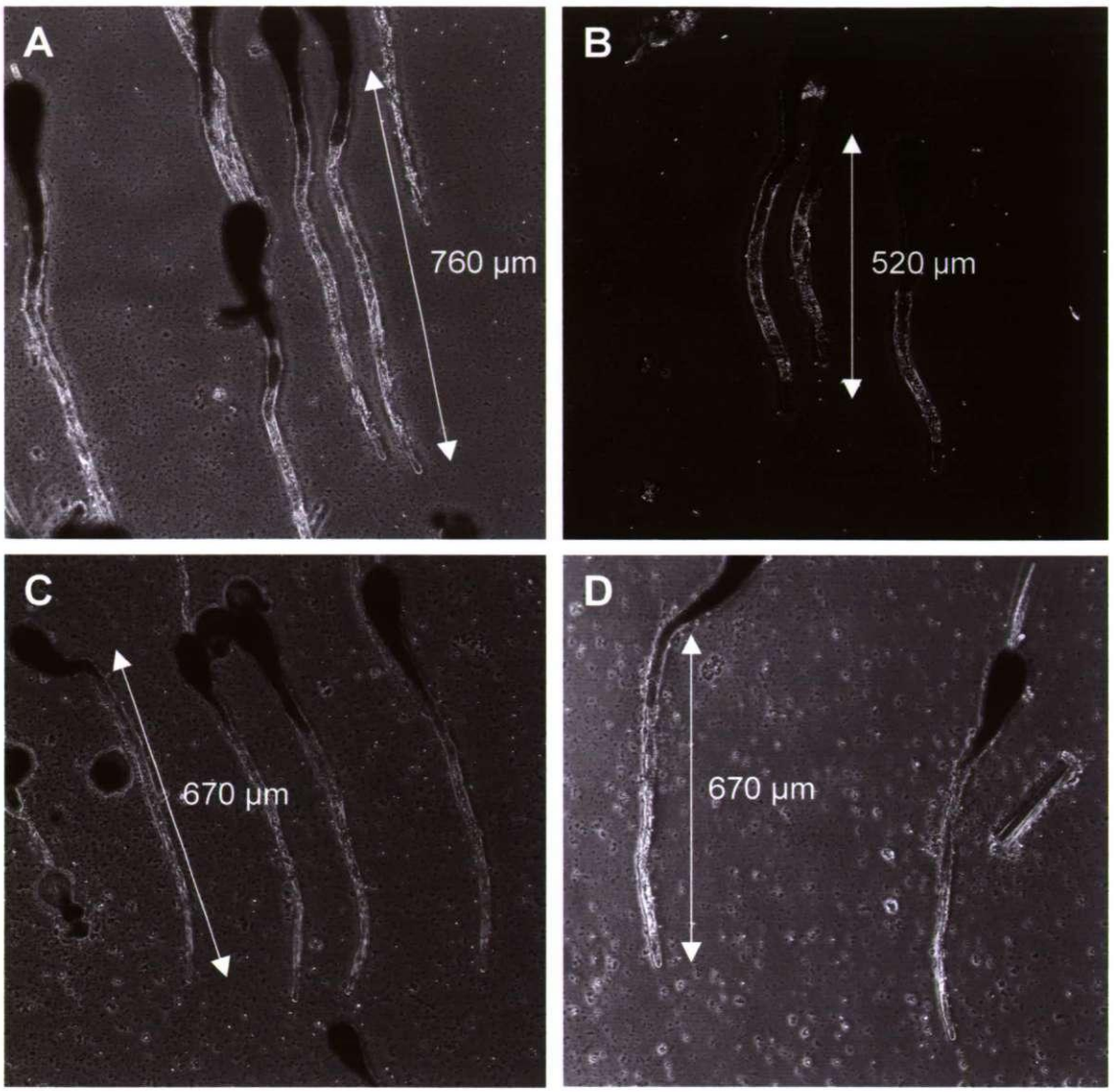

Figure 3.16. Examples of rhizoid elongation after 10 days of incubation. Wembury embryos in Cu^{2+} free control medium (**A**) and medium containing 211 nM Cu^{2+} (**B**), and Restronguet embryos in Cu^{2+} free medium (**C**) and medium containing 211 nM free Cu^{2+} (**D**).

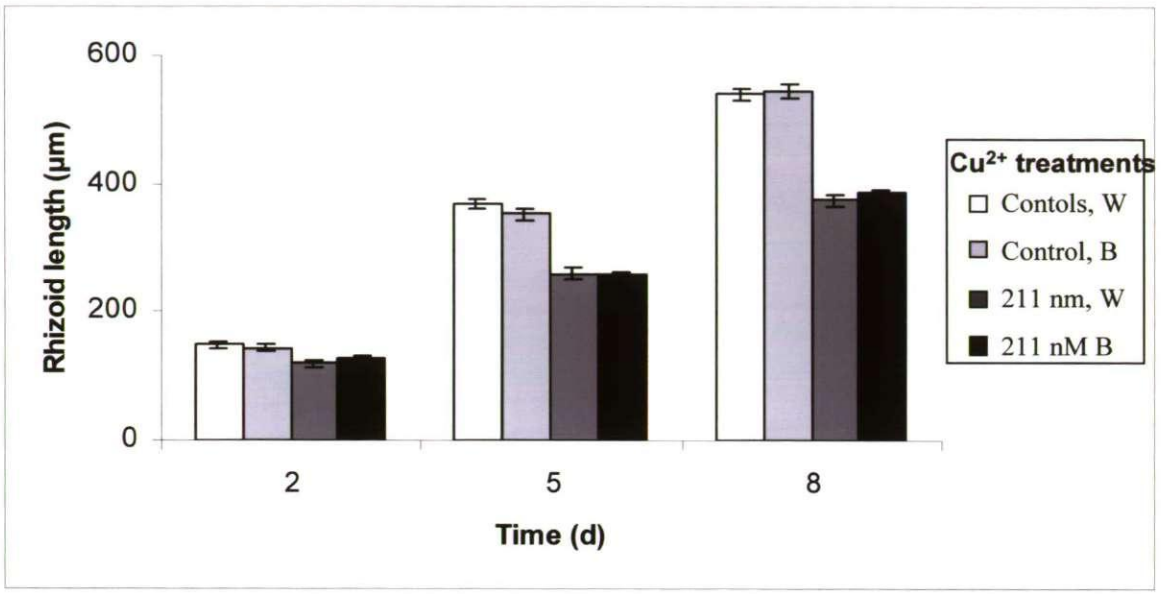

Figure 3.17. Effect of Cu^{2+} on rhizoid elongation in embryos from Wembury Beach (**W**) and Bantham Quay (**B**), which are not naturally exposed to Cu^{2+}. Germinated embryos were incubated for 8 days in Cu^{2+} free control medium and medium containing a Cu^{2+} concentration which was above the tolerance limit for embryos from a non-tolerant population, but within the tolerance limit for embryos from a Cu^{2+} tolerant population. Average rhizoid length for >25 embryos in each treatment was measured. Values represents means ± 1 SD (n= 3)

incubated in 211 nM Cu^{2+} ($p<0.05$), which indicates some Cu^{2+} requirement for rhizoid elongation in Restronguet embryos. Incubation in 844 nM Cu^{2+} significantly reduced but never inhibited rhizoid elongation completely in Restronguet embryos. On the 4th day of measurement and thereafter, embryos incubated in 844 nM Cu^{2+} produced significantly shorter rhizoids than embryos in the other treatments ($p<0.05$) but rhizoid elongation was never arrested ($P<0.05$).

It was important to determine whether the difference in Cu^{2+} tolerance limits between embryos obtained from the Restronguet Creek and Wembury Beach populations was caused by true adaptation in the Restronguet embryos or by other inter-population differences. Rhizoid elongation was therefore investigated in embryos from two unexposed populations incubated in 0 and 211 nM Cu^{2+} for 8 days. The results (Figure 3.17) clearly show that the two unexposed populations had the same Cu^{2+} tolerance limit. There was a significant increase in rhizoid elongation in embryos from both populations in both treatments throughout the experiment ($p<0.05$), although rhizoid elongation in embryos was significantly reduced when exposed to 211 nM Cu^{2+} compared with 0 nM ($p<0.05$). When exposed to either 0 or 211 nM Cu^{2+} there was no difference in rhizoid elongation between zygotes from the two populations ($p>0.05$). The identical responses to Cu^{2+} exposure in these two populations strongly suggests that the consistently better tolerance of the Restronguet population represent a true adaptation to elevated Cu^{2+}.

3.3.2.3. Cell division

In addition to rhizoid elongation, cell division is essential for growth in the *Fucus* embryo and effects of Cu^{2+} on cell division were therefore investigated. Ungerminated Wembury zygotes were exposed to a range of [Cu^{2+}] and the number of cells per zygote was counted at 24 and 40h AF. The results (Figure 3.18) show that low to moderate [Cu^{2+}] had a

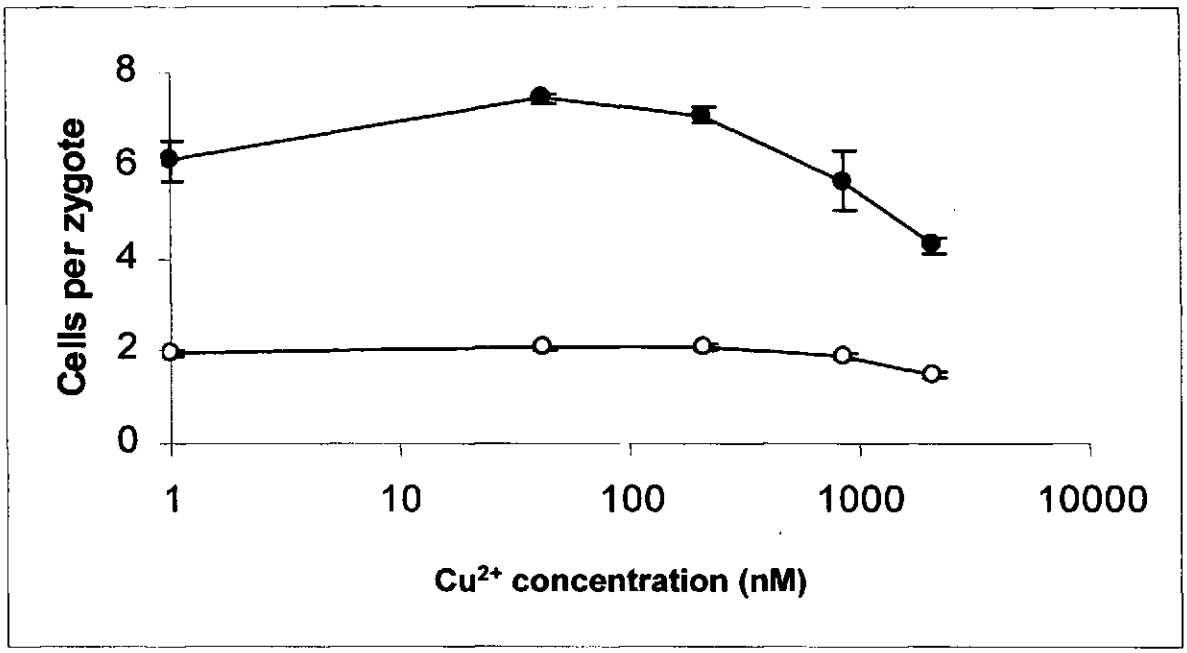

Figure 3.18. Effects of Cu^{2+} on cell division in Wembury *Fucus* zygotes. Zygotes were exposed to Cu^{2+} 2h after fertilisation (AF) and the number of cell divisions measured at 24 h AF (○) and 40 h AF (●). Values represents means ± 1 SD (n= 3)

positive effect on cell division, and that the inhibitory effect of high [Cu^{2+}] was most pronounced by 40h AF.

By 24h AF the mean number of cells per embryo was 1.95 in the control treatment. Exposure of zygotes to 42.2 and 211 nM Cu^{2+} had a positive effect on cell division. In these concentrations the average number of cells was 2.05 and 2.10 respectively. This was significantly higher than in control embryos ($p<0.05$). Upon an increase in [Cu^{2+}] to 844 nM there was a decrease in number of cells per embryo to 1.88, which is equivalent to the number of divisions in controls ($p>0.05$). Exposure of zygotes to 2110 nM Cu^{2+} resulted in 1.48 cells per embryo by 24h AF, which was significantly lower than in control embryos and any other treatment ($p<0.05$).

By 40h AF the average number of cells per control embryo was 6.09. There was a positive effect of 42.2 nM Cu^{2+} on cell division as the average number of cells per embryo was 7.45, which was significantly higher than in control embryos ($p<0.05$). Increasing [Cu^{2+}] to 211 and 844 nM resulted in a reduction in the number of cells per embryo to the level of control embryos ($p>0.05$). Further increase in [Cu^{2+}] had an inhibitory effect on cell division. Exposure to 2110 nM Cu^{2+} resulted in an average 4.27 cells per embryo which is significantly lower than in control zygotes ($p<0.05$) and equivalent to a reduction of 43% compared with incubation in 42.2 nM.

Examples of cell divisions in embryos incubated in medium containing 42.2 nM Cu^{2+} and 2110 nM Cu^{2+} are shown in Figure 3.19. Cu^{2+} clearly had a significant disruptive influence on the cell division pattern in the *Fucus* embryo. By 40 h AF 51.5±4.6% of embryos incubated in 2110 nM Cu^{2+} had a cell division pattern which deviated from the normal

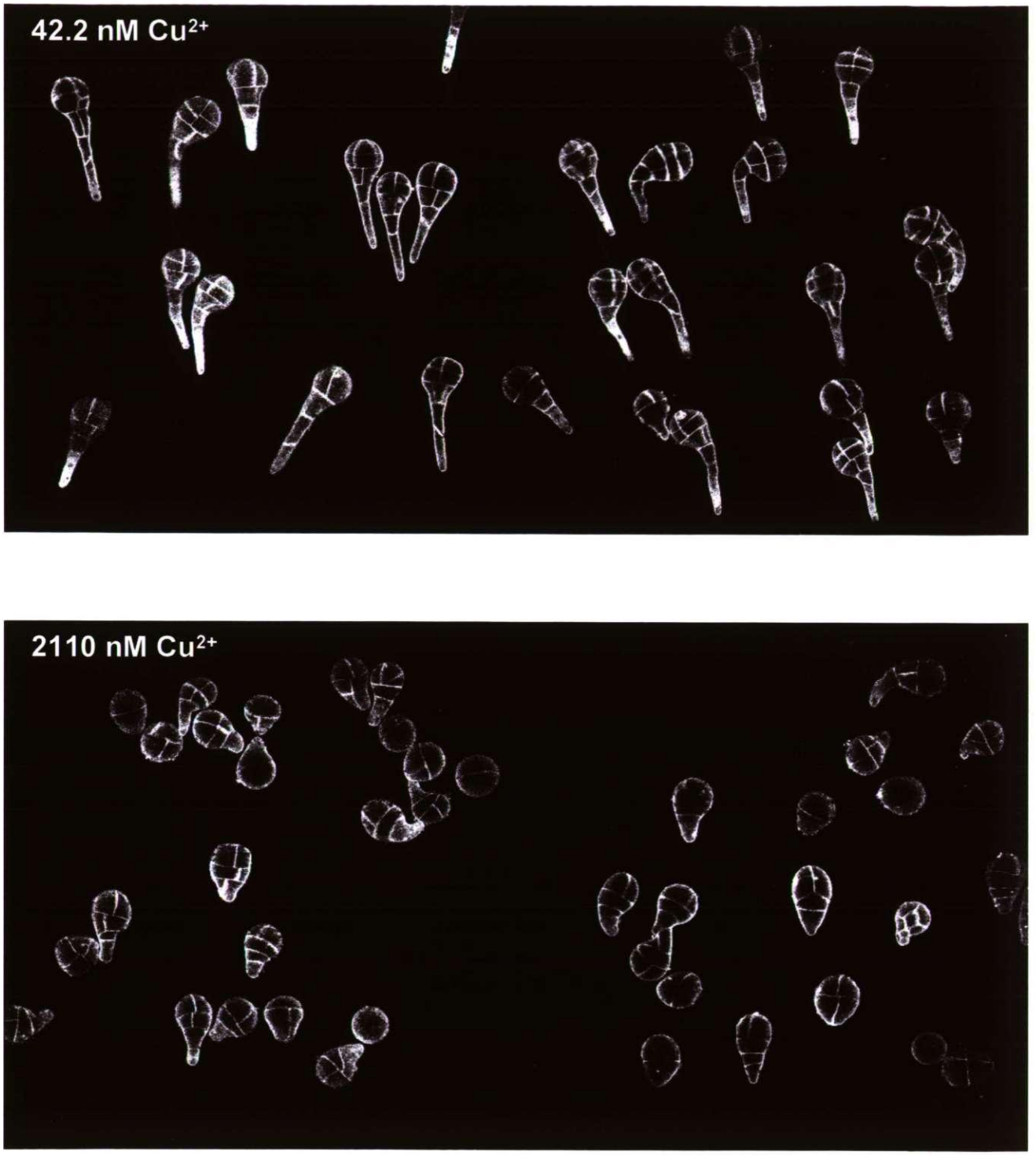

Figure 3.19. Examples of cell divisions in embryos stained with the cell wall dye FM 1-43 after 40h of incubation in medium containing either 42.2 nM Cu^{2+} (top) or 2110 nM Cu^{2+} (bottom).

pattern for *Fucus* embryos at this age. Only 5.8±3.7% of embryos incubated with 42.2 nM Cu^{2+} had a deviant cell division pattern.

3.3.3. Effects of Cu^{2+} on cytosolic Ca^{2+} in the *Fucus* rhizoid

3.3.3.1. Effects of Cu^{2+} on the Ca^{2+} gradient

Figure 3.20 shows an example of the cytosolic Ca^{2+} response to an 80% hypo-osmotic shock in the rhizoid of a *Fucus* embryo not pre-treated with Cu^{2+}. Within 10 seconds of exposure to hypo-osmotic conditions there was an abrupt increase in apical Ca^{2+} in the rhizoid cell. The Ca^{2+} elevation occurred in a restricted area near the cell membrane and extended a few μm into the cytoplasm. Apical Ca^{2+} remained at an elevated level for at least 1 min. This response was observed in all 3 control embryos and was therefore characteristic for embryos that were not pre-treated with Cu^{2+}.

Figure 3.21 shows examples of rhizoid cytosolic Ca^{2+} during an 80% hypo-osmotic shock in embryos pre-treated with medium containing 422 nM free Cu^{2+} for 5 min. In 4 out of 6 embryos investigated there was no elevation at all in apical Ca^{2+} upon exposure to an 80% hypo-osmotic shock. In the remaining two embryos a slight increase in apical Ca^{2+} was observed. The extent and duration of the Ca^{2+} elevation in these embryos, however, was much less than in the control embryos (Figure 3.20). An example of cytosolic Ca^{2+} in the rhizoid cell of embryos pre-incubated for 3 h in Aquil containing 422 nM free Cu^{2+} is shown in Figure 3.22. In this example, no apical Ca^{2+} elevation was present before and during exposure to an 80% hypoosmotic shock. This response in apical Ca^{2+} was observed in 5 out of 7 embryos investigated.

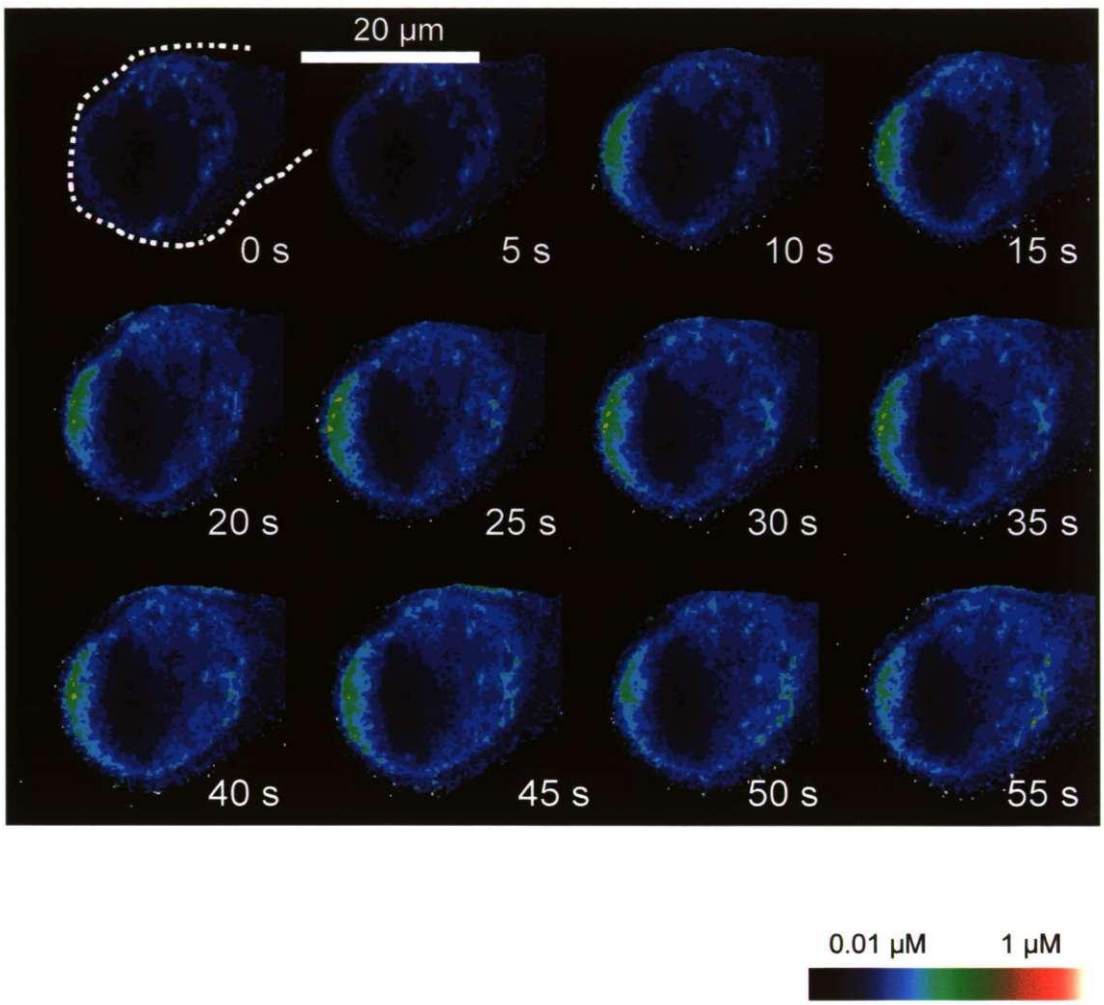

Figure 3.20. Calcium Green/Texas Red images of Ca^{2+} in the apex of a rhizoid cell during the first 55 seconds after exposure to an 80% hypo-osmotic shock. The hypo-osmotic shock was applied at t=0 s. Only the rhizoid tip is shown and it is outlined in white in the first image. The colour bar (bottom right indicates the Ca^{2+}concentration.

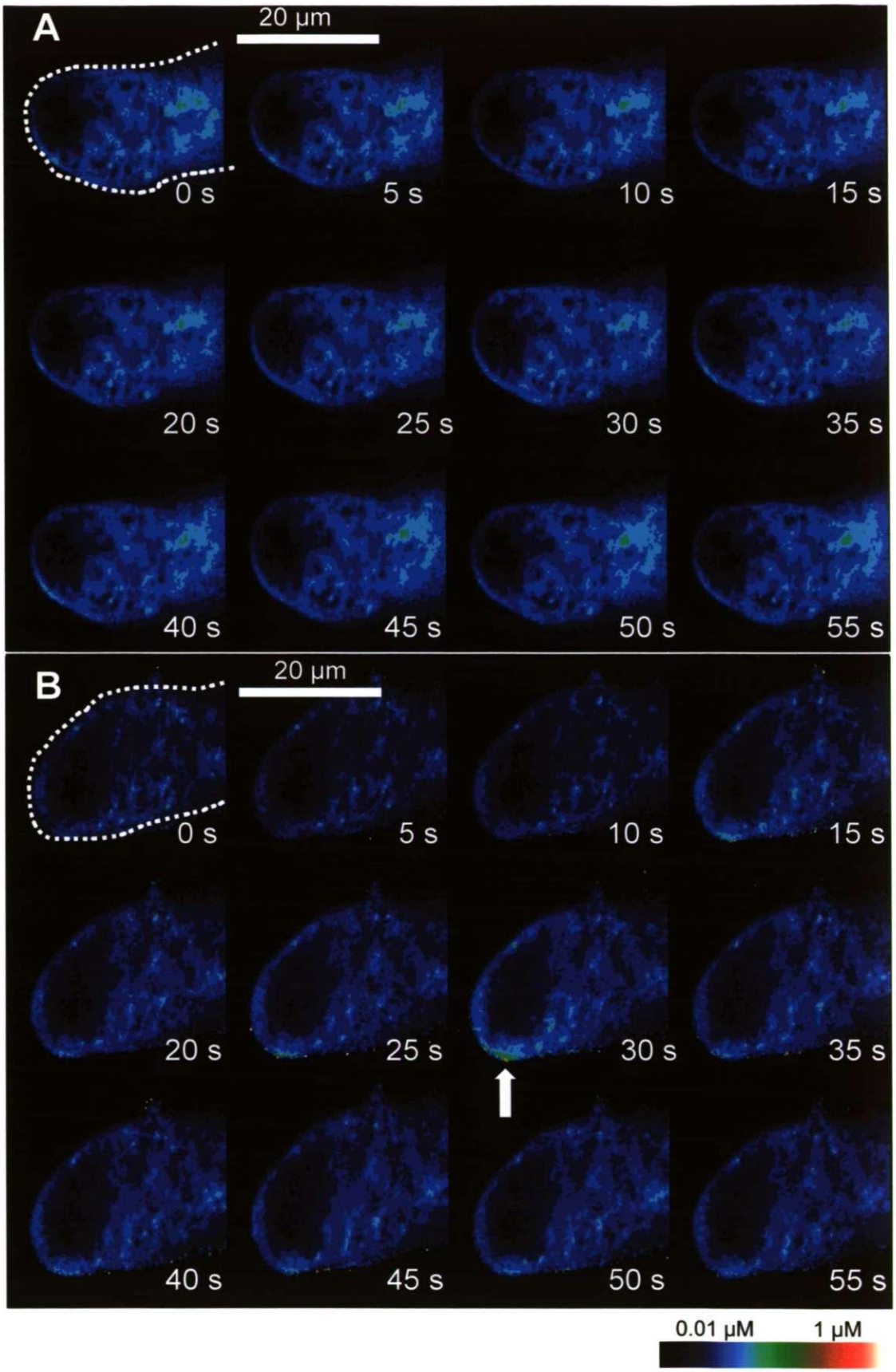

Figure 3.21. Calcium Green/Texas Red ratio images of apical cell Ca^{2+} in the rhizoid of two embryos pre-incubated for 5 min. in medium containing 422 nM Cu^{2+} and subsequently given an 80% hypo-osmotic shock. In 4/6 zygotes (**A**) no change in apical and sub-apical Ca^{2+} was observed. In 2/6 there was a slight increase in apical Ca^{2+} (**B**), this is indicated by an arrow. The colour bar (bottom right indicates the Ca^{2+}concentration.

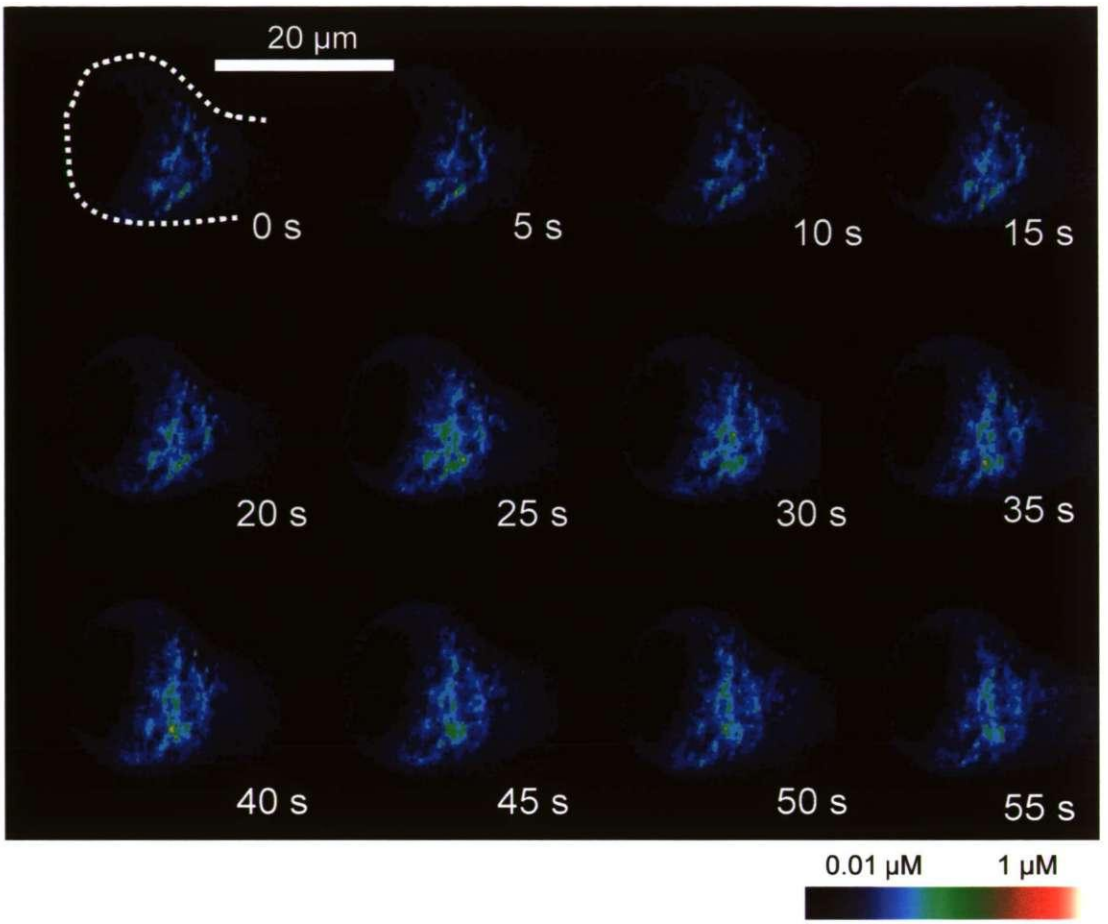

Figure 3.22. Calcium Green/Texas Red ratio of changes in cell Ca^{2+} in a rhizoid tip during an 80% hypo-osmotic shock given subsequent to 3h exposure to 422 nM Cu^{2+}. No apical changes in Ca^{2+} were observed. Sub-apical Ca^{2+} started to increase 15-20 seconds after the hypo-osmotic shock was given. The colour bar (bottom right) indicates the Ca^{2+} concentration.

To quantify the [Ca^{2+}_{cyt}] responses in Cu^{2+} pre-treated and control embryos during hypo-osmotic treatment, changes in apical and sub-apical [Ca^{2+}] were determined. Fluorescence in the ratio images was converted into [Ca^{2+}] on the basis of the calibration curve (Figure 3.07b). The average changes in apical [Ca^{2+}] in experimental embryos during hypo-osmotic shock are shown in Figure 3.23. Apical [Ca^{2+}] in control embryos increased from 0.1 to approximately 1 μM upon exposure to hypo-osmotic conditions. This is equivalent to a 100-fold increase in $[Ca^{2+}]_{cyt}$. At 55 seconds after the hypo-osmotic treatment was applied, the apical [Ca^{2+}] had gradually decreased by about 50%. In embryos pre-treated with Cu^{2+} for either 5 min or 3h before the hypo-osmotic treatment, only minor changes in apical [Ca^{2+}] were observed.

Figure 3.24. shows average changes in sub-apical [Ca^{2+}] during the hypo-osmotic treatment. Sub-apical resting [Ca^{2+}] in control embryos before the hypo-osmotic treatment was about 0.1 μM, whereas sub-apical resting [Ca^{2+}] in Cu^{2+} treated embryos of about 0.15 μM was 50% higher. This was independent of the duration of the Cu^{2+} exposure. The predominant response in embryos pre-incubated with Cu^{2+} for 3h was an increase in $[Ca^{2+}]_{cyt}$ from about 0.15 to 0.3 μM approximately 15-20 seconds after exposure to hypo-osmotic conditions (Figure 3.24). This result was based on calculations of sub-apical [Ca^{2+}] in the 5 out of 7 embryos where the response was observed. In 2 out of 3 control embryos and 4 out of 6 embryos pre-treated with Cu^{2+} for 5 min, some increase in sub-apical [Ca^{2+}] during the hypo-osmotic treatment was observed (Figure 3.24). However, with a relative increase in sub-apical Ca^{2+} in these embryos of no more than 10-15%, this increase was less than half of what was observed in 5 out of 7 embryos pre-treated with Cu^{2+} for 3 h before the osmotic shock treatment.

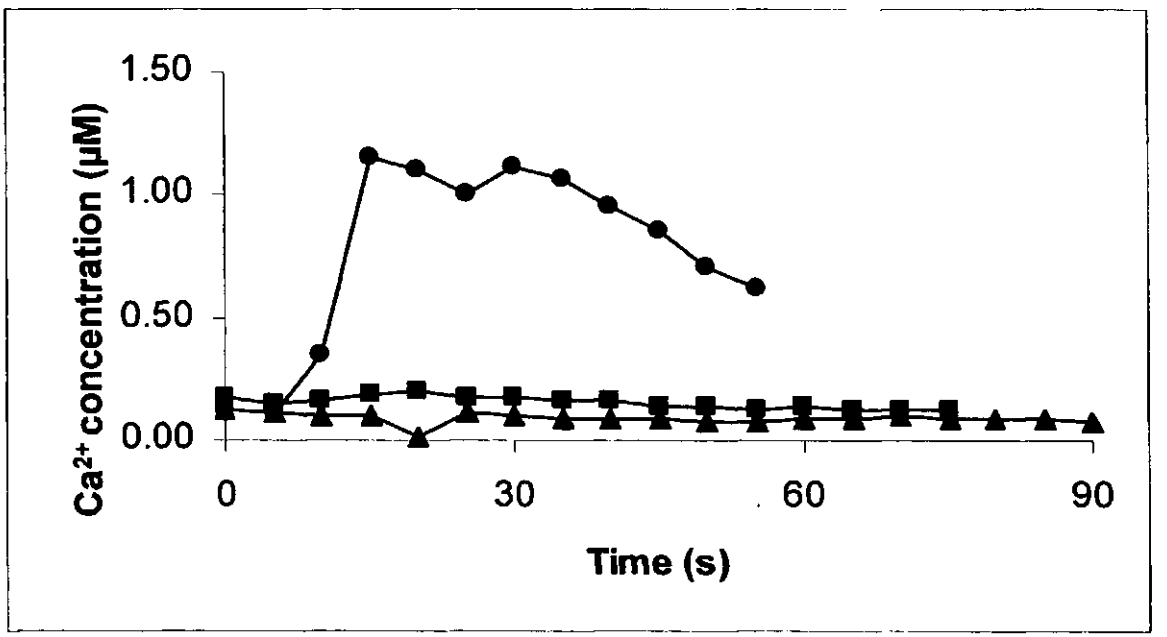

Figure 3.23. Average changes in the apical Ca^{2+} concentration during exposure to an 80% hypo-osmotic shock in embryos exposed to 422 nM µM Cu^{2+} for 5 min., n=6 (■), 3h., n=7 (▲), and in control embryos, n=3 (●).

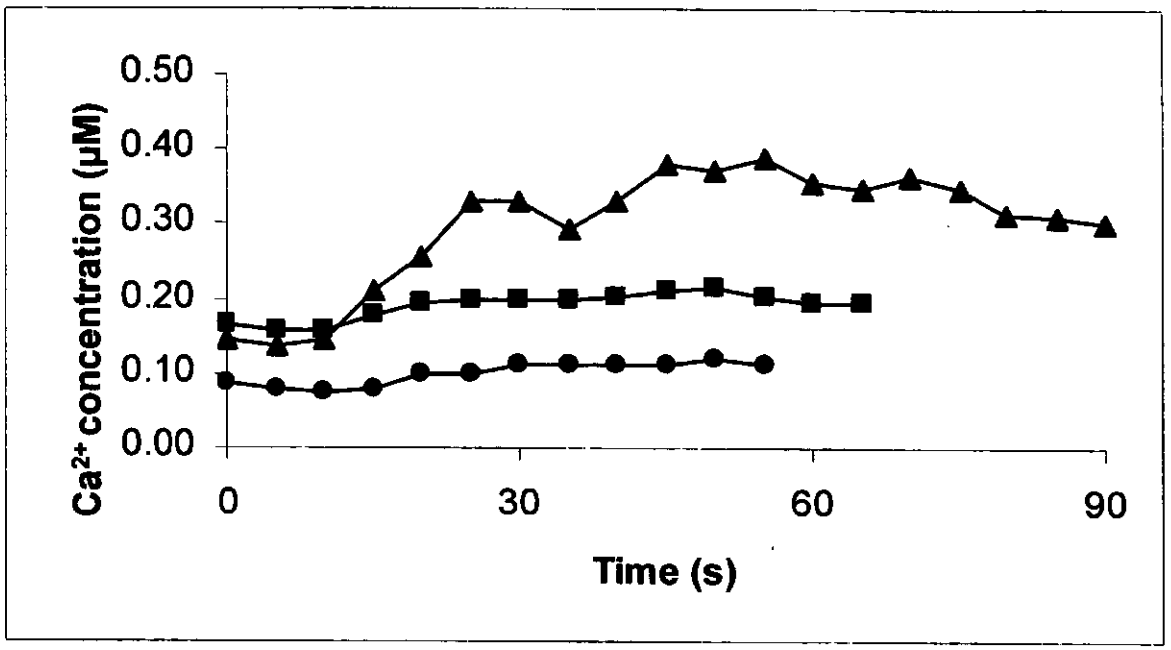

Figure 3.24. Average relative changes in sub-apical Ca^2 concentration during an 80% hypo-osmotic shock in embryos pre-treated with 422 nM Cu^{2+} for 5 min., n=4 (■), 3 h., n=5 (▲), and in control embryos, n=2 (●).

3.3.3.2. Effects of acute Cu^{2+} exposure on Ca^{2+} homeostasis

Figure 3.25 shows an example of the cellular Ca^{2+} response to acute exposure to 2110 nM free Cu^{2+} in a rhizoid cell. Within 30 seconds of application of Cu^{2+} there was a dramatic increase in Ca^{2+} throughout the rhizoid and the global Ca^{2+} remained at this level for at least 2 min. In particular the sub-apical Ca^{2+} level remained high for about 10 min. A dramatic increase in Ca^{2+} relative to the level before acute exposure to high [Cu^{2+}] was a general response in the rhizoid. This increase was independent of free [Cu^{2+}] at 2110 nM and above (Figure 3.26). In one embryo exposed to 844 nM free Cu^{2+}, the Ca^{2+} elevation lasted for about 300 s and eventually decreased to below the level measured at time 0. This would reflect dye loss or errors in ratio due to low signals in the ratio images. In embryos exposed to 2110 nM free Cu^{2+}, the cell Ca^{2+} remains at the elevated level until about 2400 seconds after Cu^{2+} was applied, at which time the cell Ca^{2+} had decreased to the resting level. The general trend for cell Ca^{2+} observed in the 3 embryos exposed to the extreme [Cu^{2+}] of 8440 nM was a global increase in cell Ca^{2+}, lasting for several minutes. In one of these embryos a sudden decrease in cell Ca^{2+} was observed about 2000 seconds after Cu^{2+} exposure. The nature of this decrease indicates that it probably was caused by dye loss from a dying cell.

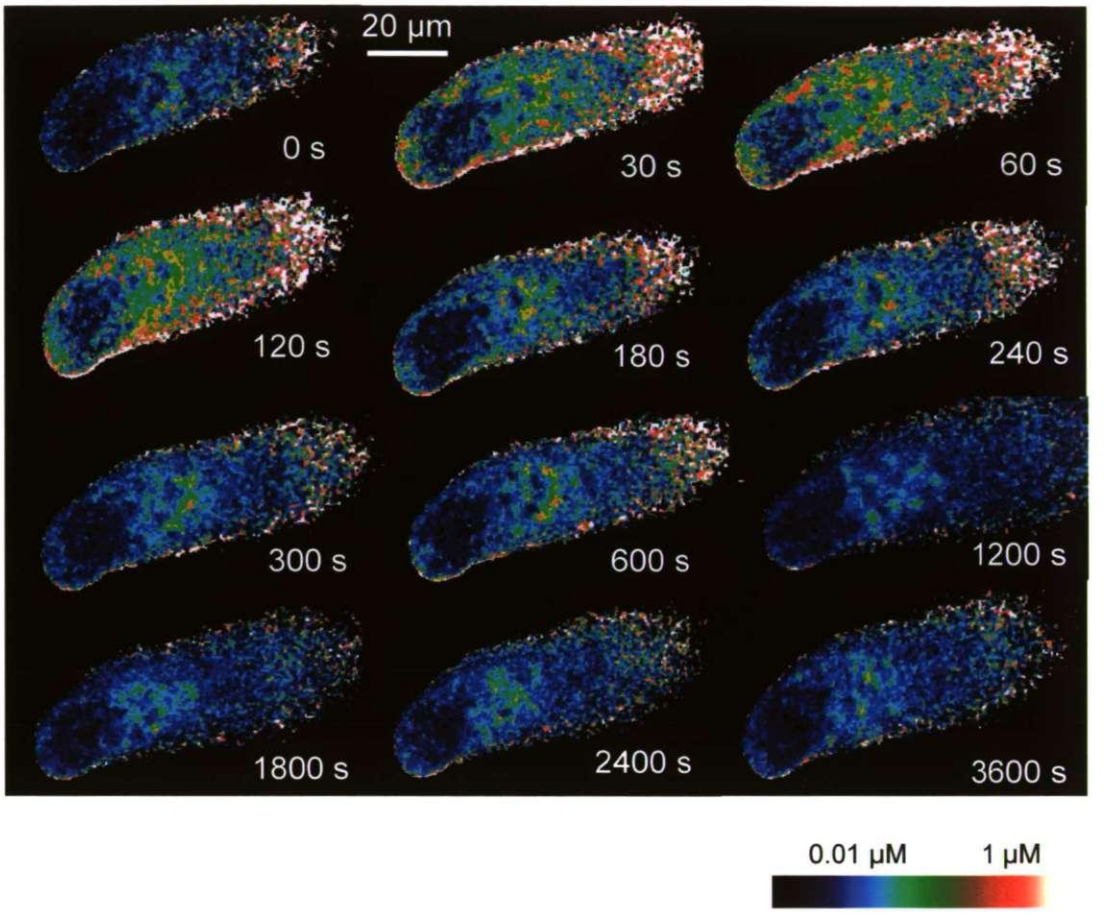

Figure 3.25. Example of the Calcium Green/Texas Red images of the Ca^{2+} elevation observed in *Fucus* rhizoid cells subject to acute Cu^{2+} exposure. The colour bar (bottom right indicates the Ca^{2+} concentration.

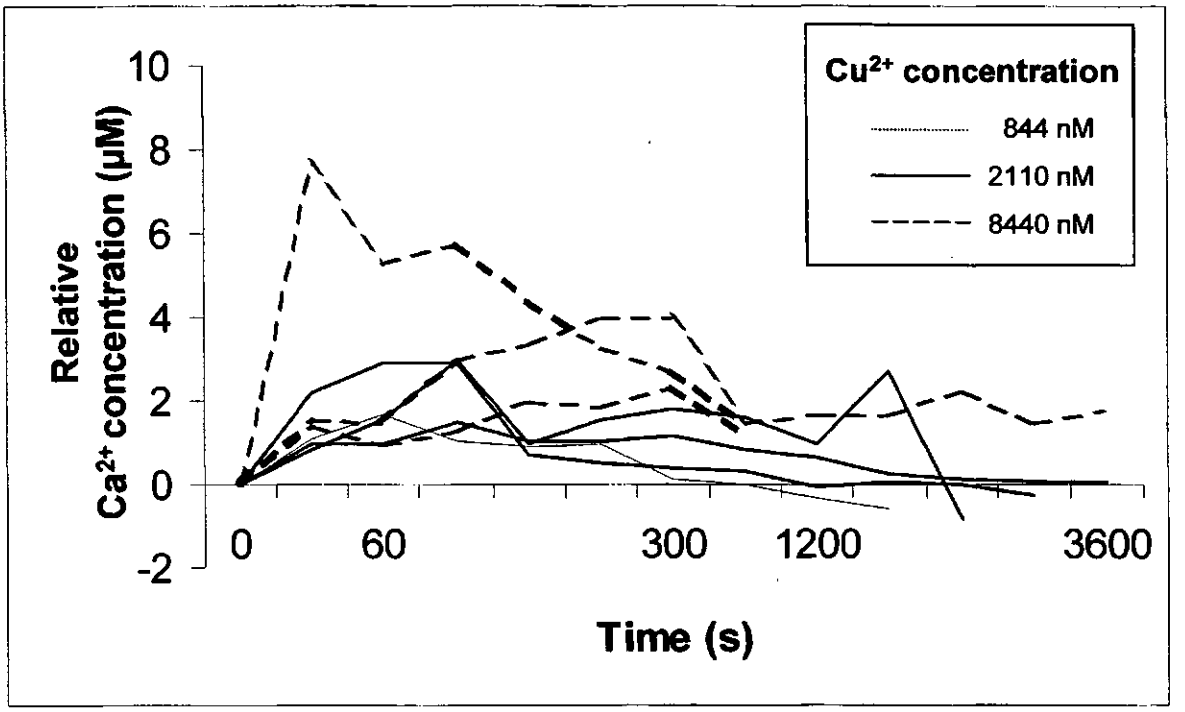

Figure 3.26. Relative changes in global cell Ca^{2+} in 7 rhizoid cells during acute exposure to three different concentrations of Cu^{2+}. Cu^{2+} concentrations used are indicated in the figure.

3.4. Discussion

Polar axis establishment in the *Fucus* zygote is dependent on a sequence of complex physiological processes of which the best known are localisation of F-actin, establishment of an apical Ca^{2+} gradient, and localised secretion of fucoidin into the cell wall. The same processes are underlying rhizoid elongation, which occur as tip growth. In the present study it was shown that Cu^{2+} selectively targets these physiological processes and consequently reduces and arrests polarisation with possible consequences for further development of the embryo, and inhibits rhizoid elongation. Similarly, it has been shown by other workers, that Cu^{2+} may target very early processes in the *Fucus* zygote (Anderson and Kautsky, 1996), and reduce and even arrest rhizoid elongation and growth of the embryos (Bond *et al.*, 1999; Gledhill *et al.*, 1999).

3.4.1. Effects of Cu^{2+} on embryo growth and osmoregulation

3.4.1.1. Osmoregulation

The rhizoid cell of the *Fucus* zygote possesses the ability to osmoregulate during exposure to hypo-osmotic conditions by controlling the concentration of ions and water within the cell (Taylor *et al.*, 1996; Goddard, 2000). Hypo-osmotic treatment of a *Fucus* zygote initiates a Ca^{2+} wave at the apex of the rhizoid as it begins to swell (Taylor *et al.*, 1996, 1997). The Ca^{2+} wave propagates to the sub-apical region by release of Ca^{2+} from internal stores (Goddard *et al.*, 2000), and the Ca^{2+} signal is involved in mediating ion efflux through Cl^-- and K^+-channels in the cell membrane, which in turn regulate hypo-osmotic swelling. Cu^{2+} is known to be a potent inhibitor of ion channels in both plants and animals (Kiss *et al.*, 1991; Osipenko *et al.*, 1992; Amesheh and Weber, 1999; Demidchik *et al.*,

1997; 2001). Therefore it was expected that Cu^{2+} would affect plasma membrane ion channels and consequently have negative effects on the osmoregulatory process. In the present study osmoregulation in the *Fucus* zygote was unaffected by Cu^{2+} at concentrations up to 844 nM during exposure to a 50% and 25% hypoosmotic shock. However, 2110 nM Cu^{2+} improved the ability of the rhizoid cell to osmoregulate. Although it is possible that Cu^{2+} did have an inhibitory effect on the activity of plasma membrane ion channels, and in this way diminish the ability of zygotes to osmoregulate, Cu^{2+} may still have had a positive effect on osmoregulation. A rigid cell wall protects the thallus cell of the *Fucus* zygote from uncontrolled swelling during hypo-osmotic treatment, whereas the cell wall at the rhizoid tip is soft and allows the cell to swell (Taylor *et al.*, 1996). In a cellulose cell wall the cellulose and hemicellulose fibres are held together by hydrogen bonds (Fry, 1994). Hydrogen bonds are relatively weak, and it is therefore possible that Cu^{2+} may have a direct strengthening effect on the cell wall by forming stronger cross links between the cell wall components. Furthermore, cell wall softening during turgor-driven cell enlargement in flowering plants is effected by a specific group of cell wall proteins (expansins) which may act by breaking hydrogen bonds between hemicellulose and cellulose (Fry, 1994; Cosgrove, 1996). The existence of expansins in *Fucus* has not been shown, but cell wall softening enzymes would be required during growth, and a similar mechanism to that in flowering plants is likely to exist. Cu^{2+} has a high affinity for –SH groups and may therefore inhibit enzymes at elevated concentrations by cross-linking sulfhydryl groups and cause conformational changes (Stauber and Florance, 1987; Rijstenbil *et al.*, 1994; von Stedniak *et al.*, 1997). It is therefore possible that the positive effect of Cu^{2+} on osmoregulation is caused by inhibition of cell wall softening expansin-like proteins within the cell wall of the rhizoid. Hence, elevated concentrations of Cu^{2+} could result in a more rigid cell wall, and consequently prevent bursting during hypo-osmotic conditions. Cu^{2+} may have had other effects on the cell wall. Inhibition of secretion of the cell wall

component fucoidin, has been shown to have a positive effect on osmoregulation in *Pelvetia* zygotes (Bisgrowe and Kropf, 2001). Adding 5 μg l^{-1} Brefeldin A to germinated zygotes 4-6 h prior to hypoosmotic treatment inhibited secretion of fucoidin, destroyed Golgi membranes and increased the percentage of zygotes which could withstand transfer to distilled water from 55% to 85% (Bisgrowe and Kropf, 2001). In that work it was suggested that the improved osmoregulation in zygotes exposed to the inhibitor of secretion was coursed by strengthening of the cellulose cell wall, which was doubled in thickness in response to Brefeldin A as revealed by electron microscopy. Secretion of fucoidin in the *Fucus* zygote is initiated during the time when zygotes in the osmoregulation experiment were pre-incubated with Cu^{2+} (Wagner *et al.*, 1992; Shaw and Quatrano, 1996). Furthermore, it was shown in the present work (see below, 3.4.2.2.), that Cu^{2+} has a strong inhibitory effect on localised secretion of fucoidin. It is therefore a possibility that the inhibitory effects of Cu^{2+} on secretion may have resulted in strengthening of the cellulose cell wall at the rhizoid tip of the *Fucus* zygotes analogous with the results presented by Bisgrove and Kropf (2001). However, the inhibitors (Brefeldin A and Cu^{2+}) may have changed the osmotic potential of the zygotes during the pre-incubation period, which offers an alternative explanation. It was shown in Chapter 2 and by other workers (Plöz, 1991; Yruela *et al.*, 1996; Ciscto, 1997) that Cu^{2+} is a potent inhibitor of photosynthesis. Consequently, Cu^{2+} may have reduced the photosynthetic capacity and lowered the carbohydrate content of the zygotes. This in turn could have lowered the osmotic potential of the zygotes and resulted in less swelling during the hypo-osmotic treatment, and have given the impression of improved osmoregulation.

3.4.1.2. Cell division

The first cell division in the *Fucus* embryo is orientated perpendicular to the polar axis and subsequent divisions occur in a specific pattern (Kropf *et al.*, 1990). In the present study,

2110 nM Cu^{2+} resulted in abnormal cell division patterns in the *Fucus* zygote from non-tolerant populations, and this effect could be the result of the inhibition of Cu^{2+} on axis fixation. Failure of the *Fucus* zygote to establish a polar axis results in loss of the ability to orientate the first division plane correctly (Allan and Kropf, 1992; Shaw and Quatrano, 1996). Consequently, the abnormal and often random cell division patterns observed in the present study could be the result of the inhibitory effect of Cu^{2+} on axis fixation during Cu^{2+} exposure. Although Cu^{2+} had a severe effect on the cell division pattern, cell division rate was unaffected or even increased at concentrations below 2110 nM. At low concentrations, 42.2 and 211 nM, Cu^{2+} had a positive effect on cell division rate, whereas 844 nM Cu^{2+} had no effect on cell division rate even though this concentration is 20-fold higher than the tolerance limit for axis fixation and rhizoid elongation, and is equivalent to the concentration which eventually arrested rhizoid elongation in Cu^{2+}-intolerant embryos. In fucoid zygotes, negative regulators of the cell cycle (DNA replication checkpoints) may ensure accurate transmission of genetic information by preventing mitosis until DNA is fully replicated (Corellou *et al.*, 2000). It is a possibility that Cu^{2+} has increased the cell division rate by inhibiting the action of the DNA replication checkpoints, which would result in mitosis and completion of cell cycle before DNA replication was completed. DNA replication check points may also be involved in regulation of spindle alignment prior to cell division (Corellou *et al.*, 2000). Therefore, disruption the DNA replication checkpoints by Cu^{2+} as well as incomplete replication of DNA, may have contributed to the abnormal cell division pattern observed. Only in embryos exposed to 2110 nM Cu^{2+} was the cell division rate observed to slow down compared to control embryos.

3.4.1.3. Rhizoid elongation and Cu^{2+} tolerance

This study showed that rhizoid elongation in *F. serratus* embryos have different tolerance limits to Cu^{2+}, which reflects the Cu^{2+} status in the habitat from which they were obtained.

Physiological experiments carried out on adult *F. serratus* from the same locations revealed that the adult algae also have different Cu^{2+} tolerance limits, which are dependent on the Cu^{2+} status in their natural environment (Chapter 2). By comparing results on embryos and adults from the same locations it is revealed that the Cu^{2+} tolerance limit in the embryos mirrors the tolerance limit in the adults. Cu^{2+} tolerant Restronguet embryos even displayed some Cu^{2+} requirement during axis fixation. Chelating of Cu^{2+} by polyphenols, which are present in cytoplasmic physodes and in the cell wall (Smith *et al.*, 1986; Schoenwaelder and Clyton, 1998), and secretion of copper complexing ligands to the medium (Gledhill *et al.*, 1999), may be a general Cu^{2+} tolerance mechanism in *Fucus* embryos as well as adults. Hence, other mechanisms may be responsible for the higher tolerance limit in the Restronguet population, and the similar response pattern in embryos and adults suggests that genetic adaptation is involved. Metallothionein genes, which are transcribed at higher rate in tolerant strains of *Silene* and *Arabidopsis* than in non-tolerant strains (Murphy and Taiz, 1995; van Hoof *et al.*, 2001), have been identified in *Fucus* (Morris *et al.*, 1999). Consequently, inter-population differences similar to those of flowering plants are likely to occur in *Fucus*.

The Cu^{2+} tolerance limit for rhizoid elongation in embryos obtained from uncontaminated sites was 42.2 nM. Higher [Cu^{2+}] resulted in inhibition of rhizoid elongation. Similarly, Cu^{2+} has been shown to have an inhibitory effect on apical cell elongation in *Fucus* embryos and pollen tubes. Thus, 10 μM total copper reduced the elongation of *Lilium longiflorum* pollen tubes to about 15% of control tubes within 60 minutes of application (Sawidis and Reiss, 1995), and similar observations were made on *Lilium* pollen tubes exposed to elevated concentrations of Pb^{2+} (Röderer and Reiss, 1988). Cu^{2+}, together with Cd^{2+} is a much stronger inhibitor of pollen tube elongation than other divalent metals such as Co^{2+}, Fe^{2+}, Mn^{2+}, Hg^{2+}, and Zn^{2+} (Sawidis and Reiss, 1995). Furthermore, growth in *F.*

spiralis embryos, measured as relative increase in zygote area, was significantly reduced at free Cu^{2+} concentrations above 42.2 nM, and became irreversibly arrested at 844 nM (Bond *et al.*, 1999; Gledhill *et al.*, 1999). Total embryo area correlates with rhizoid elongation as the main embryo expansion during the first days occurs as rhizoid elongation. Although Cu^{2+} eventually arrested rhizoid elongation completely in the present study, the effect of Cu^{2+} on rhizoid elongation at 844 nM Cu^{2+} was more pronounced in the experiment by Bond *et al.* (1999) as those embryos grew very short stunted rhizoids. It is a possibility that there are different tolerance limits of Cu^{2+} in *F. serratus* (used in the present study) and *F. spiralis* (Bond *et al.*, 1999). However, the timing of adding Cu^{2+} to the incubation medium is a more likely explanation. Exposing *F. vesicolusus* embryos to Cu^{2+} at the time of germination rather than at the time of fertilisation increased their tolerance limit about 10-fold (Anderson and Kautsky, 1996). In the study by Bond and co-workers (1999), Cu^{2+} was added after fertilisation as soon as the zygotes had settled in the incubation chambers, before axis fixation had occurred. Therefore, what was measured was the effect of Cu^{2+} on axis establishment as well as rhizoid elongation. In the present study, Cu^{2+} was not added until after rhizoid germination when the initial developmental processes had taken place and effects of Cu^{2+} on axis fixation were not included in the results. Rhizoid elongation in the *Fucus* embryo is the result of tip growth, which may share common processes to those in axis fixation (Kropf and Quatrano, 1987; Speksnijder *et al.*, 1989; Roberts *et al.*, 1993; Taylor *et al.*, 1996; 1997). Therefore, studying mechanisms of Cu^{2+} toxicity during polar axis establishment would not only reveal effects of Cu^{2+} during early development but also shed light on toxicity mechanisms in rhizoid elongation.

3.4.2. Cu^{2+} toxicity in early development

3.4.2.1. Axis formation and fixation

Polar axis establishment in *Fucus* occurs a few hours after fertilisation. The polar axis is first formed and then irreversibly fixed in response to polarising light (Quatrano, 1973; Kropf, 1992). In this study it was determined that axis formation in *F. serratus* occurs between 3 and 7 h AF, and subsequently becomes irreversibly fixed between 7 and 13 h AF. Similar timing of events has previously been shown for *F. serratus* (Berger and Brownlee, 1994; Love *et al.*, 1997). Early developmental events in *Fucus* are sensitive to metal toxicity, and copper is known to be a potent inhibitor of growth in *Fucus* embryos during early development (Andersson and Kautsky, 1996; Bond *et al.*, 1999). In the present study it was shown that Cu^{2+} toxicity in the *Fucus* zygote targets axis fixation, whereas axis formation was unaffected, even when exposed to very high concentrations of Cu^{2+}. During axis formation the polarising light vector is first detected and translated into spatial information. Excitation of photoreceptors in the plasma membrane on one side of the zygote may result in asymmetrically enhanced redox activity at the cell surface, which in turn initiates Ca^{2+} asymmetries (Berger and Brownlee, 1994; Love *et al.*, 1997). Alternatively, in a process which involves retinal, the polarising light signal promotes asymmetric cyclic GMP activity, which in turn, may result in increased F-actin polymerisation by the rhizoid pole (Robinson and Miller, 1997; Robinson *et al.*, 1998). Although our understanding of light detection in the *Fucus* zygote remains vague, it is clear that the pigments involved are unaffected by Cu^{2+} even at relatively high concentrations. Similarly, the mechanism of translating the light signal into spatial information, whether it involves an increase in redox chain activity or cyclic GMP activity, is apparently unaffected by elevated concentrations of Cu^{2+}.

Axis fixation in the *Fucus* zygote is a complex process and many different events are involved. The exact timing and order of events is unclear, and only a few have been subject to detailed study. Three of the major processes thought to be involved in axis fixation are localisation of F-actin (Bouget *et al.*, 1996; Alessa and Kropf, 1999; Pu *et al.*, 2000), establishment of a Ca^{2+} gradient (Specksnijder *et al.*, 1989; Taylor *et al.*, 1992) and localised secretion of fucoidin into the cell wall (Wagner at al 1992; Shaw and Quatrano 1996b). The present study focused on each of these three processes, as they all, either singly or in combination, were potential principal targets of Cu^{2+} toxicity during early development in the *Fucus* zygote.

3.4.2.2. Localised secretion of fucoidin

Direct effects of Cu^{2+} on secretion of fucoidin, or processes upstream of secretion, may have caused the negative effect of Cu^{2+} on axis fixation. It was shown in this study that fucoidin was secreted into the cell wall at the rhizoid pole in 77% of control zygotes during axis fixation, and similar results have been presented by other workers (Wagner *et al.*, 1992; Shaw and Quatrano, 1996b). However, 211 nM Cu^{2+} considerably inhibited secretion of fucoidin, as the proportion of secreting zygotes was reduced to 15% when treated with this concentration during axis fixation. This is within the concentration range which also had an inhibitory effect on axis fixation although the inhibitory effect of Cu^{2+} on secretion of fucoidin was more pronounced. Preliminary experiments (data not shown) revealed that the adhesion of zygotes was unaffected by up to 2110 nM Cu^{2+} and suggests that secretion of polysaccharides and mucus in general was unaffected by Cu^{2+}. Furthermore, secretion of Cu^{2+} complexing ligands by *Fucus* zygotes was not inhibited by increasing $[Cu^{2+}]$. On the contrary it was increased (Gledhill *et al.*, 1999). Such secretion in fucoid embryos is performed by exocytosis (Schoenwaelder and Clyton, 1998) in a similar way as localised secretion (Shaw and Quatrano, 1996b). Consequently the effects

of Cu^{2+} on secretion in *Fucus* zygotes may be targeted exclusively at localised secretion of fucoidin at the rhizoid tip. It is likely that the negative effect of Cu^{2+} on axis fixation is related to effects on secretion or upstream processes. In the suggested model for axis fixation (Goodner and Quatrano, 1999), Golgi-derived vesicles containing fucoidin are guided towards the rhizoid pole by actin filaments in response to the polar Ca^{2+} signal. The direct effects of Cu^{2+} on secretion of fucoidin could involve peroxidation of Golgi membranes through production of free radicals. The strong oxidative properties of Cu^{2+} are known to cause the production of reactive oxygen species (ROS) and result in peroxidation and damage to internal membranes (Luna *et al.*, 1994; Yruela *et al.*, 1996; Navari-Izzo *et al.*, 1998;). However, Cu^{2+} has been shown to result in accumulation of light- and electron microscope translucent vesicles in *F. spiralis* rhizoids and *Lilium* pollen tubes at concentrations which inhibited cell elongation, and which were within the range used in the present experiment (Sawidis and Reiss, 1995; Bond *et al.*, 1999). It is very likely that the accumulated vesicles contained Golgi-derived substances, which have not been secreted into the apical plasma membrane and cell wall. Consequently, vesicles are still derived from the Golgi during Cu^{2+} exposure in these organisms. These results suggest that the inhibitory effect of Cu^{2+} on transport and secretion of secretory vesicles is likely to cause the pronounced negative effect on secretion, rather than direct effects of Cu^{2+} on the Golgi apparatus. Hence, F-actin localisation and establishment of the Ca^{2+} gradient are potential targets for Cu^{2+} toxicity in the developing *Fucus* zygote.

3.4.2.3. F-actin localisation

The inhibitory effect of Cu^{2+} during axis fixation was downstream of F-actin localisation, as even [Cu^{2+}] as high as 2110 nM did not inhibit F-actin localisation greatly. In agreement with previous results (Kropf *et al.*, 1989; Bouget *et al.*, 1996; Alessa and Kropf, 1999; Pu *et al.*, 2000), it was shown that F-actin localises at the rhizoid pole in the *Fucus* zygotes

during axis establishment. Heavy metal ions may cause depolymerisation of the F-actin cytoskeleton, as Cd^{2+} ions were shown to be responsible for loss of actin filaments in vascular muscle cells (Wang *et al.*, 1996). The effect of metal ions on F-actin depolymerisation, however, was very specific for Cd^{2+}, as a number of different divalent metal ions, including Cu^{2+}, were tested and found ineffective (Wang *et al.*, 1996). In the present study, even during exposure to 2110 nM Cu^{2+}, as many as 80% of zygotes localised F-actin during the axis fixation period. Although this is 17% less than the proportion of zygotes which had localised F-actin in the control treatment, it is not enough to account for the 66% decrease in axis fixation, and the significant effect of Cu^{2+} on secretion of fucoidin. Consequently the main target for Cu^{2+} during axis fixation in the *Fucus* zygote must be upstream of secretion of fucoidin and downstream of F-actin localisation.

3.4.3. Effects of Cu^{2+} on cytosolic Ca^{2+} in the *Fucus* rhizoid

3.4.3.1. The Ca^{2+} gradient

The Ca^{2+} gradient at the *Fucus* rhizoid tip is initiated during axis establishment (Berger and Brownlee, 1993; Pu and Robinson, 1998), and becomes very localised during rhizoid germination and growth (Roberts *et al.*, 1993; Taylor *et al.*, 1996). Sustaining the apical Ca^{2+} gradient is very important for continued apical growth in both the *Fucus* zygote and other tip growing systems, as can be seen from microinjecting Ca^{2+} buffers such as BAPTA that disrupt the Ca^{2+} gradient and attenuate apical growth (Speksnijder *et al.*, 1989; Roberts *et al.*, 1993; Pierson *et al.*, 1994; Malhó *et al.*, 1995; Taylor *et al.*, 1996). Maintenance of the apical Ca^{2+} gradient may involve influx of external Ca^{2+} across the plasma membrane through mechanosensitive Ca^{2+} channels, which are activated by

localised stretching of the membrane at the apex by cell turgor (Taylor *et al.*, 1996; 1997). By monitoring $[Ca^{2+}]_{cyt}$ in a *Fucus* zygote microinjected with Ca^{2+} sensitive dye, and simultaneously patch clamping the plasma membrane during hypo-osmotic treatment it was shown that voltage- and mechanosensitive Ca^{2+} channels play a major part in apical Ca^{2+} signalling in the *Fucus* zygote (Taylor *et al.*, 1997). Furthermore, this work (Taylor *et al.*, 1997) also suggests that the mechanisms of establishing the growth related Ca^{2+} gradient and the hypo-osmotic Ca^{2+} elevation in the *Fucus* rhizoid may be linked.

Amplification of the apical Ca^{2+} gradient is a general response in the *Fucus* rhizoid when exposed to slight hypo-osmotic conditions. Goddard *et al.* (2000) showed that transfer of embryos from SW to 80% SW resulted in pronounced apical Ca^{2+} elevations in all embryos tested (n=20). Similarly in the present study, an abrupt, 10-fold increase in apical $[Ca^{2+}]$ was observed upon transfer from ASW to 80% ASW. Due to the soft cell wall at the rhizoid tip during rhizoid germination and apical growth, the cell turgor increase may result in localised activation of stretch activated Ca^{2+} channels and influx of Ca^{2+}, which contribute to maintenance of the Ca^{2+} gradient (Taylor *et al.*, 1996; 1997).

Inhibition of the Ca^{2+} gradient is a general feature of Cu^{2+} toxicity in the *Fucus* zygote. In 4 out of 6 experimental zygotes, exposure to 422 nM Cu^{2+} instantly and completely inhibited their ability to abruptly increase apical Ca^{2+} during slight hypo-osmotic conditions. The apical Ca^{2+} elevation in the remaining 2 out of 6 experimental zygotes was very limited. The rapid effect of the attenuation of the Ca^{2+} gradient suggests that the Cu^{2+} toxicity is due to inhibition of ion channels in the plasma membrane. A number of ion channels have been associated with the plasma membrane of the *Fucus* zygote. Voltage-gated mechanosensitive cation channels have been identified by patch clamp experiments (Taylor and Brownlee, 1993; Taylor *et al.*, 1992; 1996; 1997). Applying a mechanical

pressure of 0.5-2 kPa to the rhizoid plasma membrane or stretching it by inducing hypoosmotic swelling of the rhizoid resulted in increased cation channel activity (Taylor *et al.*, 1996; 1997). Membrane depolarisation and single channel recordings of these mechanosensitive channels revealed that the conductance was carried by an outward K^+ current and an inward Ca^{2+} current (Taylor *et al.*, 1996). This ion channel was blocked by Gd^{3+} (Taylor *et al.*, 1996) which also blocks mechanosensitive Ca^{2+} ion channels in other systems (Yang and Sachs, 1989; Amasheh and Weber, 1999). By the use of an extracellular vibrating probe it was shown that the positive inward current, observed at the rhizoid apex in the *Fucus* zygote, appears to be carried partly by Cl^- efflux (Nuccitelli and Jaffe, 1976).

Cu^{2+} is known to be a potent inhibitor of the current passing through different types of ion channels, antiporters and ATPases in different organisms, but the effect of Cu^{2+} is complex and there is no general response of the different types of ion channels to Cu^{2+}. The numerous examples include the inhibitory effects of Cu^{2+} on $Na^+/K^+/Ca^{2+}$-ATPase (Li *et al.*, 1996; Viarengo *et al.*, 1996), H^+-ATPase (Demidchik, 1997; 2001) and Na^+/Ca^{2+}-antiporter (Viarengo *et al.*, 1996). Patch clamp experiments have revealed that Cu^{2+} depresses current passing through Ca^{2+} channels in both plant and animal endo- and plasma-membranes (Kasai and Neher, 1992; Osipenko *et al.*, 1992; Viarengo *et al.*, 1996; Klusener at al 1997). Cu^{2+} strongly inhibited the conductivity through a non-specific Ca^{2+} channel in the *Bryonia dioica* ER membrane (Klusner *et al.*, 1997), and elevated $[Cu^{2+}]$ reduced the inward current through voltage activated Ca^{2+} channels in neuronal plasma membranes (Kasai and Neher, 1992; Osipenko *et al.*, 1992). Furthermore, Kasai and Neher (1992) found that Gd^{3+} was a potent inhibitor of the same neuronal Ca^{2+} channel. Cu^{2+} is also known to inhibit current through Cl^- channels (Kiss *et al.*, 1991; Demidchik, 1997; Amasheh and Weber, 1999). Amasheh and Weber (1999) found that elevated $[Cu^{2+}]$ is a

potent inhibitor of the current passing through Ca^{2+}-activated Cl^- channels in the *Xenopus laevis* oocyte plasma membrane. Interestingly, applying Gd^{3+} to the membrane had a similar inhibitory effect on the Ca^{2+}-activated Cl^- channel conductivity (Amasheh and Weber, 1999). It is very interesting to notice at least two examples where Cu^{2+} and Gd^{3+} ions are shown to be potent inhibitors of the conductance through the same type of ion channels (Kasai and Neher, 1992; Amasheh and Weber, 1999). Although there is no general effect of different ions on different types of ion channels, it is possible that the effects of Cu^{2+} and Gd^{3+} on other types of ion channels may be similar. Gd^{3+} is known to be a very potent inhibitor of stretch activated Ca^{2+} channels (Yang and Sachs, 1989; Zhang *et al.*, 1998), and has also been shown to inhibit inward Ca^{2+} current through stretch-activated ion channels in the apex of the *Fucus* rhizoid (Taylor *et al.*, 1996). Therefore, the coincident effect of Gd^{3+} and Cu^{2+} on Ca^{2+}- and Cl^--ion channels suggests that Cu^{2+} is also a potential inhibitor of stretch activated Ca^{2+} channels. Cu^{2+} may act by either blocking Ca^{2+}-channels in the *Fucus* rhizoid or changing the protein configuration.

3.4.3.2. Effects of Cu^{2+} on Ca^{2+} release from internal stores

Ca^{2+} signalling in the *Fucus* rhizoid is not solely dependent on the influx of Ca^{2+} from the external medium, but also relies on release of Ca^{2+} across internal membranes (Goddard *et al.*, 2000). The mobilisation of Ca^{2+} from internal Ca^{2+} stores across endomembranes in plants is gated by both ligand- and voltage-activated Ca^{2+} channels (Sanders *et al.*, 1999). Evidence for hyperpolarisation- and depolarisation-activated Ca^{2+} channels in endomembranes of higher plants has been presented (Johannes *et al.*, 1992; Ward and Schroeder, 1994; Allan and Sanders, 1994, 1996;). Furthermore, both inositol 1,4,5-trisphosphate (IP_3)- and cyclic ADP-ribose (cADPR)-activated Ca^{2+} channels have been identified in plants, where IP_3 and cADPR stimulate distinct Ca^{2+} release pathways from both vacuoles and the ER (Gilroy *et al.*, 1990; Allen *et al.*, 1995; Muir and Sanders, 1997).

IP_3-induced Ca^{2+} release from endomembranes may occur in the *Fucus* zygote. Photorelease of caged IP_3 was shown to induce a rapid increase in $[Ca^{2+}]_{cyt}$ in *Fucus* rhizoids (Goddard *et al.*, 2000). This finding suggests the involvement of IP_3 in the generation of Ca^{2+} signalling in the *Fucus* zygote (Goddard *et al.*, 2000). Ca^{2+} itself acts as a co-agonist in IP_3 induced Ca^{2+} release from internal stores, and the activity of the IP_3-receptor is regulated by the IP_3- and Ca^{2+}-concentration in the cytoplasm (Finch *et al.*, 1991; Combettes *et al.*, 1994; Kaftan *et al.*, 1997; Hirose *et al.*, 1998). The Ca^{2+} dependence of the IP_3-receptor is described by a bell-shaped curve which means that Ca^{2+} has a negative feedback on the IP_3-receptor below and above the Ca^{2+} optimum which is dependent on $[IP_3]$ (Combettes *et al.*, 1994; Kaftan *et al.*, 1997). The membrane-bound enzyme phospholipase C (PLC) catalyses the hydrolysis of the membrane lipid phosphatidylinositol 4,5-bisphosphate (PIP_2) to IP_3 and diacylglycerol (Burgess *et al.*, 1984; Runnels and Scarlata, 1998). Cu^{2+} is able to inhibit PLC activity and thereby effect the IP_3 dependent Ca^{2+} signalling (Panfoli *et al.*, 2000). Incubating gills and digestive glands of mussel, *Mytilus galloprovincialis*, with elevated $[Cu^{2+}]$ for 30 minutes resulted in an inhibitory effect on the PLC activity (Panfoli *et al.*, 2000). This finding led to the conclusion that the inhibitory effect of Cu^{2+} on the enzyme was due to lipid peroxidation and changed configuration induced by ROS production (Panfoli *et al.*, 2000). Furthermore, Cu^{2+} and other metals have been shown to form complexes with IP_3 (Haug *et al.*, 1994; Persson, 1998), which may obstruct the role of IP_3 as a messenger. The inhibitory effect of Cu^{2+} on IP_3 production and consequently on IP_3 controlled Ca^{2+} release from internal Ca^{2+} stores may play a role in the disruption of Ca^{2+} signalling in the *Fucus* zygote during long term exposure to moderate concentrations of Cu^{2+}.

3.4.3.3. Effects of acute Cu^{2+} exposure on Ca^{2+} homeostasis

Damage to the plasma membrane and changes to the total ionic current are some of the primary effects of Cu^{2+} toxicity at the cellular level (Kiss and Osipenko, 1994). Elevated $[Cu^{2+}]$ is known to cause lesions in plant plasma membranes, which may result in disrupted ion homeostasis in *Arabidopsis* seedlings (Murphy *et al.*, 1999) and the freshwater algae *Nitella flexilis* (Demidchik *et al.*, 1997; 2001). Increased membrane permeability resulted in increased ion current, which was carried by K^+ efflux (Murphy *et al.*, 1999) and Ca^{2+} influx (Demidchik *et al.*, 2001). In the experiment by Demidchik and co-workers (2001) the increased membrane permeability seemed to be unrelated to lipid peroxidation by ROS, as addition of antioxidants had no effect on the increased current. However, there are numerous examples of membrane lipid peroxidation caused by the highly oxidative properties of Cu^{2+}, which induces oxidative damage (De Vos *et al.*, 1991; 1993; Luna *et al.*, 1994; von Stedniak *et al.*, 1997; Cuypers *et al.*, 1999; Teisseire and Guy, 2000).

Ca^{2+} signalling is dependent on the ability of the cell to maintain $[Ca^{2+}]_{cyt}$ at a low level by exporting Ca^{2+} against a concentration gradient into vacuoles and the external medium (Bush, 1995; Sanders *et al.*, 1999). However, lipid peroxidation of ER membranes by ROS in neurons resulted in highly increased Ca^{2+} permeability of these membranes (Racay *et al.*, 1997; Lehotsky *et al.*, 1999). Oat leaves exposed to elevated concentrations of Cu^{2+} were subject to membrane peroxidation and chlorophyll breakdown, which are common symptoms of oxidative damage (Luna *et al.*, 1994). Highly increased antioxidant enzyme activity and production of free radicals has been found in response to elevated $[Cu^{2+}]$ in different plant species including *Lemna minor* (Teisseire and Guy, 2000). Similarly in the present study, acute exposure of the *Fucus* zygote to extreme (2-20 μM) $[Cu^{2+}]$ resulted in an abrupt increase in $Ca^{2+}{}_{cyt}$ within 30 seconds. This response is likely to be caused by loss of cellular control of internal Ca^{2+} stores, and external Ca^{2+} due to membrane peroxidation

by Cu^{2+}, and consequently flooding of the cytoplasm with Ca^{2+}. Therefore, the cytosolic Ca^{2+} elevations observed in the *Fucus* zygote in response to extreme acute and moderate chronic Cu^{2+} conditions may be the result of Cu^{2+} promoting the production of free radicals and lesions in plasma and endo-membranes.

3.4.4. Summary of discussion

Effects of Cu^{2+} on early development in the *Fucus* zygote and on growth of germlings acquired from populations with different tolerance limits were addressed in the present chapter.

By studying effects of Cu^{2+} on rhizoid elongation it was established that Restronguet embryos had a higher tolerance limit than Bantham and Wembury embryos. Furthermore, the Cu^{2+} tolerance during axis fixation was higher for Restronguet than Wembury zygotes. These results are mirrored both in the tolerance limit for adult *Fucus* (Chapter 2) and the natural copper status at the locations from which the algae were collected (Chapter 1).

Cu^{2+} was shown to have a positive effect on osmoregulation in non-tolerant embryos. This observation could be a direct strengthening effect of Cu^{2+} on the cell wall, or an indirect effect through lower osmotic potential of the zygotes due to inhibited photosynthesis.

It was shown that initiation of the polar axis in polarising zygotes was unaffected by high $[Cu^{2+}]$, whereas Cu^{2+} had a pronounced inhibitory effect on axis fixation. This effect may, in turn, have resulted in the abnormal cell division pattern observed, as alignment of the division plane is dependent on correct establishment of the polar axis.

The inhibitory effect of Cu^{2+} on axis fixation and rhizoid elongation was caused by inhibitory effects on secretion of fucoidin and/or the apical Ca^{2+} gradient, whereas F-actin localisation was largely unaffected. Cu^{2+} had the ability to rapidly and completely attenuating the apical Ca^{2+} gradient, which is an absolute requirement for axis fixation and rhizoid elongation. This effect may be the result of Cu^{2+} blocking apical Ca^{2+} carrying ion channels, which are partly responsible for maintenance of the gradient. Cu^{2+} may also interfere with IP_3 controlled Ca^{2+}-release from internal stores, and in this way contribute to the loss of the apical Ca^{2+} gradient.

Acute exposure of zygotes to extreme $[Cu^{2+}]$ resulted in largely increased $[Ca^{2+}]_{cyt}$. This effect may be the result of Cu^{2+} induced ROS production, which potentially could result in lipid peroxidation of endo- and plasmamembranes, which in turn could cause the flooding of the cytoplasm with Ca^{2+}.

CHAPTER 4

General Discussion

Fucus spp. have the ability to tolerate the presence of toxic metals in the environment, as evidenced by the presence of luxuriant populations in highly contaminated costal areas influenced by anthropogenic mineral exploitation. Such metal resistance is not a general feature of the genus and strains of tolerant and non-tolerant *Fucus* populations have developed in locations with varying metal status. In the present study, *Fucus serratus* obtained from Restronguet Creek which has been exposed to high levels of Cu^{2+} for decades, generally had a much higher level of resistance to imposed Cu^{2+} stress than populations from Bantham Quay and Wembury Beach, which have no history of Cu^{2+} pollution. The differences in Cu^{2+} tolerance were manifested by highly reduced and even negative growth rates of fronds from Bantham and Wembury populations compared with those from the Restronguet population that were largely unaffected during both short and long term exposure to high $[Cu^{2+}]$.

The tolerant and non-tolerant populations of *Fucus* have been shown to have different strategies for responding to high $[Cu^{2+}]$. Adult Bantham and Wembury *Fucus* responded to Cu^{2+} by accumulating it in high concentrations in the tissue, indicating that large quantities of Cu^{2+} were chelated internally. This is consistent with the demonstration by Smith and co-workers (1986) that Cu^{2+} was chelated internally and probably stored in vacuoles and/or cell walls of brown algae. Bantham and Wembury fronds accumulated Cu^{2+} to similar high levels whereas Restronguet fronds accumulated significantly less total copper per gram dry weight than Bantham and Wembury fronds. This suggests that the superior tolerance of the Restronguet population may be based, at least in part, on exclusion mechanisms. The natural exposure of *Fucus* from Restronguet Creek to excess Cu^{2+} may have led to the development of relatively few Cu^{2+} uptake sites in the plasma membrane which would contribute to avoidance of copper uptake. In addition, the population may have a higher level of metallothionein expression than non-tolerant

populations, analogous with tolerant and non-tolerant strains of *Arabidopsis* and *Silene* (Murphy and Taiz, 1995; van Hoof *et al.*, 2001).

Large quantities of organic substances were released from the Bantham and Wembury fronds in response to elevated Cu^{2+}. Production and secretion of ligands may lower [Cu^{2+}] in the water surrounding the algae (Gledhill *et al.*, 1999), although such ligands might easily be washed away and diluted. The large efflux of organic substances from Bantham and Wembury fronds may therefore include polyphenols or other chelators secreted with Cu^{2+} already bound, to lower the concentration of Cu^{2+} accumulated in the tissue. Alternatively, the high concentrations of organic substances measured in the incubation medium during Cu^{2+} exposure in non-tolerant algae, may reflect leakage of cell contents as a result of oxidative membrane damage. Cu^{2+}-induced lipid peroxidation, which resulted in leakage of cell contents through lesions in the cell membrane, has been demonstrated in *Arabidopsis* seedlings after 4h exposure to 30 μM $CuSO_4$ (Murphy *et al.*, 1999). In that study, leakage of cell contents was studied by measuring the K^+ concentration of the incubation medium by flame photometry. Similar measurements from *Fucus* during Cu^{2+} exposure would indicate whether Cu^{2+} led to solute leakage. If K^+ efflux was unaffected during Cu^{2+} exposure this would indicate that organic substances were selectively secreted. Increased K^+ efflux would indicate a general loss of cell content through lesions in the cell membrane.

Cu^{2+} appears to reduce the photosynthetic efficiency and capacity of *Fucus* by targeting two distinct parts of the photosynthetic apparatus. Furthermore, the tolerant population of *Fucus* from Restronguet Creek was more resistant to inhibitory effects of Cu^{2+} on photosynthesis than non-tolerant populations. Inhibitory effects of Cu^{2+} on the photosynthetic efficiency of photosystem II was expressed by a negative impact on the

quantum yield in photosynthetically saturating light, whereas the quantum yield of the dark-adapted state was unaffected after long-term (23 days) exposure. This suggests that Cu^{2+} reduced the tolerance of *Fucus* to saturating light. These results are consistent with the findings of Ouzounidou *et al.* (1997) who showed that Cu^{2+} reduces the quantum yield of the light- but not the dark-adapted stage of maize seedlings after 15 days exposure to elevated [Cu^{2+}]. Unlike Bantham and Wembury fronds, Restronguet fronds appeared to be able to divert the excess light energy, resulting from inhibitory effects on photosynthetic efficiency, by converting it to thermal energy through non-photochemical quenching (NPQ). The observed increase in NPQ of the Restronguet fronds may in turn result from a more resistant xanthophyll pool. A large xanthophyll pool and NPQ activity in brown algae is normally associated with sun-adaptation (Harker *et al.*, 1999) and these results therefore suggest that sun-adapted fronds may have a higher tolerance to Cu^{2+} than shade-adapted fronds. Although there was some increase in NPQ in Bantham and Wembury fronds at intermediate [Cu^{2+}], high concentrations had an inhibitory effect on NPQ. However, the non-tolerant populations may have responded to the increased sensitivity to high irradiances by increasing their production of accessory pigments to screen the photosynthetic apparatus from excess light. Bantham and Wembury fronds exposed to high [Cu^{2+}] became increasingly dark brown during the course of the experiment. Although this darkening in part may have been caused by accumulation of polyphenols, it could have been the result of fucoxanthin accumulation.

In addition to the inhibitory effects of Cu^{2+} on photosynthetic efficiency, there may have been a negative effect on the photosynthetic capacity of *Fucus*. This was indicated by a reduction in maximum fluorescence (F'_m) in saturating light. The observed reduction in the fluorescence signal, particularly in Bantham and Wembury fronds, may have been the result of increased pigmentation. However, the darkening effect of Cu^{2+} was only observed

in non-tolerant fronds, yet there was still some inhibitory effect of Cu^{2+} on the fluorescence of Restronguet fronds. Furthermore, the reduced fluorescence coincided with a reduction in the chlorophyll *a* pool of non-tolerant populations. Production of reactive oxygen species (ROS) and breakdown of chlorophyll *a*, particularly in the non-tolerant populations, may be an additional cause of reduced photosynthesis in *Fucus*, which was apparent after both short- and long-term exposure. Excess light energy and elevated $[Cu^{2+}]_{cyt}$ in non tolerant species may have contributed to increased production of reactive oxygen species (ROS) which, in turn, may have resulted in the breakdown of the chlorophyll *a* pool. Cu^{2+} seems to affect the pigment composition in *Fucus* as both chlorophyll and carotenoids may have been affected. Moreover, the pigmentation during Cu^{2+} exposure seems to be dependent on the degree of Cu^{2+} tolerance of the algae. It would therefore be highly relevant to carry out a detailed study of the content of chlorophylls and different carotenoids in different populations of *Fucus* after long-term exposure to Cu^{2+}. Furthermore, it would be interesting to compare effects of Cu^{2+} on the photosynthetic apparatus in sun- and shade-adapted *Fucus*, to clarify the possibility of higher Cu^{2+} tolerance in sun-adapted fronds.

In the present study it was shown that the level of Cu^{2+} tolerance of *Fucus* embryos and young zygotes mirrors that of the adults from which they were acquired. Bantham and Wembury zygotes and embryos were more sensitive to Cu^{2+} than Restronguet ones. There was some inhibitory effect of Cu^{2+} on rhizoid elongation of Restronguet embryos although this was more pronounced in Bantham and Wembury embryos. Similarly, inhibitory effects of Cu^{2+} on developmental processes of young zygotes occurred at lower concentrations in Wembury zygotes than Restronguet ones, which even displayed some Cu^{2+} requirement at this stage in the life cycle.

Cu^{2+} targets the establishment of the polar growth axis in the *Fucus* zygote in a very selective manner. Polarisation of the *Fucus* zygote occurs as a sequence of complex physiological processes. The polar axis is initiated during photopolarisation by the detection and translation of a determining environmental vector, usually light, into spatial information (Berger and Brownlee, 1994). Subsequently the polar axis is irreversibly fixed in a sequence of physiological processes at the rhizoid pole, involving F-actin localisation (Bouget *et al.*, 1998a), secretion of fucoidin (Shaw and Quatrano, 1996b) and establishment of a Ca^{2+} gradient (Taylor *et al.*, 1992). Photopolarisation was unaffected in non-tolerant zygotes even at extreme [Cu^{2+}] whereas there were inhibitory effects on the axis fixation process in both non-tolerant and, to a lesser extent, tolerant zygotes. Failure of zygotes to fix their polar axis correctly affected their further development. Whereas the cell division rate of *Fucus* embryos was largely unaffected, there was an abnormal pattern of cell division in the developing embryo in response to Cu^{2+} exposure. Such abnormalities may be related to the inhibitory effects of Cu^{2+} on axis fixation, as fixation of the polar axis is a requirement for correct orientation of the cell division plane (Shaw and Quatrano, 1996b).

The inhibitory effects of Cu^{2+} on axis fixation appeared to be downstream of F-actin localisation, which was largely unaffected by Cu^{2+}, and upstream of polarised secretion of fucoidin into the rhizoid apex, which was severely inhibited by Cu^{2+}. Cu^{2+} may specifically target the localised secretion of fucoidin, as secretion of mucusand cell wall components, other than fucoidin, appeared to be unaffected, and secretion of polypohenols may have been increased by Cu^{2+}. Other workers (Bond *et al.*, 1999) have demonstrated the accumulation of vesicles inside the *Fucus* rhizoid cell which coincided with the development of very stunted rhizoids in *Fucus* zygotes exposed to Cu^{2+} during polarisation. These vesicles may contain fucoidin, the incorporation of which into the cell

wall may be prevented by Cu^{2+}. Hence, rather than inhibitory effects on fucoidin synthesis in the Golgi, Cu^{2+} may impair intracellular polar vesicle transport. During intracellular transport, vesicles are guided along actin filaments by motor proteins such as myosin and kinesin (Rogers and Gelfand, 2000). Cu^{2+} is unlikely to impair vesicle transport by affecting the axially-arranged actin filaments, as it has been shown in this and other studies (Wang *et al.*, 1996) that F-actin polymerisation is largely unaffected by Cu^{2+} exposure. Cu^{2+} may, however, target myosin, kinesin and other motor proteins, which are responsible for the actual movement of vesicles. Intracellular vesicle transport can be visualised *in vivo* by labelling motor protein subunits with green fluorescent protein and imaging vesicular transport using confocal microscopy (Orozco *et al.*, 1999). In their work, Orozco and co-workers (1999) imaged polar vesicular transport in cilia. It would be very interesting and useful to adapt and develop the method of Orozco and co-workers (1999) for monitoring vesicle transport in polarising *Fucus* zygotes.

It was shown that the maintenance of the localised Ca^{2+} gradient is one of the key targets for Cu^{2+} toxicity in *Fucus* zygote development. Exposure of germinated zygotes to a slight hypo-osmotic shock results in a noticeable amplification of the apical Ca^{2+} gradient (Goddard *et al.*, 2000), which is dependent on Ca^{2+}-conducting ion channels in the plasma membrane (Taylor *et al.*, 1996, 1997). Exposure to Cu^{2+} immediately inhibited the Ca^{2+} elevation at the rhizoid apex in response to hypo-osmotic conditions. This result suggests that Cu^{2+} specifically targets the apical Ca^{2+} gradient in the *Fucus* zygote by inhibiting inward Ca^{2+} flux through Ca^{2+} conducting ion channels. This in turn would result in loss of the polar signal which is a prerequisite for both axis fixation and rhizoid elongation. Hence, such inhibition could in itself cause the observed inhibitory effects on Cu^{2+} on both axis fixation and rhizoid elongation. Consequently it would be of great relevance to monitor the direct effect of Cu^{2+} on ion channel activity in the plasma membrane of the

Fucus zygote using patch clamp techniques. Existing protocols for patch clamping of the zygote membrane during hypo-osmotic treatment of rhizoids (Taylor and Brownlee, 1993; Taylor *et al.*, 1996, 1997) could be used for monitoring the effect of Cu^{2+} on Ca^{2+} channel activity.

In addition to influx of Ca^{2+} from the external medium, the apical Ca^{2+} gradient in *Fucus* is dependent on Ca^{2+} release from internal stores in an inositol 1,4,5-trisphosphate (IP_3) controlled process (Goddard *et al.*, 2000). The membrane bound enzyme, phosholipase C, catalyses the production of IP_3 (Runnels and Scarlata, 1998) which in turn induces the release of Ca^{2+} from internal stores such as the ER *via* IP_3 -sensitive Ca^{2+} channels (Hirose *et al.*, 199). Phospholipase C is itself activated by localised Ca^{2+} elevations in a positive feedback mechanism and IP_3-induced Ca^{2+} release is a process downstream of Ca^{2+} entry from the external medium (Goddard *et al.*, 2000). Hence, inactivation of the IP_3 pathway in the *Fucus* zygote may be a result of inhibitory effects on the stretch-activated Ca^{2+} channels at the rhizoid apex. There are, however, several other potential targets for Cu^{2+} in the IP_3-pathway. For example, Cu^{2+} has the ability to inhibit the phospholipase C activity in mussel gill membranes (Panfoli *et al.*, 2000) and to form complexes directly with IP_3, hence disrupting its role as a messenger (Persson *et al.*, 1998). Furthermore, Cu^{2+} has been shown to strongly inhibit the conductivity of Ca^{2+} channels in *Bryonia dioica* ER membranes (Klusener *et al.*, 1997). Cu^{2+} may therefore also target the IP_3 -sensitive Ca^{2+} channels, which are controlling internal Ca^{2+} release in *Fucus*. It would be interesting to study the effects of Cu^{2+} on IP_3-induced Ca^{2+} release in the *Fucus* zygote. By microinjecting germinated rhizoids with Calcium Green/Texas Red and caged IP_3, and subsequently induce localised photorelease of IP_3 with a UV pulse, IP_3-induced Ca^{2+} release can be monitored by the use of a confocal microscope (Goddard *et al.*, 2000). A negative effect of Cu^{2+} on the Ca^{2+} release from internal stores would result from direct

inhibitory effects on the IP_3 pathway, which could be caused either by complex formation between Cu^{2+} and IP_3, or by inhibitory effects of Cu^{2+} on the IP_3 sensitive Ca^{2+} channels in internal membranes.

In adults, production of ROS and oxidative damage was indicated by chlorophyll *a* breakdown and possible lesions in the plasma membrane. Exposure of embryos to high [Cu^{2+}] resulted in an immediate large elevation of Ca^{2+} throughout the rhizoid cell, which lasted for several minutes. Such a response may be the result of the induction of ROS by Cu^{2+} which in turn may cause lipid peroxidation and membrane damage. Cu^{2+}-induced damage to endo- and plasma membranes in the embryo would have allowed flux of Ca^{2+} into the cytoplasm from the external medium and vacuoles, which holds several-fold higher [Ca^{2+}]. It would be highly relevant to study the effect of Cu^{2+} on ROS production in *Fucus* embryos to clarify the role of ROS in Cu^{2+} toxicity in *Fucus*. This could be achieved by loading embryos with fluorescent indicators and subsequently exposing them to Cu^{2+} and monitor the response on a confocal microscope.

Resistance to environmental stress requires an appropriate stress response. Several stress responses in plants involve both Ca^{2+} and H_2O_2 signalling (Bowler and Fluhr, 2000). This also appears to be the case following exposure of *Fucus* embryos to a hyper-osmotic shock (Coelho *et al.*, unpublished data). The embryo responded to hyper-osmotic treatment by a burst of reactive oxygen species, which correlated with elevated Ca^{2+} to promote a cellular stress response involving a complex signalling pathway (Coelho *et al.*, unpublished data). Ca^{2+} signalling during exposure of a plant cell to a stress factor appears to be specific, due to controlled release and spatial location of the signal. H_2O_2 signalling, on the other hand, may induce similar cellular responses to different stresses, and H_2O_2 induction by exposure to one form of stress may induce several defence-related genes (Bowler and Fluhr, 2000).

H_2O_2 signalling may therefore induce cross-tolerance in plants as illustrated by higher pathogen resistance in plants treated with UV radiation compared with untreated plants (Bowler and Fluhr, 2000). Similarly, the Cu^{2+}-resistant Restronguet population may have a higher tolerance limit to pollutants and environmental factors other than Cu^{2+} compared with the Bantham and Wembury populations, which are not tolerant to Cu^{2+}. A generally higher stress tolerance of the Restronguet population than both the Bantham and Wembury populations was reflected by the higher relative growth rates of Restronguet control fronds after 2 days. It would be very interesting to study the tolerance limits of Cu^{2+} tolerant and non-tolerant *Fucus* to other environmental factors such as metals other than Cu^{2+}, hydrocarbons, UV radiation, herbicides *etc.*

The present study indicated that Cu^{2+} tolerance in *Fucus* is an inherited character. There were no differences in the level of Cu^{2+} tolerance of *F. serratus* expressed as axis fixation of zygotes and growth of germinated embryos and adults from the same population. All of these stages were, however, more sensitive than axis formation, which occurs approximately 2h after fertilisation, and was the earliest developmental stage studied. The strategies of Cu^{2+} resistance (metallothionein and exclusion mechanisms) which were suggested to distinguish tolerant adult *Fucus* from non-tolerant specimens (Chapter 2) are also likely to exist in tolerant zygotes and embryos. Metallothionein genes which are expressed in *Fucus* during Cu^{2+} exposure (Morris *et al.*, 1999) may be transcribed at higher rates in tolerant than non-tolerant strains (van Hoof *et al.*, 2001). Furthermore, gene expression in young *Fucus* zygotes may rely almost entirely on maternal mRNA during the first hours after fertilisation. Early experiments showed that inhibition of mRNA synthesis in *Fucus* zygotes had no effect on early developmental processes, which suggests the presence of maternal mRNA in the zygotes and that this mRNA is required and sufficient for protein synthesis during zygote development (Quatrano, 1968). The presence of mRNA

in *Fucus* zygotes was further supported by the finding that unfertilised eggs contain large quantities of actin mRNA which is not required until polarisation in the fertilised zygote (Masters *et al.*, 1992). Assuming that *Fucus* provides its progeny with maternal metallothionein, the Restronguet zygotes were likely to synthesise higher levels of metallothionein than non-tolerant zygotes regardless of the Cu^{2+} treatment. Such default induction of metallothionein may be the physiological difference which allowed Restronguet zygotes to fix their polar axes at higher [Cu^{2+}] than Bantham and Wembury zygotes and may have resulted in the Cu^{2+} requirement, which was expressed in Restronguet zygotes exposed to Cu^{2+}-free medium during axis fixation. The assumption that metallothionein production in Restronguet zygotes is dependent on gene expression of the parents rather than on [Cu^{2+}] in the environment of the zygote is extremely interesting. This could be tested further by quantifying metallothionein gene expression in eggs, embryos and adults exposed to different [Cu^{2+}]. Furthermore, the hypothesis that metallothionein is synthesised at higher levels in Cu^{2+}-tolerant than non-tolerant populations of *Fucus* also suggests an interesting study. The *Fucus* metallothionein gene has been identified and methods for quantification of metallothionein mRNA have been developed (Morris *et al.*, 1999).

Very few studies have addressed the issue of inherited versus acquired Cu^{2+} tolerance in macroalgae. Similar to the fucoids, green algae such as *Enteromorpha compressa* are known to develop Cu^{2+} tolerant strains which may become dominant in habitats exposed to elevated [Cu^{2+}] (Correa *et al.*, 1996). However, in contrast to the present study, Correa and co-workers (1996) showed that rather than being an inherited character, Cu^{2+} tolerance of *E. compressa* is acquired during the development of the algae. There was a significant difference in the tolerance limit of adult *E. compressa* measured as relative elongation of segments, which was 10 μM total copper for algae from a 'clean' habitat and 100 μM for

algae from a Cu^{2+} polluted habitat. In comparison, there was no difference in the Cu^{2+} tolerance limit for the progeny from the two populations which was comparable to the adults from the clean habitat (Correa *et al.*, 1996). The higher level of Cu^{2+} tolerance in *E. compressa* adults than in their progeny may indicate that there is a higher selection pressure on the young, and non-tolerant young may therefore die before they reach maturity. This would result in rapid selection, as only tolerant individuals would live to reproduce, Alternatively, Cu^{2+} tolerance may be acquired by all individuals during their development into adults. In *Fucus* there appeared to be no difference in the tolerance limit for Cu^{2+} in zygote, embryos and adults, and the selection for Cu^{2+} tolerance therefore appears to be equal at all stages. Earlier developmental stages may, however, express higher sensitivity to Cu^{2+}. It has been shown that *Fucus* is much more sensitive to Cu^{2+} during fertilisation than at the time of germination (Andersson and Kautsky, 1996). Such sensitivity could imply that there is a negative effect on the gametes as well as on the fertilisation process itself. Egg activation in *Fucus* and resumption of the cell cycle and metabolism is dependent on the fertilisation potential, which is initiated by ion channel-mediated flux of external Na^{+} and Ca^{2+} across the plasma membrane into the cytoplasm of the zygote in response to fertilisation (Taylor and Brownlee, 1993). The present study indicated that Cu^{2+} may inhibit channel-mediated flux of Ca^{2+} across the plasma membrane of the *Fucus* zygote, hence Cu^{2+} may also inhibit the fertilisation potential, which initiates zygote development. It is therefore possible that there is a larger selection pressure for Cu^{2+} tolerance on the *Fucus* zygote during fertilisation and within the first 1-2h after fertilisation, or that Cu^{2+} tolerance is acquired during this very early life cycle stage. To establish the effect of Cu^{2+} on *Fucus* gametes and fertilisation more precisely it would be relevant to carry out simple comparative germination experiments of zygotes exposed to Cu^{2+} as gametes prior to fertilisation, during fertilisation and immediately after fertilisation has taken place. Such experiments may confirm that fertilisation and/or the first few hours

after fertilisation is the stage in the *Fucus* life cycle which experiences a larger selection pressure for Cu^{2+} tolerance than any subsequent developmental stage.

Restronguet Creek has been exposed to Cu^{2+} pollution for more than a century and the Cu^{2+} tolerance of the *Fucus* population growing within the Creek is well established. Consequently, this population does not provide much information about the development of a tolerant population. However, habitats which are not exposed to continuous discharge of Cu^{2+} may be affected by more unpredictable sources of Cu^{2+}. Anti-fouling paint on ships is a known source of Cu^{2+} release into the marine environment. Furthermore, a ship may represent a strong selection pressure for the development of Cu^{2+} tolerance as numerous zygotes may settle on a ship. Cu^{2+} in anti-fouling paint would then favour the few which have an unusually high Cu^{2+} tolerance due to natural variability. As Cu^{2+} tolerance in *Fucus* is inherited, these individuals may release Cu^{2+} tolerant gametes once maturity is reached. Consequently the presence of ships painted with Cu^{2+}-containing paints represents not only a source of Cu^{2+} but also of individuals with extremely high Cu^{2+} tolerance, which may then be released into an environment with naturally very low concentrations of Cu^{2+}.

The present work has focused on the physiological responses of *Fucus* subjected to Cu^{2+} exposure. Apical portions of fronds were used as they were easier to handle than whole individuals and facilitated a range of different measurements on tissue of approximately the same age. This approach, however, did not provide any information about the responses of sub-apical portions. Different responses are likely to occur in different parts of the thallus. For example apical parts of *Ascophyllum nodosum* thalli accumulated more copper and were more sensitive to changes in $[Cu^{2+}]_{ext}$ than other parts of the alga (Stengel and Dring, 2000). Consequently, additional information on physiological effects of *Fucus* exposed to toxic metals could be gained by studying segments from other parts of the

thallus and whole algae. Inter-population differences in the physiological responses of *Fucus* during Cu^{2+} exposure were studied by including three populations which were either not exposed to Cu^{2+} or exposed to very high concentrations in their natural environment. Three populations is the minimum required for the study of inter-population differences. Although the results of the present study clearly indicate that exposure of *Fucus* to Cu^{2+} in its natural environment results in the development of tolerant populations, it would be statistically more convincing to include a larger number of both exposed and unexposed populations in the work.

The *Fucus* zygote provides an excellent model for assessment of environmental impact on early embryo development. The zygote is very easily obtained and cultured in synchronous populations and the developmental events following fertilisation are relatively well known, and both adult and microscopic stages of brown algae are often used in toxicity testing and biomonitoring. Some of the methods in this study could be developed further and used in such programmes. Biological monitoring of metal pollution often occurs as straightforward measurement of the tissue metal content of an organism such as *Fucus*. On the basis of the present study it is evident that such measurements may give a biased impression of the effects of heavy metals on an organism and underestimate the actual toxicity level in a habitat. The Cu^{2+}-tolerant Restronguet population accumulated far less copper than the non-tolerant Bantham and Wembury populations during exposure to the same [Cu^{2+}], whereas the Wembury population accumulated much less copper than both the Restronguet and Bantham populations during exposure to low [Cu^{2+}]. A much more useful approach would be to measure the metal content of transplanted material using the tissue from one reference station with known accumulation thresholds combined with measurements made on local tissue. Transplantation experiments of this kind would provide more specific information about the conditions the biota are subject to in a particular habitat, although

the approach does not provide the instant results that are often desirable in environmental monitoring. Use of *Fucus* zygotes, which respond to pollutants within a few hours after the exposure, may therefore be a useful addition or alternative to tests on adult tissue.

Microscopic stages of brown algae are useful in biomonitoring programmes as they are very easy to obtain and culture in large numbers and the tests gives a fairly rapid indication of how the organism is affected by exposure to particular environmental conditions. Standardised protocols have been developed for the use of the brown alga *Ecklonia radiata* in toxicity testing in Southern Australia (Bidwell *et al.*, 1998; Burridge *et al.*, 1998). Axis fixation in *Fucus* is affected by very low (nM) [Cu^{2+}], and since this developmental stage is easily assessed by simple manipulative experiments the system could be further developed for use in toxicity testing. However, this approach would only provide information which is relevant to the time when the sample was taken whereas monitoring metal accumulation in adult *Fucus* does provide information about the time-integrated effects. Combined use of zygotes and adults would provide a detailed description of the conditions for the biota in a particular environment.

The present study has provided insight into some of the mechanisms of Cu^{2+} toxicity in both zygotes and adults of *F. serratus*. There are, however, still unanswered questions, which would add to knowledge of toxicity effects in *Fucus*:

- Ca^{2+} signalling, which is important for the development of the *Fucus* zygote, is interrupted by Cu^{2+}. To determine more precisely the targets for Cu^{2+} in Ca^{2+} signalling, future studies should focus on the effects of Cu^{2+} on Ca^{2+} ion channels in the plasma membrane and on Ca^{2+} release from internal stores.

- The inhibitory effects of Cu^{2+} on Ca^{2+} signalling may be a determining factor in inhibition of localised secretion at the rhizoid apex. Localised secretion may also be interrupted by inhibitory effects on the attachment and movement of motor proteins on the actin filaments. Inhibitory effects of Cu^{2+} on the actual vesicle transport along actin filaments should therefore be studied.
- Cu^{2+} may induce ROS production in *Fucus* embryos and adults as well as lesions in the plasma membrane, which may result in leakage of the cell content, and these responses should therefore be studied.
- Photosynthesis is a primary target for Cu^{2+} in the physiology of *Fucus*. Cu^{2+} inhibited photosynthetic electron transport and appeared to lower the resistance of fronds to saturating light and to change their pigment composition. Future work on the effects of Cu^{2+} on the photosynthetic apparatus in *Fucus* should therefore include detailed studies of effects of Cu^{2+} on the pigment composition of fronds as well as on the role of adaptation to high irradiances in Cu^{2+} tolerance.
- Cu^{2+} tolerance in *Fucus* is an inherited character. The tolerance level of zygotes and embryos is equivalent to that of adult algae from the same population. The tolerance of zygotes and embryos may therefore depend on the expression of maternal metallothionein mRNA. Consequently it would be highly relevant to monitor metallothionein gene expression of eggs, zygotes and adults from tolerant and non-tolerant populations. Instead of inherited Cu^{2+}-tolerance, tolerance may be acquired immediately after fertilisation and it is therefore relevant to study the effects of Cu^{2+} on these early stages.
- Cross tolerance may occur with environmental stresses other than Cu^{2+} and it is therefore relevant to test the tolerance level of Cu^{2+} tolerant populations to other stress factors.

Fucus provides a useful system for studying the toxic effects on development and physiology of algae and may be a suitable candidate for inclusion in standardised toxicity testing. With the present day concerns over environmental impacts, not only by heavy metals but also other stressors such as hydrocarbons and UV radiation, *Fucus* should continue to be a valuable model system for environmental science in the future.

APPENDICES

Appendix 1

Composition of Aquil, modified from Morel *et al.* (1979).

Constituent	Amount added g l^{-1} nano pure water	Concentration in stock (M)	Final concentration in Aquil (M)
Synthetic Ocean Water (SOW)			
NaCl	24.03		4.20×10^{-1}
Na_2SO_4	4.09		2.88×10^{-2}
KBr	0.10		8.40×10^{-4}
KCl	0.70		9.39×10^{-3}
H_3BO_3	0.03		4.85×10^{-4}
$NaHCO_3$	0.20		2.38×10^{-3}
Make sure all anhydrated salts are completely dissolved before adding the hydrated salts			
$CaCl_2 \cdot 2H_2O$	1.51		1.05×10^{-2}
$MgCl_2 \cdot 6H_2O$	11.10		5.46×10^{-2}
Nutrients			
$SrCl_2 \cdot 6H_2O$	1.70	$6.38 \cdot 10^{-2}$	6.38×10^{-5}
NaF	0.30	$7.14 \cdot 10^{-2}$	7.14×10^{-5}
KI	0.04	$2.40 \cdot 10^{-4}$	2.40×10^{-7}
$NaNO_3$	1.70	$2.00 \cdot 10^{-2}$	2.00×10^{-5}
NaH_2PO_4	0.276	$2.00 \cdot 10^{-3}$	2.00×10^{-6}
Make each stock individually and add each at 1 ml l^{-1} to SOW			
Trace metals			
Solution 1	*g l^{-1} 0.01 M HCl*		
$FeCl_3 \cdot 6H_2O$	0.122	$4.51 \cdot 10^{-4}$	4.51×10^{-7}
Solution 2A	*g 100ml^{-1} 0.01 M HCl*		
$Na_2MoO_4 \cdot 2H_2O$	2.42	$1.00 \cdot 10^{-1}$	1.00×10^{-7}
$CoCl_2 \cdot 6H_2O$	0.595	$2.50 \cdot 10^{-2}$	2.50×10^{-8}
Solution 2B	*g 100l^{-1} 0.01 M HCl*		
$ZnSO_4 \cdot 7H_2O$	0.115	$4.00 \cdot 10^{-3}$	4.00×10^{-9}
$MnCl_2 \cdot 4H_2O$	0.460	$2.30 \cdot 10^{-2}$	2.30×10^{-8}
Add solution 2A and 2B at 1 ml l^{-1} each to solution 1. Then add solution 1 at 1 ml l^{-1} to SOW			

Appendix 2

Summary of the preparation of copper enriched Aquil and initial concentrations of total copper and free Cu^{2+}

[total copper] of stock (mM)	Volume (µl) copper stock per 100 ml Aquil	Initial total copper (µM) in Aquil	Initial free Cu^{2+} (µM) in Aquil
0.2	50	0.1	0.0422
0.2	100	0.2	0.0844
2.0	25	0.5	0.211
2.0	50	1.0	0.422
2.0	100	2.0	0.844
2.0	250	5.0	2.11
20.0	100	20.0	8.44

REFERENCES

Ahner, B. A., Kong, S. and Morel, F. M. M. (1995). Phytochelatin production in marine algae. I. An interspecies comparison. *Limnol. Oceanogr.*, **40**, 649-657

Alberts, J. J. and Filip, Z. (1998). Metal binding in estaurine humic and fluvic acids: FTIR analysis of humic acid-metal complexes. *Environ. Technol.*, **19**, 923-931

Alessa, L. and Kropf, D. L. (1999). F-actin marks the rhizoid pole in living *Pelvetia compressa* zygotes. *Development*, **126**, 201-220

Alexandre, J. Lassalles, J. P. and Kado, R. T. (1990). Opening of Ca^{2+} channels in isolated red beet root vacuole membrane by inositol 1,4,5-triphosphate. *Nature*, **343**, 567-570

Al-Farawati, R. and Van den Berg, C. M. G. (1999). Metal-sulfide complexation in seawater. *Mar. Chem.*, **63**, 331-352

Allen, V. and Kropf, D. L. (1992). Nuclear rotation and lineage specification in *Pelvetia* embryos. *Development*, **115**, 873-883

Allen, G. J., Muir, S. R. and Sanders, D. (1995). Release of Ca^{2+} from individual plant vacuoles by both InsP3 and cyclic ADP-ribose. *Science*, **268**, 735-737

Allen, H. E. and Hansen, D. J. (1996). The importance of trace metal speciation to water quality criteria. *Water Environ. Res.*, **68**, 42-54

Allen, R. D., Jacobsen, J. J. and Jaffe, L. F. (1970). Ionic concentration in developing *Pelvetia* eggs. *Dev. Biol.* **27**, 538-545

Amasheh, S. and Weber, W.-M. (1999). Further characteristics of the Ca^{2+}-inactivated Cl^- channel in *Xenopus laevis* oocytes. *J. Membrane Biol.*, **172**, 169-179

Anderson, B. S., Hunt, J. W., Turpen, S. L., Conlon, A. R. and Martin, M. (1990). Copper toxicity to microscopic stages of giant kelp *Macrocystis pyrifera*: interpopulation comparisons and temporal variability. *Mar. Ecol. Prog. Ser.*, **68**, 147-156

Anderson, D. M. and Morel, F. M. M. (1978). Copper sencitivity of *Gonyaulax tamarensis*. *Limnol. Oceanogr.* **23**, 283-295

Andersson, S. and Kautsky, L. (1996). Copper effects on reproductive stages of Baltic Sea *Fucus vesiculosus*. *Mar. Biol.* **125**, 171-176

Apte, S. C., Gardner, M. J., Gunn, A. M., Ravenscroft, J. E. and Vale, J. (1990). Trace metals in the Severn Estuary: a reappraisal. *Mar. Pol. Bull.*, **21**, 393-396

Ashley, J. T. F. (1996). Adsorption of Cu(II) and Zn(II) by estuarine, rivearine and terrestrial humic acids. *Chemosphere*, **33**, 2175-2187

Atkins, P. W. (1989). *General Chemistry*. Scientific American Inc., New York, 989 p.

Babcock, G. T. and Wikström (1992). Oxygen activation and the conservation of energy in cell respiration. *Nature*, **356**, 301-308

Babu, Y. S., Bugg, C. E. and Cook, W. J. (1988). Structure of calmodulin refined at 2.2 Å resolution. *J. Mol. Biol.*, **204**, 191-204

Baker, A. J. M. (1987). Metal tolerance. *New Pyhtol.*, **106** (suppl.), 93-111

Battey, N. H. and Blackbourn, H. D. (1993). The control of endocytosis in plant cells. *New Pytol.*, **125**, 307-338

Beers, J., Glerum, D. M. and Tzagoloff, A. (1997). Purification, characterization and localization of yeast Cox17p, a mitochondrial copper shuttle. *J. Biol. Chem.*, **272**, 33191-33196

Bentrup, F. W. (1963). Vergleichende Unterscuchen zur Polaritätsinduktion durc das Licht an der *Equisetum*-spore und des *Fucus*-zygotes. *Planta.* **59,** 472-491

Bentrup, F. W., Sandan, T, and Jaffe, L. (1966). Induction of polarity in *Fucus* eggs by potassium ion gradients. *Protoplasma,* **64,** 254-266

Berger, F. and Brownlee, C. (1993). Ratio confocal imaging of free cytoplasmic calcium gradients in polarising and polarised *Fucus* zygotes. *Zygote.* **1,** 9-15

Berger, F. and Brownlee, C. (1994). Photopolarization of the *Fucus* sp. zygote by blue light involves a plasma membrane redox chain. *Plant Physiol.,* **105,** 519-527

Berger, F., Taylor, A. and Brownlee, C. (1994). Cell fate determination by cell wall in early *Fucus* development. *Science,* **263,** 1421-1423

Berkaloff, C. and Rousseau, B. (1979). Ultrastructure of male gametogenesis in *Fucus serratus* (Phaeophyceae). *J. Phycol.,* **15,** 163-173.

Berleth, T., Mattsson, J. and Hardtke, C. S. (2000). Vascular continuity, cell axialisation and auxin. *Plant Growth Reg.,* **32,** 173-185

Bidwell, J. R., Wheeler, K. W. and Burridge, T. R. (1998). Toxicant effects on the zoospore stage of the marine macroalga *Ecklonia radiata* (Phaeophyta: Laminariales). *Mar. Ecol. Prog. Ser.,* **163,** 259-265

Bisgrove, S. R. and Kropf, D. L. (1998). Alignment of centrosomal and growth axes is a late event during polarisation of *Pelvetia compressa* zygotes. *Devel. Biol.,* **194,** 246-256

Bisgrove, S. R. and Kropf, D. L. (2001). Cell wall deposition during morphogenesis in fucoid algae. *Planta,* **212,** 648-658

Bond, P. R., Brown, M. T., Moate, R. M., Gledhill, M., Hill, S. J. and Nimmo, M. (1999). Arrested development in *Fucus spiralis* (Phaeophyceae) germlings exposed to copper. *Eur. J. Phycol.,* **34,** 513-521

Bouget, F. -Y., Berger, F. and Brownlee, C. (1998). Position dependent control of cell fate in the *Fucus* embryo: role of intercellular communication. *Development,* **125,** 1999-2008

Bouget, F. -Y., Gertulla, S., Shaw, S. L. and Quatrano, R. S. (1998). Localization of actin mRNA during the establishment of cell polarity and early cell division in *Fucus* embryos. *The Plant Cell,* **8,** 189-201

Bowler, C. and Fluhr, R. (2000). The role of calcium and activated oxygens as signals for controlling cross-tolerance. *Trends Plant Sci.,* **5,** 241-246

Boyle, E. A., Chapnick, S. D., Bai, X. X. and Spivack, A. (1985). Trace metal enrichments in the Mediterranean Sea. *Earth Planet. Sci. Let.,* **74,** 405-419

Brand, L. E., Sunda, W. G. and Guillard, R. R. L. (1986). Reduction of marine phytoplankton reproduction rates by copper and cadmium. *J. Exp. Mar. Biol. Ecol.,* **96,** 225-250

Brawley, S. H. (1991). The fast block against polyspermy in *Fucoid* algae is an electrical block. *Devel. Biol.,* **144,** 94-106

Brawley, S. H., Quatrano, R. S. and Weatherbee, R. (1977). Fine structure studies of the gametes and embryo of *Fucus vesiculosus* L. (Phaeophyta). III. Cytokenesis and the multicellular embryo. *J. Cell Sci.,* **24,** 275-294

Breton, C., Faure, J. E. and Dumas, C. (1995). From in vitro fertilisation to early embryogenesis in maize. *Protoplasma,* **187,** 3-12

Brownlee, C. and Berger, F. (1995) Extracellular matrix and pattern in plant embryos: on the lookout for developmental information. *Trends in Genetics,* **11,** 344-348

Brownlee, C. and Wood, J. W. (1986). A gradient of cytoplasmic free calcium in growing rhizoid cells of *Fucus serratus. Nature,* **320,** 624-626

Bruland, K. W. (1980). Oceanographic distributions of cadmium, zinc, nickel, and copper in the North Pacific. *Earth a Planet. Sci. Let.* **47,** 176-198

Bruland, K. W., Rue, E. L., Donat, J. R., Skrabel, S. A. and Moffett, J. W. (2000). Intercomparison of voltammetric techniques to determine the chemical speciation of dissolved copper in a coastal seawater sample. *Anal. Chim. Acta,* **405,** 99-113

Bryan, G. W. (1971). Effects of heavy metals (other than mercury) on marine and estuarine organisms. *Proc. R. Soc. Lond. B.*, **177,** 389-410

Bryan, G. W. and Gibbs, P. E. (1983). Heavy metals in the Fal Estuary, Cornwall: A study of long-term contamination by mining waste and its effects on estuarine organisms. *Occ. Publ. Mar. Biol. Ass.*, **2**

Bryan, G. W. and Hummerstone, L. G. (1973). Brown seaweed as an indicator of heavy metals in estuaries in South-West England. *J. Mar. Biol. Ass.*, **53,** 705-720

Bryan, G. W. and Langston, W. J. (1992). Bioavailability, accumulation and effects of heavy metals in sediments with special reference to United Kingdom estuaries: a review. *Envir. Pollt.*, **76,** 89-131

Brzezinkski, M. A. (1995). The Si:C:N ratio of marine diatomes: interspecific variability and the effect of some environmental variables. *J. Phycology,* **21,** 347-357

Buckley, J. A. (1994). The susceptibility of superoxide dismutase in *Lemna minor* to systemic copper cencentrated from wastewater. *Wat. Res.*, **28,** 2469-2476

Bueno, P., Varela, J., Giménez-Gallego, K. and del Rio, L. A. (1995). Peroxisomal copper,zinc superoxide dismutase. *Plant Physiol.*, **108,** 1151-1160

Burgess, G. M., Godfrey, P. P., McKinney, J. S., Berridge, M. J., Irvine, R. F., and Putney, J. W. (1984). The second messenger linking receptor activation to internal Ca^{2+} release in liver. *Nature,* **309,** 63-66

Burridge, T. R., Karistianos, M. and Bidwell, J. (1998). The use of aquatic macrophyte ecotoxicological assays in monitoring coastal effluent discharges in Southern Australia. *Mar. Poll. Bull.*, **39,** 89-96

Bush, D. S. (1995). Calcium regulation in plant cells and its role in signalling. *Ann. Rev. Plant Physiol. Plant Mol. Biol.*, **46,** 95-122

Byrne, R. H., Kump, L. R. and Cantrell, K. J. (1988). The influence of temperature and pH on trace metal speciation in seawater. *Mar. Chem.*, **25,** 163-181

Byrne, R. H. and Miller, W. L. (1985). Copper(II) carbonate complexation in seawater. *Geochim. Cosmochim. Acta,* **49,** 1837-1844

Callow, J. A. (1985). Sexual recognition and reproduction in brown algae. *J. Cell Sci. Suppl.* **2,** 219-232

Camoni, L., Fullone, M. R., Marra, M. and Aducci, P. (1998). The plasma membrane H^+-ATPase from maize roots is phosphorylated in the C-terminal domain by a calcium dependent protein kinase. *Physiol. Plant.,* **104,** 549-555

Capaldi, R. A. (1990). Structure and function of cytochrome *c* oxidase. *Annu. Rev. Biochem.*, **59,** 569-596

Chung, I. K. and Brinkhuis, B. H. (1986). Copper effects in early stages of the kelp, *Laminaria saccharina. Mar. Poll. Bul.*, **17,** 213-218

Ciscato, M., Valcke, R., Van Loven, K., Clijsters, H. and Navari-Izzo, F. (1997). Effects of *in vivo* copper treatment on the photosynthetic apparatus of two *Triticum durum* cultivars with different stress sensitivity. *Physiol. Plant.*, **100,** 901-908

Coale, K. H. and Bruland, K. W. (1988). Copper complexation in the Northeast Pacific. *Limnol. Oceanogr.*, **33,** 1084-1101

Coale, K. H. and Bruland, K. W. (1990). Spatial and temporal variability in copper complexation in the North Pacific. *Deep-Sea Res.*, **37,** 317-336

Coelho, S., Rijstenbil, J. W., Sousa-Pinto, I. and Brown, M. T. (2001). Cellular responses to elevated light levels in *Fucus spiralis* embryos during the first days after fertilisation. *Plant Cell Envir.*, **24,** 801-810

Colman, P. M., Freeman, H. C., Guss, J. M., Murata, M., Norris, V. A., Ramshaw, J. A. M. and Venkatappa, M. P. (1978). X-ray crystal structure analysis of plastocyanin at 2.7 Å resolution. *Nature*, **272,** 319-324

Combettes, L., Hannaert-Merah, Z., Coquil, J.-F., Rousseau, C., Claret, M., Swillens, S. and Champeil, P. (1994). Rapid filtration studies of the effect of cytosolic Ca^{2+} on inositol 1,4,5-trisphosphate-induced $^{45}Ca^{2+}$ release from cerebellar microsomes. *J. Biol. Chem.*, **269,** 17561-17571

Compos, M. L. A. M. and Van den Berg, C. M. G. (1994). Determination of copper complexation in seawater by chatodic stripping voltammetry and ligand complexation with salicylaldoxime. *Anal. Chim. Acta*, **248,** 481-496

Cooke, R. (1987). The mechanism of muscle contraction. *Crit. Rev. Biochem.* **21,** 53-118

Correa, J. A., González, P., Sánchez, P., Muñoz, J. and Orellana, M. C. (1996). Copper-algae interactions: inheritance or adaptation? *Environ. Monit. Assess.*, **40,** 41-45

Corellou, F., Bisgrove, S. R., Kropf, D. L., Meijer, L., Kloareg, B. and Bouget, F.-Y. (2000) A S/M DNA replication checkpoint prevents nuclear and cytoplasmic events of cell division including centrosomal axis alignment and inhibits activation of cyclin-dependent kinase-like proteins in fucoid zygotes. *Development*, **127,** 1651-1660

Cosgrove, D. J. (1996). Plant cell enlargement and the action of expansins. *Bio Essay*, **18,** 533-540

Croot, P. L., Moffett, J. W. and Brand, L. E. (2000). Production of extracellular Cu complexing ligands by eucaryotic phytoplankton in response to Cu stress. *Limnol. Oceanogr.* **45,** 619-627

Culotta, V. C., Klomp, L. W. J., Strain, J., Casareno, R. L. B., Krems, B. and Gitlin, J. D. (1997). The copper chaperone for superoxide dismutase. *J. Biol. Chem.*, **272,** 23469-23472

Dahmani-Muller, H., Van Orrt, F., Gélie, B. and Balabane, M. (2000). Strategies of heavy metal uptake by three plant species growing near a metal smelter. *Env. Pol.*, **109,** 231-238

Dancis, A., Yuan, D. S., Haile, D., Askwith, C., Eide, D., Moehle, C., Kaplan, J. and Klausner, R. D. (1994). Molecular characterization of copper transport protein in *S. cerevisiae*: An unexpected role for copper ion transport. *Cell*, **76,** 393-402

De Vos, C. H. R., Vonk, M. J., Vooijs, R., and Schat, H. (1992). Glutathione depletion due to copper-induced phytochelatin synthesis causes oxidative stress in *Silene cucubalus*. *Plant Physiol.*, **98,** 853-858

Demidchik, V, Sokolik, A. and Yurin, V. (1997). The effect of Cu^{2+} on ion transport systems of the plant cell plasmalemma. *Plant Physiol.*, **114,** 1313-1325

Demidchik, V., Sokolik, A. and Yurin, V. (2001). Characteristics of non-specific permeability and H^+-ATPase inhibition induced in the plasma membrane of *Nitella flexilis* by excessive Cu^{2+}. *Planta*, **212,** 583-590

Demmig-Adams, B. (1998). Survey of thermal energy dissipation and pigment composition in sun and shade leaves. *Plant Cell Physiol.*, **39,** 474-482

Demmig-Adams, B. and Adams, W. W. (2000). Harvesting sunlight safely. *Nature*, **403,** 371-374

Denny and Shibata, (1989). Consequence of surf-zone turbulence for settlement and external fertilisation. *American naturalist*, **134,** 859-889

Depledge, M. H., Weeks, J. M. and Bjerregaard, P. (1994). Heavy metals. In: Calow, P. (Ed.) *Handbook of Ecotoxicology*. Blackwell Science, U. K., **11,** 543-569

Dines, H. G. (1969). *The methalliferous mining region of South-West England.* H.M.S.O., London, **1,** 508pp.

Donat, J. R., Lao, K. A., and Bruland, K. W. (1994). Speciation of dissolved copper and nickel in South San Francisco Bay: A multi-method approach. *Anal. Chim. Acta*, **284,** 547-571

Doust, J. L., Schmidt, M. and Doust, L. L. (1994). Biological assessment of aquatic pollution: A review, with emphasis on plants as biomonitors. *Biol. Rev.*, **69,** 147-186

Dring, M. J., Makarov, V., Schoschina. E., Lorenz, M. and Lüning, K. (1996). Influence of ultraviolet radiation on chlorophyll fluorescence and growth in different life-history stages of three species of Laminaria (Phaeophyta). *Mar. Biol.*, **126,** 183-191

Droppa, M., Terry, N. and Horvath, G. (1984). Effects of Cu deficiency on photosynthetic electron transport. *Proc. Natl. Acad. Sci. USA*, **81,** 2369-2373

Dyrssen, D. (1988). Sulfide complexation in surface seawater. *Mar. Chem.*, **24,** 143-153

Elliott, S., Lu, E. and Rowland, F. S. (1987). Carbonyl sulfide hydrolysid as a source of hydrogen sulfide in open ocean seawater. *Geophys. Res. Lett.*, **14,** 131-134

Elstner, E. F. (1982). Oxygen activation and oxygen toxicity. *Ann. Rev. Plant Physiol.*, **33,** 73-96

Falkowski, P. G. and Raven, J. A. (1997). *Aquatic photosynthesis.* Blackwell Science, Ltd., Oxon, UK. 375 pp.

Fernández, J. A., Ray, A. and Carballeira, R. A. (2000). An extended study of heavy metal deposition in Galicia (NW Spain) based on moss analysis. *Sci. Total Env.*, **254,** 31-44

Finch, E. A., Turner, T. J. and Goldin, S. M. (1991). Calcium as a coagonist of inositol 1,4,5-trisphosphate-induced calcium release. *Science*, **252,** 443-446

Forsberg, Å., Söderlund, S., Frank, A., Petersson, L. R. and Pedersén, M. (1988) Studies on metal content in the brown seaweed *Fucus vesiculosus*, from the Archipelago of Stockholm. *Envir. Pollut.*, **49,** 245-263

Foster, P. (1976). Concentrations and concentration factors of heavy metal in brown algae. *Environ. Pollut.*, **10,** 45-53

Frankel, S. and Mooseker, M. S. (1996). The actin-related proteins. *Cur. Opin. Cell Biol.*, **8,** 30-37

Franklin, L. and Foster, R. (1997). The changing irradiance environment: Consequence for marine macrophyte physiology, productivity and ecology. *Eur. J. Physiol.*, **32,** 207-232

Frew, R. D. and Hunter, K. A. (1992). Influence of Southern Ocean waters on the cadmium-phosphate properties of the global ocean. *Nature*, **360,** 144-146

Fridovich, I. (1989). Superoxide dismutase. *J. Biol. Chem.*, 264, 7761-7764

Fry, S. C. (1994). Unzipped by expansins. *Curr. Biol.*, **4,** 815-817

Fu, Y., Wu, G. and Yang, Z. (2001). Rop GTPase-dependent dynamics of tip-localized F-actin controls tip growth in pollen tubes. *J. Cell Biol.*, **152,** 1019-1032

Fuge, R. and James, K. H. (1974). Trace metal concentrations in *Fucus* from the Bristol Channel. *Mar. Pollut. Bull.* **5,** 9-12

Furukawa, R., and Fechheimer, M. (1997). The structure, function and assembly of actin filament bundles. *Int. Rev. Cytol.*, **175,** 29-90

Galione, A., Lee, H. C. and Busa, W. B. (1991). Ca^{2+} induced Ca^{2+} release in sea urchin egg homogenates: Modulation by cyclic ADP-Ribose. *Science*, **253,** 1143-1146

Garansson, A. (1998). Steady-state nutrition and growth responses of *Betuala pendula* of different relative supply rates of copper. *Plant Cell Environ.*, **21,** 937-944

Garrill, A., Lew, R. R. and Heath, I. B. (1992). Stretch- activated Ca^{2+} and Ca^{2+}-activated K^+ channels in the hyphal tip plasma membrane of the oomycete *Saprolegnia ferax*. *J. Cell Sci.*, **101,** 721-730

Gekeler, W., Grill, E., Winnacker, E. -L. and Zenk, M. H. (1988). Algae sequester heavy metals via synthesis of phytochelatin complexes. *Arch. Microbiol.*, **150,** 197-202

Genty, B., Briantais, J. -M. and Baker, N. R. (1989). The relationship between quantum yield of photosynthetic electron transport and quenching of chlorophyll fluorescence. *Biochim. Biophys. Acta*, **990,** 87-92

Georgatsau, E., Mavrogiannis, L. A., Fragiadakis, G. S. and Alexandraki, D. (1997). The yeast Fre1p/Fre1p cupric reductases facilitate copper uptake and are regulated by copper-modulated Mac1p activator. *J. Biol. Chem.*, **272,** 13786-13792

Gibb, J. O. T., Allen, J. R. and Hawkins, S. J. (1996). The application of biomonitors for the assessment of mine derived pollution on the west coast of the Isle of Man. *Mar. Pollut. Bull.*, **32,** 513-519

Gibbon, B. C. and Kropf, D. L. (1993). Intracellular pH and its regulation in *Pelvetia* zygotes. *Dev. Biol.*, **156,** 259-268

Gilroy, S., Bethke, P. C. and Jones, R. L. (1993). Calcium homeostasis in plants. *J. Cell Sci.* **106,** 453-462

Gilroy, S., Read, N. D. and Trewavas, A. J. (1990). Elevation of cytoplasmic calcium by caged calcium or caged inositol trisphosphate initiates stomatal closure. *Nature*, **346,** 769-771

Gledhill, M., Nimmo, M., Hill, S. J. and Brown, M. T. (1997). The toxicity of copper(II) species to marine algae, with particular reference to macroalgae. *J. Phycol.*, **33,** 2-11

Gledhill, M., Nimmo, M., Hill, S. J. and Brown, M. T. (1999). The release of copper-complexing ligands by the brown alga *Fucus vesiculosus* (Phaeophyceae) in response to increasing total copper levels. *J. Phycol.*, **35,** 501-509

Glerum, D. M., Shtanko, A. and Tzagoloff, A. (1996). Characterization of *Cox17*, a yeast gene involved in copper metabolism and assembly of cytochrome oxidase. *J. Biol. Chem.*, **271,** 14504-14509

Goddard, H., Manison, N. F. H., Tomos, D. and Brownlee, C. (2000). Elemental propagation calcium signals in response-specific patterns determined by environmental stimulus strength. *Proc. Natl. Acad. Sci. USA*, **97,** 1932-1937

Goldberg, R. B., de Paiva, G. and Yadegari, R. (1994). Plant embryogenesis: zygote to seed. *Science*, **266,** 605-614

Goode, B. L., Drubin, D. G. and Barnes, G. (2000). Functional cooperation between the microtubule and actin cytoskeletons. *Cur. Opin. Cell Biol.*, **12,** 63-71

Goodner, B. and Quatrano, R. S. (1993). *Fucus* embryogenesis: a model to study the establishment of polarity. *Plant Cell*, **5,** 1471-1481

Graham, M. (1996). Effect of high irradiance on recruitment of the giant kelp *Macrocystis* (Phaeophyta) in shallow water. *J. Phycol.*, **32,** 903-906

Green, E. J. and Carritt, D. E. (1967). New tables for oxygen saturation of seawater. *J. Mar. Res.*, **25,** 140-147

Grill, E., Winnacker, E. -L. and Zenk, M. H. (1985). Phytochelatins: The principal heavy-metal complexing peptides of higher plants. *Science*, **230,** 674-676

Gupta, A. B. and Arora, A. (1978). Morphology and physiology of *Lyngbya nigra* with reference to copper toxicity. *Physiol. Plant.*, **44,** 215-220

Hable, W. E. and Kropf, D. L. (1998). Roles of secretion and the cytoskeleton in cell adhesion and polarity establishment in *Pelvetia compressa* zygotes. *Develop. Biol.*, **198,** 45-56

Hable, W. E. and Kropf, D. L. (2000). Sperm entry induces polarity in fucoid zygotes. *Development*, **127**, 493-501

Hamer, D. H. (1986). Metallothionein. *Ann. Rev. Biochem.*, **55**, 913-951

Han, T. and Kain, J. (1996). Effects of photon irradiance and photoperiod on young sporophytes of four species of Laminariales. *Eur. J. Phycol.*, **31**, 233-240

Hanelt, D., Wiencke, C., and Karsten, U. (1997). Photoinhibition and recovery after high light stress in different developmental and life-history stages of *Laminaria saccharina* (Phaeophyta). *J. Phycol.*, **33**, 387-395

Harker, M., Berkaloff, C., Lemoine, Y., Britton, G., Young, A. J., Duval, J. –C., Rmiki, N. –E. and Rousseau, B. (1999). Effect of high light and dessication on the operation of the xanthophyll cycle in two marine brown algae. *Eur. J. Phycol.*, **34**, 35-42

Harper, J. F, Sussmann, M. R., Schaller, G. E., Putnam-Evans, C., Charbonneau, H. and Harmon, A. C. (1991). A calcium-dependent protein kinase with regulatory domain similar to calmodulin. *Science*, **252**, 951-954

Hassett, R. and Kosman, D. J. (1995). Evidence for Cu(II) reduction as a component of copper uptake by *Saccharomyces cerevisiae*. *J. Biol. Chem.*, **270**, 128-134

Haug, A., Melsom, S. and Omang, S. (1974). Estimation of heavy metal pollution in two Norwegian fjord areas by analysis of the brown algae *Ascophyllum nodosum*. *Environ. Pollut.*, **7**, 179-92

Haug, A., Shi, B. and Vitorello, V. (1994). Aluminium interaction with phosphoinositide-associated singal-transduction. *Archives of Toxicology*, **68**, 1-7

Hecky, R. E. and Kilham, P. (1988). Nutrient limitation of phytoplankton in freshwater and marine environments: a review of recent evidence on the effect of enrichment. *Limnol. Oceanogr.*, **33**, 796-822

Heizmann, C. W. and Hunziker, W. (1991). Intracellular calcium binding proteins: more sites than insights. *TIBS*, **16**, 98-103

Henry, C. A., Jordan, J. R. and Kropf, D. L. (1996). Localised membrane-wall adhesions in *Pelvetia* zygotes. *Protoplasma*, **190**, 39-52

Herbik, A., Giritch, A., Horstmann, C., Becker, R., Balzer, H.- J., Bäumlein, H. and Stephan, U. W. (1996). Iron and copper nutrition-dependent changes in protein expression in tomato wild type and the nicotianamine-free mutant *chloronerva*. *Plant Physiol.*, **111**, 533-540

Hirayama, T., Kieber, J. J., Hirayama, N., Kogan, M., Guzman, P., Nourizadeh, S., Alonso, J. M., Dailey, W. P., Dancis, A. and Ecker, J. R. (1999). Responsive-to-antagonist1, a Menkes/Wilson disease-related copper transporter, is required for ethylene signalling in *Arabidopsis*. *Cell*, **97**, 383-393

Hirose, K., Kadowaki, S. and Iino, M. (1998). Allosteric regulation by cytoplasmic Ca^{2+} and IP_3 of the gating of IP_3 receptors in permeabilized guinea-pig vascular smooth muscle cells. *J. Physiol.*, **506**, 407-414

Hopkin, R. and Kain, J. M. (1978). The effects of some pollutants on the survival, growth and respiration of *Laminaria hyperborea*. *Estuar. Coast. Mar. Sci.*, **7**, 531-553

Horton, P., Ruban, A. V., and Walters, R. G. (1996). Regulation of light harvesting in green plants. *Annu. Rev. Plant Physiol. Plant Mol. Biol.*, **47**, 655-684

Hrabak, E. M., Dickmann, L. J., Satterlee, J. S. and Susman, M. R. (1996). Characterization of eight new members of the calmodulin-likedomain protein kinase gene family from *Arabidopsis thaliana*. *Plant Mol. Biol.*, **31**, 405-412

Humphries, M. J. (2000). Integrin structure. *Biochem. Soc. Trans.*, **28**, 311-340

Hunt, R. (1982). *Plant Growth Curves*. Edward Arnold Publisher Ltd, London, 248 pp.

Hunter, K. A., Kim, J. P. and Croot, P. L. (1997). Biological roles of trace metals in natural waters (1997). *Env. Monit. Ass.*, **44**, 103-147

Hurd, A. M. (1920). Effects of unilateral monochromatic white light and group orientation on the polarity of germinating *Fucus* spores. *Bot. Gaz.*, **70**, 25-50

Ilvessalo, H. and Tuomi, J. (1989). Nutrient availability and accumulation of phenolic compounds in the brown alga *Fucus vesiculosus*. *Mar. Biol.*, **101**, 115-119

Jackson, G. A. and Morgan, J. J. (1978). Trace metal-chelator interactions and phytoplankton growth in seawater media: Theoretical analysis and comparison with reported observations. *Limnol. Oceanogr.*, **23**, 268-282

Jaffe, L. F. (1958). Tropistic responces of zygotes of the Fucaceae to polarized light. *Exp. Cell Res.* **15**, 282-299

Jaffe, L. F. (1966). Electrical currents through the developing *Fucus* egg. *Proc. Natl. Acad. Sci. USA*, **56**, 1102-1109

Jayasekera, R. and Rossbach, M. (1996). Use of seaweeds for monitoring trace elements in costal waters. *Environ. Geochem. Health*, **18**, 63-68

Jegerschöld, C., Arellano, J. B., Schröder, W. P., van Kan, P. J. M., Barón, M. and Styring, S. (1995). Copper(II) inhibition and electron transfer through photosystem II studied by EPR spectroscopy. *Biochem.*, **34**, 12747-12754

Johannes, E., Brosnan, J. M. and Sanders, D. (1992). Calcium channels in the vacuolar membrane of plants: multiple pathways for intracellular Ca^{2+} mobilization. *Philos. Trans. R. Soc. Lond. B.*, **338**, 105-112

Jürgens, G., Mayer, U., Busch, M., Lukowitz, W. and Laux, T. (1995). Pattern formation in the *Arabidopsis* embryo: a genetic perspective. *Phil. Trans. R. Soc. Lond.* B., **350**, 19-25

Kaftan, E. J., Ehrlich, B. E. and Watras, J. (1997). Inositol 1,4,5-trisphosphate ($InsP_3$) and calcium interact to increase the dynamic range of $InsP_3$ receptor-dependent calcium signalling. *J. Gen. Physiol.*, **110**, 529-538

Kaila, K. and Voipoi, J. (1985). A simple method for dry bevelling of micropipettes used in the construction of ion-sensitive microelectrodes. *J. Physiol. Lond.* **369**, 8p

Karyophyllis, D., Katsaros, C. and Galatis, B. (2000). F-actin involvement in apical cell morphogenesis of *Sphacelaria rigidula* (Phaeophyceae): mutual alignment between cortical actin filaments and cellulose microfibrils. *Eur. J. Phycol.*, **35**, 195-203

Kasai, H. and Neher, E. (1992). Dihydropyridine-sensitive and omega-conotoxin-sensitive calcium channels in a mammalian neuroblastoma-glioma cell-line. *J. Physiol. Lond.*, **448**, 161-188

Kessler, D. S. and Melton, D. A. (1994). Vertebrete embryonic induction: mesodermal and neural patterning. *Science*, **266**, 596-604

Kimble, J. (1994). An ancient molecular mechanism for establishing embryonic polarity? *Science*, **266**, 577-578

Kiss, T. and Osipenko, O. (1994). Metal ion-induced permeability changes in cell membranes: a minireview. *Cellul. Mol. Neurobiol.*, **14**, 781-789

Kiss, T., Gyori, J., Osipenko, O. and Maginyan, S. B. (1991). Copper-induced nonselective permeability changes in intracellular perfused snail neurons. *J. Appl. Toxicol.*, **11**, 349-354

Klinkhammer, G. P. (1980). Early diagenesis in sediments from the eastern equatorial Pacific, II. Pore water metal results. *Earth Planet. Sci. Let.*, **49**, 81-101

Klusener, B., Boheim, G. and Weiler, E. W. (1997). Modulation of the ER Ca^{2+} channel BCC1 from tendrils of *Bryonia dioica* by divalent cations, protons and H_2O_2. *FEBS Lett.*, **407**, 230-234

Knapp, E. (1931). Entwicklungsphysiologische untersuchungen an Fucaceeneiren. I. Zur Kenntnis der eir von *Cystosira barbata*. *Planta*, **14**, 731-751

Knight, H., Trewavas, A. J. and Knight, M. R. (1996). Cold calcium signalling in *Arabidopsis* involves two cellular pools and a change in calcium signature after acclimation. *Plant Cell*, **8**, 489-503

Koch, G. L. E. (1990). The endoplasmatic reticulum and calcium storage. *BioEssay*, **12**, 527-531

Kogut, M. B. and Voelker, B. M. (2001). Strong copper-binding behaviour of terrestrial humic substances in seawater. *Environ. Sci. Technol.*, **35**, 1149-1156

Kranz, E. and Lörz, H. (1993). In vitro fertilisation with isolated, single gametes results in zygotic embryogenesis and fertile maize plants. *Plant Cell*, **5**, 739-746

Kranz, E., von Wiegen, P. and Lörz, H. (1995). Early cytological events after induction of cell division in egg cells and zygote development following *in vitro* fertilisation in angiosperm gametes. *Plant J.*, **8**, 9-23

Krause, G. H. and Weis, E. (1991). Chlorophyll fluorescence and photosynthesis: The basics. *Ann. Rev. Plant Physiol. Mol. Biol.*, **42**, 313-349

Krieger, A. and Weis, E. (1999). The role of calcium in the pH-dependent control of photosystem-II. *Photosynt. Res.*, **37**, 117-130

Kristiansen, A., Moestrup, Ø. and Nielsen, H. (1981). *Introduktion til alger og bakterier*. NUCLEUS. Møller Nielsen Grafik, Herlev, Denmark, 190pp

Kröniger, W., Rennenberg, H. and Polle, A. (1992). Purification of two superoxide dismutase iso-zymes and their subcellular localization in needles and roots of Norway spruce (*Picea abies* L.) trees. *Plant Physiol.*, **100**, 334-340

Kropf, D. L. (1992). Establishment and expression of cellular polarity in fucoid zygotes. *Microbiol. Rev.*, **46**, 316-339

Kropf, D. L. (1994). Cytoskeletal control of cell polarity in a plant zygote. *Dev. Biol.*, **165**, 361-371

Kropf, D. L., Berge, S. K. and Quatrano, R. S. (1989). Actin localisation during *Fucus* embryogenesis. *Plant Cell*, **1**, 191-200

Kropf, D. L., Bisgrove, S. R. and Hable, W. E. (1998). Cytoskeletal control of polar growth in plant cells. *Cur. Opin. Cell Biol.*, **10**, 117-122

Kropf, D. L., Coffmann, H. R., Kloareg, B., Glen, P. and Allen, V. W. (1993). Cell wall and rhizoid polarity in *Pelvetia* embryos. *Dev. Biol.*, **160**, 303-314

Kropf, D. L., Jordan, J. R., Allen, V. W. and Gibbon, B. C. (1992). Cellular polarity in pelvetia zygotes: Studies of intracellular pH and division alignment. *Curr. Top. Plant Physiol.*, **11**, 143-152

Kropf, D. L., Kloareg, B. and Quatrano, R. S. (1988). Cell wall is required for fixation of the embryonic axis in *Fucus* zygotes. *Science*, **239**, 187-190

Kropf, D. L., Maddock, A. and Gard, D. L. (1990). Microtubule distribution and function in early *Pelvetia* development. *J. Cell Sci.*, **97**, 545-552

Kropf, D. L. and Quatrano, R. S. (1987). Localisation of membrane associated calcium during development of fucoid algae using chlorotetracyclin. *Planta*, **171**, 158-170

Küpper, H., Küpper, F., and Spiller, M. (1996). Environmental relevance of heavy metal-substituted chlorophylls using the example of water plants. *J. Exp. Bot.*, **47**, 259-266

Langston, W. J. and Spence, S. K. (1995). Biological factors involved in metal concentrations observed in aquatic organisms. In: Tessier, A. and Turner, D. E. (Eds.) *Metal speciation and bioavailability in aquatic systems*. John Wiley & Sons Ltd., New York, pp. 407-78

Larsen, T. S., Kristensen, J. A., Asmund, G. and Bjerregaard, P. (2001). Lead and zinc in sediments and biota from Maarmorilik, West Greenland: an assessment of the environmental impact of mining wastes on an Arctic fjord system. *Envir. Poll.*, **114,** 275-283

Lasker, H. R., Brazeau, J., Calderon, D.A., Coffroth, M. A., Coma, R. and Kim, K. (1996). In situ rates of fertilization among broadcast spawning gorgonian corals. *Bio. Bul.*, **190,** 45-55

Lee, J. Y., Yoo, B. C., and Harmon, A. C. (1998). Kinetic and calcium-binding properties of three calcium-dependent protein kinase isoenzymes from soyabean. *Biochemistry*, **37,** 6801-6809

Lehotsky, J., Kaplan, P., Racay, P., Matejovicova, M., Drgova, A. and Mezesova, V. (1999). Membrane ion transport systems during oxidative stress in rodent brain: Protective effects of stobadine and other antioxidants. *Life Sci.*, **65,** 1951-1958

Levitan, D. R., Sewell, M. A. and Chia, F.-S. (1992). How distribution and abundance influence fertilisation success in the sea urchin *Strongylocentrotus franciscanus. Ecology,* **73,** 248-254

Levring, T. (1947). Remarks on the surface layers and the formation of the fertilisation membrane in the *Fucus* egg. *Meddr. Göteborgs bot. trädq.*, **17,** 97-103

Levring, T. (1952). Remarks on the submicroscopical structure of eggs and spermatozoids of *Fucus* and related genera. *Physiol. Plant.*, **5,** 528-540

Li, X. –P., Björkman, O., Shih, C., Grossman, A. R., Rosenquist, M., Jansson, S. and Niyogi, K. K. (2000). A pigment-binding protein essential for regulation of photosynthetic light harvesting. *Nature*, **403,** 391-395

Li, J., Lock, R. A. C., Klaren, P. H. M., Swarts, H. G. P., Schuurmans Stekhoven, F. M. A. H., Wendelar Bonga, S. E. and Flik, G. (1996). Kinetics of Cu^{2+} inhibition of Na^+/K^+-ATPase. *Toxicol. Let.*, **87,** 31-38

Lignell, Å., Roomans, G. M. and Pedersén, M. (1982). Localization of absorbed cadmium in *Fucus vesiculosus* L. by X-ray microanalysis. *Z. Pflanzenphysiol.*, **105,** 103-109

Lord, E. M. and Sanders, L. C. (1992). Role of the extracellular matrix in plant development and pollination: a special case of cell movement in plants. *Dev. Biol.*, **153,** 16-28

Lores, E. M. and Pennock, J. R. (1998). The effect of salinity on binding of Cd, Cr, Cu and zinc to dissolved organic matter. *Chemosphere*, **37,** 861-874

Love, J., Brownlee, C. and Trewavas, A. J. (1997). Ca^{2+} and calmodulin dynamics during photopolarization in *Fucus serratus* zygotes. *Plant Physiol.*, **115,** 249-261

Luna, C. M., González, C. A. and Trippi, V. S. (1994). Oxidative damage caused by an excess of copper in oat leaves. *Plant Cell Physiol.*, **35,** 11-15

Luoma, S. N., Bryan, G. W. and Langston, W. J. (1982). Scavenging of heavy metals from particulates by brown seaweed. *Mar. Poll. Bull.*, **13,** 394-396

Lüning, K. and Neushul, M. (1978). Light and temperature demands for growth and reproduction in *Laminaria* gametophytes in Southern and Central California. *Mar. Biol.*, **45,** 297-309

MacDowall, F. D. H. (1949). The effects of some inhibitors of photosynthesis upon the photochemical reduction of a dye by isolated chloroplasts. *Plant Physiol.*, **24,** 462-480

Madsen, T. V. and Sand-Jensen, K. (1991). Photosynthetic carbon assimilation in aquatic macrophytes. *Aquat. Bot.*, **41,** 5-40

Malea, P., Haritonidis, S. and Stratis, I. (1994). Bioaccumulation of metals by Rhodophyta species at Antikyra Gulf (Greece) near an aluminium factory. *Bot. Mar.*, **37,** 505-513

Malhó, R., Moutinho, A., van der Luit, A. and Trewavas, A. J. (1998). Spatial characteristics of calcium signalling: The calcium wave as a basic unit in plant cell calcium signalling. *Phil. Trans. R. Soc. Lond.* B, **353,** 1463-1473

Malhó, R. and Trewavas, A. J. (1996). Localized apical increases of cytosolic free calcium control pollen tube orientation. *Plant Cell*, **8**, 1935-1949

Marrs, R. H. and Bannister, P. (1978). The adaptation of *Calluna vulgaris* (L.) Hull to contrasting soil types. *New Phytol.*, **81**, 753-761

Marschner, H. (1995). *Mineral nutrition of higher plants.* Academic Press, New York, 889 pp.

Marsden, A. D. and DeWreede, R. E. (2000). Marine macroalgae community structure, metal content and reproductive function near an acid mine drainage outflow. *Environ. Poll.*, **110**, 431-440

Martin, M. H., Nickless, G. and Stenner, R. D. (1997). Concentrations of cadmium, copper, lead, nickel and zinc in the alga *Fucus serratus* in the Severn Estuary from 1971 to 1995. *Chemosphere*, **34**, 325-334

Masters, A. K., Shirras, A. D. and Hetherington, A. M. (1992). Maternal mRNA and early development in *Fucus serratus*. *Plant J.*, **2**, 619-622

Mayer, U., Ruiz, R. A. T., Berleth, T., Miséra, S. and Jürgens, G. (1991). Mutations affecting body organization in the *Arabidopsis* embryo. *Nature*, **353**, 402-407

Mayer, U., Buttner, G. and Jürgens, G. (1993). Apical-basal pattern-formation in the *Arabidopsis* embryo – studies on the role of the GNOM gene. *Development*, **117**, 149-162

Maxwell, K. and Johnson, G. N. (2000). Chlorophyll fluorescence – a practical guide. *J. Exp. Bot.*, **51**, 659-668

Melhuus, A., Seip, K. L. and Mykelstad, S. (1978). A preliminary study of the use of benthic algae as biological indicators of heavy metal pollution in Sorfjorden, Norway. *Environ. Pollut.*, **15**, 101-107

McKnight, D. M. and Morel, F. M. M. (1979). Release of weak and strong copper-complexing agents by algae. *Limnol. Oceanogr.*, **24**, 823-837

McLean, M. W. and Williamson, F. B. (1977). Cadmium accumulation by the marine red algal *Porphyra umbilicalis*. *Physiol. Plant.*, **41**, 268-272

Meador, J. P. (1991). The interaction of pH, dissolved organic carbon and total copper in the determination of ionic copper and toxicity. *Aquatic Toxicol.*, **19**, 13-32

Miller, L. A. and Bruland, K. W. (1994). Determination of copper speciation in marine waters by competitive ligand equilibration/liquid-liquid extraction: an evaluation of the technique. *Anal. Chim. Acta*, **284**, 573-586

Miller, D. D., Ruijter, N. C. A., Bisseling, T. and Emons, A. M. C. (1999). The role of actin in roothair morphogenesis: studies with lipochito-oligosaccharide as a growth stimulator and cytochalasin as an actin perturbing drug. *Plant J.*, **17**, 141-154

Millero, F. J. (1991). The oxidation of H_2S in Black Sea waters. *Deep-Sea Res.*, **38**, 1139-1150

Moffett, J. W. and Brand, L. E. (1996). Production of strong, extracellular Cu chelators by marine cyanobacteria in response to Cu stress. *Limnol. Oceanogr.*, **41**, 388-395

Moffett, J. W. and Zika, R. G. (1983). Oxidation kinetics of Cu(I) in seawater: Implications for its existence in the marine environment. *Mar. Chem.*, **13**, 239-251

Moffett, J. W. and Zika, R. G. (1987). Solvent extraction of copper acetylacetonate in studies of copper (II) speciation in seawater. *Mar. Chem.*, **21**, 301-313

Moffett, J. W., Zika, R. G. and Brand, L. E. (1990). Distribution and potential sources and sinks of copper chelators in the Sargasso Sea. *Deep-Sea Res.*, **37**, 27-36

Molina-Heredia, F. P., Hervás, M., Navarro, J. A. and De la Rosa, M. A. (2001). A single arginyl residue in plastocyanin and in cytochrome c_6 from the cyanobacterium *Anabena* sp. PCC 7119 is required for efficient reduction in photosystem I. *J. Biol. Chem.*, **276**, 601-605

Monni, S., Salemaa, M., White, C., Tuittila, E. and Huopalainen, M. (2000). Copper resistance of *Calluna vulgaris* originating from the pollution gradient of a Cu-Ni smelter, in south west Finland. *Environ. Pollut.*, **109,** 211-219

Moore, J. M., Case, D. A., Chazin, W. J., Gippert, G. P., Havel, T. F., Powls, R. and Wright, P. E. (1988). Three-dimentional solution structure of plastocyanin from the green alga *Scenedesmus obliquus*. *Science*, **240,** 314-317

Morel, F. M. M., Rueter, J. G., Anderson, D. M. and Guillard, R. R. L. (1979). Aquil: a chemically defined phytoplankton culture medium for trace metal studies. *J. Phycol.*, **15,** 135-141

Morelli, E. and Scarano, G. (2001). Synthesis and stability of phytochelatin induced by cadmium and lead in the diatom *Phaeodactylum tricornutum*. *Mar. Environ. Res.*, **52,** 383-395

Morris, C. A., Nicolaus, B., Sampson, N., harwood, J. L. and Kille, P. (1999). Identification and charicterization of a recombinant metallothionein protein from a marine algae, *Fucus vesiculosus*. *Biochem. J.*, **338,** 553-560

Mostafa, H. M. and Collins, K. J. (1995). Heavy metal concentrations in sea urchin tissues from Egypt, Ireland and United Kingdom. *Chem. Ecol.*, **10,** 181-190

Muir, S. R. and Sanders, D. (1997). Inositol 1,4,5-trisphosphate-sensitive Ca^{2+} release across nonvacuolar membranes in cauliflower. *Plant Physiol.*, **114,** 1511-1521

Müller, D. G. and Gassmann, G. (1985). Sexual reproduction and the role of sperm attractants in monoecious species of the brown algae order Fucales (*Fucus, Hesperophycus, Pelvetia,* and *Pelvetiopsis*). *J. Plant Physiol.*, **118,** 401-408

Murphy, A. S., Eisinger, W. R., Shaff, J. E., Kochian, L. V. and Taiz, L. (1999). Early copper induced leakage of K^+ from *Arabidopsis* seedlings is mediated by ion channels and coupled to citrate efflux. *Plant Physiol.*, **121,** 1375-1382

Murphy, A. and Taiz, L. (1995). Comparison of metallothionein gene expression and nonprotein thiols in ten *Arabidopsis* ecotypes. Correlation with copper tolerance. *Plant Physiol.*, **109,** 945-954

Muse, J. O., Stripeikis, J. D., Fernández, F. M., d'Huicque, L., Tudino, M. B., Carducci, C. N., and Troccoli, O. E. (1999). Seaweeds in the assessment of heavy metal pollution in the Gulf San Jorge, Argentina. *Environ. Pollut.* **104,** 315-322

Navari-Izzo, F., Quartacci, M. F., Pinzino, C., Vecchia, F. D. and Sgherri, C. L. M. (1998). Thylakoid-bound and stromal antioxidative enzymes in wheat treated with excess copper. *Physiol. Plant.*, **104,** 630-638

Newman, J. E. (1998). *Physiological responses of* Gracilariopsis longissima *to copper exposure.* Ph.D. Thesis, Dept. Biol. Sci., University of Plymouth

Ng, B., Turner, A., Tyler, A. O., Falconer, R. A. and Millward, G. E. (1996) Modelling contaminant geochemistry in estuaries. *Water Res.*, **30,** 63-74

Niyogi, K. K., Grossman, A. R. and Björkman, O. (1998). *Arabidopsis* mutants define a central role for xanthophyll cycle in the regulation of photosynthetic energy conversion. *Plant Cell*, **10,** 1121-1134

Norton, T. (1978). The factors influencing the distribution of *Saccorhiza polyschides* in the region Lough Ine. *J. Mar. Biol. Ass.*, **58,** 527-536

Norton, T., Mathieson, A. and Neushul, M. (1982). A review of some aspects of form and function in seaweeds. *Bot. Mar.*, **25,** 501-510

Nriagu, J. O. and Pacyna, J. M. (1988). Quantitative assessment of worldwide contamination of air, water and soils by trace metals. *Nature*, **333,** 134-139

Nuccitelli, R. and Jaffe, L. F. (1976). Current pulses involving chloride and potassium efflux relieve excess pressure in *Pelvetia* embryos. *Planta,* **131,** 315-320

Okazaki, Y., Yoshimoto, Y., Hiramoto, Y. and Tazawa, M. (1987). Turgor regulation and cytoplasmic free Ca^{2+} in the alga *Lamprothamnium*. *Protoplasma*, **140,** 67-71

O'Leary, C. and Breen, J. (1997). Metal levels in seven species of muollusc and in seaweeds from the Shannon Estuary. *Proc. R. Irish Acad., B.*, **97,** 121-132

O'Leary, C. and Breen, J. (1998). Seasonal variation of heavy metals in *Mytilus edulis, Fucus vesiculosus*, and sediment from the Shannon Estuary. *Proc. R. Irish Acad. B.*, **98,** 153-169

Orozco, J. T., Wedaman, K. P., Signor, D., Brown, H., Rose, L. and Scholey, J. M. (1999). Movement of motor and cargo along cilia. *Nature*, **398,** 674

Orren, M. J. and Monteiro, P. M. S. (1985). Trace element geochemistry in the Southern Ocean. In: *Antarctic Cycles and Food Webs*. (Eds. Seigfield, W. R., Condy, P. R. and Laws, R. M.), Springer Verlag, Berlin, pp. 30-37

Ort, D. R. (2001). When there is too much light. *Plant Physiol.*, **125,** 29-32

Osipenko, O. N., Kiss, T. and Salanki, J. (1992). Effects of Cu^{2+}, Pb^{2+} and Zn^{2+} on voltage-activated current in *Helix pomatia* L neurons. *Environ. Monit. Assess.*, **22,** 57-72

Ouzounidou, G., Moustakas, M., and Strasser, R. J. (1997). Sites of action of copper in the photosynthetic apparatus of maize leaves: Kinetic analysis of chlorophyll fluorescence, oxygen evolution, absorption changes and thermal dissipation as monitored by photoacoustic signals. *Aust. J. Plant Physiol.*, **24,** 81-90

Pandey, A. K., Pandey, S. D. and Misra, V. (2000). Stability constants of metal-humic acid complexes and its role in environmental detoxification. *Ecotox. Environ. Safety*, **47,** 195-200

Panfoli, I., Burlando, B. and Viarengo, A. (2000). Effects of heavy metals on phospholipase C in gill and digestive gland of the marine mussel *Mytilus galloprovincialis* Lam. *Comp. Biochem. Physiol.* **127B,** 391-397

Pätsikkä, E., Aro, E. -M. and Tyystjärvi, E. (1998). Increase in the quantum yield of photoinhibition contributes to copper toxicity *in vivo*. *Plant Physiol.*, **117,** 619-627

Pawlik-Skowronska, B. (2001). Phytochelatin production in freshwater algae *Stigeoclonium* in response to heavy metals contained in mining water; effects of some environmental factors. *Aquat. Toxicol.*, **52,** 241-249

Pearson, G. A. and Brawley, S. H. (1996). Reproductive ecology of *Fucus distichus* (Phaeophyceae): an intertidal alga with successful external fertilisation. *Mar. Ecol. Prog. Ser.* **143,** 211-223

Pearson, G. A., Serrão, E. A. and Brawley, S. H. (1998). Control of gamete release in Fucoid algae: Sensing hydrodynamic conditions via carbon acquisition. *Ecology*, **79,** 1725-1739

Pearson, G. A., Serrão, E. A. and Kautsky, L. (1995). Signaling mechanisms affecting synchronous gamete release in fucoid algae. *Mol. Biol. Cell*, **6,** 522

Peña, M. M. O., Puig, S. and Thiele, D. J. (2000). Characterization of the *Saccharomyces cerevisiae* high affinity copper transporter Ctr3. *J. Biol. Chem.*, **275,** 33244-33251

Perryman, S. A. M. (1996). *The effect of heavy metal contamination on estaurine bentic fauna at varying levels of biological organisation.* Ph.D. Thesis, Dept. Biol. Sci., University of Plymouth, UK.

Persson, H., Turk, M., Nyman, M. and Sandberg, A. S. (1998). Binding of Cu^{2+}, Zn^{2+} and Cd^{2+} to inositol tri-, tetra-, penta-, and hexaphosphates. *J. Agr. Food Chem.*, **46,** 3194-3200

Phillips, D. J. H. (1990). The use of macroalgae as monitors of metal levels in estuaries and costal waters. In: *Heavy metals in the marine environment.* (Eds. Furness, R. W. and Rainbow, P. S.), CRC Press, Florida, pp. 81-99

Pierson, E. S., Miller, D. D., Gallaham, D. A., van Aken, J., Hackett, G., and Hepler, P. K. (1996). Tip-localized calcium entry fluctuations during pollen tube growth. *Devel. Biol.*, **174,** 160-173

Plötz, J. (1991). Effects of salinity and toxic heavy metals on oxygen release by *Fucus vesiculosus* L. *Acta Ichthyologica et Piscatoria*, **21,** supl., 283-290

Poovaiah, B. W. and Reddy, A. S. N. (1987). Calcium messenger systems in plants. *Crit. Rev. Plant Sci.*, **6,** 47-103

Price, A. H., Taylor, A., Ripley, S. J., Griffiths, A., Trewavas, A. J. and Knight, M. R. (1994). Oxidative signals in tobacco increase cytosolic calcium. *Plant Cell*, **6,** 1301-1310

Price, N. M., Harrison, G. I., Hering, J. G., Hudson, R. J., Nirel, P. M. V., Palenik, B. and Morel, F. M. M. (1988/89). Preparation and chemistry of the artificial alga culture medium Aquil. *Biol. Oceanogr.*, **6,** 443-461

Pu, R. and Robinson, K. R. (1998). Cytoplasmic calcium gradients and calmodulin in the early development of the fucoid alga *Pelvetia compressa*. *J. Cell Sci.* **111,** 3197-3207

Pu, R., Wozniak, M. and Robinson, K. R. (2000). Cortical actin filaments form rapidly during photopolarisation and are required for the development of calcium gradients in *Pelvetia compressa* zygotes. *Dev. Biol.*, **222,** 440-449

Pufahl, R. A., Singer, C. P., Peariso, K. L., Lin, S.- J., Schmidt, P. J., Fahrni, C. J., Culotta, V. C., Penner-Hahn, J. E. and O'Halloran, T. V. (1997). Metal ion chaperone function of soluble Cu(I) receptor Atx1. *Science*, **278,** 853-856

Quatrano, R. S. (1968). Rhizoid formation in *Fucus* zygotes: Dependence on protein and ribonucleic acid synthesis. *Science*, **151,** 468-470

Quatrano, R. S. (1973). Separation of processes associated with differentiation of two-celled *Fucus* embryos. *Dev. Biol.*, **30,** 209-213

Quatrano, R. S. and Stevens, P. T. (1976). Cell wall assembly in *Fucus* zygotes. I. Characterisation of the polysaccharide components. *Plant Physiol.*, **58,** 224-231

Quatrano, R. S., Brian, L., Aldridge, J., and Schultz, T. (1991). Polar axis fixation in *Fucus* zygotes: Components of the cytoskeleton and extracellular matrix. *Development*, **1,** 11-16

Racay, P., Kaplan, P., Mezesova, V. and Lehotsky, J. (1997). Lipid peroxidation inhibits Ca^{2+}-ATPase and increases Ca^{2+} permeability of endoplasmatic reticulum membrane. *Biochem. Mol. Biol. Int.*, **41,** 647-655

Rae, T. D., Schmidt, P. J., Pufahl, R. A., Culotta, V. C. and O'Halloran, T. V. (1999). Undetectable intracellular free copper: The requirement of a copper chaperone for superoxide dismutase. *Science*, **284,** 805-808

Ragan, M. A., Ragan, C. M. and Jensen, A. (1980). Natural chelators in seawater: detoxification of Zn^{2+} by brown algal polyphenols. *J. Exp. Mar. Biol. Ecol.*, **44,** 261-267

Ragan, A. M. (1976). Physodes and the phenolic compounds of brown algae. Composition and significance of physodes *in vivo*. *Bot. Mar.*, **19,** 145-154

Rainbow, P. S. and Phillips, D. J. H. (1993). Cosmopolitan biomonitors of trace metals. *Marine Poll. Bull.*, **26,** 593-601

Rathore, K. S., Cork, R. J. and Robinson, K. R. (1991). A cytoplasmic gradient of Ca^{2+} is correlated with the growth of lily pollen tubes. *Dev. Biol.*, **148,** 612-619

Rauser, W. E. (1990). Phytochelatins. *Ann. Rev. Biochem.*, **59,** 61-86

Rauser, W. E. and Curvetto, N. R. (1980). Metallothionein occurs in roots of *Agrostis* tolerant to excess copper. *Nature*, **287,** 563-564

Reed, R. H. and Moffat, L. (1983). Copper toxicity and copper tolerance in *Enteromorpha compressa* (L.) Grev. *J. Exp. Mar. Biol. Ecol.*, **69,** 85-103

Redfield, A. C. (1958). The biological control of chemical factors in the environment. *American scientist,* **46,** 205-221

Richards, K. D., Schott, E. J., Sharma, Y. K., Davis, K. R. and Gardner, R. C. (1998). Aluminium induces oxidative stress genes in *Arabidopsis thaliana. Plant Physiol.*, **116,** 409-418

Riget, F., Johansen, P. and Asmund, G. (1995). Natural seasonal variation of cadmium, copper, lead, and zinc in brown seaweed (*Fucus vesiculosus*). *Mar. Poll. Bull.*, **30,** 409-413

Rijstenbil, J. W., Derksen, J. W. M., Gerringa, L. J. A., Poortvliet, T. C. W., Sandee, A., van den Berg, M., van Drie, J. and Wijnholds, J. A. (1994). Oxidative stress induced by copper: Defense and damage in the marine planktonic diatom *Ditylum brightwellii*, grown in continuous cultures with high and low zinc levels. *Mar. Biol.*, **119,** 583-590

Roberts, S. K., Berger, F. and Brownlee, C. (1993). The role of calcium in signal transduction following fertilization in *Fucus serratus. J. Exp. Biol.*, **184,** 197-212

Roberts, S. and Brownlee, C. (1995). Calcium influx, fertilisation potential and egg activation in *Fucus serratus. Zygote,* **3,** 191-197

Roberts, S. K., Gillot, I. and Brownlee, C. (1994). Cytoplasmic calcium and *Fucus* egg activation. *Development,* **120,** 155-163

Robinson, K. R. (1996). Fucoid zygotes germinate from their darkest regions, not their brightest ones. *Plant Physiol.*, **112,** 1401

Robinson, K. R. and Miller, B. J., (1997). The coupling of cyclic GMP and photopolarisation of *Pelvetia* zygotes. *Devel. Biol.*, **187,** 125-130

Robinson, K. R., Lorenzi, R., Ceccarelli, N. and Gualtieri, P., (1998). Retinal identification in *Pelvetia fastigiata. Biochem. Biophys. Res. Comm.,* **243,** 776-778

Röderer, G and Reiss, H. –D. (1988). Different effects of inorganic and triethyl lead on growth and ultrastructure of lily pollen tubes. *Protoplasma,* **144,** 101-109

Rogers, S. L. and Gelfand, V. I. (2000). Membrane traffiking, organelle transport, and the cytoskeleton. *Cur. Opin. Cell Biol.*, **12,** 57-62

Ronnberg, O., Adjers, K., Ruokolahti, C. and Bondestam, M. (1990). *Fucus vesiculosus* as an indicator of heavy metal availability in a fish farm recipient in the Northern Baltic Sea. *Mar. Pollut. Bull.*, **21,** 388-392

Ruban, A. V. and Horton, P. (1999). The xanthophyll cycle modulates the kinetics of nonphotochemical energy dissipation in isolated light-harvesting complexes, intact chloroplasts, and leaves of spinach. *Plant Physiol.*, **119,** 531-542

Ruban, A. V., Young, A. J. and Horton, P. (1993). Induction of nonphotochemical energy dissipation and absorbance changes in leaves. *Plant Physiol.*, **102,** 741-750

Runnels, L. W. and Scarlata, S. F. (1998). Relulation of the rate and extend of phosphiolipase C β_2 effector activation by $\beta\gamma$ subunits of heterotrimeric G proteins. *Biochem.*, **37,** 15563-15574

Saager, P. M., De Baar, H. J. W. and Howland, R. J. (1992). Cd, Zn, Ni and Cu in the Indian Ocean. *Deep-Sea Res.*, **39,** 9-35

Sanders, D., Brownlee, C. and Harper, J. F. (1999). Communicating with calcium. *Plant Cell,* **11,** 691-706

Sandmann, G. and Böger, P. (1980). Copper-mediated lipid peroxidation processes in photosynthetic membranes. *Plant Physiol.*, **66,** 797-800

Sawidis, T. and Reiss, H. -D. (1995). Effects of heavy metals on pollen tube growth and ultrastructure. *Protoplasma,* **185,** 113-122

Say, P. J., Burrows, I. G. and Whitton, B. A. (1990). *Enteromorpha* as a monitor of heavy metals in estauries. *Hydrobiol.*, **195,** 119-126

Scanlan, C. M. and Wilkinson, M. (1987). The use of seaweeds in biotic toxicity testing. Part 1. The sensitivity of different stages in the life history of *Fucus*, and of other algae, to certain biocides. *Mar. Environ. Res.*, **21,** 11-29

Schat, H. and Kalff, M. M. A. (1992). Are phytochelatins involved in differential metal tolerance or do they merely reflect metal-imposed strains? *Plant Physiol.*, **99,** 1475-1480

Schel, J. H. N., Kieft, H. and Van Lammeren, A. A. M. (1984). Interactions between embryo and endosperm during early developmental stages of maize caryopses (*Zea mays*). *Can. J. Bot.*, **62,** 2842-2853

Schierup, H. H., Brix, H. and Madsen, T. V. (1995). *Øvelsesvejledning i ferskvandsøkoilogi.* Afd. Bot. Øk., Aarhus Universitet

Schröder, W. P., Arellano, J. B., Bittner, T., Barón, M., Eckert, H. –J. and Renger, G. (1994). Flash-induced absorption spectroscopy studies of copper interaction with photosystem II in higher plants. *J. Biol. Chem.*, **269,** 32865-32870

Schroeder, J. I. and Thuleau, P. (1991). Ca^{2+} channels in higher plant cells. *Plant Cell*, **3,** 555-559

Schoenwaelder, M. E. A. and Clayton, M. N. (1998). Secretion of phenolic substances into the zygote wall and cell plate in embryos of *Hormosira* and *Acrocarpia* (Fucales, Phaeophyceae). *J. Phycol.*, **34,** 969-980

Seeliger, U. and Cordazzo, C. (1982). Field and experimental evaluation of *Enteromorpha* sp. as a quali-quantitative monitoring organism for copper and mercury in estuaries. *Environ. Pollut.*, **29,** 197-206

Serrão, E. A., Pearson, G., Kautsky, L. and Brawley, S. H., (1996). Successful external fertilization in turbulent environments. *Proc. Nat. Acad. Sci. USA*, **93,** 5286-5290

Sharma, V. K. and Millero, F. J. (1988). Effect of ionic interactions on the rates of oxidation of Cu(I) with O_2 in natural waters. *Mar. Chem.*, **25,** 141-161

Shaw, S. L. and Quatrano, R. S. (1996a). Polar localization of a dihydropyridine receptor on living *Fucus* zygotes. *J. Cell Sci.*, **109**, 335-342

Shaw, S. L. and Quatrano, R. S. (1996b). The role of targeted secretion in the establishment of cell polarity and the orientation of the division plane in *Fucus* zygotes. *Development*, **122,** 2623-2630

Shimmen, T. and Yokota, E. (1994). Physiological and biological aspects of cytoplasmic streaming. *Int. Rev. Cyt.*, **108,** 2549-2563

Shimmen, T., Hamatani, M., Saito, S., Yokota, E., Mimura, T., Fusetani, N. and Karaki, H. (1995). Roles of actin filaments in cytoplasmic streaming and organization of transvacuolar strands in root hair cells of *Hydrocharis*. *Protoplasma*, **185,** 188-193

Small, J. V., Rottner, K. and Kaverina, I. (1999). Functional design in the actin cytoskeleton. *Cur. Opin. Cell Biol.*, **11,** 54-60

Smith, K. L., Hann, A. C. and Harwood, J. L. (1986). The subcellular localisation of absorbed copper in *Fucus*. *Physiol. Plant.*, **66,** 692-698

Söderlund, S., Fosberg, Å. and Pedersén, M. (1988). Concentrations of cadmium and other metals in *Fucus vesiculosus* L. and *Fontinalis dalecarlia* Br. Eur. from the Northern Baltic Sea and the Southern Bothnian Sea. *Environ. Pollut.*, **51,** 197-212

Sokal, R. R., and Rohlf, F. J. (1981). *Biometry*. W. H. Freeman and Company, New York. 859 pp.

Soli, A. L. and Byrne, R. H. (1989). Temperature dependence of Cu(II) carbonate complexation in naturel seawater. *Limnol. Oceanogr.*, **34,** 239-244

Somerfield, P. J., Gee, J. M. and Warwick, R. M. (1994). Soft sediment meiofaunal community structure in relation to a long-term heavy metal gradient in the Fal estuary system. *Mar. Ecol. Progr. Ser.*, **105,** 79-88

Souter, M. and Lindsey, K. (2000). Polarity and signalling in plant embryogenesis. *J. Exp. Bot.*, **51,** 971-983

South, G. R. and Wittick, A. (1988). *Introduction to phycology*. Blackwell Scientific publications, Editorial Offices, Oxford, 341 pp.

Speksnijder, J. A., Miller, A. L., Weisenseel, M. H., Chen, T.-H. and Jaffe, L. F. (1989). Calcium buffer injections block fucoid egg development by facilitating calcium diffusion. *Proc. Nat. Acad. Sci. USA,* **86,** 6607-6611

Stauber, J. L. and Florence, T. M. (1986). Reversibility of copper-thiol binding in *Nitzschia closterium* and *Chlorella pyrenoidosa*. *Aquat. Toxicol.*, **8,** 223-229

Stauber, J. L. and Florence, T. M. (1987). Mechanism of toxicity of ionic copper and copper complexes to algae. *Mar. Biol.*, 94, 511-519

Steinman, T., Gelder, N., Grebe, M., Mangold, S., Jackson, C. L., Paris, S., Gälweiler, L., Palme, K. and Jürgens, G. (1999). Co-ordinated polar localisation of auxin efflux carrier PIN1 by GNOM ARF GEF. *Science*, **286,** 316-318

Stengel, D. B. and Dring, M. J. (2000). Copper and iron concentrations in *Ascophyllum nodosum* (Fucales, Phaeophyta) from different sites in Ireland and after culture experiments in relation to thallus age and epiphytism. *J. Exp. Mar. Biol. Ecol.*, **246,** 145-161

Strömgren, T. (1980). The effect of dissolved copper on the increase in length of four species of intertidal fucoid algae. *Mar. Env. Res.*, **3,** 5-13

Sueur, S., Van den Berg, C. M. G. and Riley, J. P. (1982). Measurement of the metal complexing ability of exudates of marine macroalgae. *Limnol. Oceanogr.*, **27,** 536-543

Sun, Y., Qian, H., Xu, X.-D., Han, Y., Yen, L.-F. and Sun, D.-Y. (2000). Integrin-like proteins in the pollen tube: detection, localisation and function. *Plant Cell Physiol.*, **41,** 1136-1142

Sunda, W. G. and Guillard, R. R. L. (1976). The relationship between cupric ion activity and the toxicity of copper to phytoplankton. *J. Mar. Res.*, **34,** 511-529

Sunda, W. G and Huntsman, S. A. (1983). Effects of competitive interactions between manganese and copper on cellular manganese and growth in estuarine and oceanic species of the diatom *Thalassiosira*. *Limnol. Oceanogr.*, **28,** 924-934

Sunda, W. G and Huntsman, S. A. (1991). The use of chemiluminescence and ligand competition with EDTA to measure copper contamination and speciation in seawater. *Mar. Chem.*, **36,** 137-163

Sunda, W. G and Huntsman, S. A. (1995). Regulation of copper concentration in the oceanic nutricline by phytoplankton uptake and regeneration cycles. *Limnol. Oceanogr.* **40,** 132-137

Taylor, A. R., Roberts, S. K. and Brownlee, C., (1992). Calcium and related channels in fertilisation and early development of *Fucus*. *Phil. Trans. R. Soc. Lond.* B., **335,** 1-8

Taylor, A. and Brownlee, C. (1993). Calcium and potassium currents in the *Fucus* egg. *Planta,* **189,**109-119

Taylor, A., Manison, N. and Brownlee, C. (1997). Regulation of channel activity underlying cell volume and polarity signals in *Fucus*. *J. Exp. Bot.*, **48,** 579-588

Taylor, A. R., Manison, N., Fernandez, C., Wood, J. and Brownlee, C. (1996). Spatial organisation of calcium signalling involved in cell volume control in the *Fucus* rhizoid. *Plant Cell,* **8,** 2015-2030

Tazawa, M. Shimada, K. and Kikuyama, M. (1995). Cytoplasmic hydration triggers a transient increase in cytoplasmic Ca^{2+} concentrations in *Nitella flexilis*. *Plant Cell Physiol.*, **36,** 335-340

Teisseire, H. and Guy, V. (2000). Copper-induced changes in antioxidant enzymes activities in fronds of duckweed (*Lemna minor*). *Plant Sci.*, **153,** 65-72

Thuret, M. G. (1854). Reserches sur la fécondation des fucacés suivies d'observations sur les anthéridies des algues. *Ann. Sci. Nat.*, **4,** 197-214

Tokarnia, C. H., Dobereiner, J., Moraes, S. S., and Peixoto, P. V. (1999). Mineral deficiencies and imbalances in cattle and sheep – a review of Brazilian studies made between 1987 and 1998. *Pesquisa Veterinaria Brasileira*, **19,** 47-62

Trewavas, A. J. and Gilroy, S. (1991). Signal transduction in plant cells. *TIG*, **7,** 356-360

Tsukihara, T., Aoyama, H., Yamashita, E., Tomizaki, T., Yamaguchi, H., Shinzawa-Itoh, K., Nakashima, R., Yaono, R. and Yoshikawa, S. (1996). The whole structure of the 13-subunit oxidized cytochrome c oxidase at 2.8 Å. *Science*, **272,** 1136-1144

Turner, A. (1996). Trace-metal partitioning in estuaries: importance of salinity and particulate concentration. *Mar. Chem.*, **54,** 27-39

Turner, D. R., Whitfield, M. and Dickson, A. G. (1981). The equilibrium speciation of dissolved components in freshwater and seawater at 25°C and 1 atm. pressure. *Geochim. Cosmochim. Acta*, **45,** 855-882

Tyrell, T and Law, C. S. (1997). The oceanic N:P ratio. *Nature*, **387,** 793-796

Uhrmacher, S., Hanelt, D. and Nultsch, W. (1995). Zeaxanthin content and the degree of photoinhibition are linearly correlated in the brown alga *Dictyota dichotoma. Mar. Biol.*, **123,** 159-165

Uribe, E. G. and Stark, B. (1982). Inhibition of photosynthetic energy conversion by cupric ion. Evidence for Cu^{2+}-coupling factor 1 interactions. *Plant Physiol.*, **69,** 1040-1045

Vadas, S., Johnson, S. and Norton, T. A. (1992). Recruitment and mortality of early post-settelement of benthic algae. *Br. Phycol. J.*, **27,** 331-335

Valentine, J. S. and Gralla, E. B. (1997). Delivering copper inside yeast and human cells. *Science*, **278,** 817-818

Van den Berg, C. M. G. (1984). Organic and inorganic speciation of copper in the Irish Sea. *Mar. Chem.*, **14,** 201-212

Van den Berg, C. M. G., Wong, P. T. S. and Chau, Y. K. (1979). Measurements of complexing materials excreted from algae and their ability to ameliorate copper toxicity. *J. Fish. Res. Board. Can.*, **36,** 901-905

van Hoof, N. A. L. M., Hassinen, V. H., Hakvoort, H. W. J., Ballintijn, K. F., Schat, H., Verkleij, J. A. C., Ernst, W. H. O., Karenlampi, S. O. and Tervahauta, A. I. (2001). Enhanced copper tolerance in *Silene vulgaris* (Moench) Garcke populations from copper mines is associated with increased transcript levels of a 2b-type metallothionein gene. *Plant Physiol.*, **126,** 1519-1526

Vershinin, A. O. and Kamnev, A. N. (1996). Xanthophyll cycle in marine macroalgae. *Bot. Mar.*, **39,** 421-425

Viarengo, A., Pertica, M., Mancinelli, G., Burlando, B. Canesi, L. and Orunesu, M. (1996). *In vivo* effects of copper on calcium homeostasis mechanisms of mussel gill cell plasma membranes. *Comp. Biochem. Physiol.* **113C,** 421-425

Voelker, B. M. and Kogut, M. B. (2001). Interpretation of metal speciation data in coastal waters: the effects of humic substances on copper binding as a test case. *Mar. Chem.*, **74,** 303-318

Vroemen, C. W., Langeveld, S., Mayer, U., Ripper, G., Jürgens, G., Van Kammen, A. and De Vries, S. C. (1996). Pattern formation in the *Arabidopsis* embryo revealed by position-specific lipid transfer protein gene expression. *Plant Cell*, **8,** 783-791

Wagner, V. T., Brian, L. and Quatrano, R. S. (1992). Role of vitronectin-like molecule in embryo adhesion of the brown alga *Fucus. Proc. Natl. Acad. Sci. USA*, **89,** 3644-3648

Wang, Z., Chin, T. A. and Templeton, D. M. (1996). Calcium-independent effects of cadmium on actin assembly in mesangial and vascular smooth muscle cells. *Cell Mot. Cytoskel.*, **33**, 208-222

Ward, J. M. and Schroeder, J. I. (1994). Calcium-activated K^+ channels and calcium-induced calcium release by slow vacuolar ion channels in guard cell vacuoles implicated in the control of stomatal closure. *Plant Cell*, **6**, 669-683

Westall, J. C., Zachary, J. L. and Morel, F. M. M. (1976). *MINEQL: A computer program for the calibration of chemical equilibrium composition of aqueous systems.* Massachusetts Institute of Technology, Cambridge, 91 pp.

Weeds, A. (1982). Actin-binding proteins – regulators of cell architecture and motility. *Nature*, **296**, 811-816

Welch, M. D., Mallavarapu, A., Rosenblatt, J. and Mitchison, T. J. (1997). Actin dynamics *in vivo*. *Cur. Opin. Cell Biol.*, **9**, 54-61

White, A. J. and Critchley, C. (1999). Rapid light curves: A new fluorescence method to assess the state of the photosynthetic apparatus. *Photosynt. Res.*, **59**, 63-72

Widerlund, A. (1996). Early diagenetic remobilization of copper in near-shore marine sediments: a quantitative pore-water model. *Mar. Chem.*, **54**, 41-53

Willekens, H., Van Camp, W., Van Montagu, M., Inze, D., Langebartels, C. and Sandermann, H. (1994). Ozone, sulfur dioxide, and ultraviolet B have similar effects on mRNA accumulation of antioxidant genes in *Nicotiana plumbaginifolia* L. *Plant Physiol.*, **106**, 1007-1014

Williams, R. J. P. (1992). Calcium and calmodulin. *Cell Calsium*, **13**, 355-362

Wolfe, D. A. (1992). Selection of bioindicators of pollution for marine monitoring programmes. *Chem. Ecol.*, **6**, 149-167

Wolpert, L., Beddington, R., Brockes, J., Jessell, T., Lawrance, P. and Meyerowitz. (1998). *Principles of Development.* Current Biology Ltd. Oxford University Press. 484 pp.

Wong, S. L., Nakamoto, L. and Wainwright, J. F. (1994). Identification of toxic metals in affected algal cells in assays of wastewaters. *J. Appl. Phycol.*, **6**, 405-414

Wright, P. J. and Reed, R. H. (1990). Effects of osmotic stress on gamete size, rhizoid initiation and germling growth in fucoid algae. *Br. Phycol. J.*, **25**, 149-155

Wymer, C. L., Bibikova, T. N. and Gilroy, S. (1997). Cytoplasmic free calcium distributions during the development of root hair of *Arabidopsis thaliana*. *Plant J.*, **12**, 427-439

Yabe, K., Makino, M. and Suzuki, M. (1997). Growth inhibition on gametophytes of *Laminaria religiosa* induced by UV-B irradiation. *Fish. Sci.*, **63**, 668-670

Yamasaki, H., Sakihama, N. and Ikehara, N. (1997). Flavonoid-peroxidase reaction as detoxification mechanism of plant cells against H_2O_2. *Plant Physiol.*, **115**, 1405-1412

Yang, X. -C. and Sachs, F. (1989). Block of stretch-activated ion channels in *Xenopus* oocytes by gadolinium and calcium ions. *Science*, **243**, 1068-1071

Yruela, I., Alfonso, M., de Zarates I. O., Montoya, G, and Picorel, R. (1993). Precise location of the Cu(II)-inhibitory binding site in higher plants and bacterial photosynthetic reaction centres as probed by light-induced absorption changes. *J. Biol. Chem.*, **268**, 1684-1689

Yruela, I., Montoya, G., Alonso, P. J. and Picorel, R. (1991). Identification of the pheophytin-Q_A-Fe domain of the reducing side of the photosystem II as the Cu(II)-inhibitory binding site. *J. Biol. Chem.*, **266**, 22847-22850

Yruela, I., Pueyo, J. L., Alonso, P. J., and Picorel, R. (1996). Photoinhibition of photosystem II from higher plants. *J. Biol. Chem.*, **271**, 27408-27415

Zhang, Y., McBride, D. W. and Hamill, O. P. (1998). The ion selectivity of a membrane conductance inactivated by extracellular calcium in *Xenopus* oocytes. *J. Physiol.*, **508,** 763-776

Zhao, Y., Kappes, B., and Franklin, R. M. (1993). Gene structure and expression of an unusual protein kinase from Plasmodium falciparum homologous at its terminus with the EF hand calcium-binding proteins. *J. Biol. Chem.*, **268,** 4347-4354